

ICFA Instrumentation School

March 26 – April 6, 2001

National Accelerator Center
Faure, South Africa

Signal Processing

Helmuth Spieler

*Physics Division
Lawrence Berkeley National Laboratory
Berkeley, CA 94720*

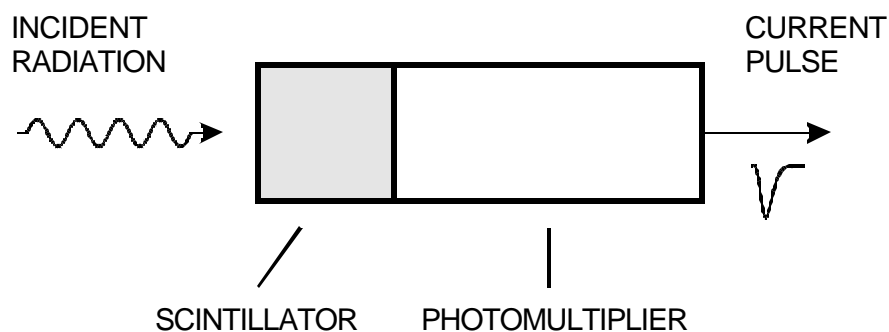
spieler@LBL.gov

*These course notes and additional tutorials are available
as pdf files at
<http://www-physics.lbl.gov/~spieler>*

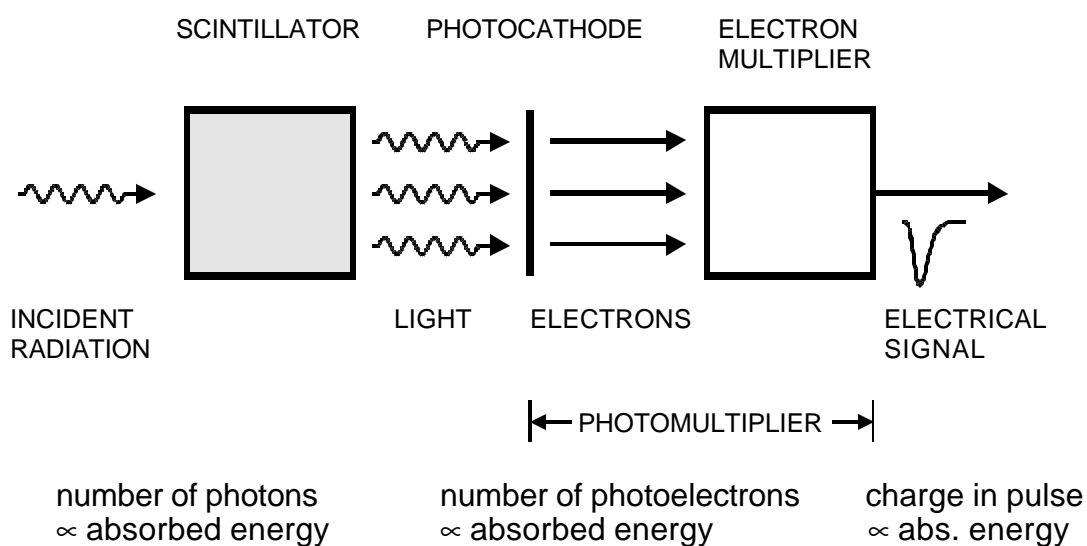
Table of Contents

1. Acquiring the Detector Signal
2. Resolution and Signal-to-Noise Ratio
 - Pulse Shaping
 - Equivalent Noise Charge
 - Sources of Electronic Noise
3. Some Other Aspects of Pulse Shaping
4. Timing Measurements
5. Digitization of Pulse and Time
 - Analog to Digital Conversion
6. Digital Signal Processing
7. Detector Systems – Some Examples
8. Why Things Don't Work
9. Summary of Considerations in Detector Electronics

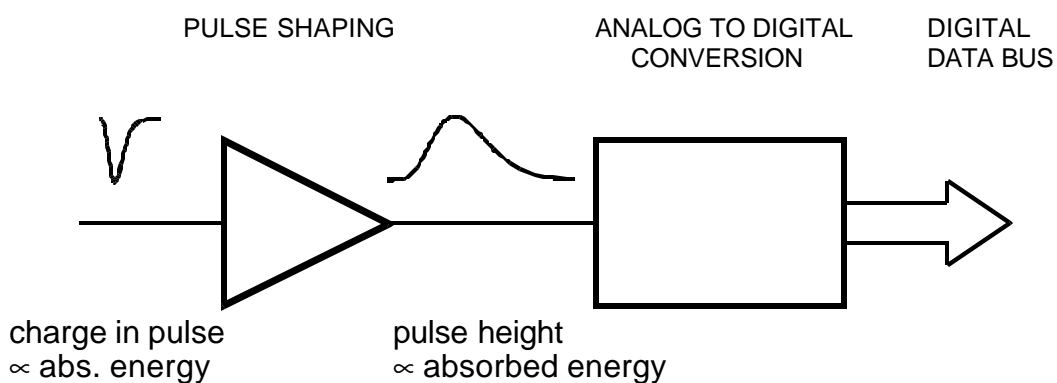
A Typical Detector System



Processes in Scintillator – Photomultiplier



Signal Processing



1. Acquiring the Detector Signal

- Determine energy deposited in detector
- Detector signal generally a short current pulse

Typical durations

Thin silicon detector (10 ... 300 μm thick):	100 ps – 30 ns
Thick ($\sim\text{cm}$) Si or Ge detector:	1 – 10 μs
Proportional chamber (gas):	10 ns – 10 μs
Gas microstrip or microgap chamber:	10 – 50 ns
Scintillator + PMT/APD:	100 ps – 10 μs

The total charge Q_s contained in the detector current pulse $i_s(t)$ is proportional to the energy deposited in the detector

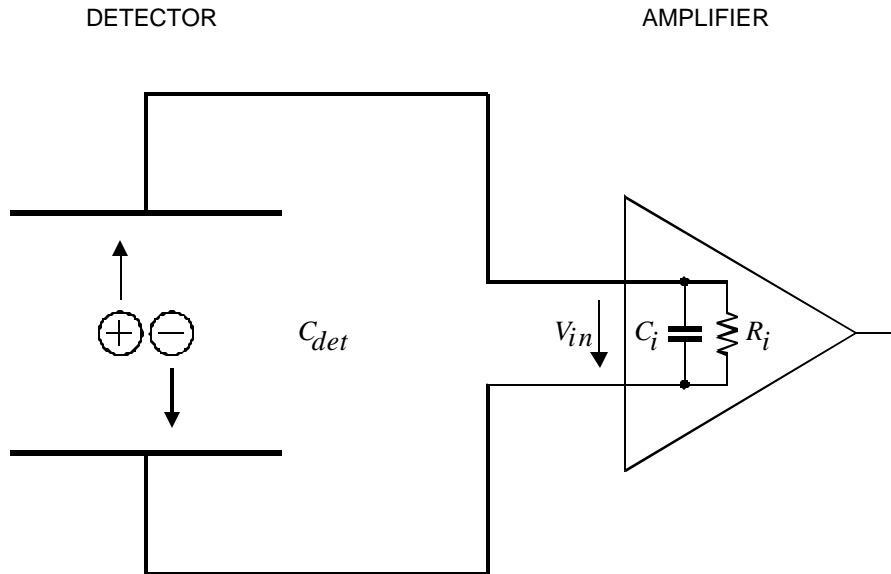
$$E \propto Q_s = \int i_s(t) dt$$

- Necessary to integrate the detector signal current.

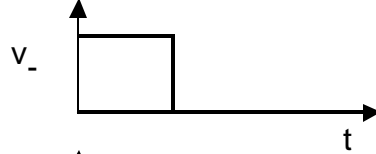
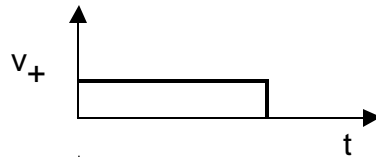
Possibilities:

1. Integrate charge on input capacitance
2. Use integrating (“charge sensitive”) preamplifier
3. Amplify current pulse and use integrating (“charge sensing”) ADC

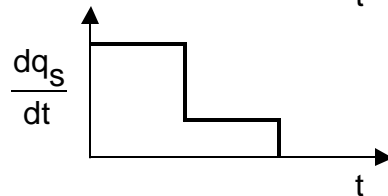
Integration on Input Capacitance



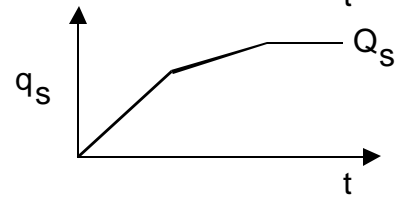
velocities of charge carriers



rate of induced charge on detector electrodes



signal charge



if $R_i \times (C_{det} + C_i) \gg$ collection time

peak voltage at amplifier input

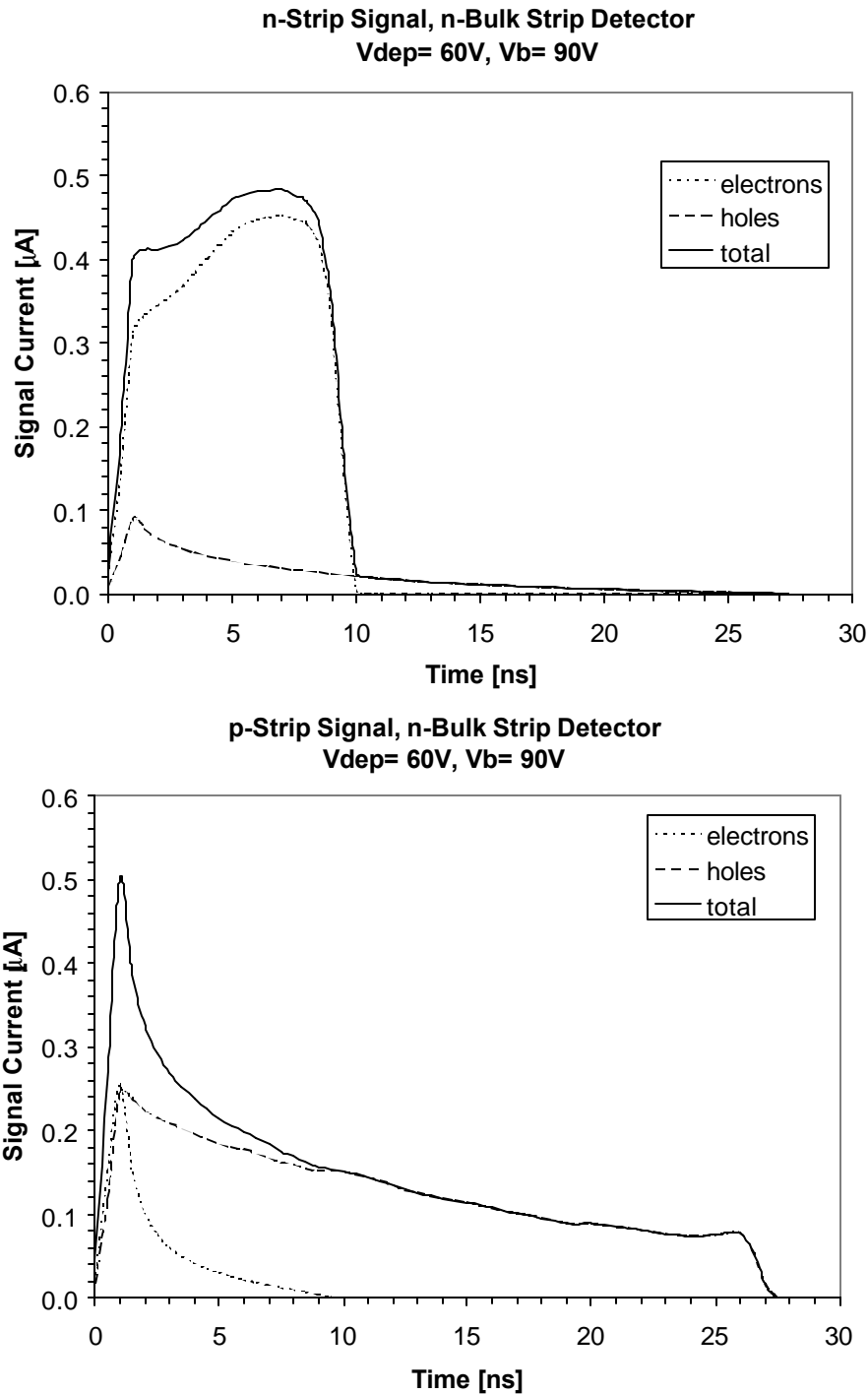
$$V_s = \frac{Q_s}{C_{det} + C_i}$$

↑

Magnitude of voltage depends on detector capacitance!

In reality the current pulses are more complex.

Current pulses on opposite sides (n-strip and p-strip) of a double-sided silicon strip detector (track traversing the detector)

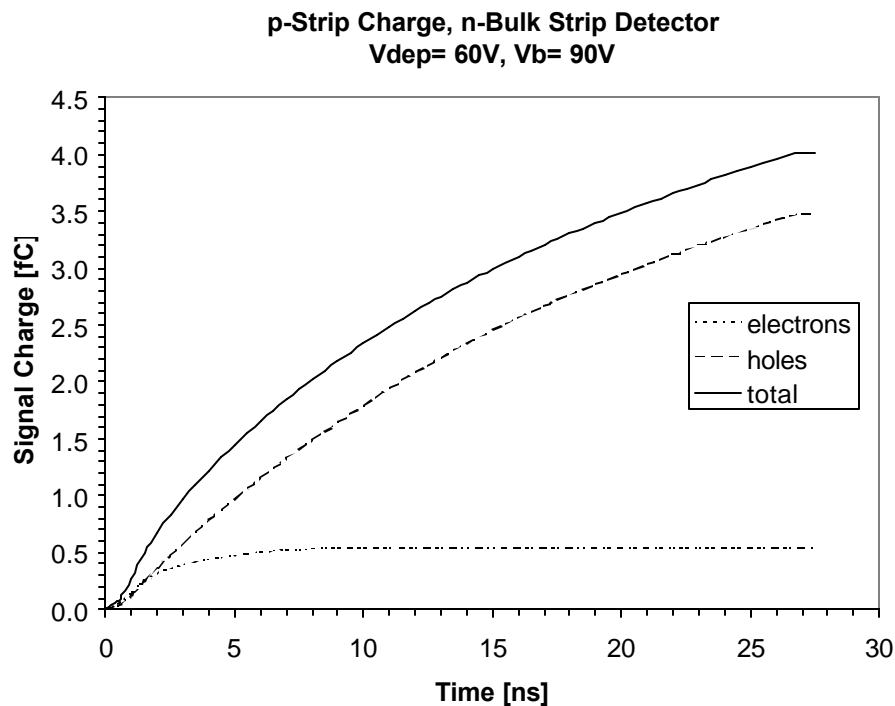
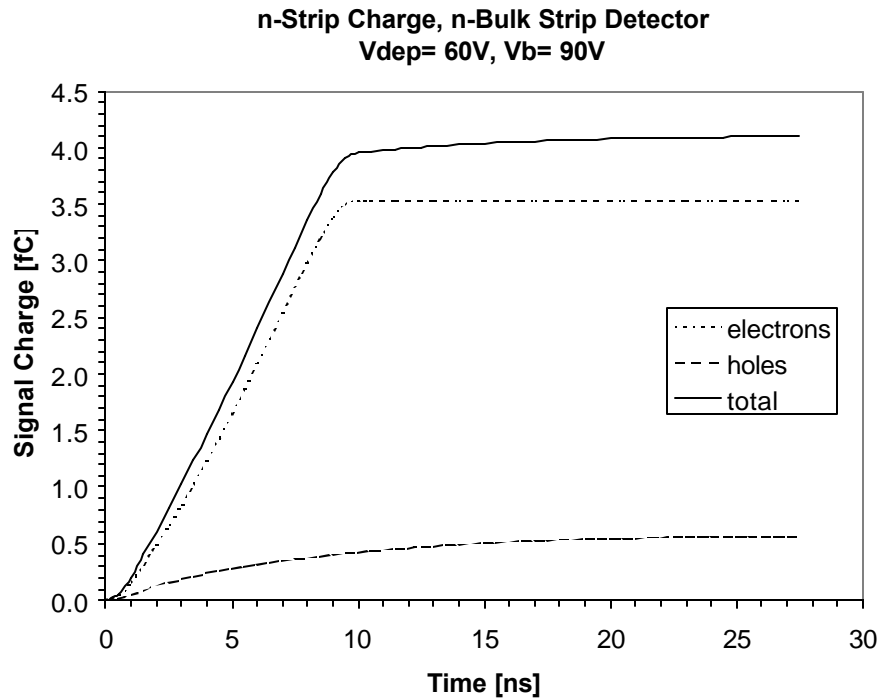


Although both pulses originate from the same particle track, the shapes are very different.

However, although the peak voltage or current signal measured by the amplifier may be quite different, the signal charge

$$Q_s = \int i_s dt$$

is the same.



⇒ **Desirable to measure signal charge**

- independent of detector pulse shape

When the input time constant RC is much greater than the signal duration, the peak voltage is a measure of the charge

$$V = \frac{1}{C} \int i_s dt = \frac{Q_s}{C}$$

The measured signal depends on the total capacitance at the input.

Awkward in system where the detector capacitance varies, e.g.

- different detector geometries
(e.g. strip detectors with different lengths)
- varying detector capacitance
(e.g. partially depleted detectors)

Use system whose response is independent of detector capacitance.

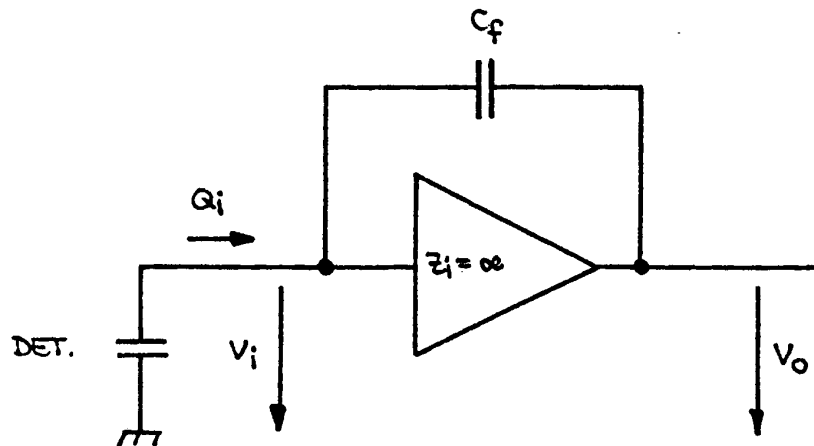
Active Integrator (“charge-sensitive amplifier”)

Start with inverting voltage amplifier

Voltage gain $dV_o/dV_i = -A \Rightarrow v_o = -A v_i$

Input impedance = ∞ (i.e. no signal current flows into amplifier input)

Connect feedback capacitor C_f between output and input.



Voltage difference across C_f : $v_f = (A+1) v_i$

\Rightarrow Charge deposited on C_f : $Q_f = C_f v_f = C_f (A+1) v_i$

$Q_i = Q_f$ (since $Z_i = \infty$)

\Rightarrow Effective input capacitance

$$C_i = \frac{Q_i}{v_i} = C_f (A+1)$$

(“dynamic” input capacitance)

Gain

$$A_Q = \frac{dV_o}{dQ_i} = \frac{A \cdot v_i}{C_i \cdot v_i} = \frac{A}{C_i} = \frac{A}{A+1} \cdot \frac{1}{C_f} \approx \frac{1}{C_f} \quad (A \gg 1)$$

Q_i is the charge flowing into the preamplifier

but some charge remains on C_{det} .

What fraction of the signal charge is measured?

$$\frac{Q_i}{Q_s} = \frac{C_i v_i}{Q_{det} + Q_i} = \frac{C_i}{Q_s} \cdot \frac{Q_s}{C_i + C_{det}}$$

$$= \frac{1}{1 + \frac{C_{det}}{C_i}} \approx 1 \text{ (if } C_i \gg C_{det} \text{)}$$

Example:

$$A = 10^2$$

$$C_f = 1 \text{ pF} \quad \Rightarrow \quad C_i = 100 \text{ pF}$$

$$C_{det} = 1 \text{ pF}: \quad Q_i / Q_s = 0.99$$

$$C_{det} = 50 \text{ pF}: \quad Q_i / Q_s = 0.67$$



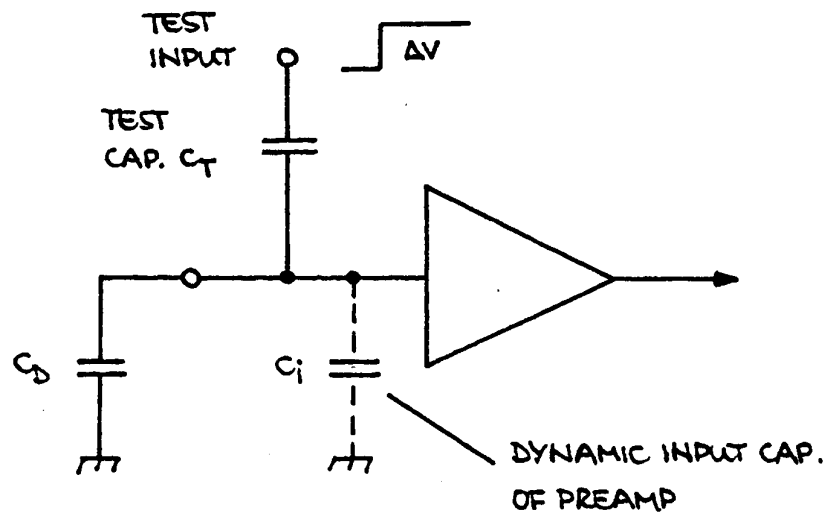
Si Det.: 50 μm thick
50 mm^2 area

Note: Input coupling capacitor must be $\gg C_i$ for high charge transfer efficiency.

Calibration

Inject specific quantity of charge - measure system response

Use voltage pulse (can be measured conveniently with oscilloscope)



$C_i \gg C_T \Rightarrow$ Voltage step applied to test input develops over C_T .

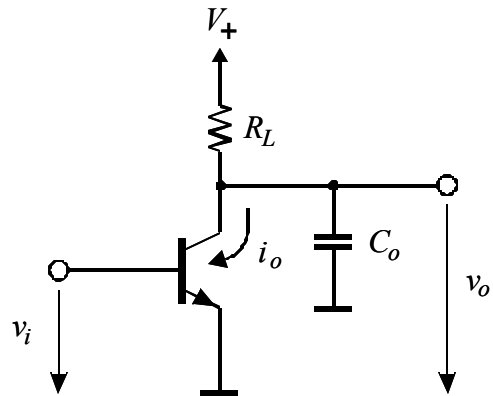
$$\Rightarrow Q_T = \Delta V \cdot C_T$$

Accurate expression:

$$Q_T = \frac{C_T}{1 + \frac{C_T}{C_i}} \cdot \Delta V \approx C_T \left(1 - \frac{C_T}{C_i} \right) \Delta V$$

Typically: $C_T/C_i = 10^{-2} - 10^{-4}$

A Simple Amplifier



Voltage gain:

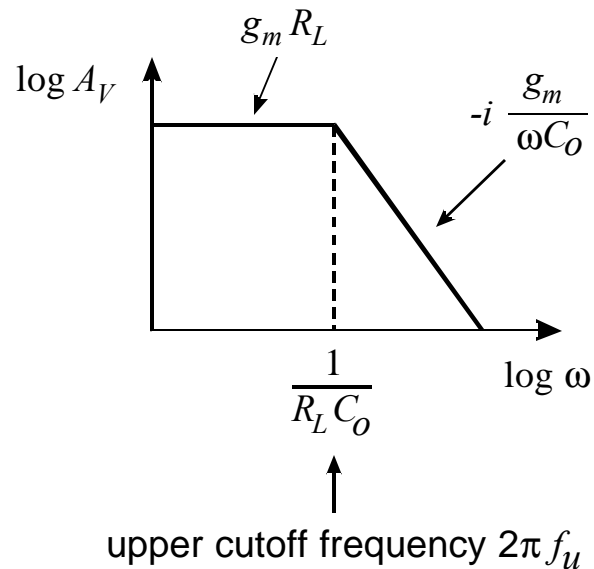
$$A_V = \frac{dv_o}{dv_i} = \frac{di_o}{dv_i} \cdot Z_L \equiv g_m Z_L$$

$g_m \equiv$ transconductance

$$Z_L = R_L // C_o$$

$$\frac{1}{Z_L} = \frac{1}{R_L} + i\omega C_o \quad \Rightarrow \quad A_V = g_m \left(\frac{1}{R_L} + i\omega C_o \right)^{-1}$$

\uparrow \uparrow
 low freq. high freq.

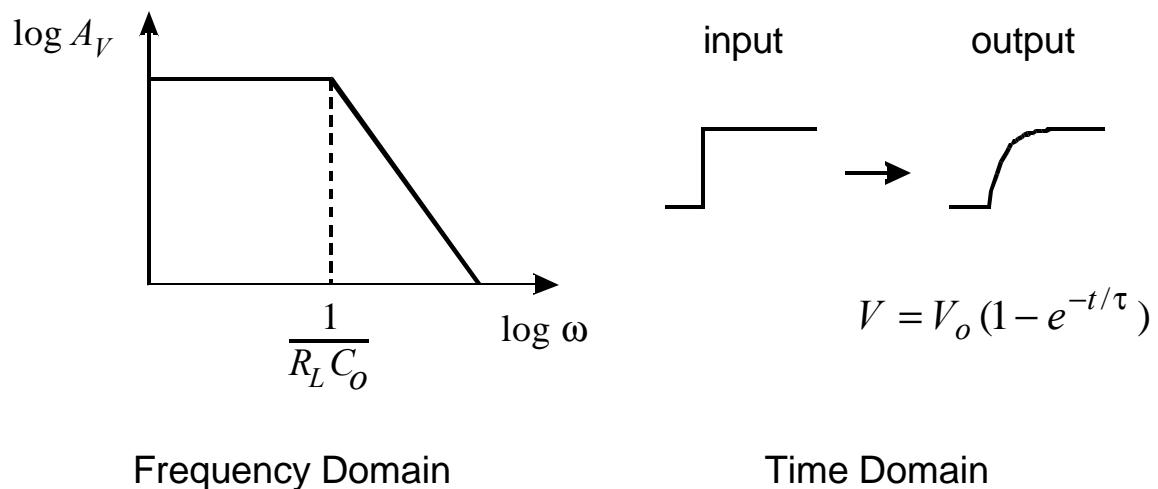


Pulse Response of the Simple Amplifier

A voltage step $v_i(t)$ at the input causes a current step $i_o(t)$ at the output of the transistor.

For the output voltage to change, the output capacitance C_o must first charge up.

⇒ The output voltage changes with a time constant $\tau = R_L C_o$



The time constant τ corresponds to the upper cutoff frequency

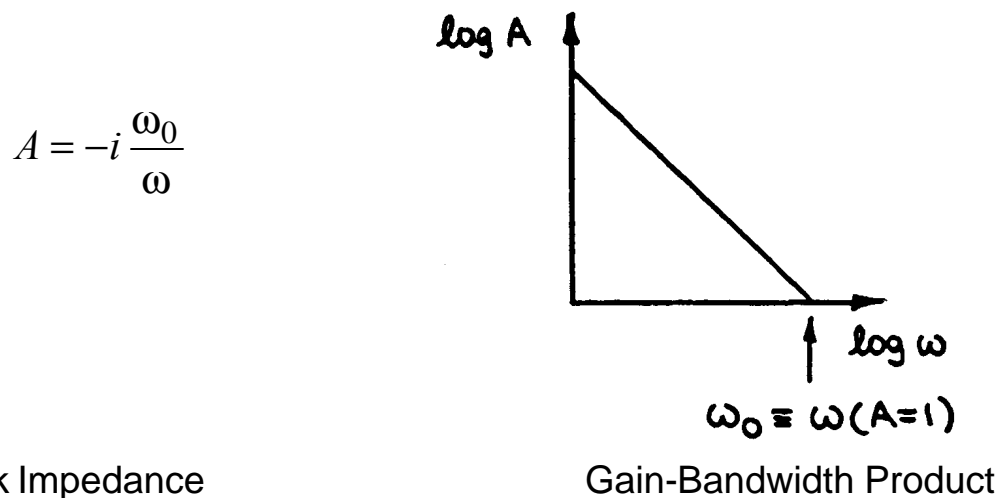
$$\tau = \frac{1}{2\pi f_u}$$

Input Impedance of a Charge-Sensitive Amplifier

Input impedance

$$Z_i = \frac{Z_f}{A+1} \approx \frac{Z_f}{A} \quad (A \gg 1)$$

Amplifier gain vs. frequency beyond the upper cutoff frequency



Feedback Impedance

$$Z_f = -i \frac{1}{\omega C_f}$$

⇒ Input Impedance

$$Z_i = -\frac{i}{\omega C_f} \cdot \frac{1}{-i \frac{\omega_0}{\omega}}$$

$$Z_i = \frac{1}{\omega_0 C_f}$$

Imaginary component vanishes ⇒ *Resistance: $Z_i \rightarrow R_i$*

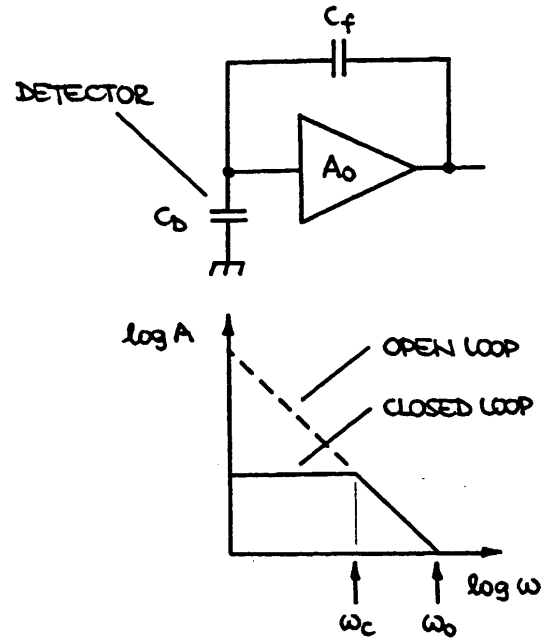
⇒ low frequencies ($f < f_u$): capacitive input
 high frequencies ($f > f_u$): resistive input

Time Response of a Charge-Sensitive Amplifier

Closed Loop Gain

$$A_f = \frac{C_D + C_f}{C_f} \quad (A_f \ll A_0)$$

$$A_f \approx \frac{C_D}{C_f} \quad (C_D \gg C_f)$$



Closed Loop Bandwidth

$$\omega_c A_f = \omega_0$$

Response Time

$$\tau_{amp} = \frac{1}{\omega_c} = C_D \frac{1}{\omega_0 C_f}$$

⇒ **Rise time increases with detector capacitance.**

Alternative Picture: Input Time Constant

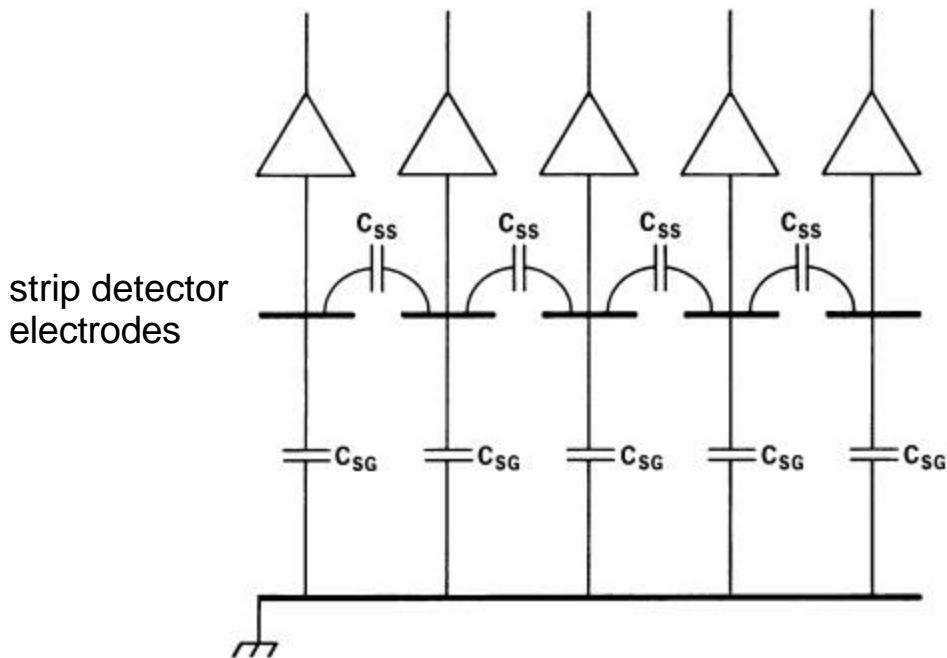
$$\tau_i = R_i C_D$$

$$\tau_i = \frac{1}{\omega_0 C_f} \cdot C_D = \tau_{amp}$$

Same result as from conventional feedback theory.

Input impedance is critical in strip or pixel detectors:

Amplifiers must have a low input impedance to reduce transfer of charge through capacitance to neighboring strips



For strip pitches that are smaller than the bulk thickness the capacitance is dominated by the fringing capacitance to the neighboring strips C_{SS} .

Typically: 1 – 2 pF/cm for strip pitches of 25 – 100 μm on a 300 μm thick Si substrate.

The backplane capacitance C_{SG} is typically 20% of the strip-to-strip capacitance.

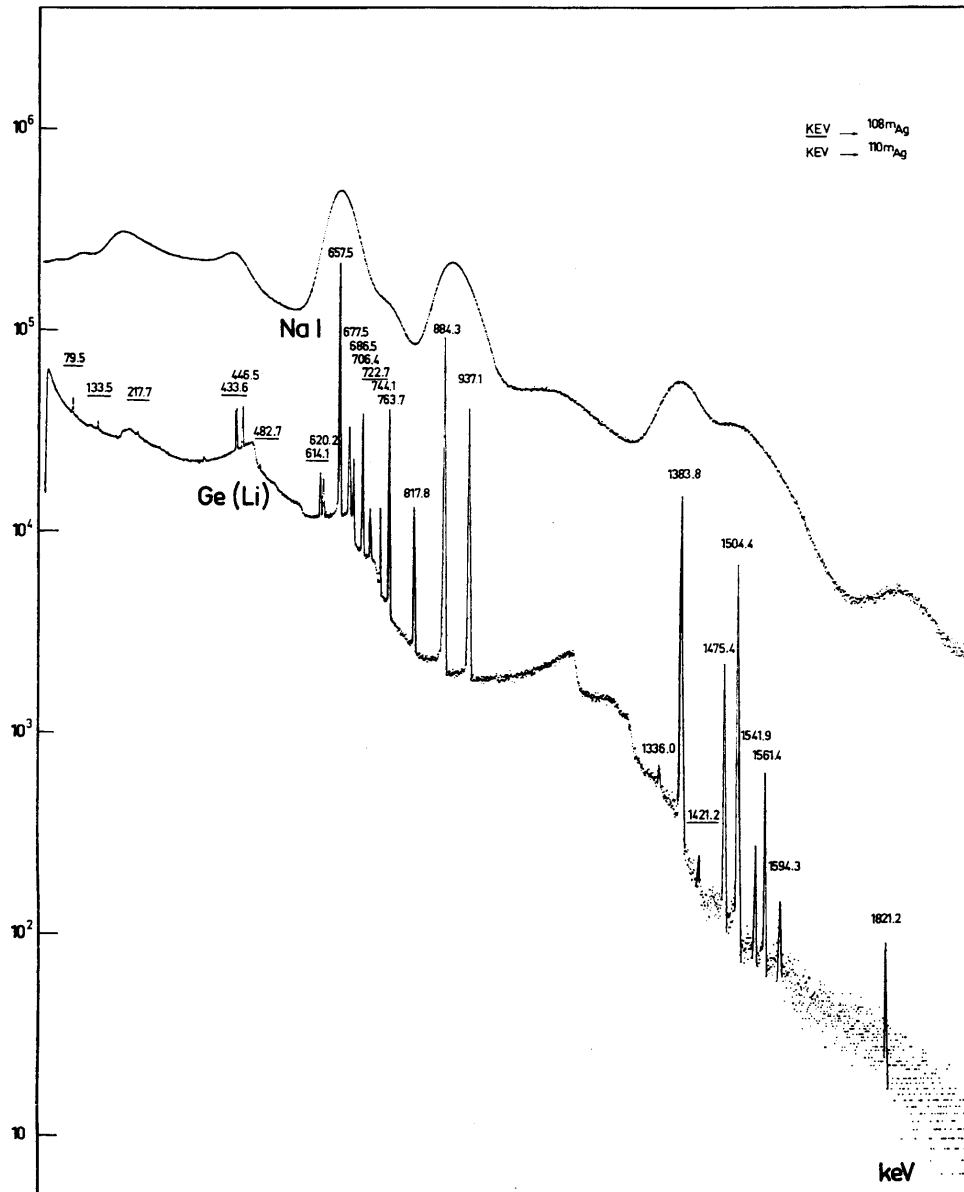
Negligible cross-coupling at times $t > (2 \dots 3) \times R_i C_D$ and if $C_i \gg C_D$.

2. Resolution and Signal-to-Noise Ratio

Why?

a) Recognize structure in spectra

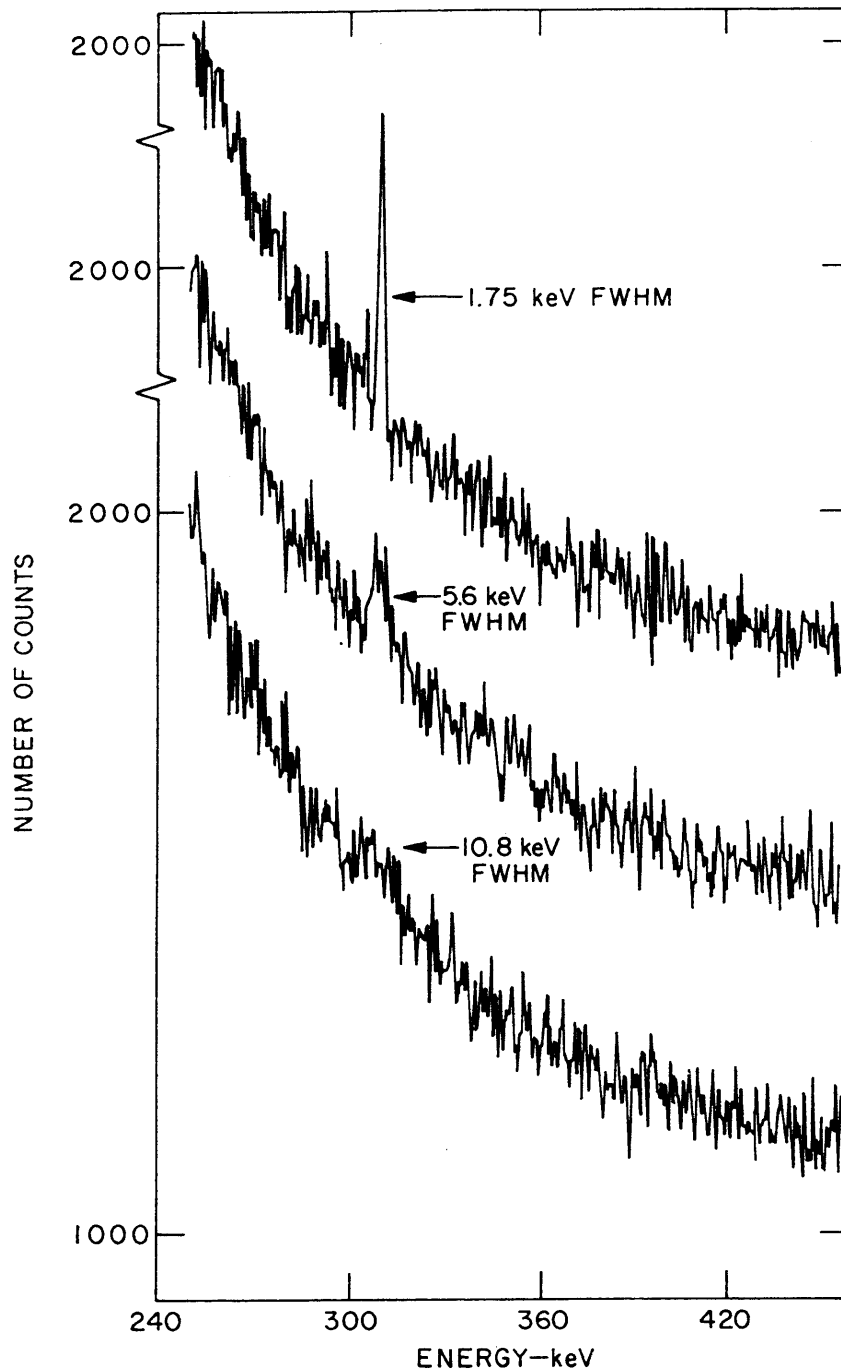
Comparison between NaI(Tl) and Ge detectors



(J.Cl. Philippot, IEEE Trans. Nucl. Sci. NS-17/3 (1970) 446)

b) Improve sensitivity

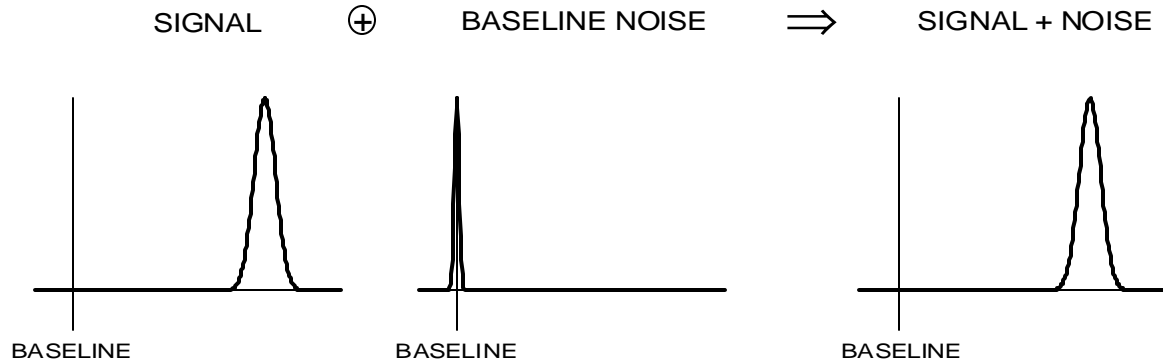
Signal to background ratio improves with better resolution
(signal counts in fewer bins compete with fewer background counts)



G.A. Armantrout *et al.*, IEEE Trans. Nucl. Sci. NS-19/1 (1972) 107

What determines Resolution?

1. Signal Variance >> Baseline Variance



⇒ Electronic (baseline) noise not important

Examples:

- High-gain proportional chambers
- Scintillation Counters with High-Gain PMTs

e.g. 1 MeV γ -rays absorbed by NaI(Tl) crystal

Number of photoelectrons

$$N_{pe} \approx 8 \cdot 10^4 [\text{MeV}^{-1}] \times E_\gamma \times QE \approx 2.4 \cdot 10^4$$

Variance typically

$$\sigma_{pe} = N_{pe}^{1/2} \approx 160 \text{ and } \sigma_{pe} / N_{pe} \approx 5 - 8\%$$

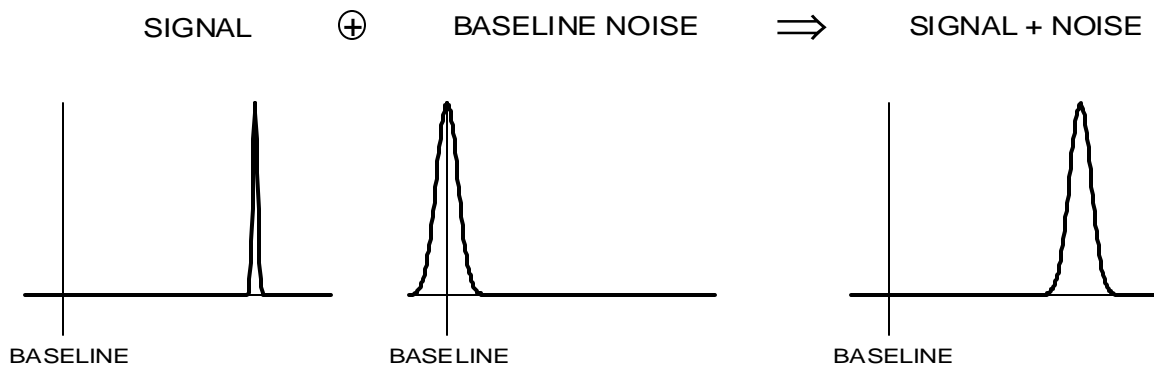
Signal at PMT anode (assume Gain= 10^4)

$$Q_{sig} = G_{PMT} N_{pe} \approx 2.4 \cdot 10^8 \text{ el and}$$

$$\sigma_{sig} = G_{PMT} \sigma_{pe} \approx 1.2 \cdot 10^7 \text{ el}$$

whereas electronic noise easily $< 10^4$ el

2. Signal Variance \ll Baseline Variance



\Rightarrow Electronic (baseline) noise critical for resolution

Examples

- Gaseous ionization chambers (no internal gain)
- Semiconductor detectors

e.g. in Si

Number of electron-hole pairs

$$N_{ep} = E_{dep} / (3.6 \text{ eV})$$

Variance

$$\sigma_{ep} = \sqrt{F \cdot N_{ep}}$$

(where F = Fano factor ≈ 0.1)

For 50 keV photons

$$\sigma_{ep} \approx 40 \text{ el} \Rightarrow \sigma_{ep} / N_{ep} = 7.5 \cdot 10^{-4}$$

obtainable noise levels are 10 to 1000 el.

Baseline fluctuations can have many origins ...

pickup of external interference

artifacts due to imperfect electronics

... etc.,

but the (practical) fundamental limit is electronic noise.

Basic Noise Mechanisms

Consider n carriers of charge e moving with a velocity v through a sample of length l . The induced current i at the ends of the sample is

$$i = \frac{n e v}{l} .$$

The fluctuation of this current is given by the total differential

$$\langle di \rangle^2 = \left(\frac{ne}{l} \langle dv \rangle \right)^2 + \left(\frac{ev}{l} \langle dn \rangle \right)^2$$

where the two terms are added in quadrature since they are statistically uncorrelated.

Two mechanisms contribute to the total noise:

- velocity fluctuations, e.g. thermal noise
- number fluctuations, e.g. shot noise
excess or '1/f' noise

Thermal noise and shot noise are both “white” noise sources, i.e.

power per unit bandwidth is constant:

≡ spectral density)

$$\frac{dP_{noise}}{df} = const.$$

or

$$\frac{dV_{noise}^2}{df} = const. \equiv e_n^2$$

whereas for “1/f” noise

$$\frac{dP_{noise}}{df} = \frac{1}{f^\alpha}$$

(typically $\alpha = 0.5 - 2$)

1. Thermal Noise in Resistors

The most common example of noise due to velocity fluctuations is the thermal noise of resistors.

Spectral noise power density vs. frequency f

$$\frac{dP_{noise}}{df} = 4kT$$

k = Boltzmann constant
 T = absolute temperature

Since

$$P = \frac{V^2}{R} = I^2 R$$

R = DC resistance

the spectral noise voltage density

$$\frac{dV_{noise}^2}{df} \equiv e_n^2 = 4kTR$$

and the spectral noise current density

$$\frac{dI_{noise}^2}{df} \equiv i_n^2 = \frac{4kT}{R}$$

The total noise depends on the bandwidth of the system. For example, the total noise voltage at the output of a voltage amplifier with the frequency dependent gain $A_v(f)$ is

$$v_{on}^2 = \int_0^{\infty} e_n^2 A_v^2(f) df$$

Note: Since spectral noise components are non-correlated, one must integrate over the noise power.

2. Shot noise

A common example of noise due to number fluctuations is “shot noise”, which occurs whenever carriers are injected into a sample volume independently of one another.

Example: current flow in a semiconductor diode
(emission over a barrier)

Spectral noise current density:

$$i_n^2 = 2q_e I$$

q_e = electronic charge

I = DC current

A more intuitive interpretation of this expression will be given later.

Note: Shot noise does not occur in “ohmic” conductors. Since the number of available charges is not limited, the fields caused by local fluctuations in the charge density draw in additional carriers to equalize the total number.

Spectral Density of Thermal Noise

Two approaches can be used to derive the spectral distribution of thermal noise.

1. The thermal velocity distribution of the charge carriers is used to calculate the time dependence of the induced current, which is then transformed into the frequency domain.
2. Application of Planck's theory of black body radiation.

The first approach clearly shows the underlying physics, whereas the second "hides" the physics by applying a general result of statistical mechanics. However, the first requires some advanced concepts that go well beyond the standard curriculum, so the "black body" approach will be used.

In Planck's theory of black body radiation the energy per mode

$$\bar{E} = \frac{h\nu}{e^{h\nu/kT} - 1}$$

and the spectral density of the radiated power

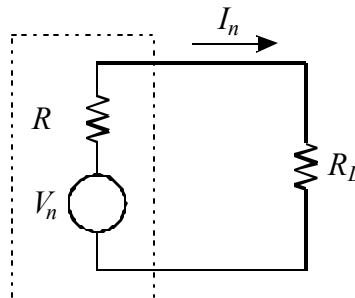
$$\frac{dP}{d\nu} = \frac{h\nu}{e^{h\nu/kT} - 1}$$

i.e. this is the power that can be extracted in equilibrium. At low frequencies $h\nu \ll kT$

$$\frac{dP}{d\nu} \approx \frac{h\nu}{\left(1 + \frac{h\nu}{kT}\right) - 1} = kT,$$

so at low frequencies the spectral density is independent of frequency and for a total bandwidth B the noise power that can be transferred to an external device $P_n = kTB$.

To apply this result to the noise of a resistor, consider a resistor R whose thermal noise gives rise to a noise voltage V_n . To determine the power transferred to an external device consider the circuit



The power dissipated in the load resistor R_L

$$\frac{V_{nL}^2}{R_L} = I_n^2 R_L = \frac{V_n^2 R_L}{(R + R_L)^2}$$

The maximum power transfer occurs when the load resistance equals the source resistance $R_T = R$, so

$$V_{nL}^2 = \frac{V_n^2}{4}$$

Since the power transferred to R_L is kTB

$$\frac{V_{nL}^2}{R} = \frac{V_n^2}{4R} = kTB$$

$$P_n = \frac{V_n^2}{R} = 4kTB$$

and the spectral density of the noise power

$$\frac{dP_n}{d\nu} = 4kT$$

Spectral Density of Shot Noise

If an excess electron is injected into a device, it forms a current pulse of duration τ . In a thermionic diode τ is the transit time from cathode to anode (see IX.2), for example. In a semiconductor diode τ is the recombination time (see IX-2). If these times are short with respect to the periods of interest $\tau \ll 1/f$, the current pulse can be represented by a δ pulse. The Fourier transform of a delta pulse yields a “white” spectrum, i.e. the amplitude distribution in frequency is uniform

$$\frac{dI_{n,pk}}{df} = 2q_e$$

Within an infinitesimally narrow frequency band the individual spectral components are pure sinusoids, so their rms value

$$i_n \equiv \frac{dI_n}{df} = \frac{2q_e}{\sqrt{2}} = \sqrt{2}q_e$$

If N electrons are emitted at the same average rate, but at different times, they will have the same spectral distribution, but the coefficients will differ in phase. For example, for two currents i_p and i_q with a relative phase ϕ the total rms current

$$\langle i^2 \rangle = (i_p + i_q e^{i\phi})(i_p + i_q e^{-i\phi}) = i_p^2 + i_q^2 + 2i_p i_q \cos\phi$$

For a random phase the third term averages to zero

$$\langle i^2 \rangle = i_p^2 + i_q^2 ,$$

so if N electrons are randomly emitted per unit time, the individual spectral components simply add in quadrature

$$i_n^2 = 2Nq_e^2$$

The average current

$$I = Nq_e ,$$

so the spectral noise density

$$i_n^2 \equiv \frac{dI_n^2}{df} = 2q_e I$$

Noise Bandwidth vs. Signal Bandwidth

Consider an amplifier with the frequency response $A(f)$. This can be rewritten

$$A(f) \equiv A_0 G(f)$$

where A_0 is the maximum gain and $G(f)$ describes the frequency response.

For example, in the simple amplifier described above

$$A_V = g_m \left(\frac{1}{R_L} + i\omega C_o \right)^{-1} = g_m R_L \frac{1}{1 + i\omega R_L C_o}$$

and using the above convention

$$A_0 \equiv g_m R_L \quad \text{and} \quad G(f) \equiv \frac{1}{1 + i(2\pi f R_L C_o)}$$

If a “white” noise source with spectral density v_{ni} is present at the input, the total noise voltage at the output is

$$V_{no} = \sqrt{\int_0^{\infty} v_{ni}^2 |A_0 G(f)|^2 df} = v_{ni} A_0 \sqrt{\int_0^{\infty} G^2(f) df} \equiv v_{ni} A_0 \sqrt{\Delta f_n}$$

Δf_n is the “noise bandwidth”.

Note that, in general, the noise bandwidth and the signal bandwidth are not the same. If the upper cutoff frequency is determined by a single RC time constant, as in the “simple amplifier”, the signal bandwidth

$$\Delta f_s = f_u = \frac{1}{2\pi RC}$$

and the noise bandwidth

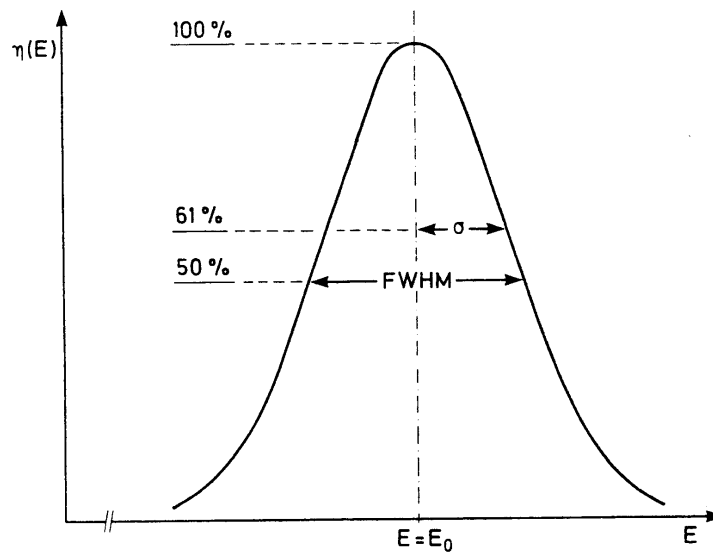
$$\Delta f_n = \frac{1}{4RC} = \frac{\pi}{2} f_u$$

Individual noise contributions add in quadrature
(additive in noise power)

$$V_{n,tot} = \sqrt{\sum_i V_{ni}^2}$$

Both thermal and shot noise are purely random.

⇒ amplitude distribution is gaussian

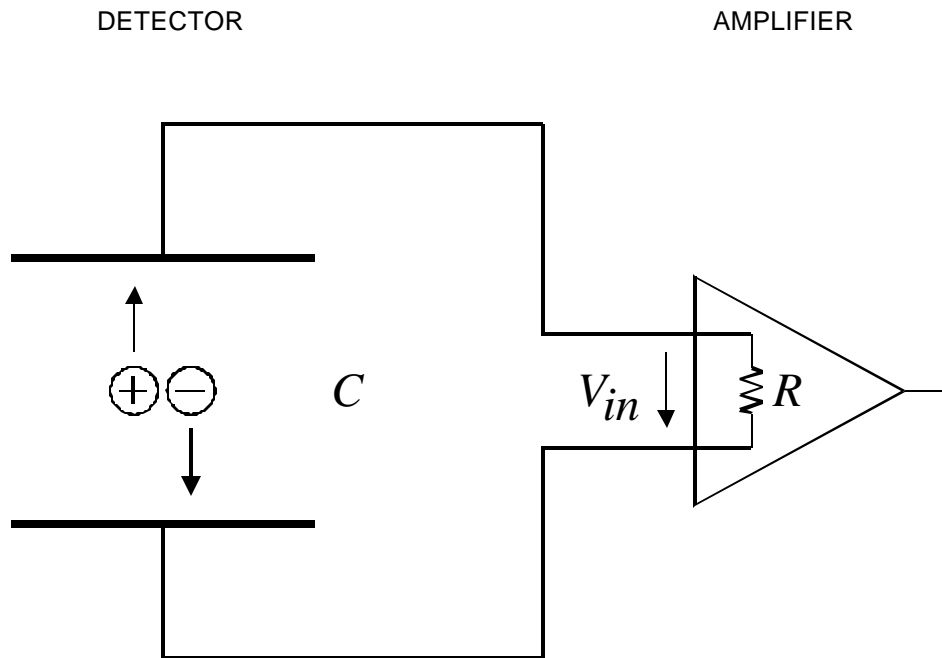


⇒ noise modulates baseline

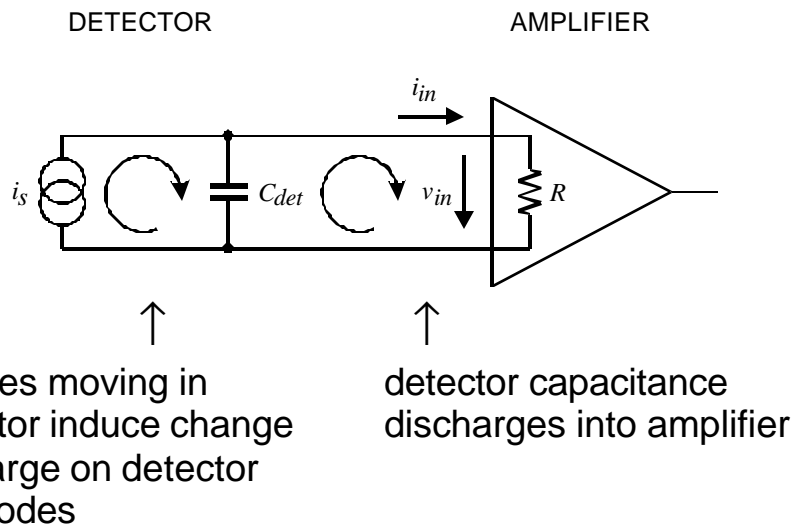
⇒ baseline fluctuations superimposed on signal

⇒ output signal has gaussian distribution

Signal-to-Noise Ratio vs. Detector Capacitance



Equivalent Circuit

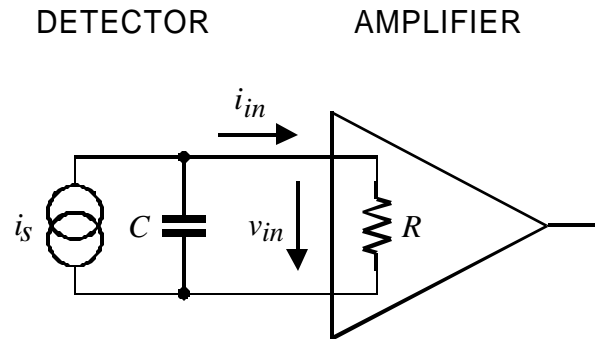


Assume an amplifier with constant noise. Then signal-to-noise ratio (and the equivalent noise charge) depend on the signal magnitude.

Pulse shape registered by amplifier depends on the input time constant RC_{det} .

Assume a rectangular detector current pulse of duration T and magnitude I_s .

Equivalent circuit



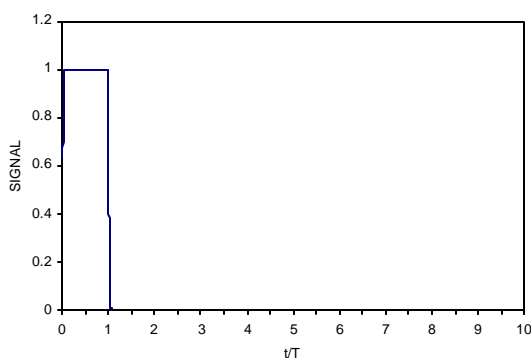
Input current to amplifier

$$0 \leq t < T : \quad i_{in}(t) = I_s \left(1 - e^{-t/RC} \right)$$

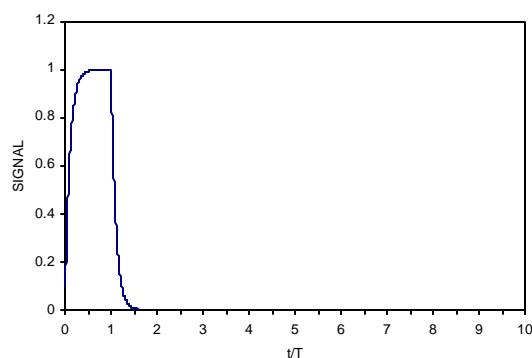
$$T \leq t \leq \infty : \quad i_{in}(t) = I_s \left(e^{T/RC} - 1 \right) \cdot e^{-t/RC}$$

At short time constants $RC \ll T$ the amplifier pulse approximately follows the detector current pulse.

$RC = 0.01 T$

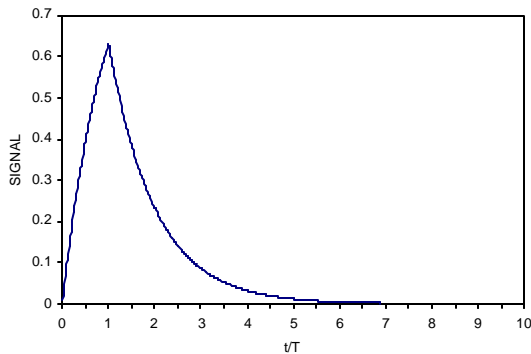


$RC = 0.1 T$

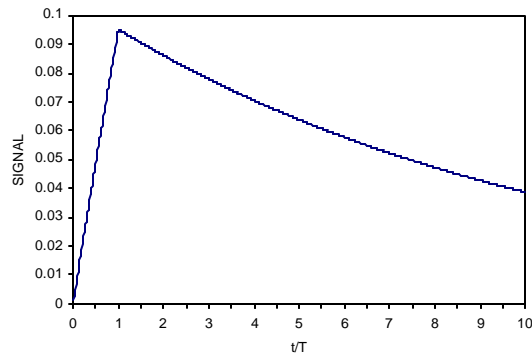


As the input time constant RC increases, the amplifier signal becomes longer and the peak amplitude decreases, although the integral, i.e. the signal charge, remains the same.

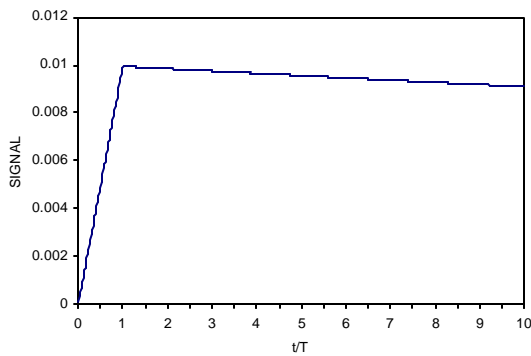
$RC = T$



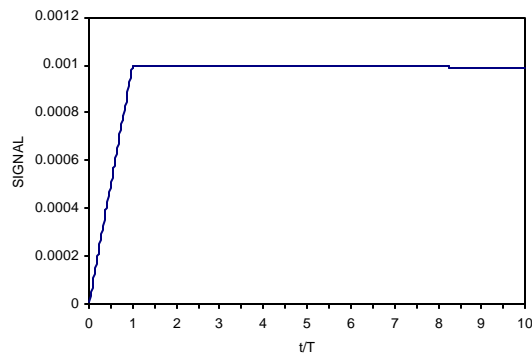
$RC = 10 T$



$RC = 100 T$



$RC = 10^3 T$

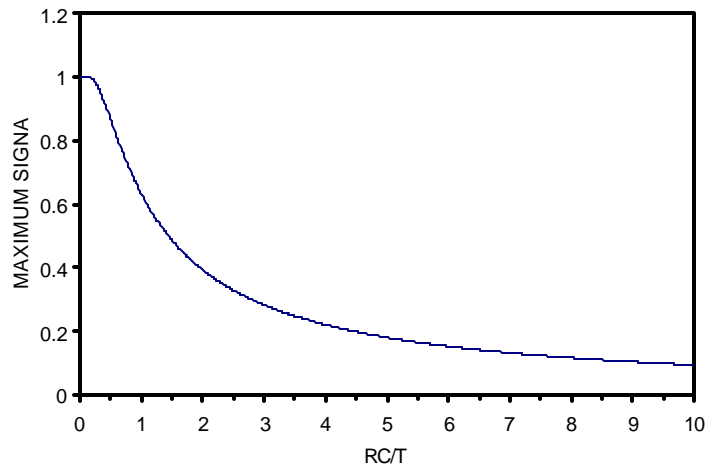


At long time constants the detector signal current is integrated on the detector capacitance and the resulting voltage sensed by the amplifier

$$V_{in} = \frac{Q_{det}}{C} = \frac{\int i_s dt}{C}$$

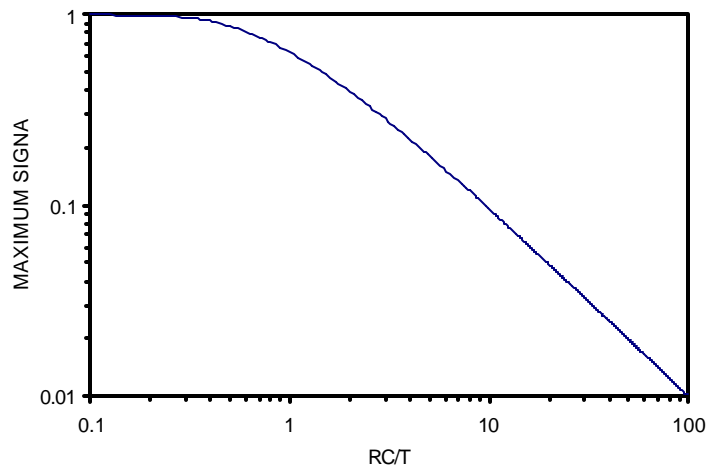
Then the peak amplifier signal is inversely proportional to the **total capacitance at the input**, i.e. the sum of detector capacitance, input capacitance of the amplifier, and stray capacitances.

Maximum signal vs. capacitance



At small time constants the amplifier signal approximates the detector current pulse and is independent of capacitance.

At large input time constants ($RC/T > 5$) the maximum signal falls linearly with capacitance.



⇒ For input time constants large compared to the detector pulse duration the signal-to-noise ratio decreases with detector capacitance.

Caution when extrapolating to smaller capacitances:

If $S/N = 1$ at $RC/T = 100$, decreasing the capacitance to 1/10 of its original value ($RC/T = 10$), increases S/N to 10.

However, if initially $RC/T = 1$, the same 10-fold reduction in capacitance (to $RC/T = 0.1$) only yields $S/N = 1.6$.

Charge-Sensitive Preamplifier Noise vs. Detector Capacitance

In a voltage-sensitive preamplifier

- noise voltage at the output is essentially independent of detector capacitance,
i.e. the *equivalent input noise voltage* $v_{ni} = v_{no} / A_v$.
- input signal decreases with increasing input capacitance, so signal-to-noise ratio depends on detector capacitance.

In a charge-sensitive preamplifier, the signal at the amplifier output is independent of detector capacitance (if $C_i \gg C_{det}$).

What is the noise behavior?

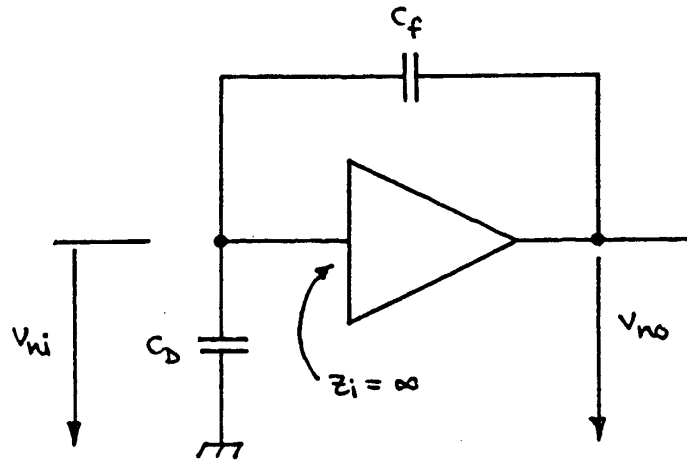
- Noise appearing at the output of the preamplifier is fed back to the input, decreasing the output noise from the open-loop value $v_{no} = v_{ni} A_{v0}$.
- The magnitude of the feedback depends on the shunt impedance at the input, i.e. the detector capacitance.

Note, that although specified as an equivalent input noise, the dominant noise sources are typically internal to the amplifier. Only in a fed-back configuration is some of this noise actually present at the input. In other words, the primary noise signal is not a physical charge (or voltage) at the amplifier input, to which the loop responds in the same manner as to a detector signal.

⇒ **S/N at the amplifier output depends on feedback.**

Noise in charge-sensitive preamplifiers

Start with an output noise voltage v_{no} , which is fed back to the input through the capacitive voltage divider $C_f - C_d$.



$$v_{no} = v_{ni} \frac{X_{C_f} + X_{C_D}}{X_{C_D}} = v_{ni} \frac{\frac{1}{\omega C_f} + \frac{1}{\omega C_D}}{\frac{1}{\omega C_D}}$$

$$v_{no} = v_{ni} \left(1 + \frac{C_D}{C_f} \right)$$

Equivalent input noise charge

$$Q_{ni} = \frac{v_{no}}{A_Q} = v_{no} C_f$$

$$Q_{ni} = v_{ni} (C_D + C_f)$$

Signal-to-noise ratio

$$\frac{Q_s}{Q_{ni}} = \frac{Q_s}{v_{ni}(C_D + C_f)} = \frac{1}{C} \frac{Q_s}{v_{ni}}$$

Same result as for voltage-sensitive amplifier, but here

- *the signal is constant and*
- *the noise grows with increasing C .*

As shown previously, the pulse rise time at the amplifier output also increases with total capacitive input load C , because of reduced feedback.

In contrast, the rise time of a voltage sensitive amplifier is not affected by the input capacitance, although the equivalent noise charge increases with C just as for the charge-sensitive amplifier.

Conclusion

In general

- optimum S/N is independent of whether the voltage, current, or charge signal is sensed.
- S/N cannot be *improved* by feedback.

Practical considerations, i.e. type of detector, amplifier technology, can favor one configuration over the other.

Pulse Shaping

Two conflicting objectives:

1. Improve Signal-to-Noise Ratio S/N

Restrict bandwidth to match measurement time

⇒ Increase pulse width

Typically, the pulse shaper transforms a narrow detector current pulse to

a broader pulse
(to reduce electronic noise),

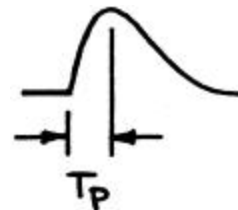
with a gradually rounded maximum at the peaking time T_P
(to facilitate measurement of the amplitude)

Detector Pulse



⇒

Shaper Output

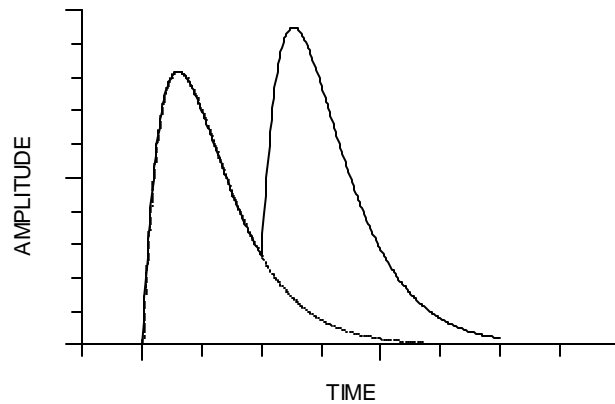


If the shape of the pulse does not change with signal level, the peak amplitude is also a measure of the energy, so one often speaks of pulse-height measurements or pulse height analysis. The pulse height spectrum is the energy spectrum.

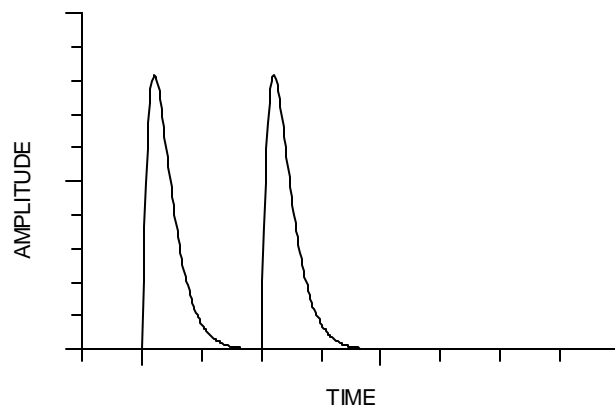
2. Improve Pulse Pair Resolution

⇒ Decrease pulse width

Pulse pile-up
distorts amplitude
measurement



Reducing pulse
shaping time to
1/3 eliminates
pile-up.

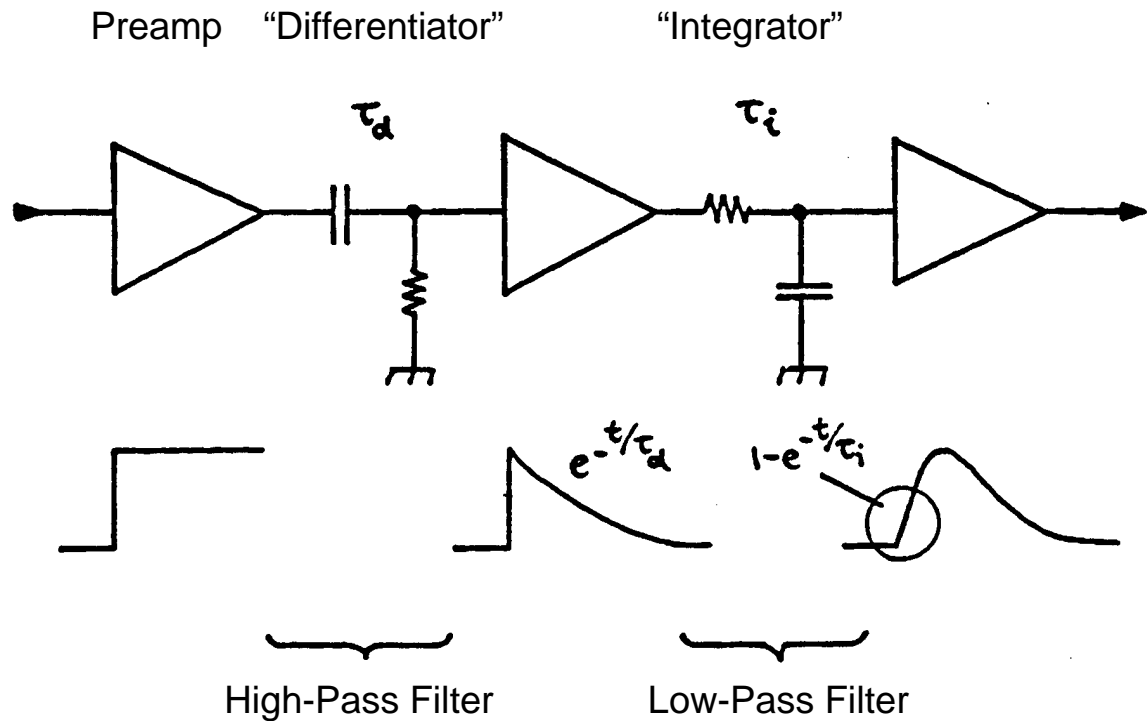


Necessary to find balance between these conflicting requirements. Sometimes minimum noise is crucial, sometimes rate capability is paramount.

Usually, many considerations combined lead to a “non-textbook” compromise.

- “*Optimum shaping*” depends on the application!
- Shapers need not be complicated –
Every amplifier is a pulse shaper!

Simple Example: CR-RC Shaping



Simple arrangement: Noise performance only 36% worse than optimum filter with same time constants.

⇒ Useful for estimates, since simple to evaluate

Key elements

- lower frequency bound
- upper frequency bound
- signal attenuation

important in all shapers.

Pulse Shaping and Signal-to-Noise Ratio

Pulse shaping affects both the

- total noise
- and
- peak signal amplitude

at the output of the shaper.

Equivalent Noise Charge

Inject known signal charge into preamp input
(either via test input or known energy in detector).

Determine signal-to-noise ratio at shaper output.

Equivalent Noise Charge \equiv Input charge for which $S/N = 1$

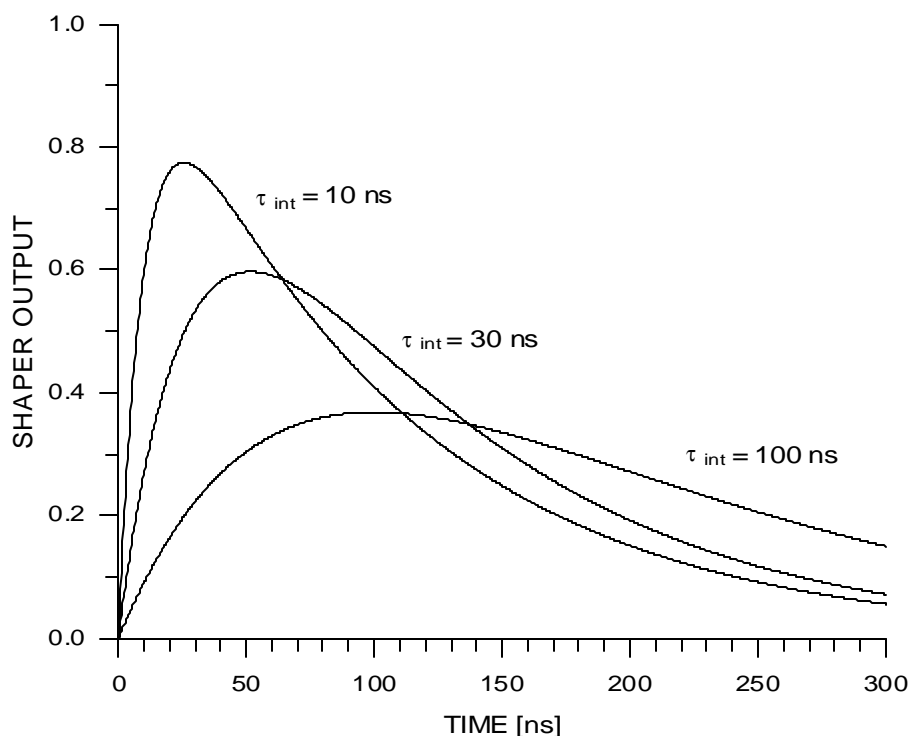
Effect of relative time constants

Consider a *CR-RC* shaper with a fixed differentiator time constant of 100 ns.

Increasing the integrator time constant lowers the upper cut-off frequency, which decreases the total noise at the shaper output.

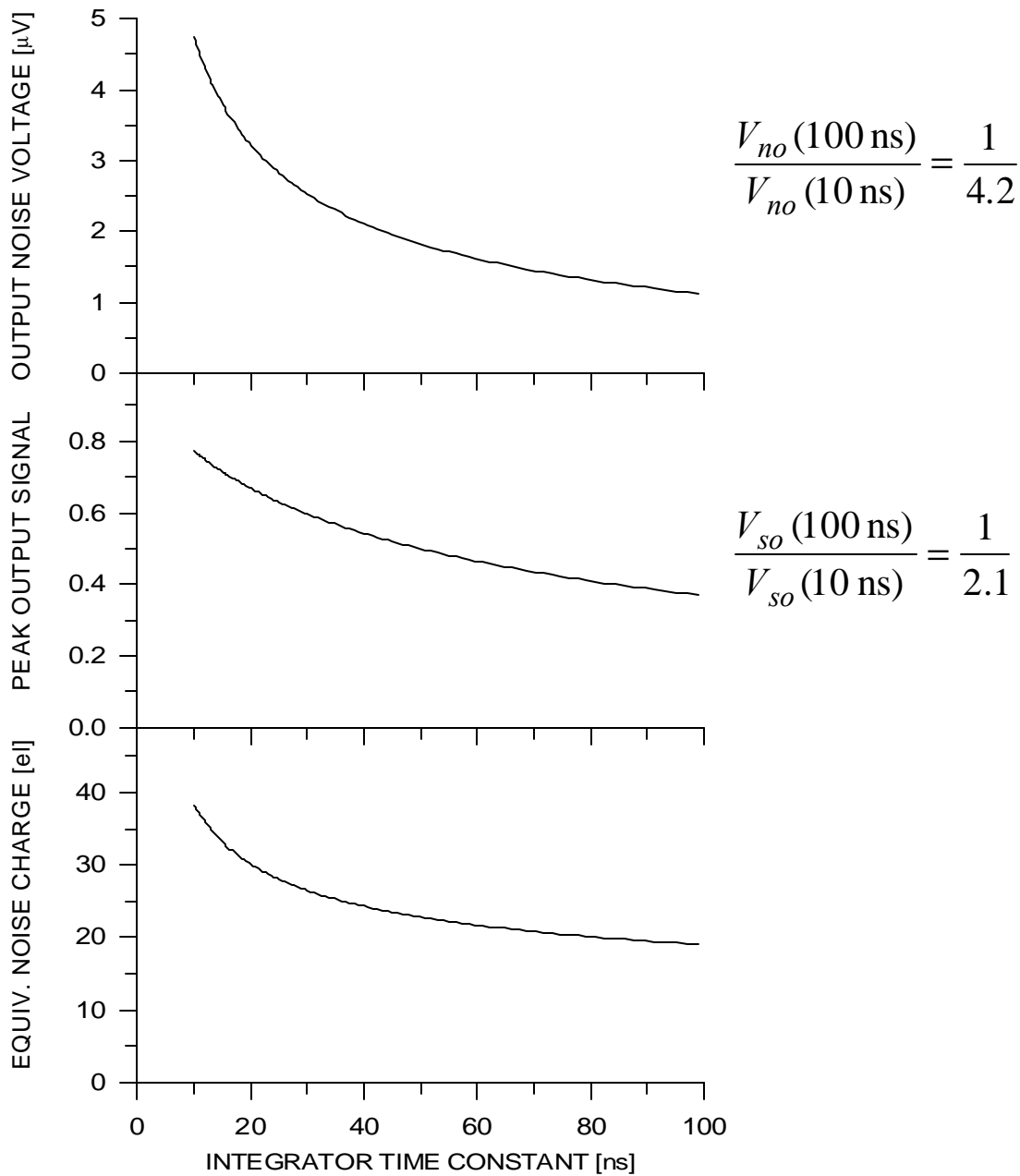
However, the peak signal also decreases.

CR-RC SHAPER
FIXED DIFFERENTIATOR TIME CONSTANT = 100 ns
INTEGRATOR TIME CONSTANT = 10, 30 and 100 ns



Still keeping the differentiator time constant fixed at 100 ns, the next set of graphs shows the variation of output noise and peak signal as the integrator time constant is increased from 10 to 100 ns.

OUTPUT NOISE, OUTPUT SIGNAL AND EQUIVALENT NOISE CHARGE
 CR-RC SHAPER - FIXED DIFFERENTIATOR TIME CONSTANT = 100 ns
 ($e_n = 1 \text{ nV}/\sqrt{\text{Hz}}$, $i_n = 0$, $C_{\text{TOT}} = 1 \text{ pF}$)



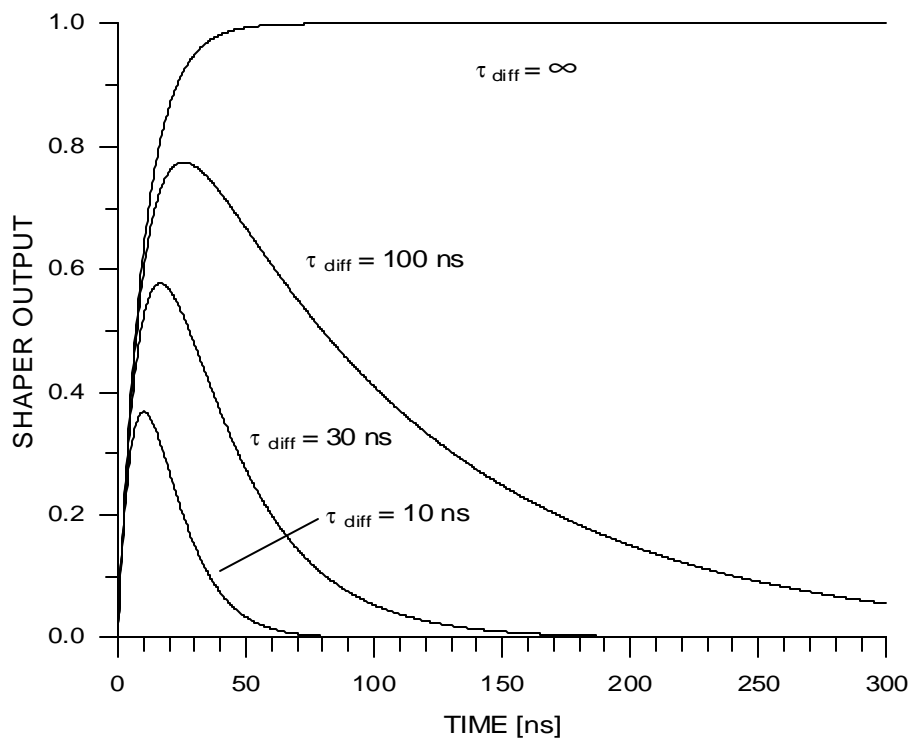
The roughly 4-fold decrease in noise is partially compensated by the 2-fold reduction in signal, so that

$$\frac{Q_n(100 \text{ ns})}{Q_n(10 \text{ ns})} = \frac{1}{2}$$

For comparison, consider the same $CR-RC$ shaper with the integrator time constant fixed at 10 ns and the differentiator time constant variable.

As the differentiator time constant is reduced, the peak signal amplitude at the shaper output decreases.

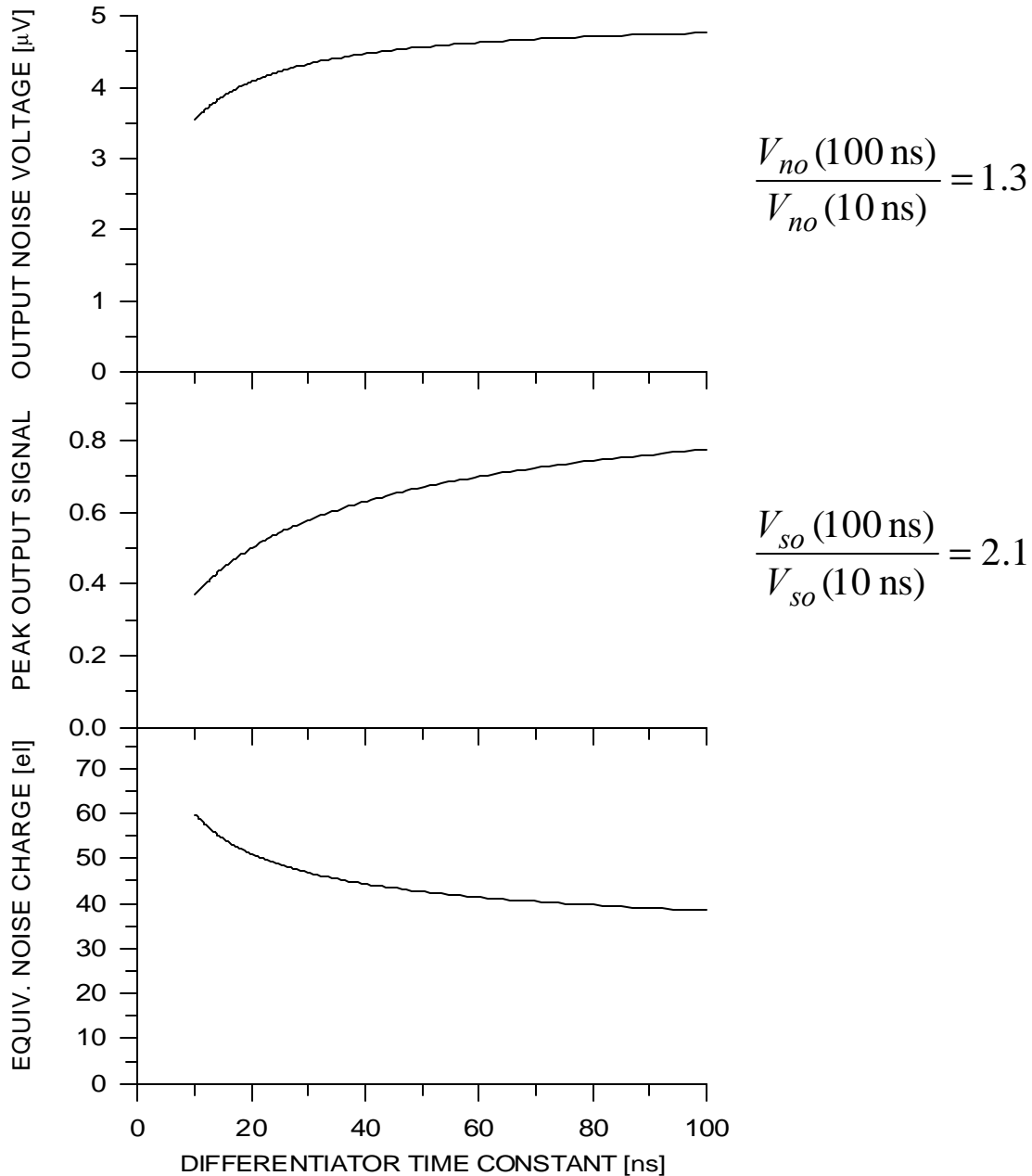
CR-RC SHAPER
FIXED INTEGRATOR TIME CONSTANT = 10 ns
DIFFERENTIATOR TIME CONSTANT = ∞ , 100, 30 and 10 ns



Note that the need to limit the pulse width incurs a significant reduction in the output signal.

Even at a differentiator time constant $\tau_{diff} = 100$ ns = $10 \tau_{int}$ the output signal is only 80% of the value for $\tau_{diff} = \infty$, i.e. a system with no low-frequency roll-off.

OUTPUT NOISE, OUTPUT SIGNAL AND EQUIVALENT NOISE CHARGE
 CR-RC SHAPER - FIXED INTEGRATOR TIME CONSTANT = 10 ns
 ($e_n = 1 \text{ nV}/\sqrt{\text{Hz}}$, $i_n = 0$, $C_{\text{TOT}} = 1 \text{ pF}$)



Although the noise grows as the differentiator time constant is increased from 10 to 100 ns, it is outweighed by the increase in signal level, so that the net signal-to-noise ratio improves.

$$\frac{Q_n(100 \text{ ns})}{Q_n(10 \text{ ns})} = 1.6$$

Summary

To evaluate shaper noise performance

- Noise spectrum alone is inadequate

Must also

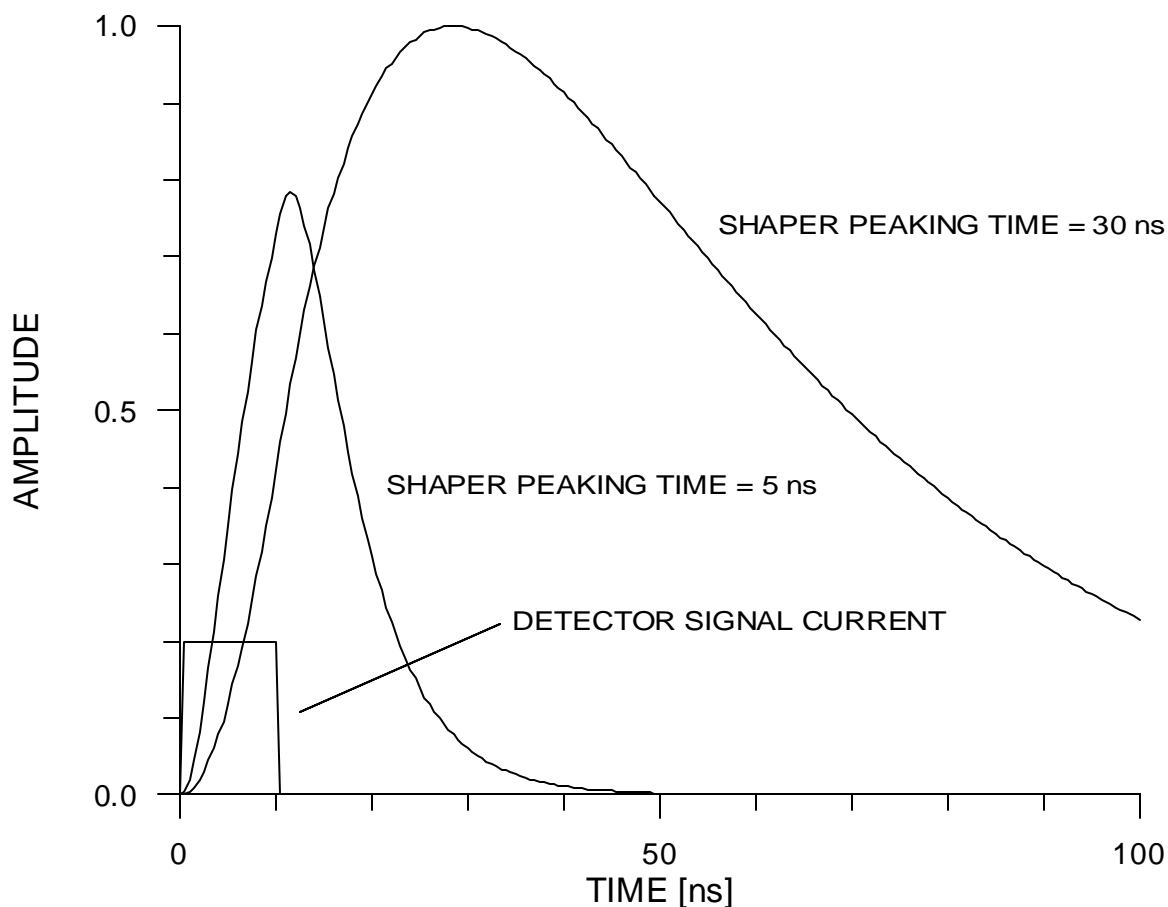
- Assess effect on signal

Signal amplitude is also affected by the relationship of the shaping time to the detector signal duration.

If peaking time of shaper $<$ collection time

\Rightarrow signal loss (“ballistic deficit”)

Loss in Pulse Height (and Signal-to-Noise Ratio) if Peaking Time of Shaper < Detector Collection Time



Note that although the faster shaper has a peaking time of 5 ns, the response to the detector signal peaks after full charge collection.

Evaluation of Equivalent Noise Charge

A. Experiment

Inject an input signal with known charge using a pulse generator set to approximate the detector signal (possible ballistic deficit). Measure the pulse height spectrum.

peak centroid \Rightarrow signal magnitude

peak width \Rightarrow noise (FWHM= 2.35 rms)

If pulse-height digitization is not practical:

1. Measure total noise at output of pulse shaper
 - a) measure the total noise power with an rms voltmeter of sufficient bandwidth
 - or
 - b) measure the spectral distribution with a spectrum analyzer and integrate (the spectrum analyzer provides discrete measurement values in N frequency bins Δf_n)

$$V_{no} = \sqrt{\sum_{n=0}^N (v_{no}^2(n) \cdot \Delta f)}$$

The spectrum analyzer shows if “pathological” features are present in the noise spectrum.

2. Measure the magnitude of the output signal V_{so} for a known input signal, either from detector or from a pulse generator set up to approximate the detector signal.
3. Determine signal-to-noise ratio $S/N = V_{so} / V_{no}$ and scale to obtain the equivalent noise charge

$$Q_n = \frac{V_{no}}{V_{so}} Q_s$$

B. Numerical Simulation (e.g. SPICE)

This can be done with the full circuit including all extraneous components. Procedure analogous to measurement.

1. Calculate the spectral distribution and integrate

$$V_{no} = \sqrt{\sum_{n=0}^N v_{no}^2(n) \cdot \Delta f}$$

2. Determine the magnitude of output signal V_{so} for an input that approximates the detector signal.
3. Calculate the equivalent noise charge

$$Q_n = \frac{V_{no}}{V_{so}} Q_s$$

C. Analytical Simulation

1. Identify individual noise sources and refer to input
2. Determine the spectral distribution at input for each source k

$$v_{ni,k}^2(f)$$

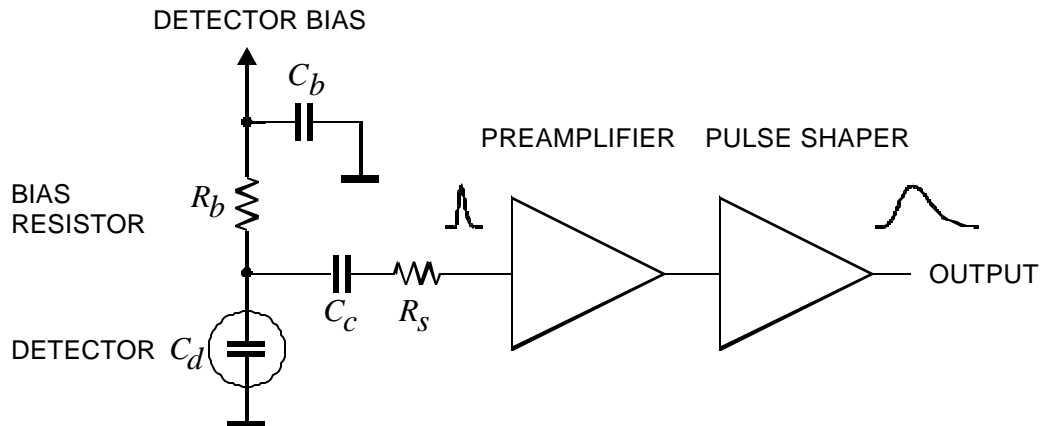
3. Calculate the total noise at shaper output ($G(f)$ = gain)

$$V_{no} = \sqrt{\int_0^{\infty} G^2(f) \left(\sum_k v_{ni,k}^2(f) \right) df} \equiv \sqrt{\int_0^{\infty} G^2(\omega) \left(\sum_k v_{ni,k}^2(\omega) \right) d\omega}$$

4. Determine the signal output V_{so} for a known input charge Q_s and realistic detector pulse shape.
5. Equivalent noise charge

$$Q_n = \frac{V_{no}}{V_{so}} Q_s$$

Analytical Analysis of a Detector Front-End



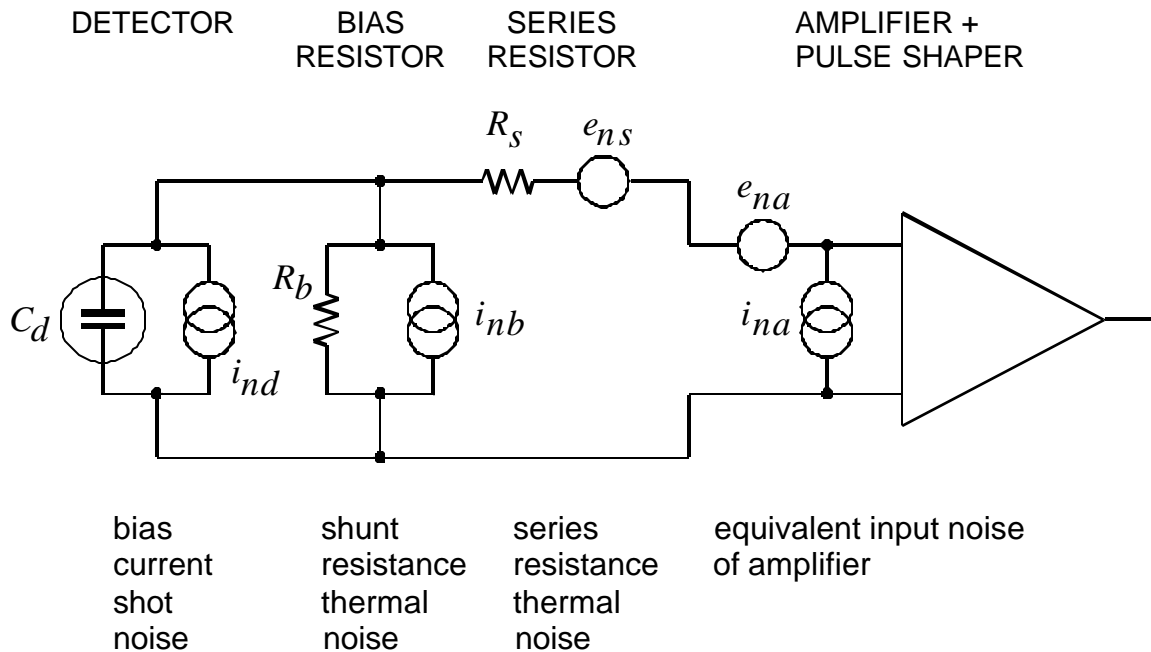
Detector bias voltage is applied through the resistor R_B . The bypass capacitor C_B serves to shunt any external interference coming through the bias supply line to ground. For AC signals this capacitor connects the “far end” of the bias resistor to ground, so that R_B appears to be in parallel with the detector.

The coupling capacitor C_C in the amplifier input path blocks the detector bias voltage from the amplifier input (which is why a capacitor serving this role is also called a “blocking capacitor”).

The series resistor R_S represents any resistance present in the connection from the detector to the amplifier input. This includes

- the resistance of the detector electrodes
- the resistance of the connecting wires
- any resistors used to protect the amplifier against large voltage transients (“input protection”)
- ... etc.

Equivalent circuit for noise analysis



In this example a voltage-sensitive amplifier is used, so all noise contributions will be calculated in terms of the noise voltage appearing at the amplifier input.

Resistors can be modeled either as voltage or current generators.

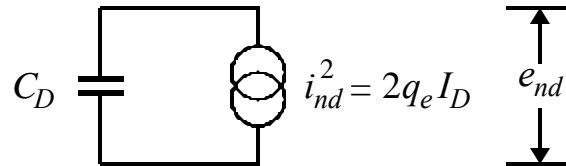
- Resistors in parallel with the input act as current sources
- Resistors in series with the input act as voltage sources.

Steps in the analysis:

1. Determine the frequency distribution of the noise voltage presented to the amplifier input from all individual noise sources
2. Integrate over the frequency response of a CR-RC shaper to determine the total noise output.
3. Determine the output signal for a known signal charge and calculate equivalent noise charge (signal charge for $S/N= 1$)

Noise Contributions

1. Detector bias current



This model results from two assumptions:

1. The input impedance of the amplifier is infinite
2. The shunt resistance R_P is much larger than the capacitive reactance of the detector in the frequency range of the pulse shaper.

Does this assumption make sense?

If R_P is too small, the signal charge on the detector capacitance will discharge before the shaper output peaks. To avoid this

$$R_P C_D \gg t_P \approx \frac{1}{\omega_P}$$

where ω_P is the midband frequency of the shaper.

Therefore,

$$R_P \gg \frac{1}{\omega_P C_D}$$

as postulated.

Under these conditions the noise current will flow through the detector capacitance, yielding the voltage

$$e_{nd}^2 = i_{nd}^2 \frac{1}{(\omega C_D)^2} = 2q_e I_D \frac{1}{(\omega C_D)^2}$$

⇒ the noise contribution decreases with increasing frequency (shorter shaping time)

Note: Although shot noise is “white”, the resulting noise spectrum is strongly frequency dependent.

In the time domain this result is more intuitive. Since every shaper also acts as an integrator, one can view the total shot noise as the result of “counting electrons”.

Assume an ideal integrator that records all charge uniformly within a time T . The number of electron charges measured is

$$N_e = \frac{I_D T}{q_e}$$

The associated noise is the fluctuation in the number of electron charges recorded

$$\sigma_n = \sqrt{N_e} \propto \sqrt{T}$$

Does this also apply to an AC-coupled system, where no DC current flows, so no electrons are “counted”?

Since shot noise is a fluctuation, the current undergoes both positive and negative excursions. Although the DC component is not passed through an AC coupled system, the excursions are. Since, on the average, each fluctuation requires a positive and a negative zero crossing, the process of “counting electrons” is actually the counting of zero crossings, which in a detailed analysis yields the same result.

2. Parallel Resistance

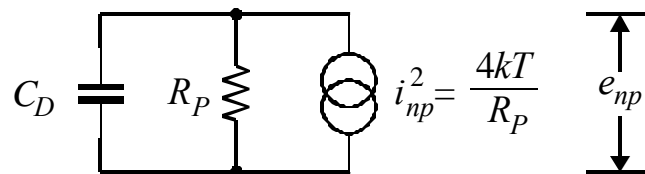
Any shunt resistance R_P acts as a noise current source. In the specific example shown above, the only shunt resistance is the bias resistor R_b .

Additional shunt components in the circuit:

1. bias noise current source
(infinite resistance by definition)
2. detector capacitance

The noise current flows through both the resistance R_P and the detector capacitance C_D .

⇒ equivalent circuit



The noise voltage applied to the amplifier input is

$$e_{np}^2 = \frac{4kT}{R_P} \left(\frac{R_P \cdot -i/\omega C_D}{R_P - i/\omega C_D} \right)^2$$

$$e_{np}^2 = 4kTR_P \frac{1}{1 + (\omega R_P C_D)^2}$$

Comment:

Integrating this result over all frequencies yields

$$\int_0^{\infty} e_{np}^2(\omega) d\omega = \int_0^{\infty} \frac{4kTR_P}{1 + (\omega R_P C_D)^2} d\omega = \frac{kT}{C_D}$$

which is independent of R_P . Commonly referred to as “ kTC ” noise, this contribution is often erroneously interpreted as the “noise of the detector capacitance”.

An ideal capacitor has no thermal noise; all noise originates in the resistor.

So, why is the result independent of R_P ?

R_P determines the primary noise, but also the noise bandwidth of this subcircuit. As R_P increases, its thermal noise increases, but the noise bandwidth decreases, making the total noise independent of R_P .

However,

If one integrates e_{np} over a bandwidth-limited system

$$E_n^2 = \int_0^{\infty} 4kTR_P \left| \frac{G(i\omega)}{1 - i\omega R_P C_D} \right|^2 d\omega$$

the total noise decreases with increasing R_P .

3. Series Resistance

The noise voltage generator associated with the series resistance R_S is in series with the other noise sources, so it simply contributes

$$e_{nr}^2 = 4kTR_S$$

4. Amplifier input noise

The amplifier noise voltage sources usually are not physically present at the amplifier input. Instead the amplifier noise originates within the amplifier, appears at the output, and is referred to the input by dividing the output noise by the amplifier gain, where it appears as a noise voltage generator.

$$e_{na}^2 = e_{nw}^2 + \frac{A_f}{f}$$

\uparrow
 “white
noise”

\uparrow
 $1/f$ noise
 (can also originate in
external components)

This noise voltage generator also adds in series with the other sources.

- Amplifiers generally also exhibit input current noise, which is physically present at the input. Its effect is the same as for the detector bias current, so the analysis given in 1. can be applied.

Determination of equivalent noise charge

1. Calculate total noise voltage at shaper output
2. Determine peak pulse height at shaper output for a known input charge
3. Input signal for which $S/N=1$ yields equivalent noise charge

First, assume a simple CR-RC shaper with equal differentiation and integration time constants $\tau_d = \tau_i = \tau$, which in this special case is equal to the peaking time.

The equivalent noise charge

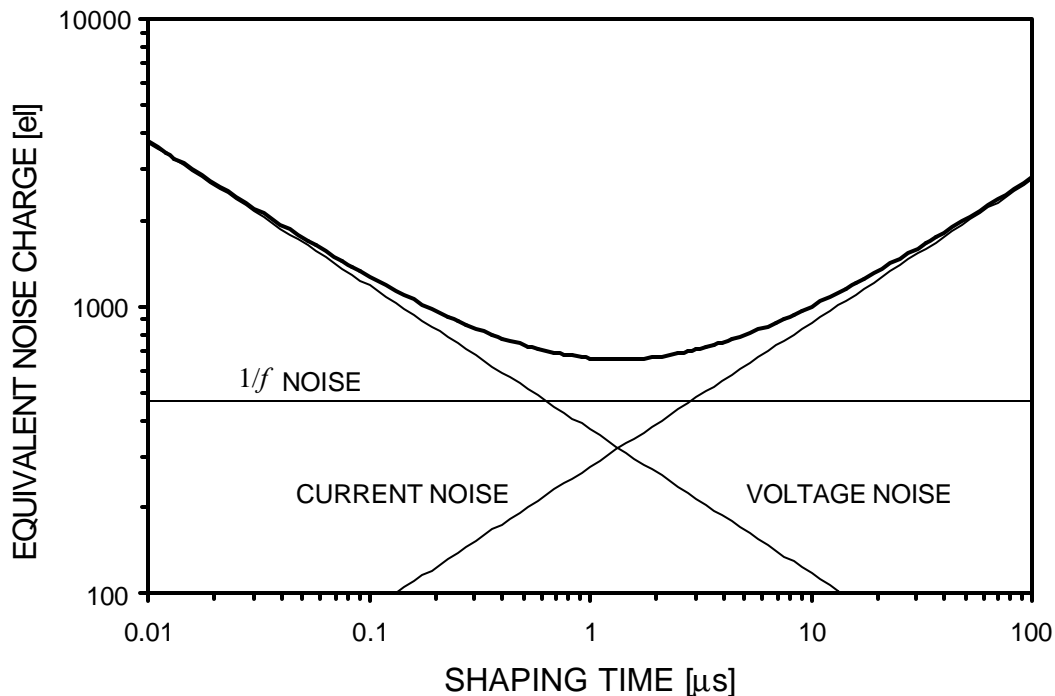
$$Q_n^2 = \left(\frac{e^2}{8} \right) \left[\left(2q_e I_D + \frac{4kT}{R_P} + i_{na}^2 \right) \cdot \tau + \left(4kTR_S + e_{na}^2 \right) \cdot \frac{C_D^2}{\tau} + 4A_f C_D^2 \right]$$

↑	↑	↑
current noise	voltage noise	1/f noise
$\propto \tau$	$\propto 1/\tau$	independent
independent of C_D	$\propto C_D^2$	of τ
		$\propto C_D^2$

- Current noise is independent of detector capacitance, consistent with the notion of “counting electrons”.
- Voltage noise increases with detector capacitance (reduced signal voltage)
- $1/f$ noise is independent of shaping time.
In general, the total noise of a $1/f$ source depends on the ratio of the upper to lower cutoff frequencies, not on the absolute noise bandwidth. If τ_d and τ_i are scaled by the same factor, this ratio remains constant.

The equivalent noise charge Q_n assumes a minimum when the current and voltage noise contributions are equal.

Typical Result



↑
dominated by voltage noise

↑
current noise

For a CR-RC shaper the noise minimum obtains for $\tau_d = \tau_i = \tau$.

This criterion does not hold for more sophisticated shapers.

Caution: Even for a CR-RC shaper this criterion only applies when the differentiation time constant is the primary parameter, i.e. when the pulse width must be constrained.

When the rise time, i.e. the integration time constant, is the primary consideration, it is advantageous to make $\tau_d > \tau_i$, since the signal will increase more rapidly than the noise, as was shown previously

Note:

For sources connected in parallel, currents are additive.

For sources connected in series, voltages are additive.

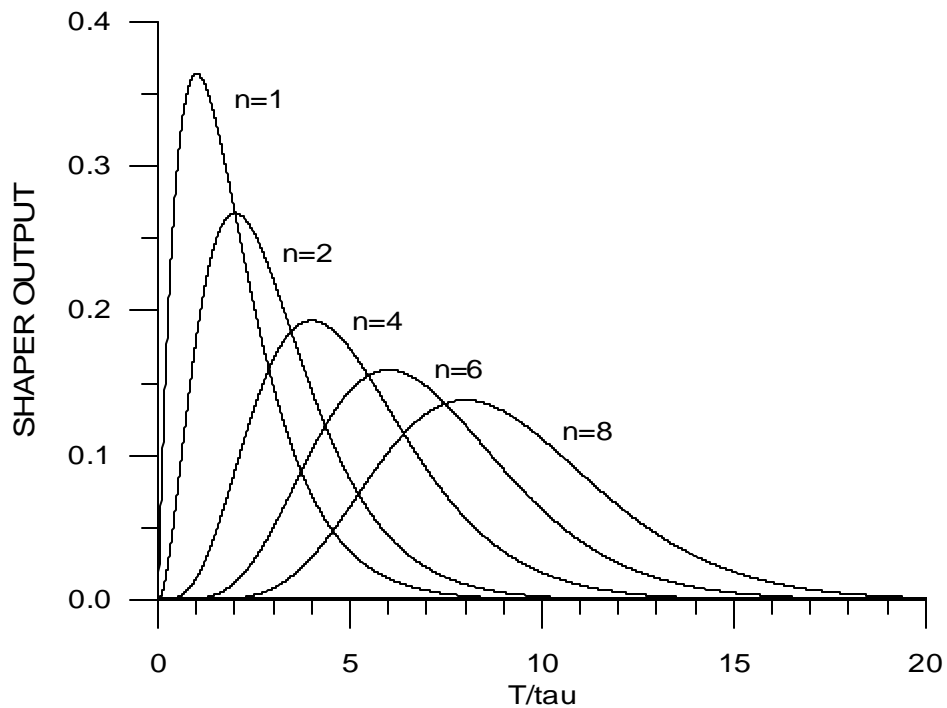
⇒ In the detector community voltage and current noise are often called “series” and “parallel” noise.

The rest of the world uses equivalent noise voltage and current.

Since they are physically meaningful, use of these widely understood terms is preferable.

CR-RC Shapers with Multiple Integrators

- a. Start with simple *CR-RC* shaper and add additional integrators ($n= 1$ to $n= 2, \dots n= 8$) with the same time constant τ .

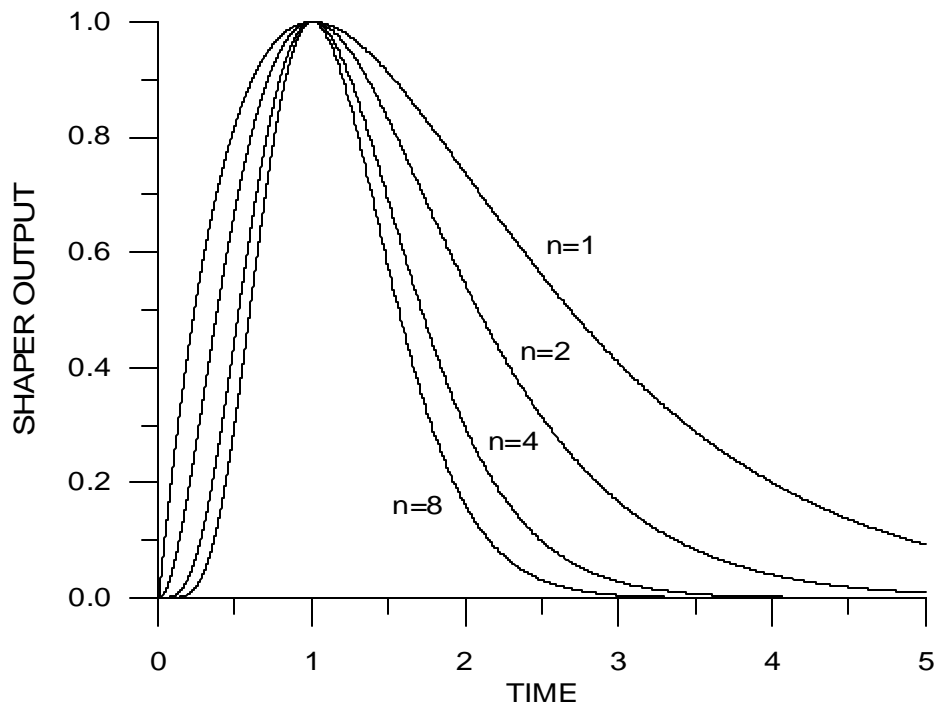


With additional integrators the peaking time T_p increases

$$T_p = n\tau$$

b) Time constants changed to preserve the peaking time

$$(\tau_n = \tau_{n=1}/n)$$



Increasing the number of integrators makes the output pulse more symmetrical with a faster return to baseline.

⇒ improved rate capability at the same peaking time

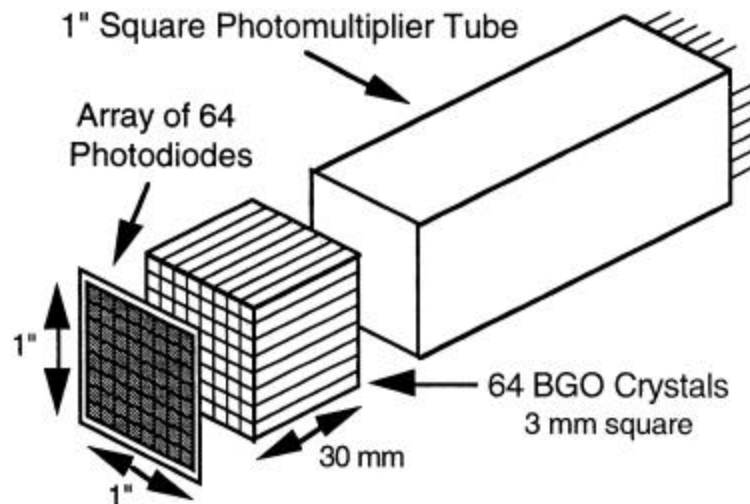
Shapers with the equivalent of 8 RC integrators are common. Usually, this is achieved with active filters (i.e. circuitry that synthesizes the bandpass with amplifiers and feedback networks).

Examples

1. Photodiode Readout

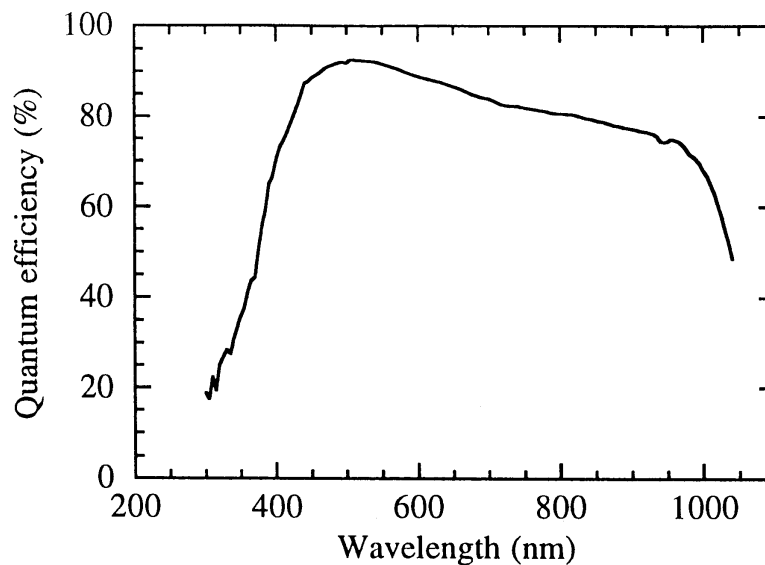
(S. Holland, N. Wang, I. Kipnis, B. Krieger, W. Moses, LBNL)

Medical Imaging (Positron Emission Tomography)



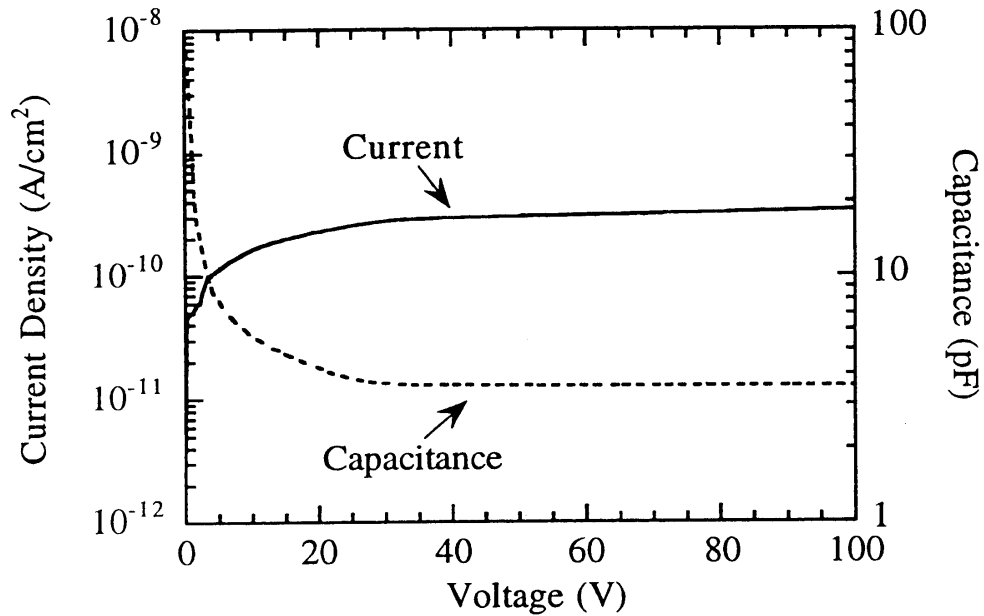
Read out 64 BGO crystals with one PMT (timing, energy) and tag crystal by segmented photodiode array.

Requires thin dead layer on photodiode to maximize quantum efficiency.



Thin electrode must be implemented with low resistance to avoid significant degradation of electronic noise.

Furthermore, low reverse bias current critical to reduce noise.



Photodiodes designed and fabricated in LBNL Microsystems Lab.

Front-end chip (preamplifier + shaper):

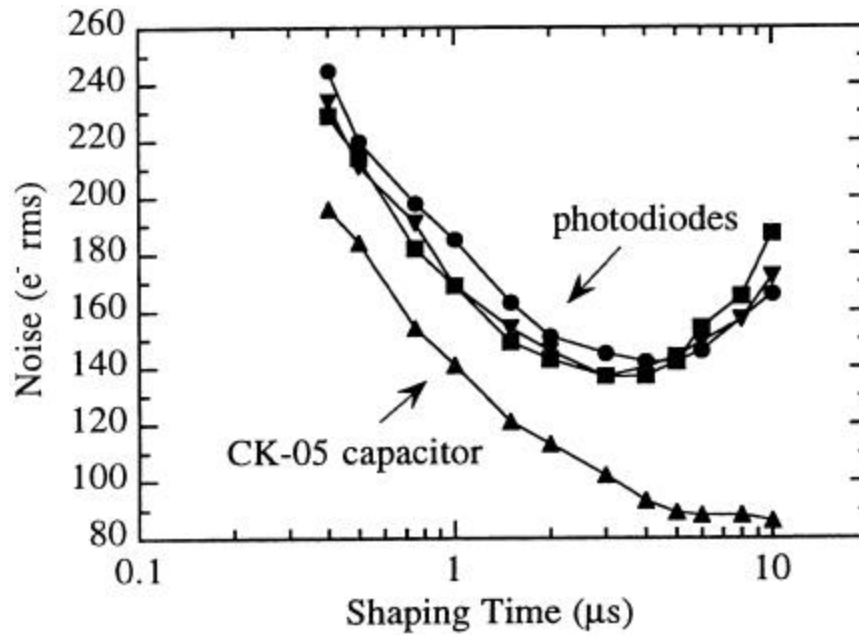
16 channels per chip

die size: 2 x 2 mm²,
1.2 μm CMOS

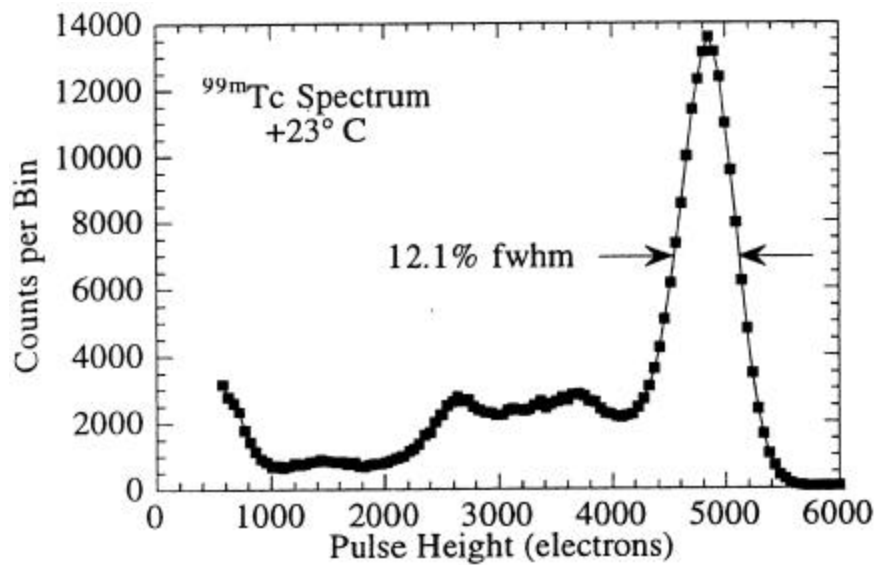
continuously adjustable shaping time (0.5 to 50 μs)

gain: 100 mV per 1000 el.

Noise vs. shaping time



Energy spectrum with BGO scintillator



2. High-Rate X-Ray Spectroscopy

(B. Ludewigt, C. Rossington, I. Kipnis, B. Krieger, LBNL)

Use detector with multiple strip electrodes

not for position resolution

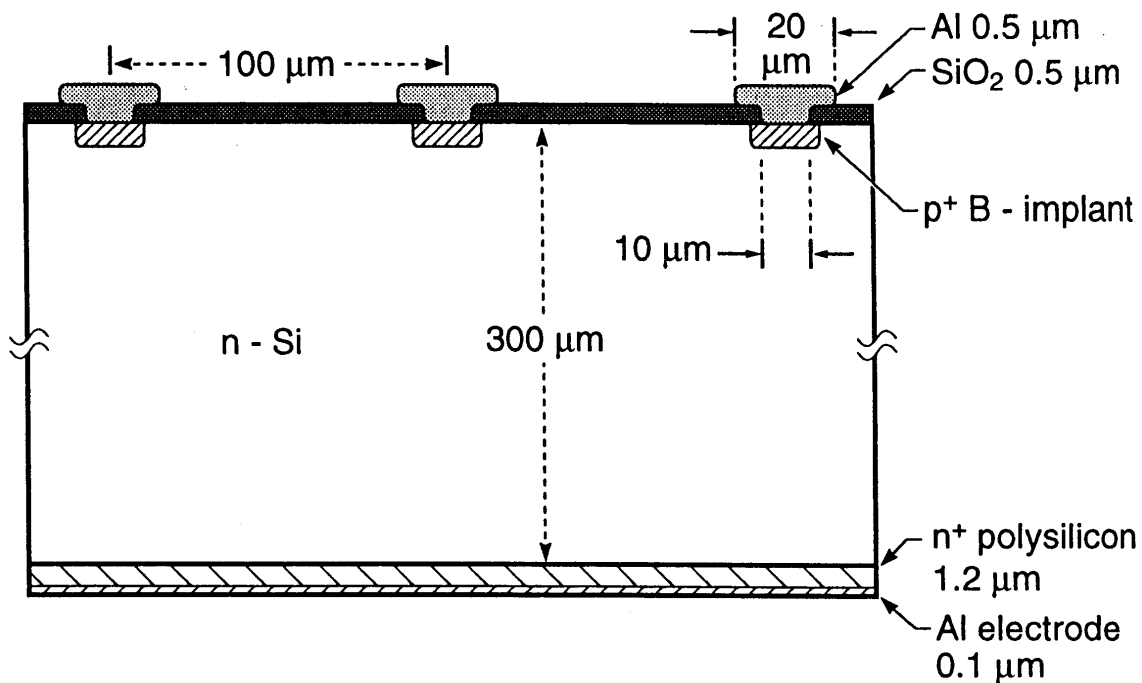
but for

- segmentation \Rightarrow distribute rate over many channels
- \Rightarrow reduced capacitance
- \Rightarrow low noise at short shaping time
- \Rightarrow higher rate per detector element

For x-ray energies 5 – 25 keV \Rightarrow photoelectric absorption dominates
(signal on 1 or 2 strips)

Strip pitch: 100 μm

Strip Length: 2 mm (matched to ALS)

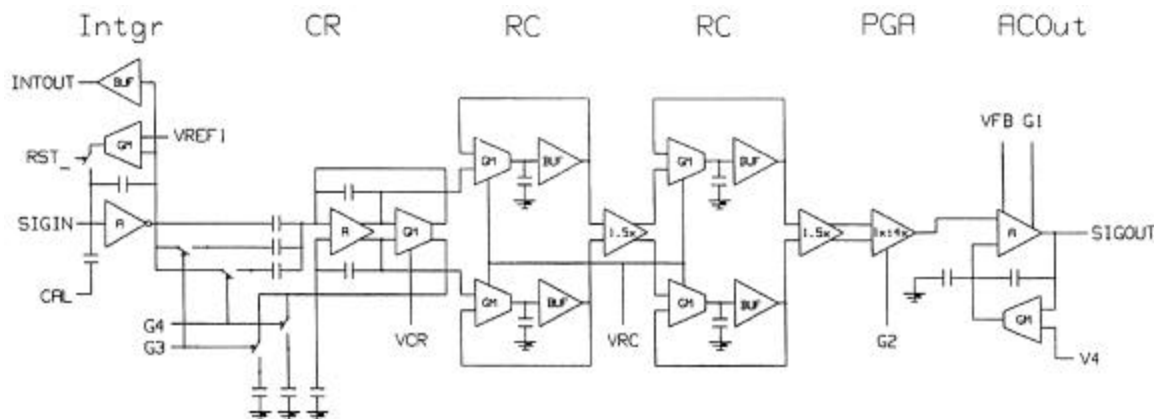
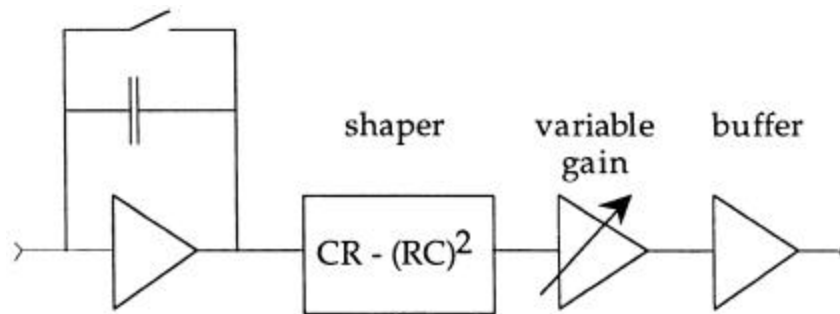


Readout IC tailored to detector

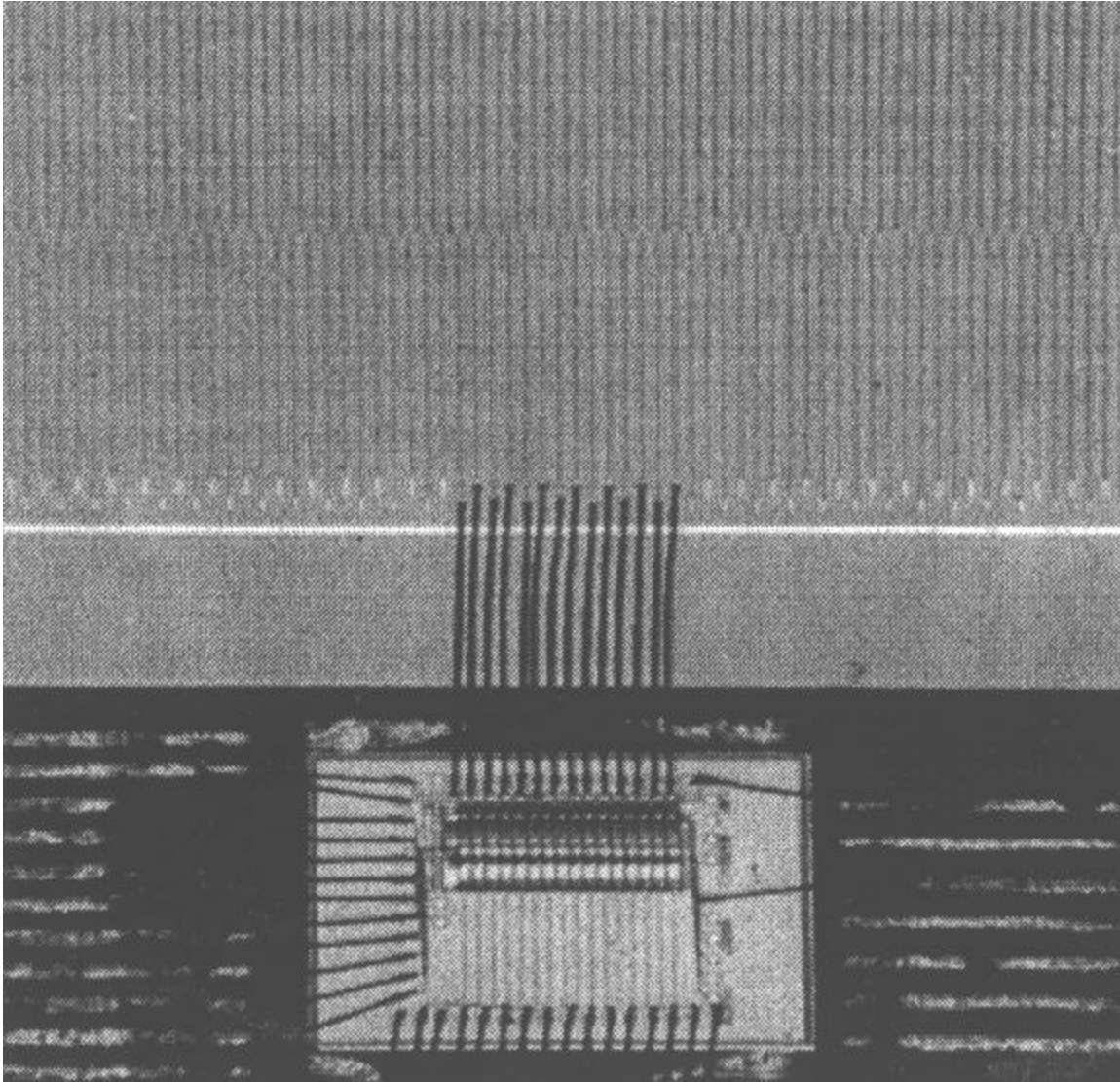
Preamplifier + CR-RC² shaper + cable driver to bank of parallel ADCs
(M. Maier + H. Yaver)

Preamplifier with pulsed reset.

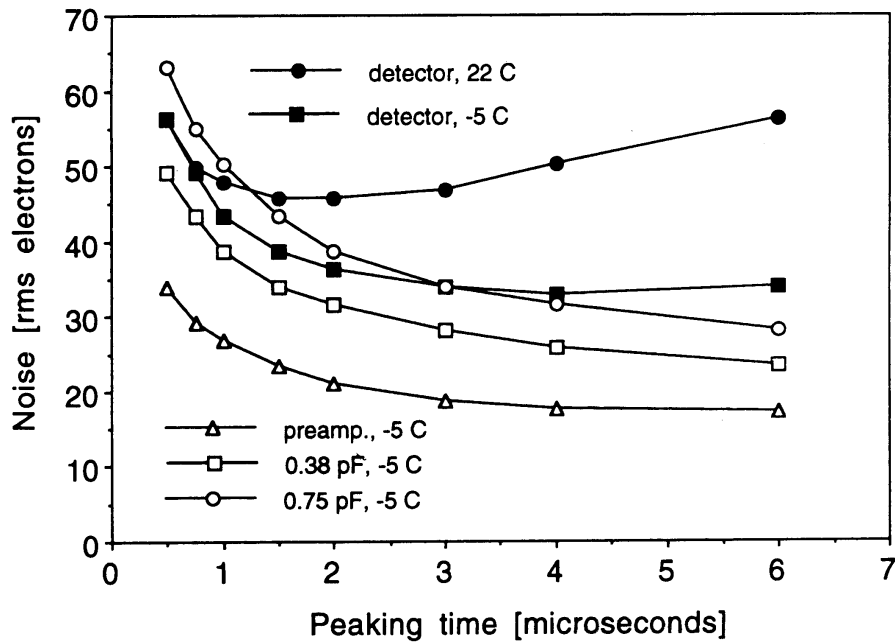
Shaping time continuously variable 0.5 to 20 μ s.



Chip wire-bonded to strip detector

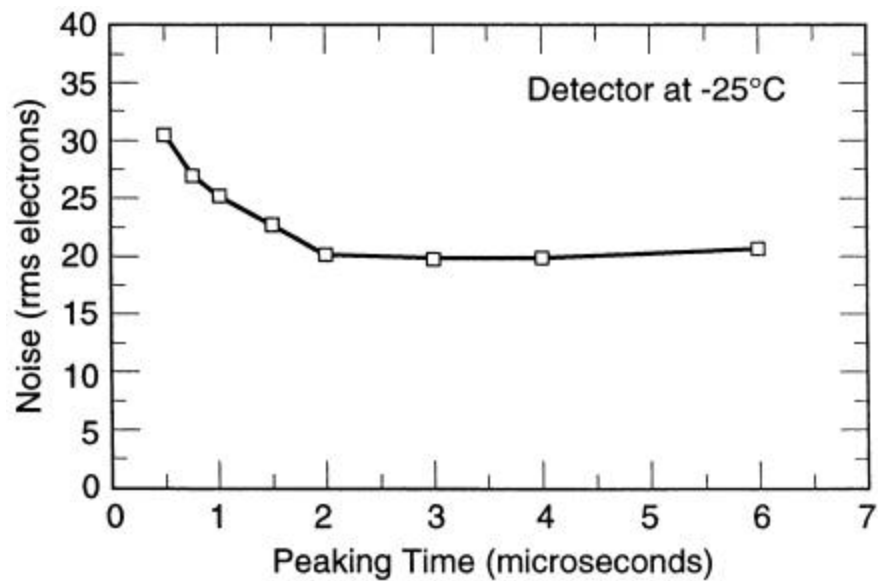


Initial results



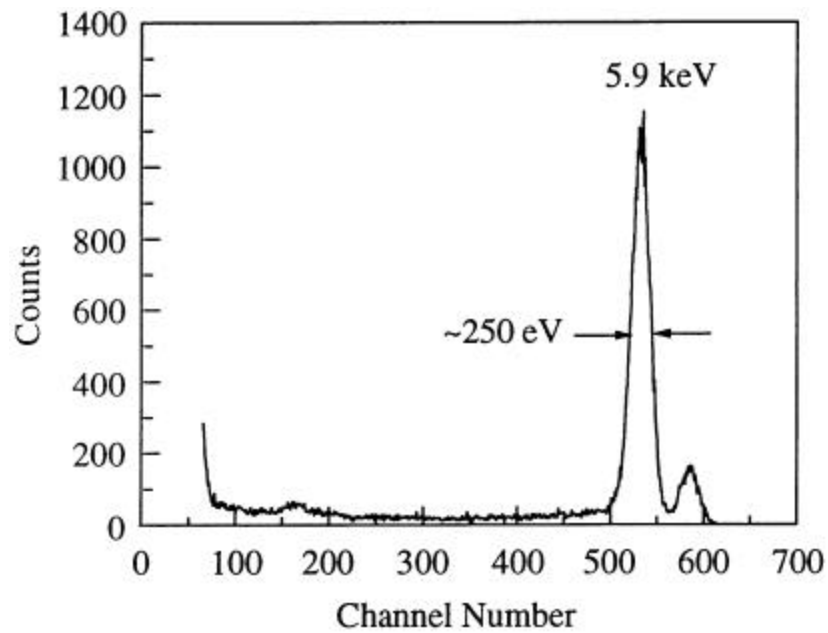
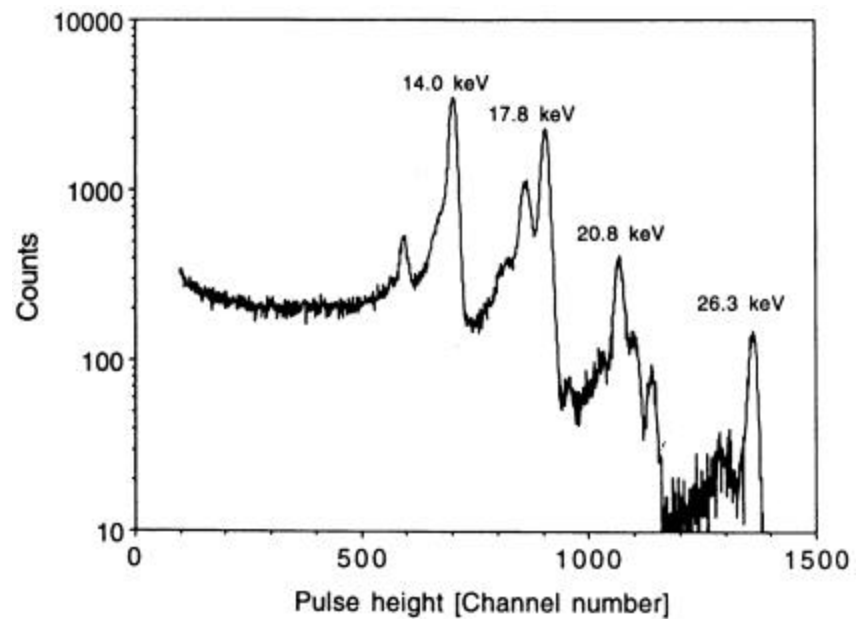
Connecting detector increases noise because of added capacitance and detector current (as indicated by increase of noise with peaking time). Cooling the detector reduces the current and noise improves.

Second prototype



Current noise negligible because of cooling – “flat” noise vs. shaping time indicates that $1/f$ noise dominates.

Measured spectra

 ^{55}Fe  ^{241}Am 

Frequency vs. Time Domain

The noise analysis of shapers is rather straightforward if the frequency response is known.

On the other hand, since we are primarily interested in the pulse response, shapers are often designed directly in the time domain, so it seems more appropriate to analyze the noise performance in the time domain also.

Clearly, one can take the time response and Fourier transform it to the frequency domain, but this approach becomes problematic for time-variant shapers.

The CR-RC shapers discussed up to now utilize filters whose time constants remain constant during the duration of the pulse, i.e. they are time-invariant.

Many popular types of shapers utilize signal sampling or change the filter constants during the pulse to improve pulse characteristics, i.e. faster return to baseline or greater insensitivity to variations in detector pulse shape.

These time-variant shapers cannot be analyzed in the manner described above. Various techniques are available, but some shapers can be analyzed only in the time domain.

The basis of noise analysis in the time domain is Parseval's Theorem

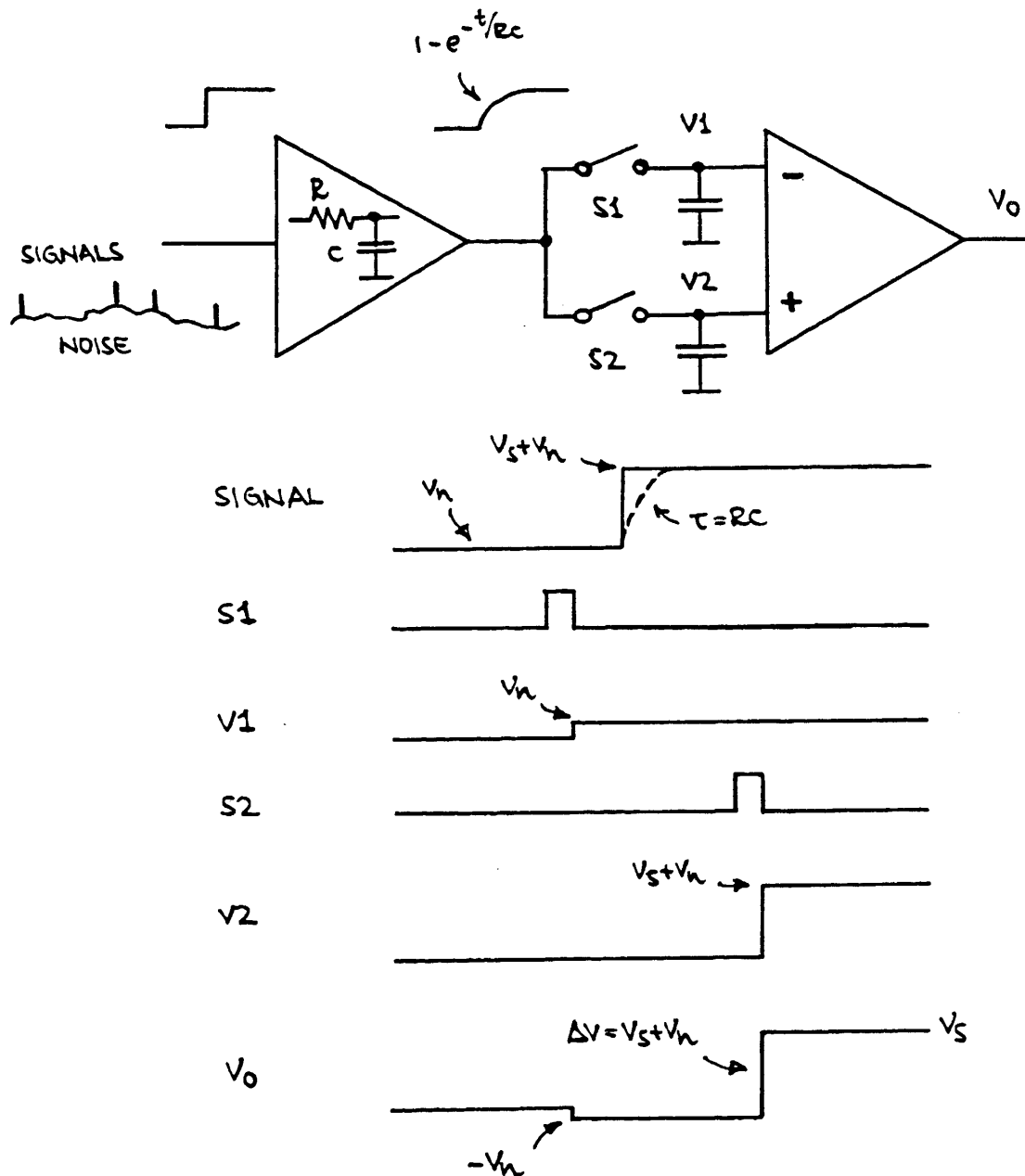
$$\int_0^{\infty} A(f)df = \int_{-\infty}^{\infty} F(t)dt ,$$

which relates the spectral distribution of a signal in the frequency domain to its time dependence. However, a more intuitive approach will be used here.

First an example:

A commonly used time-variant filter is the correlated double-sampler. This shaper can be analyzed exactly only in the time domain.

Correlated Double Sampling



1. Signals are superimposed on a (slowly) fluctuating baseline
2. To remove baseline fluctuations the baseline is sampled prior to the arrival of a signal.
3. Next, the signal + baseline is sampled and the previous baseline sample subtracted to obtain the signal

Noise Analysis in the Time Domain

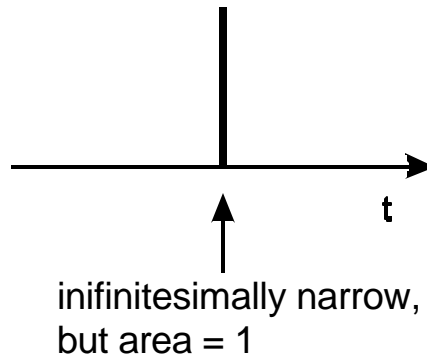
What pulse shapes have a frequency spectrum corresponding to typical noise sources?

1. voltage noise

The frequency spectrum at the input of the detector system is “white”, i.e.

$$\frac{dA}{df} = \text{const.}$$

This is the spectrum of a δ impulse:

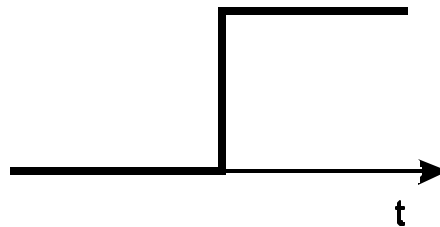


2. current noise

The spectral density is inversely proportional to frequency, i.e.

$$\frac{dA}{df} \propto \frac{1}{f}$$

This is the spectrum of a step impulse:



- Input noise can be considered as a sequence of δ and step pulses whose rate determines the noise level.
- The shape of the primary noise pulses is modified by the pulse shaper:

δ pulses become longer,

step pulses are shortened.

- The noise level at a given measurement time T_m is determined by the cumulative effect (superposition) of all noise pulses occurring prior to T_m .
- Their individual contributions at $t = T_m$ are described by the shaper's "weighting function" $W(t)$.

References:

V. Radeka, Nucl. Instr. and Meth. **99** (1972) 525
 V. Radeka, IEEE Trans. Nucl. Sci. **NS-21** (1974) 51
 F.S. Goulding, Nucl. Instr. and Meth. **100** (1972) 493
 F.S. Goulding, IEEE Trans. Nucl. Sci. **NS-29** (1982) 1125

Consider a single noise pulse occurring in a short time interval dt at a time T prior to the measurement. The amplitude at $t = T$ is

$$a_n = W(T)$$



If, on the average, $n_n dt$ noise pulses occur within dt , the fluctuation of their cumulative signal level at $t = T$ is proportional to

$$\sqrt{n_n dt}$$

The magnitude of the baseline fluctuation is

$$\sigma_n^2(T) \propto n_n [W(t)]^2 dt$$

For all noise pulses occurring prior to the measurement

$$\sigma_n^2 \propto n_n \int_0^{\infty} [W(t)]^2 dt$$

where

n_n determines the magnitude of the noise

and

$\int_0^{\infty} [W(t)]^2 dt$ describes the noise characteristics of the shaper – the “noise index”

The Weighting Function

a) current noise

$W_i(t)$ is the shaper response to a step pulse, i.e. the “normal” output waveform.

b) voltage noise

$$W_v(t) = \frac{d}{dt} W_i(t) \equiv W'(t)$$

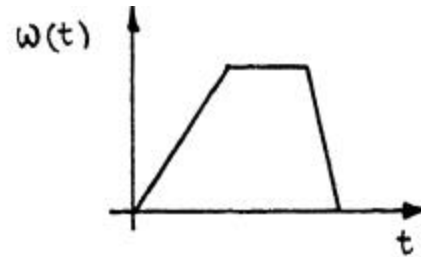
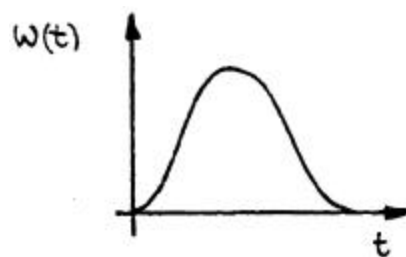
(Consider a δ pulse as the superposition of two step pulses of opposite polarity and spaced infinitesimally in time)

Examples:

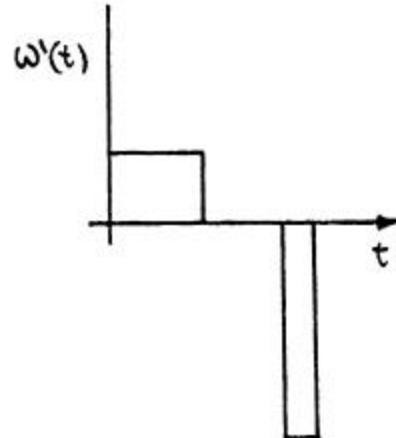
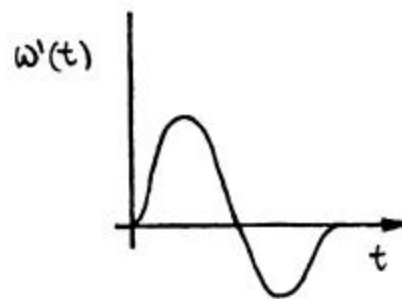
1. Gaussian

2. Trapezoid

current
 (“step”)
 noise



voltage
 (“delta”)
 noise



Goal: Minimize overall area to reduce current noise contribution
 Minimize derivatives to reduce voltage noise contribution

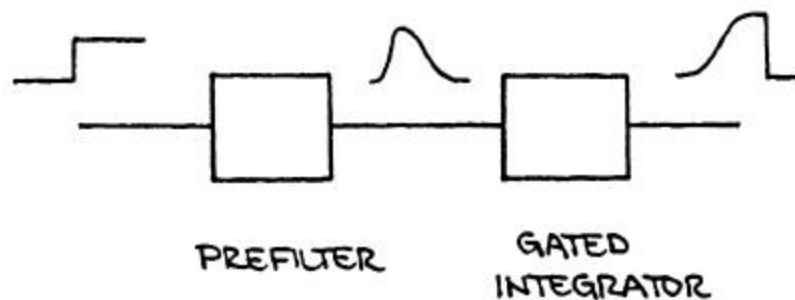
⇒ For a given pulse duration a symmetrical pulse provides the best noise performance.
 Linear transitions minimize voltage noise contributions.

Time-Variant Shapers

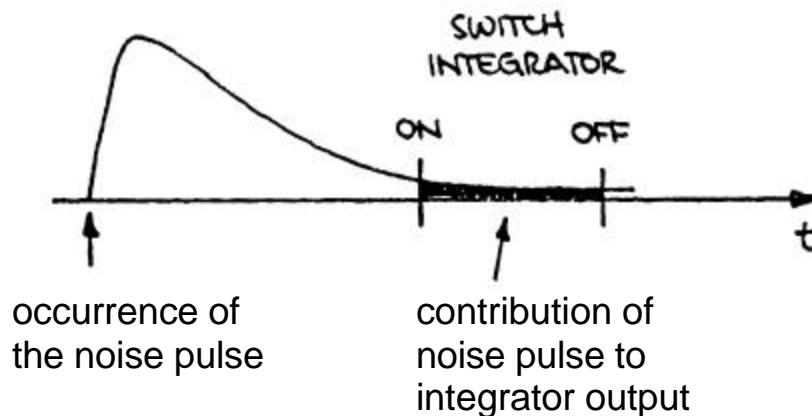
Example: gated integrator with prefilter

The gated integrator integrates the input signal during a selectable time interval (the “gate”).

In this example, the integrator is switched on prior to the signal pulse and switched off after a fixed time interval, selected to allow the output signal to reach its maximum.



Consider a noise pulse occurring prior to the “on time” of the integrator.



For W_1 = weighting function of the time-invariant prefilter

W_2 = weighting function of the time-variant stage

the overall weighting function is obtained by convolution

$$W(t) = \int_{-\infty}^{\infty} W_2(t') \cdot W_1(t - t') dt'$$

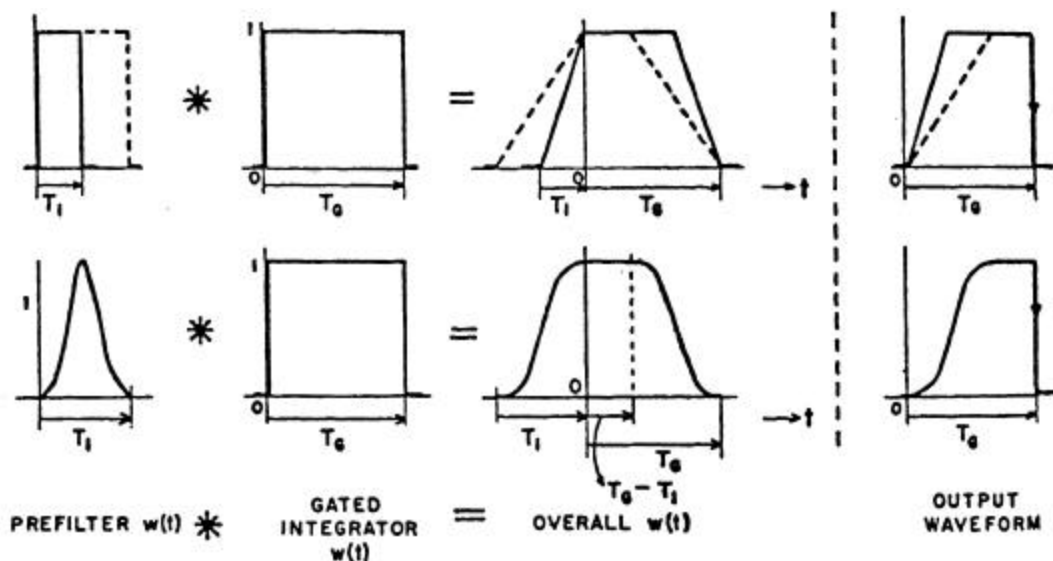
Weighting function for current (“step”) noise: $W(t)$

Weighting function for voltage (“delta”) noise: $W'(t)$

Example

Time-invariant prefilter feeding a gated integrator

(from Radeka, IEEE Trans. Nucl. Sci. **NS-19** (1972) 412)



Comparison between a time-invariant and time-variant shaper

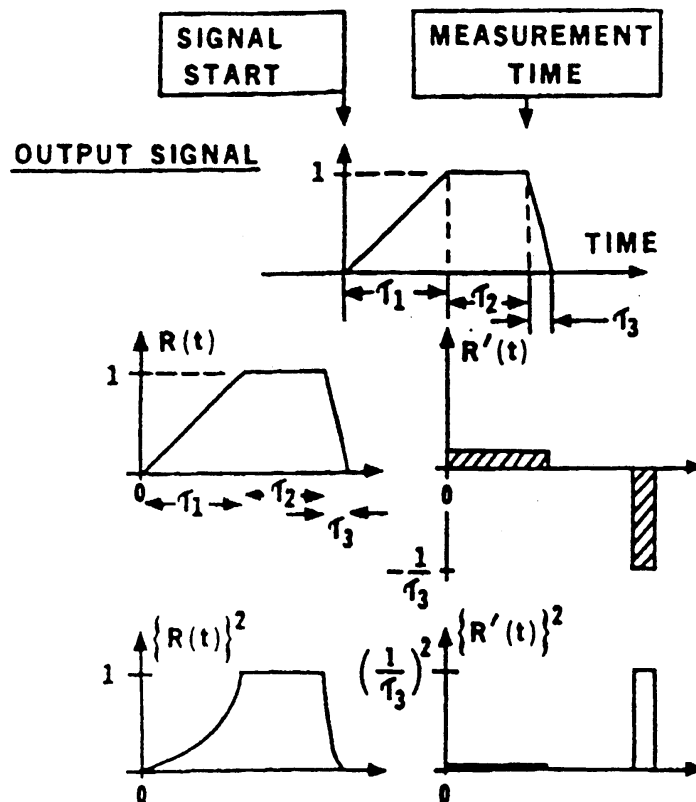
(from Goulding, NIM **100** (1972) 397)

Example: trapezoidal shaper

Duration= 2 μ s

Flat top= 0.2 μ s

1. Time-Invariant Trapezoid



Current noise

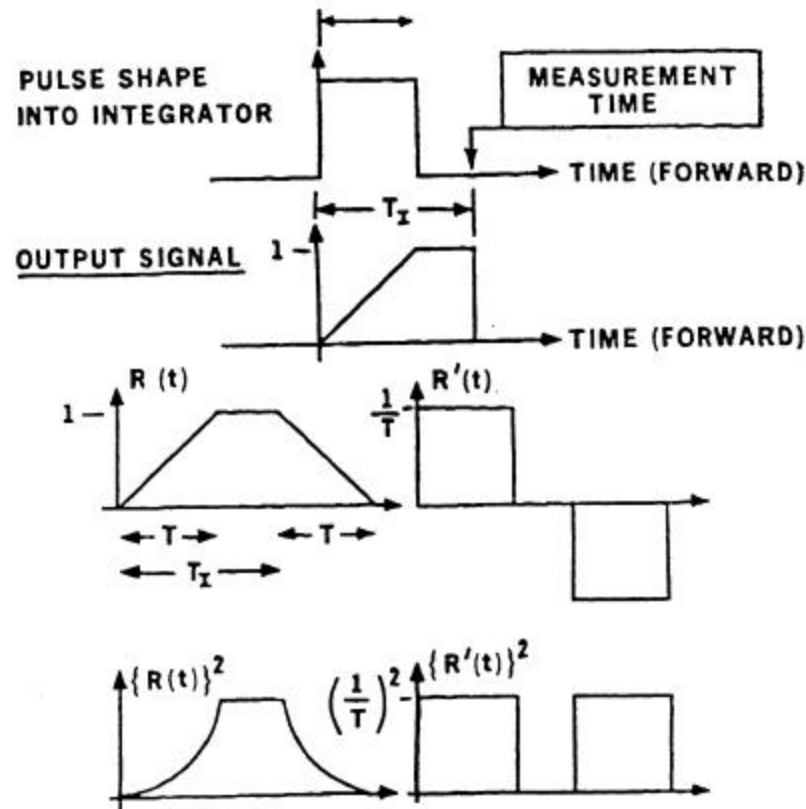
$$N_i^2 = \int_0^{\infty} [W(t)]^2 dt = \int_0^{\tau_1} \left(\frac{t}{\tau_1}\right)^2 dt + \int_{\tau_1}^{\tau_2} (1)^2 dt + \int_{\tau_2}^{\tau_2 + \tau_3} \left(\frac{t - \tau_2}{\tau_3}\right)^2 dt = \tau_2 + \frac{\tau_1 + \tau_3}{3}$$

Voltage noise

$$N_v^2 = \int_0^{\infty} [W'(t)]^2 dt = \int_0^{\tau_1} \left(\frac{1}{\tau_1}\right)^2 dt + \int_{\tau_2}^{\tau_2 + \tau_3} \left(\frac{1}{\tau_3}\right)^2 dt = \frac{1}{\tau_1} + \frac{1}{\tau_3}$$

Minimum for $\tau_1 = \tau_3$ (symmetry!) $\Rightarrow N_i^2 = 0.8, N_v^2 = 2.2$

Gated Integrator Trapezoidal Shaper



Current Noise

$$N_i^2 = 2 \int_0^T \left(\frac{t}{T} \right)^2 dt + \int_T^{T_I-T} (1)^2 dt = T_I - \frac{T}{3}$$

Voltage Noise

$$N_v^2 = 2 \int_0^T \left(\frac{1}{T} \right)^2 dt = \frac{2}{T}$$

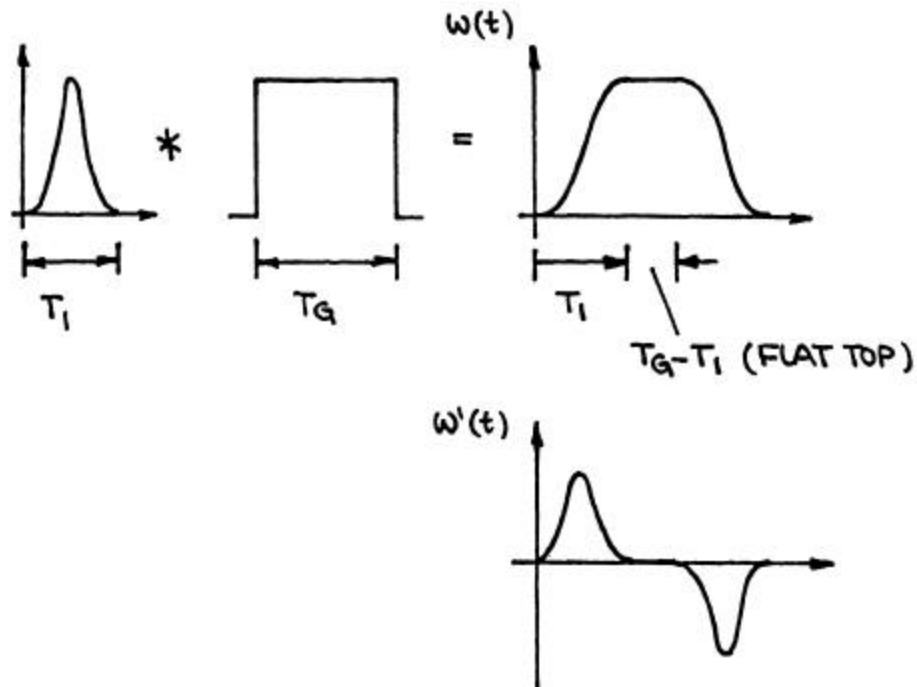
⇒ time-variant shaper $N_i^2 = 1.4$, $N_v^2 = 1.1$

time-invariant shaper $N_i^2 = 0.8$, $N_v^2 = 2.2$

time-variant trapezoid has more current noise, less voltage noise

Interpretation of Results

Example: gated integrator



Current Noise

$$Q_{ni}^2 \propto \int [W(t)]^2 dt$$

Increases with T_I and T_G (i.e. width of $W(t)$)

(more noise pulses accumulate within width of $W(t)$)

Voltage Noise

$$Q_{nv}^2 \propto \int [W'(t)]^2 dt$$

Increases with the magnitude of the derivative of $W(t)$

(steep slopes \rightarrow large bandwidth — *determined by prefilter*)

Width of flat top irrelevant

(δ response of prefilter is bipolar: net= 0)

Quantitative Assessment of Noise in the Time Domain

(see Radeka, IEEE Trans. Nucl. Sci. **NS-21** (1974) 51)

$$Q_n^2 = \frac{1}{2} i_n^2 \int_{-\infty}^{\infty} [W(t)]^2 dt + \frac{1}{2} C^2 e_n^2 \int_{-\infty}^{\infty} [W'(t)]^2 dt$$

\uparrow
 current noise

\uparrow
 voltage noise

Q_n = equivalent noise charge [C]

i_n = input current noise spectral density [A/ $\sqrt{\text{Hz}}$]

e_n = input voltage noise spectral density [V/ $\sqrt{\text{Hz}}$]

C = total capacitance at input

$W(t)$ normalized to unit input step response

or rewritten in terms of a characteristic time $t \rightarrow T/t$

$$Q_n^2 = \frac{1}{2} i_n^2 T \int_{-\infty}^{\infty} [W(t)]^2 dt + \frac{1}{2} C^2 e_n^2 \frac{1}{T} \int_{-\infty}^{\infty} [W'(t)]^2 dt$$

This result can be written in a general form that applies to any shaper.

$$Q_n^2 = i_n^2 T F_i + C^2 e_n^2 \frac{1}{T} F_v + C^2 A_f F_{vf}$$

The individual current and voltage noise contributions are combined:

current noise
$$i_n^2 = 2q_e I_b + \frac{4kT}{R_p} + i_{na}^2$$

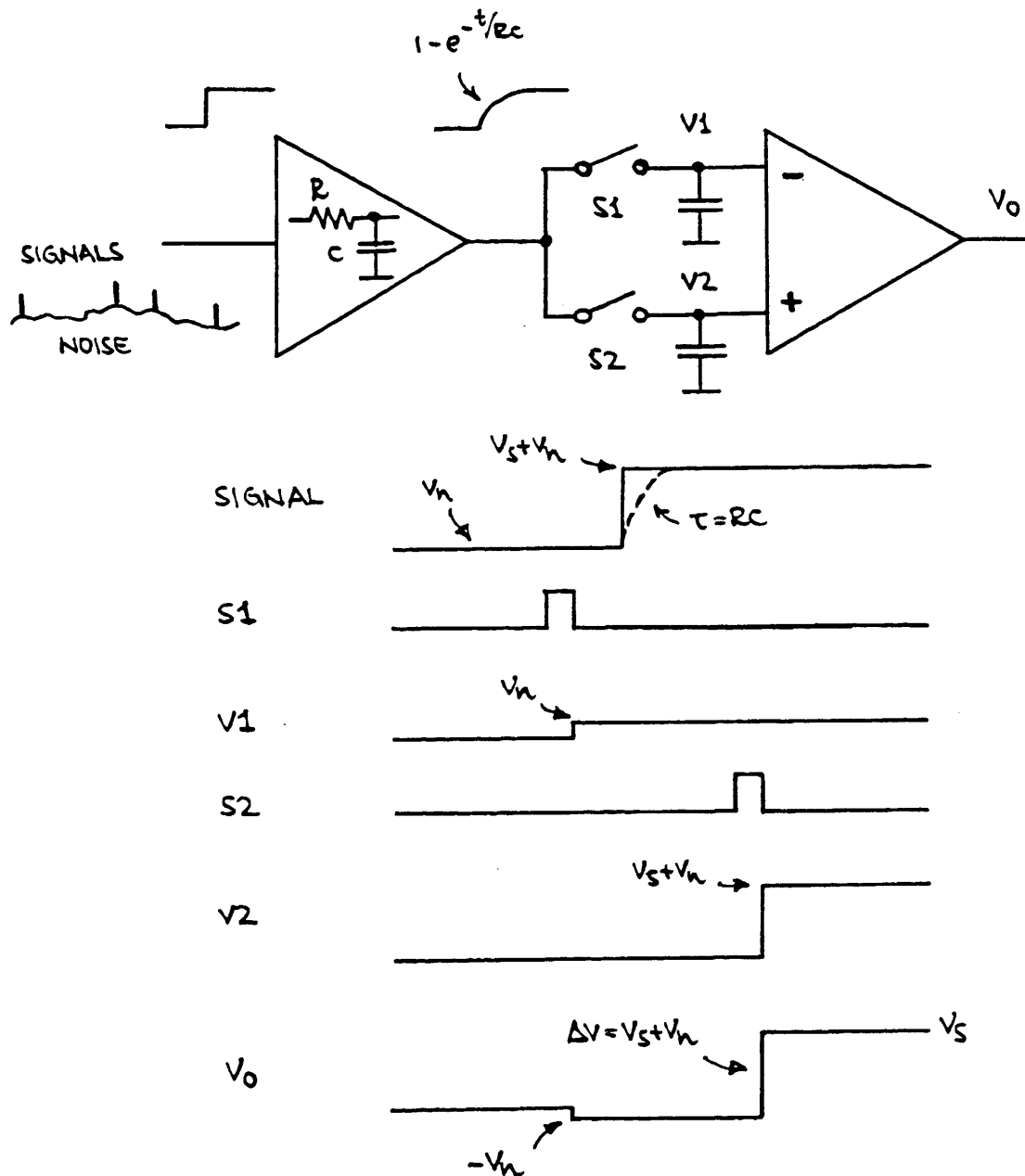
and voltage noise
$$e_n^2 = 4kTR_S + e_{na}^2$$

The shaper is characterized by noise coefficients F_i , F_v and F_{vf} , which depend only on the shape of the pulse. The noise bandwidth scales with a characteristic time T . In the specific case of a CR-RC shaper T is equal to the peaking time T_p , the time at which the pulse assumes its maximum value. For a correlated double sampler, the sampling time is an appropriate measure.

The first term describes the current noise contribution, whereas the second and third terms describe the voltage noise contributions due to white and $1/f$ noise sources.

- Generally, the noise indices or “shape factors” F_i , F_v and F_{vf} characterize the type of shaper, for example $CR-RC$ or $CR-(RC)^4$.
- They depend only on the ratio of time constants τ_d/τ_i , rather than their absolute magnitude.
- The noise contribution then scales with the characteristic time T . The choice of characteristic time is somewhat arbitrary. so any convenient measure for a given shaper can be adopted in deriving the noise coefficients F .

Correlated Double Sampling



1. Signals are superimposed on a (slowly) fluctuating baseline
2. To remove baseline fluctuations the baseline is sampled prior to the arrival of a signal.
3. Next, the signal + baseline is sampled and the previous baseline sample subtracted to obtain the signal

1. Current Noise

Current (shot) noise contribution:

$$Q_{ni}^2 = \frac{1}{2} i_n^2 \int_{-\infty}^{\infty} [W(t)]^2 dt$$

Weighting function (T = time between samples):

$$t < 0: \quad W(t) = 0$$

$$0 \leq t \leq T: \quad W(t) = 1 - e^{-t/\tau}$$

$$t > T: \quad W(t) = e^{-(t-T)/\tau}$$

Current noise coefficient

$$F_i = \int_{-\infty}^{\infty} [W(t)]^2 dt$$

$$F_i = \int_0^T (1 - e^{-t/\tau})^2 dt + \int_T^{\infty} e^{-2(t-T)/\tau} dt$$

$$F_i = \left(T + \frac{\tau}{2} e^{-T/\tau} - \frac{\tau}{2} e^{-2T/\tau} \right) + \frac{\tau}{2}$$

so that the equivalent noise charge

$$Q_{ni}^2 = \frac{1}{2} i_n^2 \left[T + \frac{\tau}{2} (e^{-T/\tau} - e^{-2T/\tau} + 1) \right]$$

$$Q_{ni}^2 = i_n^2 \tau \frac{1}{4} \left(\frac{2T}{\tau} + e^{-T/\tau} - e^{-2T/\tau} + 1 \right)$$

Reality Check 1:

Assume that the current noise is pure shot noise

$$i_n^2 = 2q_e I$$

so that

$$Q_{ni}^2 = q_e I \tau \frac{1}{2} \left(\frac{2T}{\tau} + e^{-T/\tau} - e^{-2T/\tau} + 1 \right)$$

Consider the limit Sampling Interval \gg Rise Time, $T \gg \tau$:

$$Q_{ni}^2 \approx q_e I \cdot T$$

or expressed in electrons

$$Q_{ni}^2 \approx \frac{q_e I \cdot T}{q_e^2} = \frac{I \cdot T}{q_e}$$

$$Q_{ni} \approx \sqrt{N_i}$$

where N_i is the number of electrons “counted” during the sampling interval T .

2. Voltage Noise

Voltage Noise Contribution

$$Q_{nv}^2 = \frac{1}{2} C_i^2 e_n^2 \int_{-\infty}^{\infty} [W'(t)]^2 dt$$

Voltage Noise Coefficient

$$F_v = \int_{-\infty}^{\infty} [W'(t)]^2 dt$$

$$F_v = \int_0^T \left(\frac{1}{\tau} e^{-t/\tau} \right)^2 dt + \int_T^{\infty} \left(\frac{1}{\tau} e^{-2(t-T)/\tau} \right)^2 dt$$

$$F_v = \frac{1}{2\tau} \left(1 - e^{-2T/\tau} \right) + \frac{1}{2\tau}$$

$$F_v = \frac{1}{2\tau} \left(2 - e^{-2T/\tau} \right)$$

so that the equivalent noise charge

$$Q_{nv}^2 = C_i^2 e_n^2 \frac{1}{\tau} \frac{1}{4} \left(2 - e^{-2T/\tau} \right)$$

Reality Check 2:

In the limit $T \gg \tau$:

$$Q_{nv}^2 = C_i^2 \cdot e_n^2 \cdot \frac{1}{2\tau}$$

Compare this with the noise on an RC low-pass filter alone (i.e. the voltage noise at the output of the pre-filter):

$$Q_n^2(RC) = C_i^2 \cdot e_n^2 \cdot \frac{1}{4\tau}$$

(see the discussion on noise bandwidth)

so that

$$\frac{Q_n(\text{double sample})}{Q_n(RC)} = \sqrt{2}$$

If the sample time is sufficiently large, the noise samples taken at the two sample times are uncorrelated, so the two samples simply add in quadrature.

3. Signal Response

The preceding calculations are only valid for a signal response of unity, which is valid at $T \gg \tau$.

For sampling times T of order τ or smaller one must correct for the reduction in signal amplitude at the output of the prefilter

$$V_s / V_i = 1 - e^{-T/\tau}$$

so that the equivalent noise charge due to the current noise becomes

$$Q_{ni}^2 = i_n^2 \tau \frac{\frac{2T}{\tau} + e^{-T/\tau} - e^{-2T/\tau} + 1}{4(1 - e^{-T/\tau})^2}$$

The voltage noise contribution is

$$Q_{nv}^2 = C_i^2 v_n^2 \frac{1}{\tau} \frac{2 - e^{-2T/\tau}}{4(1 - e^{-T/\tau})^2}$$

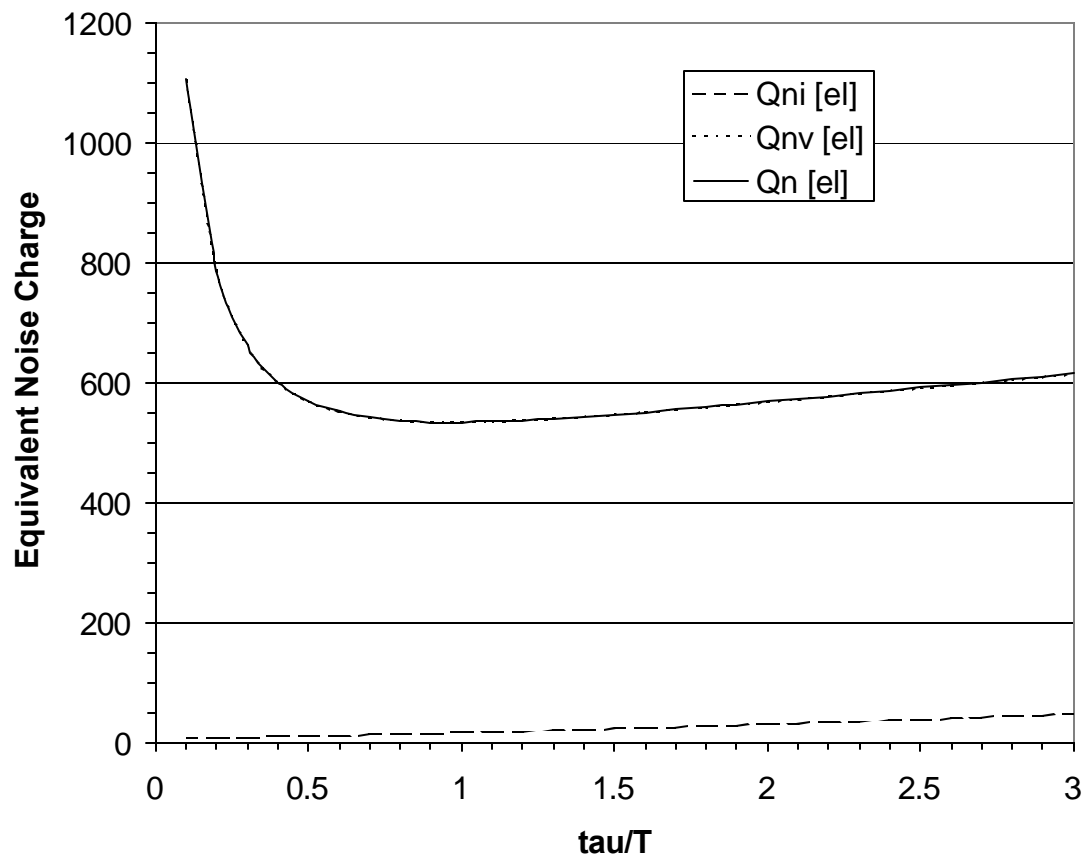
and the total equivalent noise charge

$$Q_n = \sqrt{Q_{ni}^2 + Q_{nv}^2}$$

Optimization

1. Noise current negligible

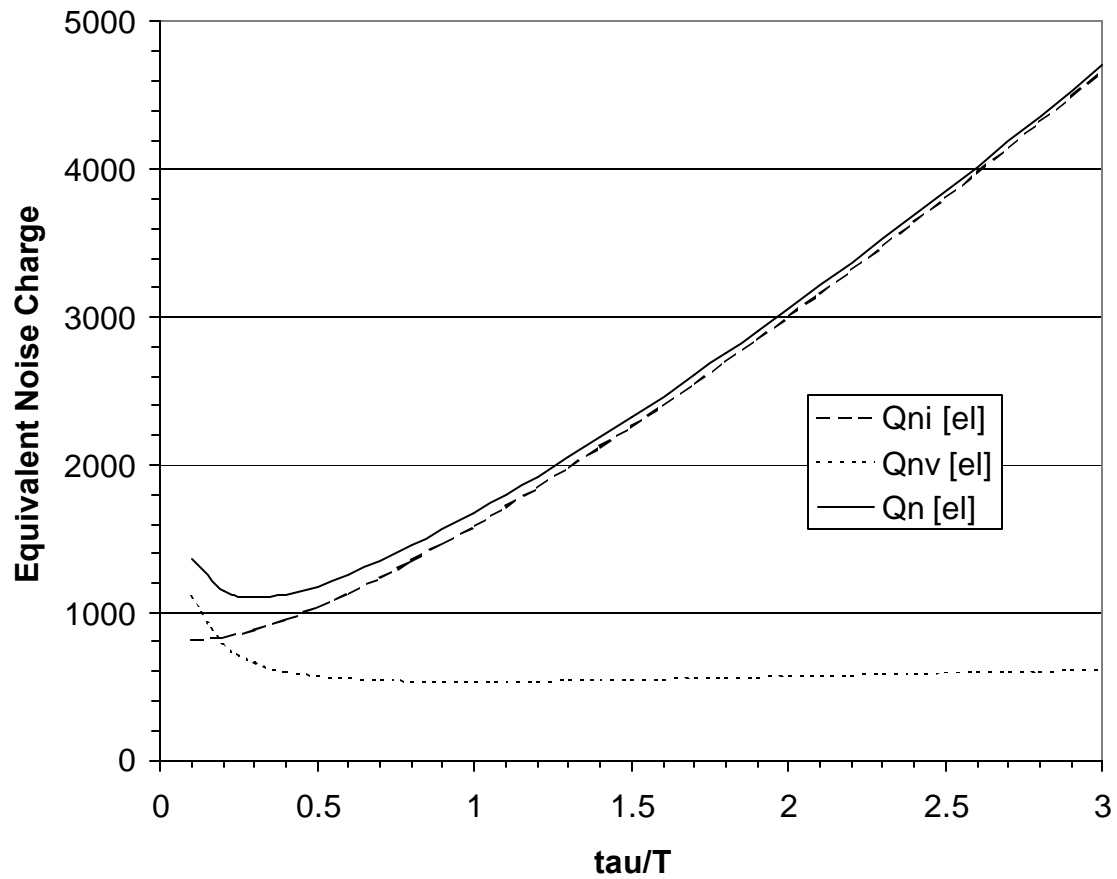
Parameters: $T = 100$ ns
 $C_d = 10$ pF
 $e_n = 2.5$ nV/ $\sqrt{\text{Hz}}$
 $\rightarrow i_n = 6$ fA/ $\sqrt{\text{Hz}}$ ($I_b = 0.1$ nA)



Noise attains shallow minimum for $\tau = T$.

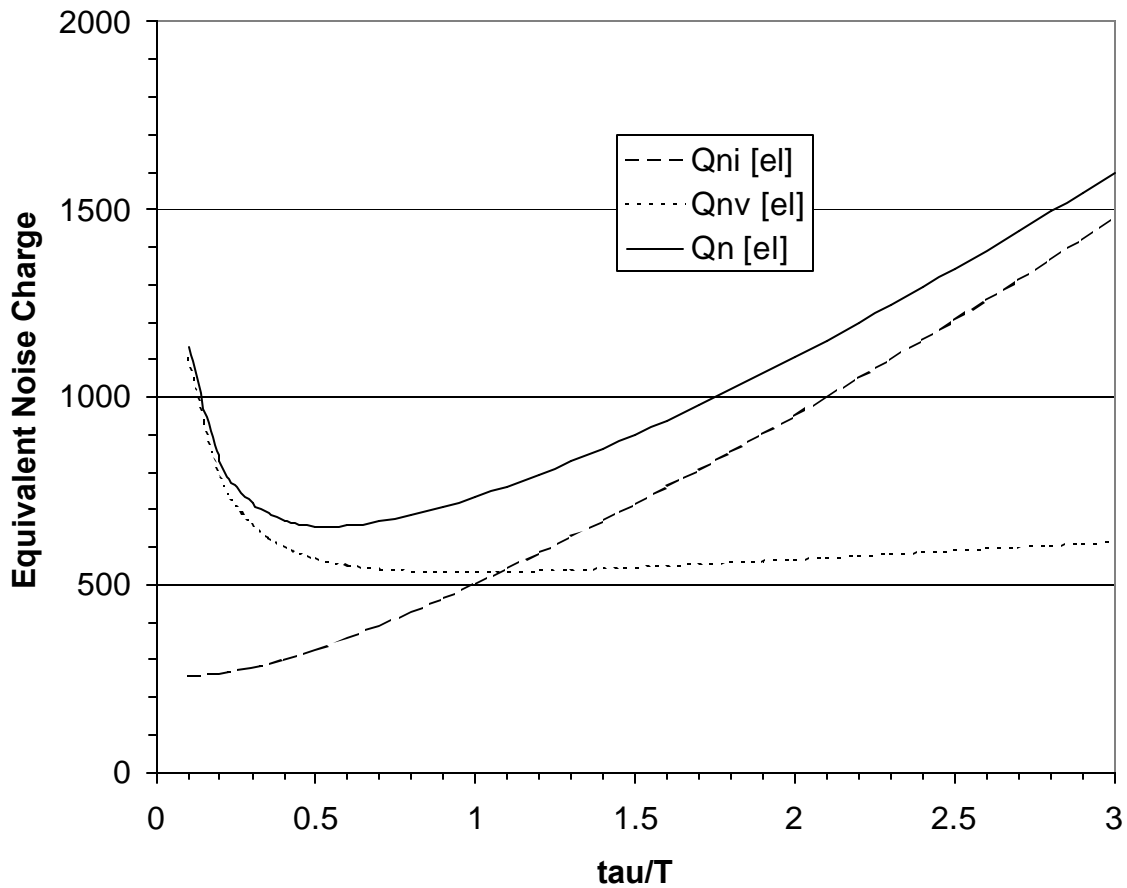
2. Significant current noise contribution

Parameters: $T = 100 \text{ ns}$
 $C_d = 10 \text{ pF}$
 $e_n = 2.5 \text{ nV}/\sqrt{\text{Hz}}$
 $\rightarrow i_n = 0.6 \text{ pA}/\sqrt{\text{Hz}} \quad (I_b = 1 \text{ }\mu\text{A})$



Noise attains minimum for $\tau = 0.3 T$.

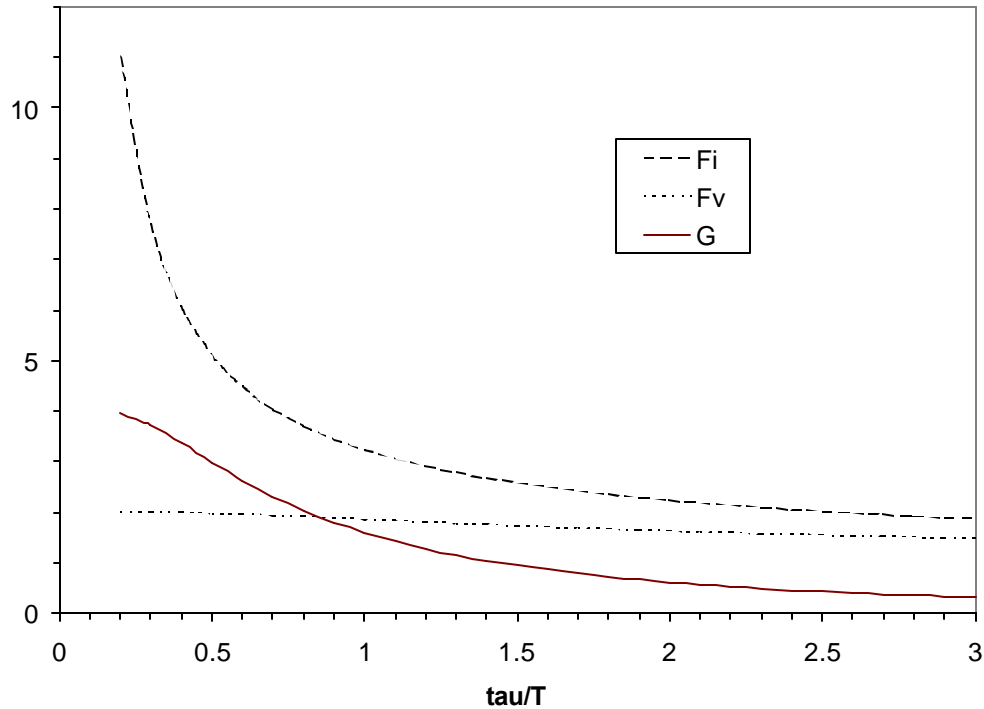
Parameters: $T = 100$ ns
 $C_d = 10$ pF
 $e_n = 2.5$ nV/√Hz
 $\rightarrow i_n = 0.2$ pA/√Hz ($I_b = 100$ nA)



Noise attains minimum for $\tau = 0.5 T$.

3. Shape Factors F_i , F_v and Signal Gain G vs. τ / T

Note: In this plot the form factors F_i , F_v are not yet corrected by the gain G .



The voltage noise coefficient is practically independent of τ / T .

Voltage contribution to noise charge dominated by C_i/τ .

The current noise coefficient increases rapidly at small τ / T .

At small τ / T (large T) the contribution to the noise charge increases because the integration time is larger.

The gain dependence increases the equivalent noise charge with increasing τ / T (as the gain is in the denominator).

Noise in Transistors

a) Noise in Field Effect Transistors

The primary noise sources in field effect transistors are

- a) thermal noise in the channel
- b) gate current in JFETs

Since the area of the gate is small, this contribution to the noise is very small and usually can be neglected.

Thermal velocity fluctuations of the charge carriers in the channel superimpose a noise current on the output current.

The spectral density of the noise current at the drain is

$$i_{nd}^2 = \frac{N_{C,tot} q_e}{L^2} \mu_0 4k_B T_e$$

The current fluctuations depend on the number of charge carriers in the channel $N_{C,tot}$ and their thermal velocity, which in turn depends on their temperature T_e and low field mobility μ_0 . Finally, the induced current scales with $1/L$ because of Ramo's theorem.

To make practical use of the above expression it is necessary to express it in terms of directly measurable device parameters. Since the transconductance in the saturation region

$$g_m \propto \frac{W}{L} \mu N_{ch} d$$

one can express the noise current as

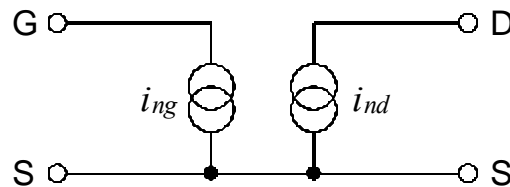
$$i_{nd}^2 = \gamma_n g_m 4k_B T_0$$

where $T_0 = 300\text{K}$ and γ_n is a semi-empirical constant that depends on the carrier concentration in the channel and the device geometry.

In a JFET the gate noise current is the shot noise associated with the reverse bias current of the gate-channel diode

$$i_{ng} = 2q_e I_G$$

The noise model of the FET



The gate and drain noise currents are independent of one another.

However, if an impedance Z is connected between the gate and the source, the gate noise current will flow through this impedance and generate a voltage at the gate

$$e_{ng} = Z i_{ng}$$

leading to an additional noise current at the output $g_m v_{ng}$, so that the total noise current at the output becomes

$$i_{no}^2 = i_{nd}^2 + (g_m Z i_{ng})^2$$

To allow a direct comparison with the input signal this cumulative noise will be referred back to the input to yield the equivalent input noise voltage

$$e_{ni}^2 = \frac{i_{no}^2}{g_m^2} = \frac{i_{nd}^2}{g_m^2} + Z^2 i_{ng}^2 \equiv e_n^2 + Z i_n^2$$

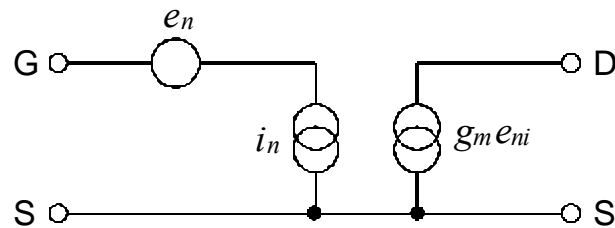
i.e. referred to the input, the drain noise current i_{nd} translates into a noise voltage source

$$e_n^2 = 4k_B T_0 \frac{\gamma_n}{g_m}$$

The noise coefficient γ_n is usually given as 2/3, but is typically in the range 0.5 to 1 (exp. data will shown later).

This expression describes the noise of both JFETs and MOSFETs.

In this parameterization the noise model becomes



where e_n and i_n are the input voltage and current noise. As was shown above, these contribute to the input noise voltage e_{ni} , which in turn translates to the output through the transconductance g_m to yield a noise current at the output $g_m e_{ni}$.

The equivalent noise charge

$$Q_n^2 = i_n^2 F_i T + e_n^2 C_i^2 \frac{F_v}{T}$$

For a representative JFET $g_m = 0.02$, $C_i = 10$ pF and $I_G < 150$ pA. If $F_i = F_v = 1$

$$Q_n^2 = 1.9 \cdot 10^9 T + \frac{3.25 \cdot 10^{-3}}{T}$$

As the shaping time T is reduced, the current noise contribution decreases and the voltage noise contribution increases. For $T = 1$ μ s the current contribution is 43 el and the voltage contribution 3250 el, so the current contribution is negligible, except in very low frequency applications.

Optimization of Device Geometry

For a given device technology and normalized operating current I_D/W both the transconductance and the input capacitance are proportional to device width W

$$g_m \propto W \quad \text{and} \quad C_i \propto W$$

so that the ratio

$$\frac{g_m}{C_i} = \text{const}$$

Then the signal-to-noise ratio can be written as

$$\left(\frac{S}{N}\right)^2 = \frac{(Q_s / C)^2}{v_n^2} = \frac{Q_s^2}{(C_{\text{det}} + C_i)^2} \frac{g_m}{4k_B T_0 \Delta f}$$

$$\left(\frac{S}{N}\right)^2 = \frac{Q_s^2}{\Delta f} \frac{1}{4k_B T_0} \left(\frac{g_m}{C_i}\right) \frac{1}{C_i \left(1 + \frac{C_{\text{det}}}{C_i}\right)^2}$$

S/N is maximized for $C_i = C_{\text{det}}$ (capacitive matching).

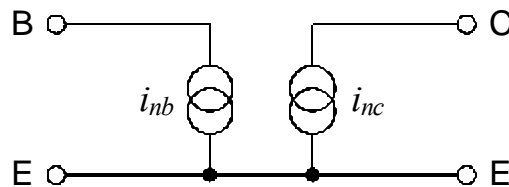
$C_i \ll C_{\text{det}}$: The detector capacitance dominates, so the effect of increased transistor capacitance is negligible. As the device width is increased the transconductance increases and the equivalent noise voltage decreases, so S/N improves.

$C_i > C_{\text{det}}$: The equivalent input noise voltage decreases as the device width is increased, but only with $1/W$, so the increase in capacitance overrides, decreasing S/N .

b) Noise in Bipolar Transistors

In bipolar transistors the shot noise from the base current is important.

The basic noise model is the same as shown before, but the magnitude of the input noise current is much greater, as the base current will be 1 – 100 μA rather than <100 pA.



The base current noise is shot noise associated with the component of the emitter current provided by the base.

$$i_{nb}^2 = 2q_e I_B$$

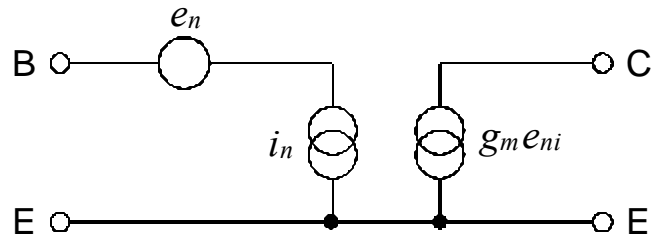
The noise current in the collector is the shot noise originating in the base-emitter junction associated with the collector component of the emitter current.

$$i_{nc}^2 = 2q_e I_C$$

Following the same argument as in the analysis of the FET, the output noise current is equivalent to an equivalent noise voltage

$$e_n^2 = \frac{i_{nc}^2}{g_m^2} = \frac{2q_e I_C}{(q_e I_C / k_B T)^2} = \frac{2(k_B T)^2}{q_e I_C}$$

yielding the noise equivalent circuit



where i_n is the base current shot noise i_{nb} .

The equivalent noise charge

$$Q_n^2 = i_n^2 F_i T + e_n^2 C^2 \frac{F_v}{T} = 2q_e I_B F_i T + \frac{2(k_B T)^2}{q_e I_C} C^2 \frac{F_v}{T}$$

Since $I_B = I_C / \beta_{DC}$

$$Q_n^2 = 2q_e \frac{I_C}{\beta_{DC}} F_i T + \frac{2(k_B T)^2}{q_e I_C} C^2 \frac{F_v}{T}$$

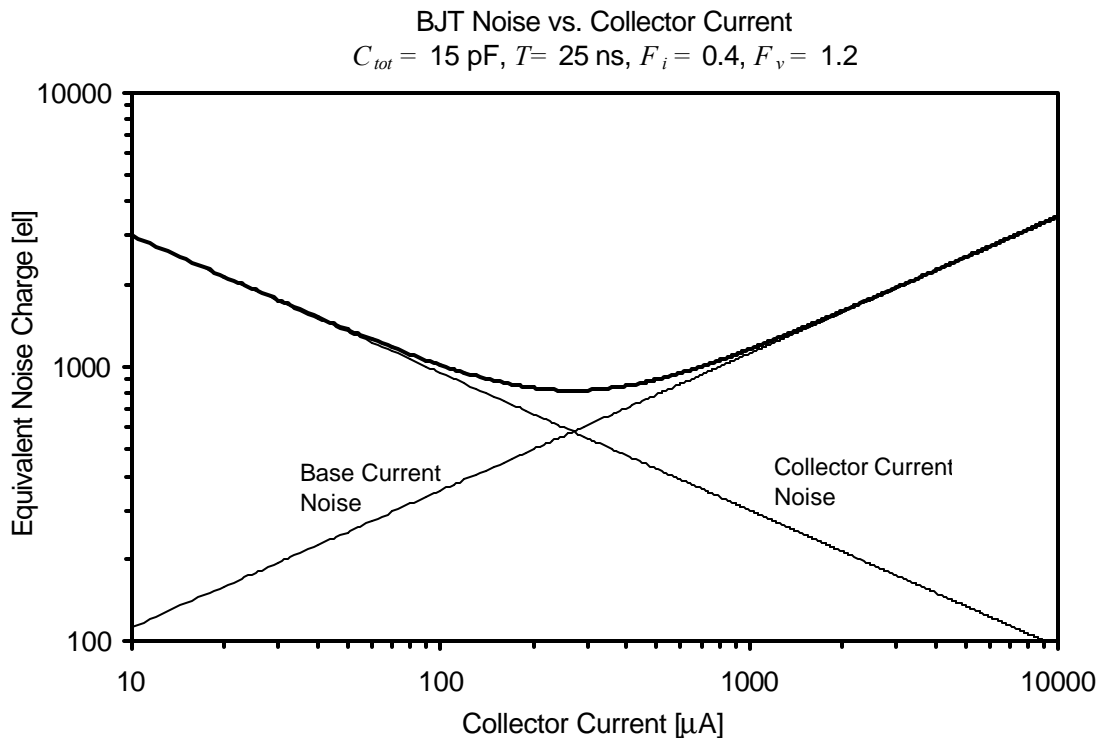
The current noise term increases with I_C , whereas the second (voltage) noise term decreases with I_C .

Thus, the noise attains a minimum

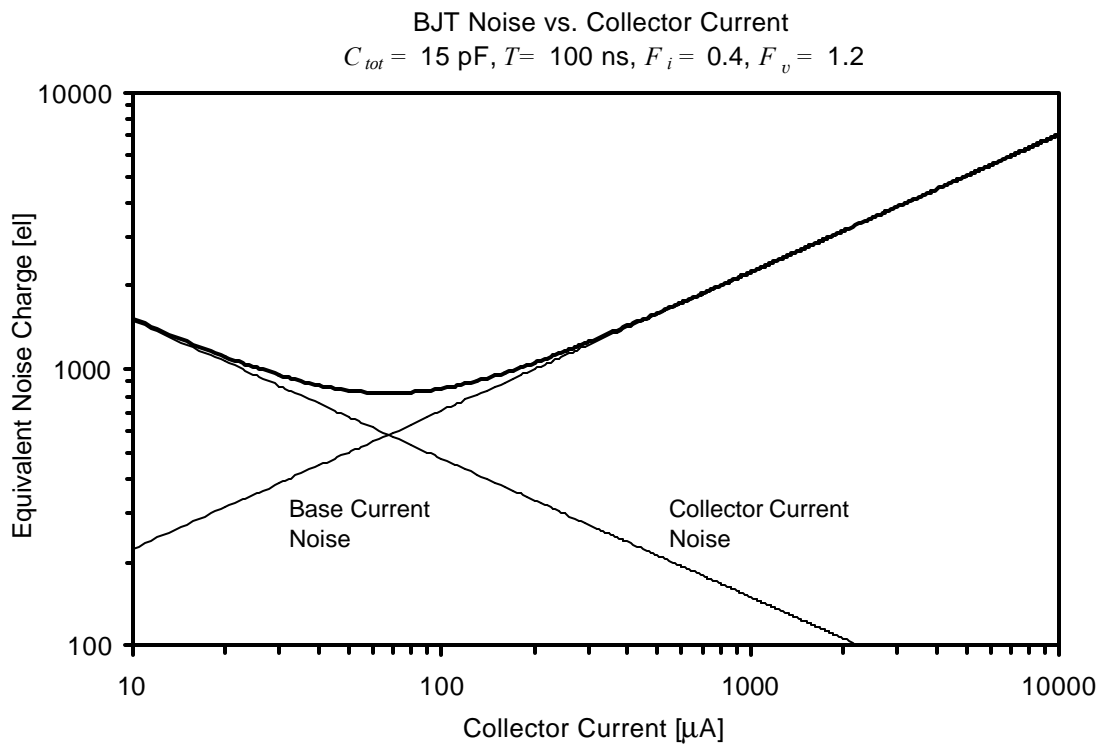
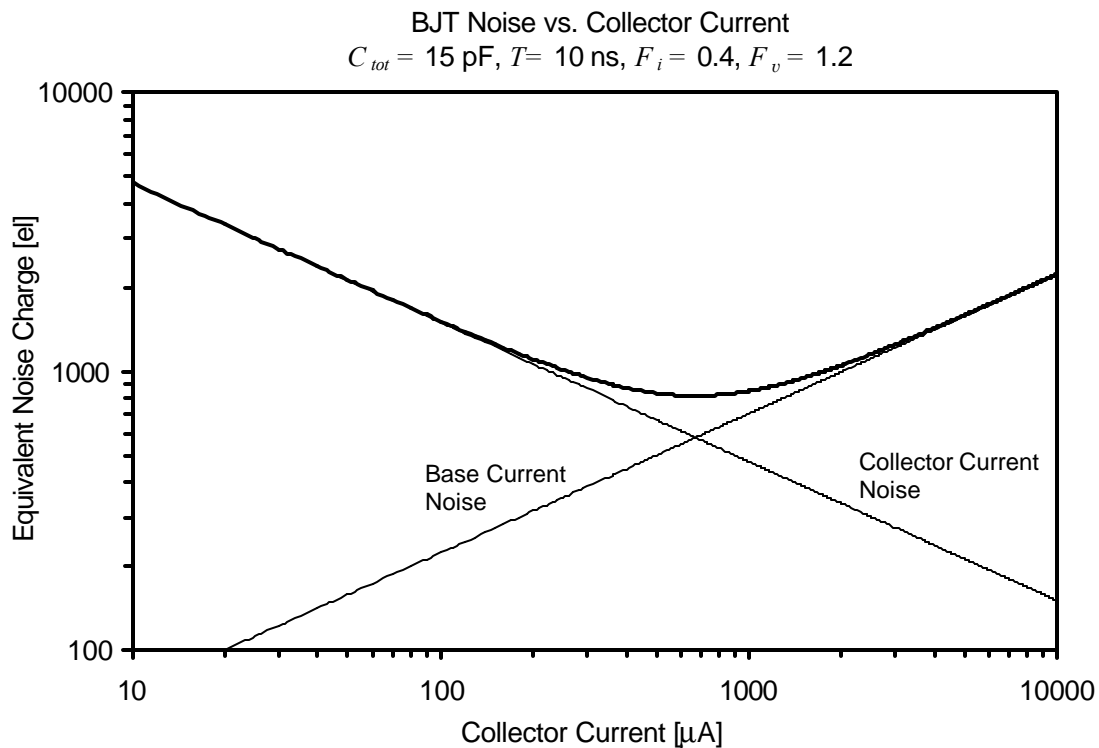
$$Q_{n,\min}^2 = 4k_B T \frac{C}{\sqrt{\beta_{DC}}} \sqrt{F_i F_v}$$

at a collector current

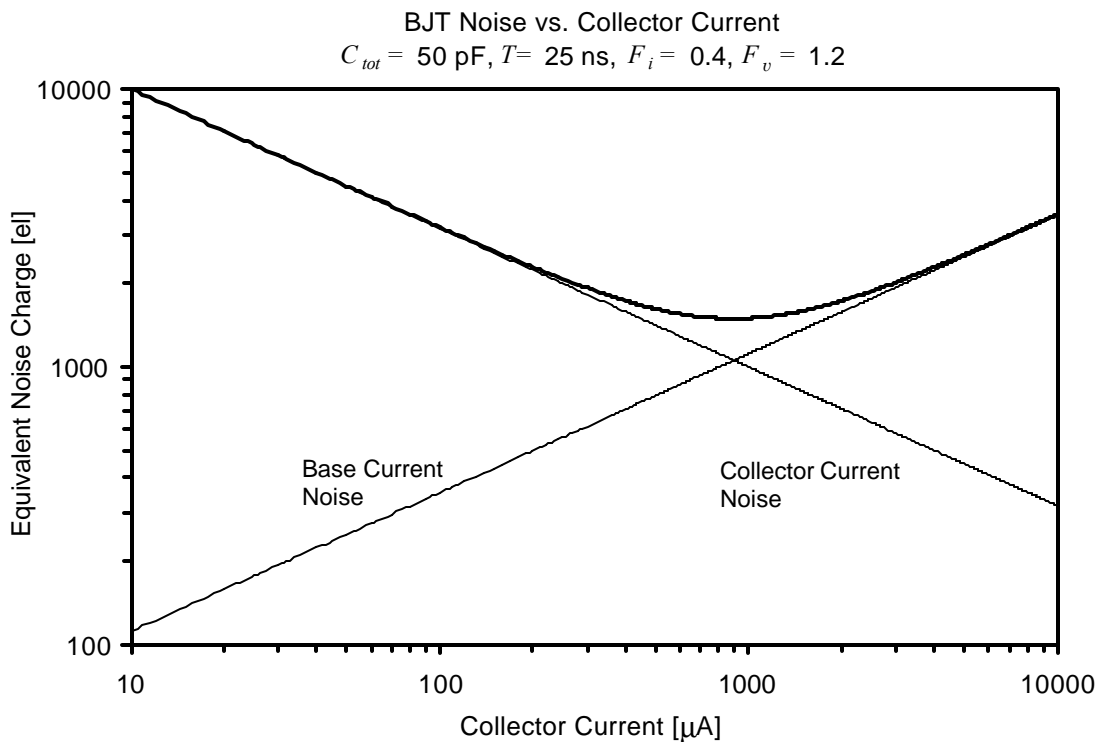
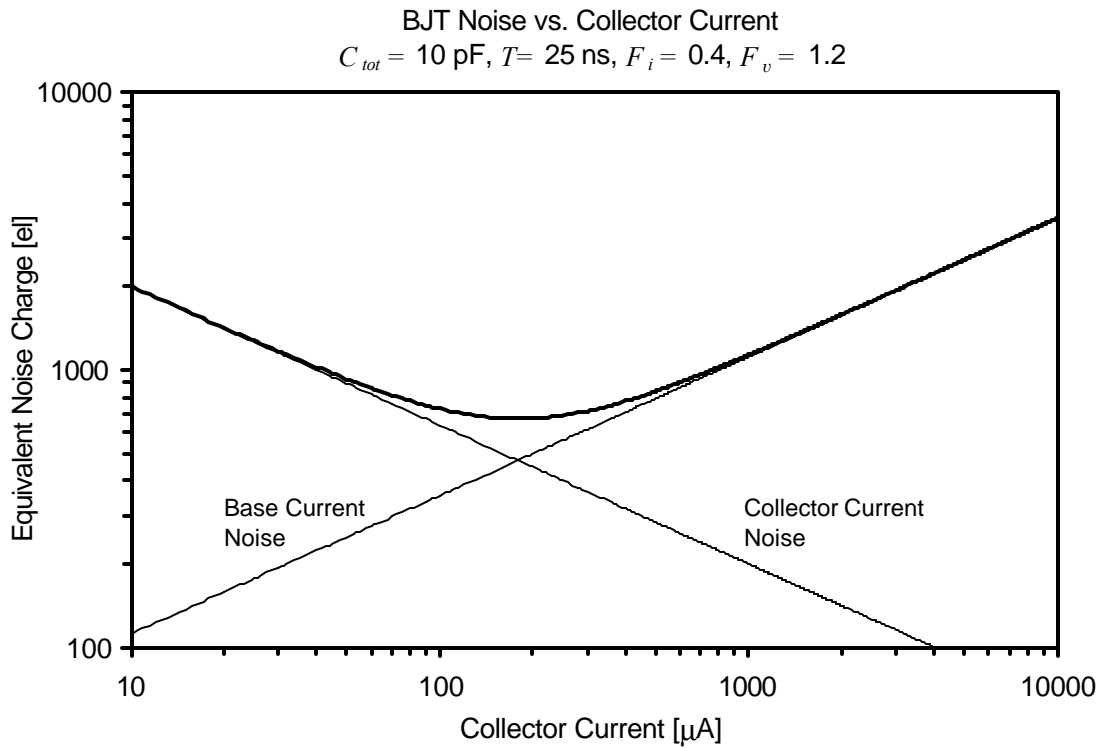
$$I_C = \frac{k_B T}{q_e} C \sqrt{\beta_{DC}} \sqrt{\frac{F_v}{F_i}} \frac{1}{T} .$$



- For a given shaper, the minimum obtainable noise is determined only by the total capacitance at the input and the DC current gain of the transistor, *not by the shaping time*.
- The shaping time only determines the current at which this minimum noise is obtained

$T = 100 \text{ ns}$

 $T = 10 \text{ ns}$


Increasing the capacitance at the input shifts the collector current noise curve upwards, so the noise increases and the minimum shifts to a higher current.



Simple Estimate of obtainable BJT noise

For a CR-RC shaper

$$Q_{n,\min} = 772 \left[\frac{el}{\sqrt{pF}} \right] \cdot \frac{\sqrt{C}}{\sqrt[4]{\beta_{DC}}}$$

obtained at
$$I_c = 26 \left[\frac{\mu A \cdot ns}{pF} \right] \cdot \frac{C}{\tau} \sqrt{\beta_{DC}}$$

Since typically $\beta_{DC} \approx 100$, these expressions allow a quick and simple estimate of the noise obtainable with a bipolar transistor.

Note that specific shapers can be optimized to minimize either the current or the voltage noise contribution, so both the minimum obtainable noise and the optimum current will be change with respect to the above estimates.

The noise characteristics of bipolar transistors differ from field effect transistors in four important aspects:

1. The equivalent input noise current cannot be neglected, due to base current flow.
2. The total noise does not decrease with increasing device current.
3. The minimum obtainable noise does not depend on the shaping time.
4. The input capacitance is usually negligible.

The last statement requires some explanation.

The input capacitance of a bipolar transistor is dominated by two components,

1. the geometrical junction capacitance, or transition capacitance C_{TE} , and
2. the diffusion capacitance C_{DE} .

The transition capacitance in small devices is typically about 0.5 pF.

The diffusion capacitance depends on the current flow I_E through the base-emitter junction and on the base width W , which sets the diffusion profile.

$$C_{DE} = \frac{\partial q_B}{\partial V_{be}} = \frac{q_e I_E}{k_B T} \left(\frac{W}{2D_B} \right) \equiv \frac{q_e I_E}{k_B T} \cdot \frac{1}{\omega_{Ti}}$$

where D_B is the diffusion constant in the base and ω_{Ti} is a frequency that characterizes carrier transport in the base. ω_{Ti} is roughly equal to the frequency where the current gain of the transistor is unity.

Inserting some typical values, $I_E=100 \mu\text{A}$ and $\omega_{Ti}=10 \text{ GHz}$, yields $C_{DE}=0.4 \text{ pF}$. The transistor input capacitance $C_{TE}+C_{DE}=0.9 \text{ pF}$, whereas FETs providing similar noise values at comparable currents have input capacitances in the range 5 – 10 pF.

Except for low capacitance detectors, the current dependent part of the BJT input capacitance is negligible, so it will be neglected in the following discussion. For practical purposes the amplifier input capacitance can be considered constant at 1 ... 1.5 pF.

This leads to another important conclusion.

Since the primary noise parameters do not depend on device size and there is no significant linkage between noise parameters and input capacitance

- Capacitive matching does not apply to bipolar transistors.

Indeed, capacitive matching is a misguided concept for bipolar transistors. Consider two transistors with the same DC current gain but different input capacitances. Since the minimum obtainable noise

$$Q_{n,\min}^2 = 4k_B T \frac{C}{\sqrt{\beta_{DC}}} \sqrt{F_i F_v} ,$$

increasing the transistor input capacitance merely increases the total input capacitance C_{tot} and the obtainable noise.

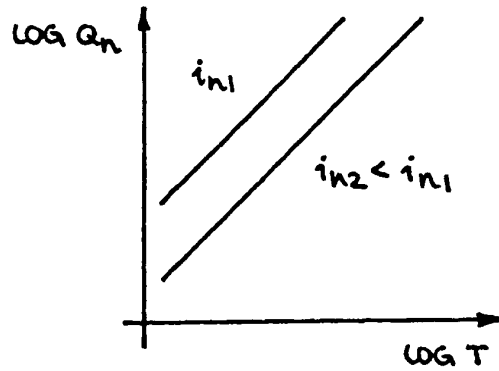
When to use FETs and when to use BJTs?

Since the base current noise increases with shaping time, bipolar transistors are only advantageous at short shaping times.

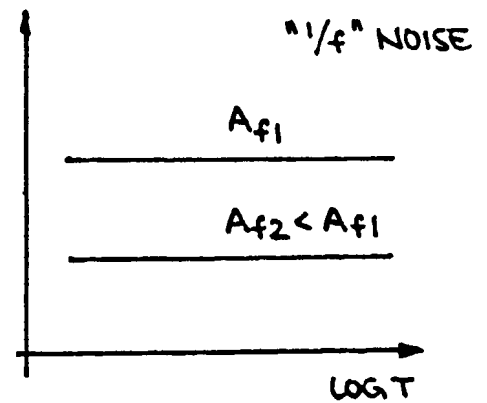
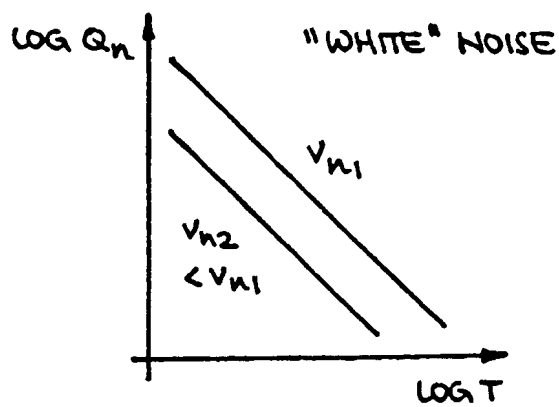
With current technologies FETs are best at shaping times greater than 50 to 100 ns, but decreasing feature size of MOSFETs will improve their performance.

1. Equivalent Noise Charge vs. Pulse Width

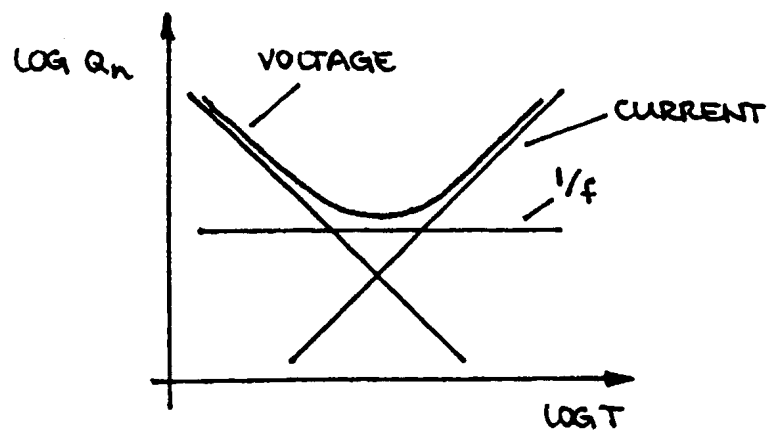
Current Noise vs. T



Voltage Noise vs. T



Total Equivalent Noise Charge



2. Equivalent Noise Charge vs. Detector Capacitance ($C = C_d + C_a$)

$$Q_n = \sqrt{i_n^2 F_i T + (C_d + C_a)^2 e_n^2 F_v \frac{1}{T}}$$

$$\frac{dQ_n}{dC_d} = \frac{2C_d e_n^2 F_v \frac{1}{T}}{\sqrt{i_n^2 F_i T + (C_d + C_a)^2 e_n^2 F_v \frac{1}{T}}}$$

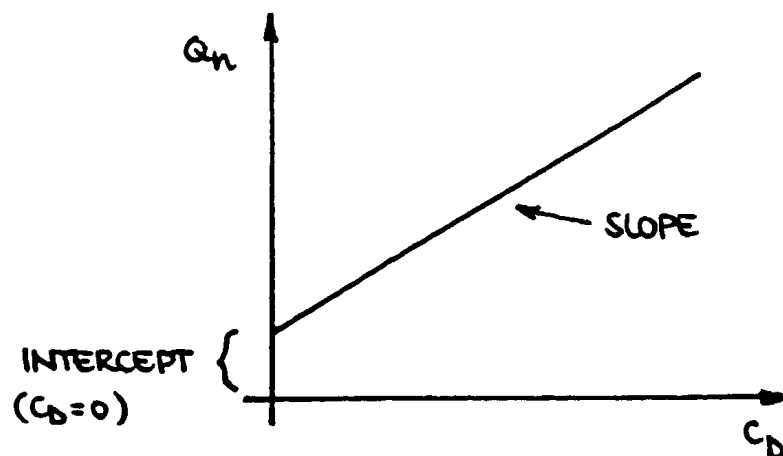
If current noise $i_n^2 F_i T$ is negligible

$$\frac{dQ_n}{dC_d} \approx 2e_n \cdot \sqrt{\frac{F_v}{T}}$$

\uparrow \uparrow
 input shaper
 stage

Zero intercept

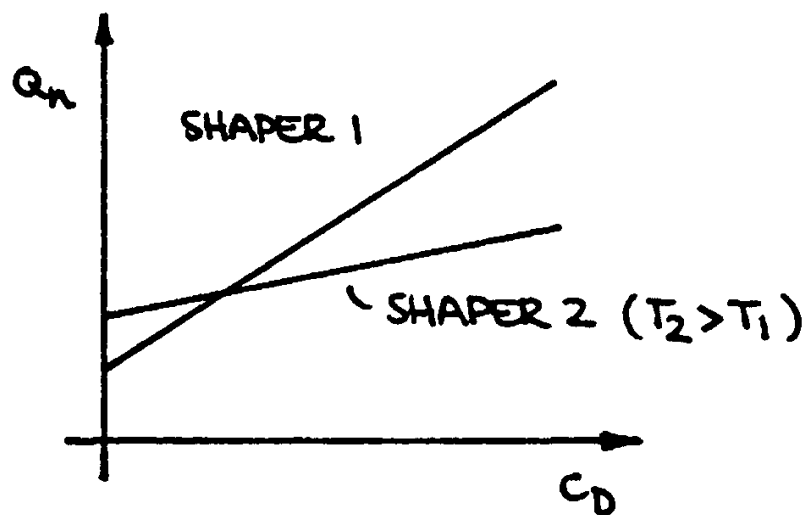
$$Q_n|_{C_d=0} = C_a e_n \sqrt{F_v / T}$$



Noise slope is a convenient measure to compare preamplifiers and predict noise over a range of capacitance.

Caution: both noise slope and zero intercept depend on *both the preamplifier and the shaper*

Same preamplifier, but different shapers:



Caution: Noise slope is only valid when current noise negligible.

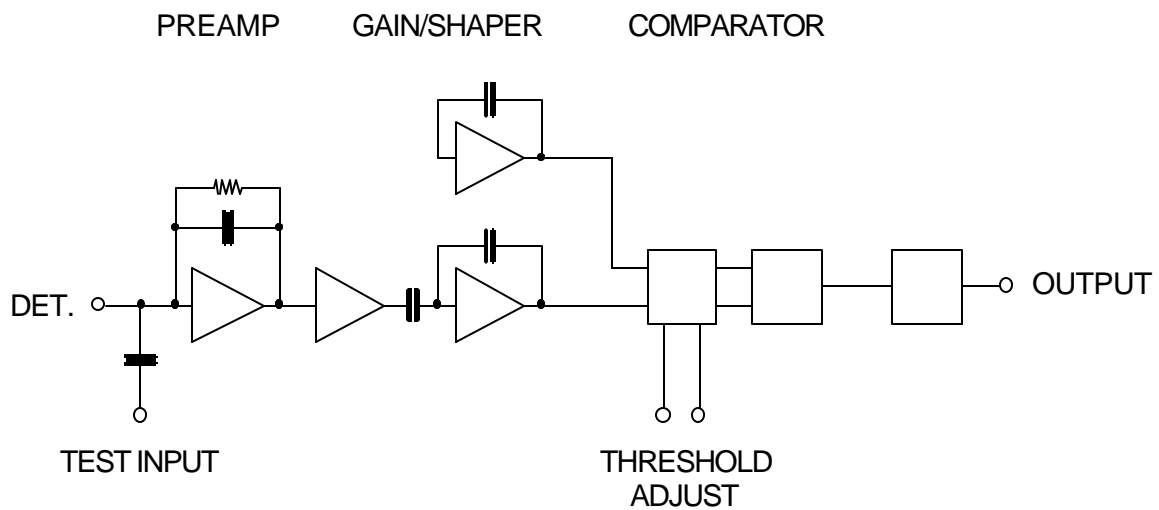
Current noise contribution may be negligible at high detector capacitance, but not for $C_d=0$ where the voltage noise contribution is smaller.

$$Q_n|_{C_d=0} = \sqrt{i_n^2 F_i T + C_a^2 e_n^2 F_v / T}$$

Rate of Noise Pulses in Threshold Discriminator Systems

Noise affects not only the resolution of amplitude measurements, but also the determines the minimum detectable signal threshold.

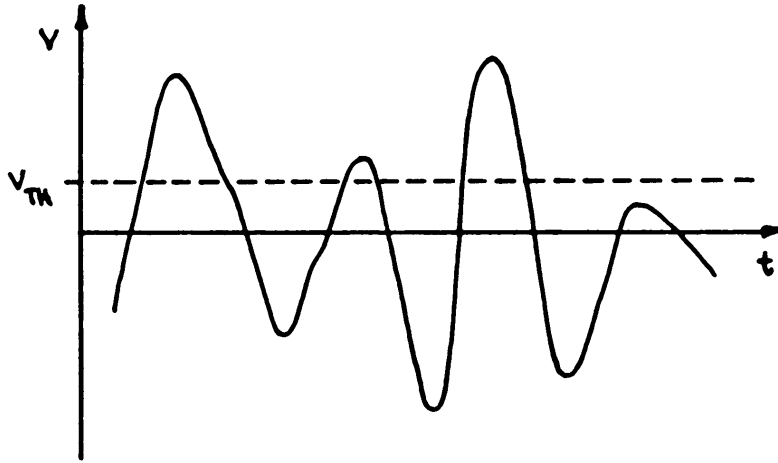
Consider a system that only records the presence of a signal if it exceeds a fixed threshold.



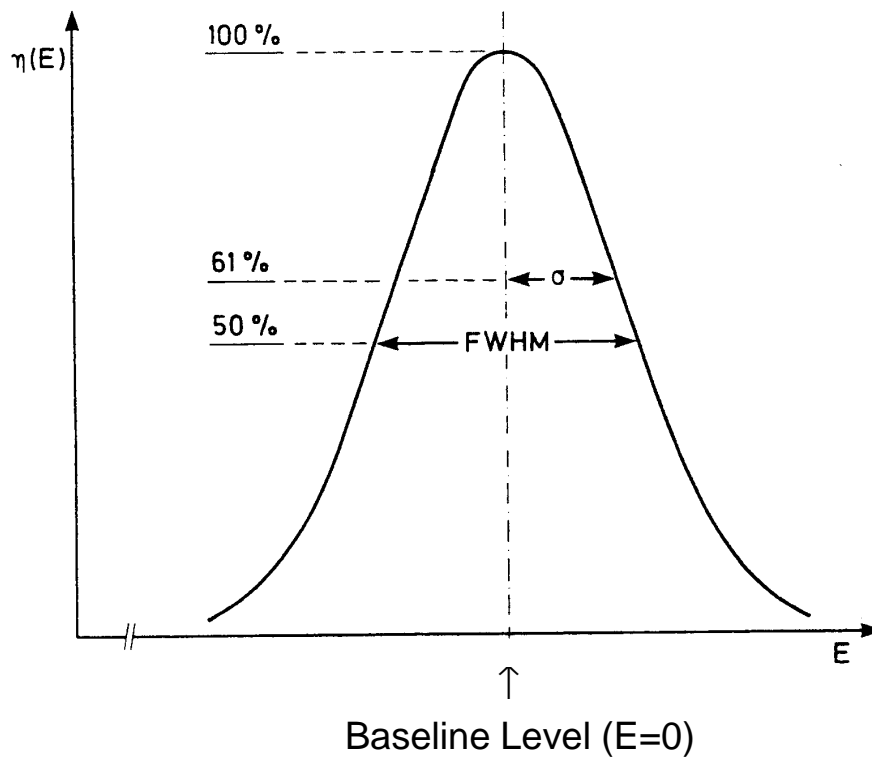
How small a detector pulse can still be detected reliably?

Consider the system at times when no detector signal is present.

Noise will be superimposed on the baseline.



The amplitude distribution of the noise is gaussian.



With the threshold level set to 0 relative to the baseline, all of the positive excursions will be recorded.

Assume that the desired signals are occurring at a certain rate.

If the detection reliability is to be >99%, then the rate of noise hits must be less than 1% of the signal rate.

The rate of noise hits can be reduced by increasing the threshold.

If the system were sensitive to pulse magnitude alone, the integral over the gaussian distribution (the error function) would determine the factor by which the noise rate f_{n0} is reduced.

$$\frac{f_n}{f_{n0}} = \frac{1}{Q_n \sqrt{2\pi}} \int_{Q_T}^{\infty} e^{-(Q/2Q_n)^2} dQ$$

where Q is the equivalent signal charge, Q_n the equivalent noise charge and Q_T the threshold level. However, since the pulse shaper broadens each noise impulse, the time dependence is equally important. For example, after a noise pulse has crossed the threshold, a subsequent pulse will not be recorded if it occurs before the trailing edge of the first pulse has dropped below threshold.

The **combined probability function** for gaussian time and amplitude distributions yields the expression for the noise rate as a function of threshold-to-noise ratio.

$$f_n = f_{n0} \cdot e^{-Q_T^2/2Q_n^2}$$

Of course, one can just as well use the corresponding voltage levels.

What is the noise rate at zero threshold f_{n0} ?

Since we are interested in the number of positive excursions exceeding the threshold, f_{n0} is $\frac{1}{2}$ the frequency of zero-crossings.

A rather lengthy analysis of the time dependence shows that the frequency of zero crossings at the output of an ideal band-pass filter with lower and upper cutoff frequencies f_1 and f_2 is

$$f_0 = 2 \sqrt{\frac{1}{3} \frac{f_2^3 - f_1^3}{f_2 - f_1}}$$

(Rice, Bell System Technical Journal, **23** (1944) 282 and **24** (1945) 46)

For a *CR-RC* filter with $\tau_i = \tau_d$ the ratio of cutoff frequencies of the noise bandwidth is

$$\frac{f_2}{f_1} = 4.5$$

so to a good approximation one can neglect the lower cutoff frequency and treat the shaper as a low-pass filter, *i.e.* $f_1 = 0$. Then

$$f_0 = \frac{2}{\sqrt{3}} f_2$$

An ideal bandpass filter has infinitely steep slopes, so the upper cutoff frequency f_2 must be replaced by the noise bandwidth.

The noise bandwidth of an *RC* low-pass filter with time constant τ is

$$\Delta f_n = \frac{1}{4\tau}$$

Setting $f_2 = \Delta f_n$ yields the frequency of zeros

$$f_0 = \frac{1}{2\sqrt{3}\tau}$$

and the frequency of noise hits vs. threshold

$$f_n = f_{n0} \cdot e^{-Q_{th}^2/2Q_n^2} = \frac{f_0}{2} \cdot e^{-Q_{th}^2/2Q_n^2} = \frac{1}{4\sqrt{3}\tau} \cdot e^{-Q_{th}^2/2Q_n^2}$$

Thus, the required threshold-to-noise ratio for a given frequency of noise hits f_n is

$$\frac{Q_T}{Q_n} = \sqrt{-2 \log(4\sqrt{3} f_n \tau)}$$

Note that the threshold-to-noise ratio determines the product of noise rate and shaping time, i.e. for a given threshold-to-noise ratio the noise rate is higher at short shaping times

- ⇒ The noise rate for a given threshold-to-noise ratio is proportional to bandwidth.
- ⇒ To obtain the same noise rate, a fast system requires a larger threshold-to-noise ratio than a slow system with the same noise level.

Frequently a threshold discriminator system is used in conjunction with other detectors that provide additional information, for example the time of a desired event.

In a collider detector the time of beam crossings is known, so the output of the discriminator is sampled at specific times.

The number of recorded noise hits then depends on

1. the sampling frequency (e.g. bunch crossing frequency) f_S
2. the width of the sampling interval Δt , which is determined by the time resolution of the system.

The product $f_S \Delta t$ determines the fraction of time the system is open to recording noise hits, so the rate of recorded noise hits is $f_S \Delta t f_n$.

Often it is more interesting to know the probability of finding a noise hit in a given interval, i.e. the occupancy of noise hits, which can be compared to the occupancy of signal hits in the same interval.

This is the situation in a storage pipeline, where a specific time interval is read out after a certain delay time (e.g. trigger latency)

The occupancy of noise hits in a time interval Δt

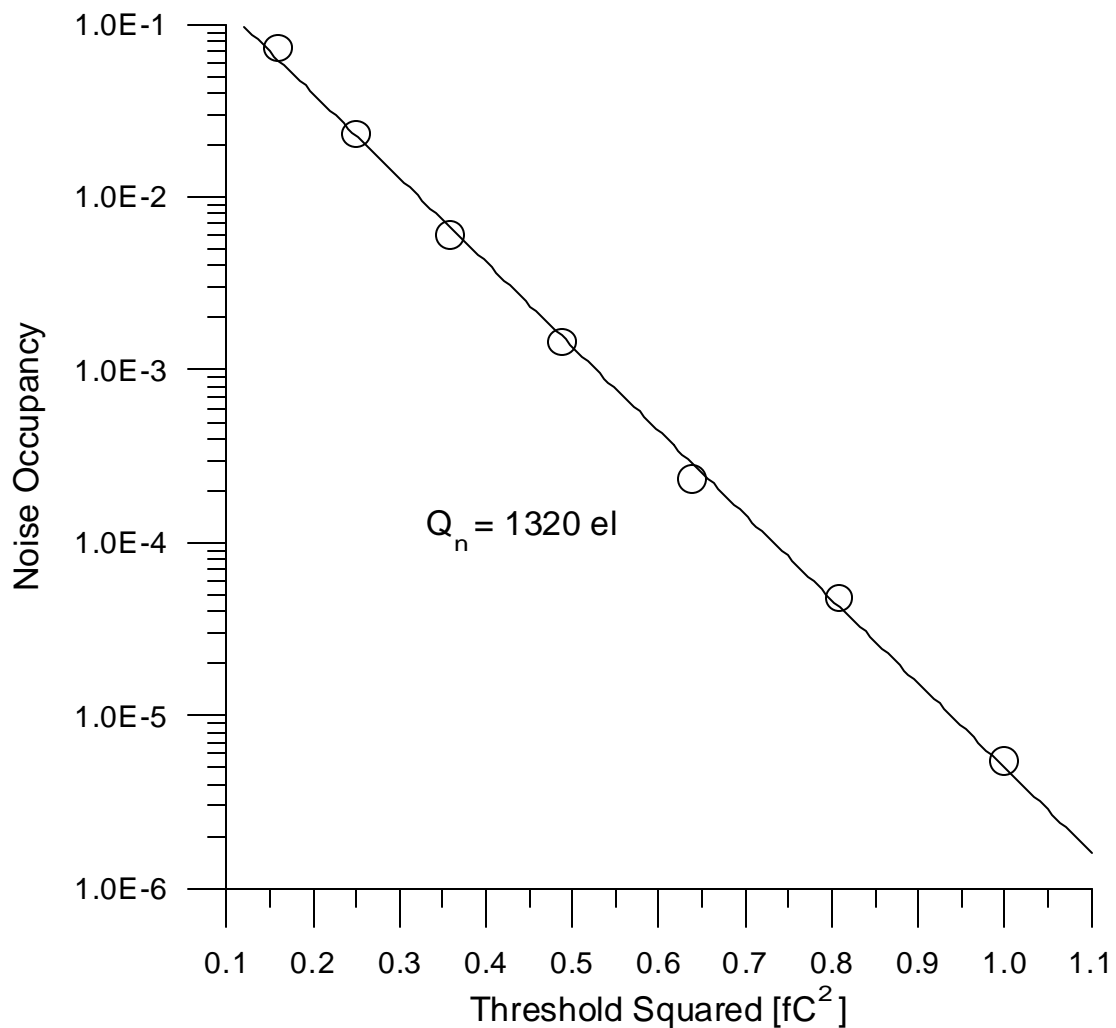
$$P_n = \Delta t \cdot f_n = \frac{\Delta t}{2\sqrt{3}\tau} \cdot e^{-Q_T^2/2Q_n^2}$$

i.e. the occupancy falls exponentially with the square of the threshold-to-noise ratio.

The dependence of occupancy on threshold can be used to measure the noise level.

$$\log P_n = \log\left(\frac{\Delta t}{2\sqrt{3}\tau}\right) - \frac{1}{2}\left(\frac{Q_T}{Q_n}\right)^2$$

so the *slope* of $\log P_n$ vs. Q_T^2 yields the noise level, *independently of the details of the shaper*, which affect only the offset.



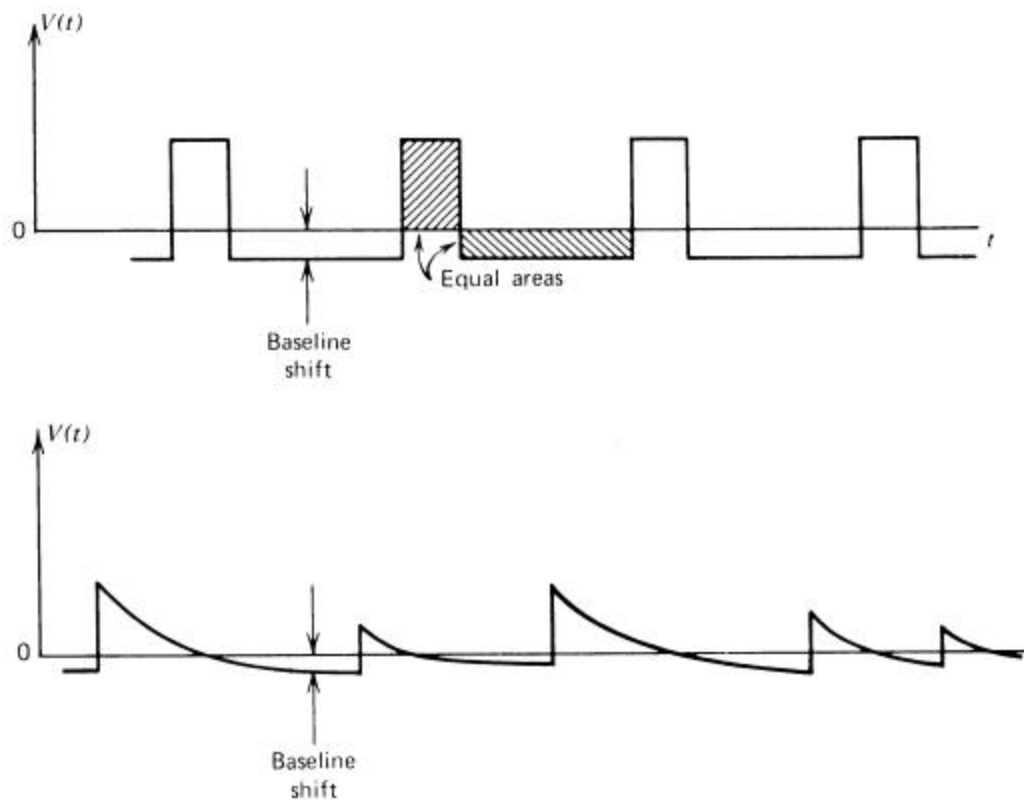
3. Some Other Aspects of Pulse Shaping

3.1 Baseline Restoration

Any series capacitor in a system prevents transmission of a DC component.

A sequence of unipolar pulses has a DC component that depends on the duty factor, i.e. the event rate.

⇒ The baseline shifts to make the overall transmitted charge equal zero.



(from Knoll)

Random rates lead to random fluctuations of the baseline shift

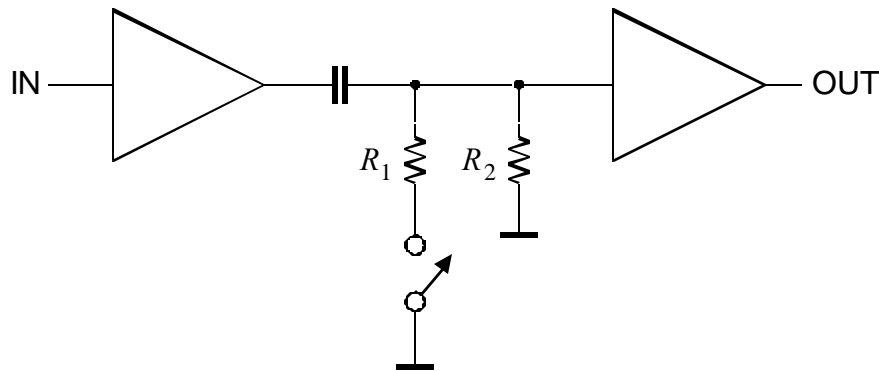
⇒ spectral broadening

- These shifts occur whenever the DC gain is not equal to the midband gain

The baseline shift can be mitigated by a baseline restorer (BLR).

Principle of a baseline restorer:

Connect signal line to ground during the absence of a signal to establish the baseline just prior to the arrival of a pulse.



R_1 and R_2 determine the charge and discharge time constants. The discharge time constant (switch opened) must be much larger than the pulse width.

Originally performed with diodes (passive restorer), baseline restoration circuits now tend to include active loops with adjustable thresholds to sense the presence of a signal (gated restorer). Asymmetric charge and discharge time constants improve performance at high count rates.

- This is a form of time-variant filtering. Care must be exercised to reduce noise and switching artifacts introduced by the BLR.
- Good pole-zero cancellation (next topic) is crucial for proper baseline restoration.

3.2 Pole Zero Cancellation

Feedback capacitor in charge sensitive preamplifier must be discharged. Commonly done with resistor.

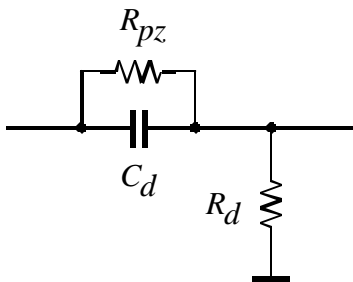
Output no longer a step, but decays exponentially

Exponential decay superimposed on shaper output.

⇒ undershoot

⇒ loss of resolution due to baseline variations

Add R_{pz} to differentiator:

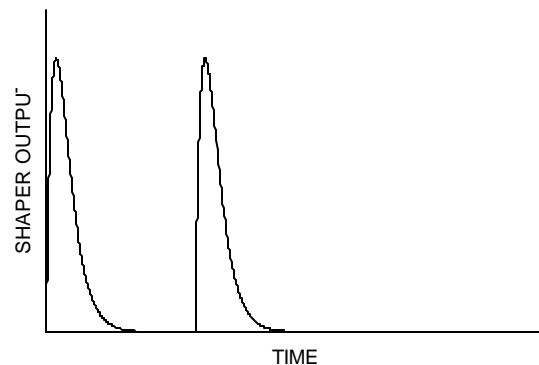
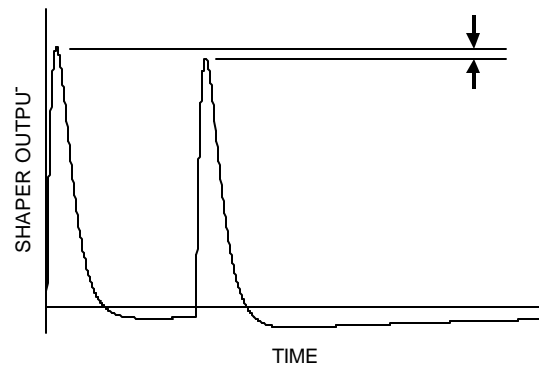
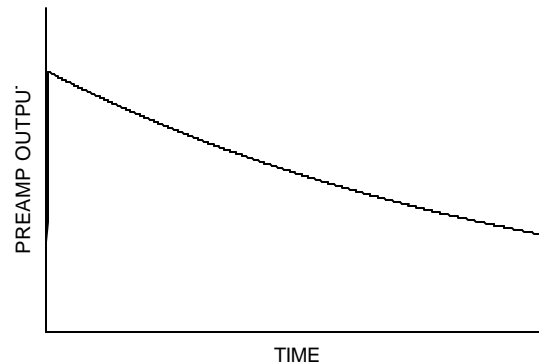
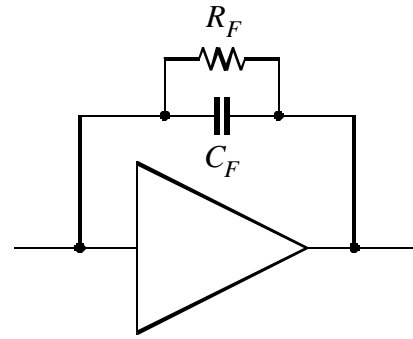


“zero” cancels “pole” of preamp when $R_F C_F = R_{pz} C_d$

Not needed in pulsed reset circuits (optical or transistor)

Technique also used to compensate for “tails” of detector pulses: “tail cancellation”

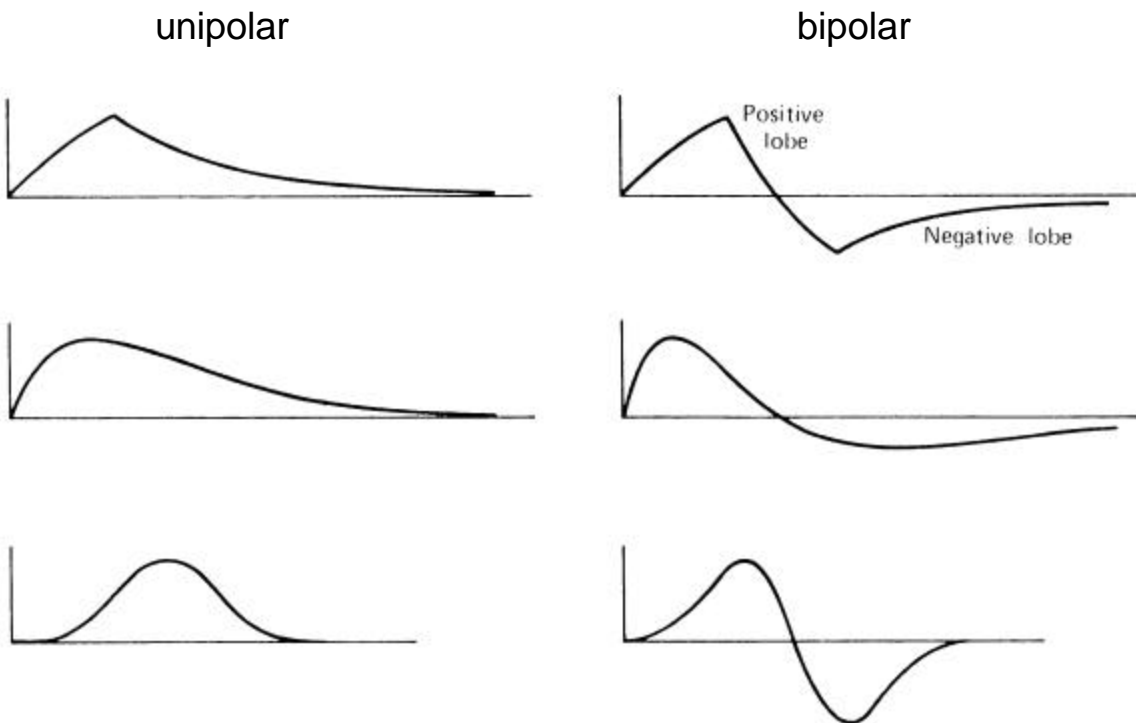
Critical for proper functioning of baseline restorer.



3.3 Bipolar vs. Unipolar Shaping

Unipolar pulse + 2nd differentiator → Bipolar pulse

Examples:



Electronic resolution with bipolar shaping typ. 25 – 50% worse than for corresponding unipolar shaper.

However ...

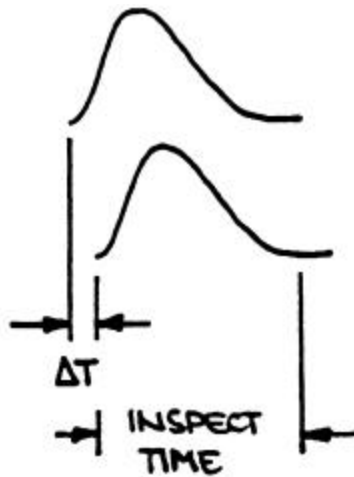
- Bipolar shaping eliminates baseline shift (as the DC component is zero).
- Pole-zero adjustment less critical
- Added suppression of low-frequency noise (see Part 7).
- Not all measurements require optimum noise performance. Bipolar shaping is much more convenient for the user (important in large systems!) – often the method of choice.

3.4 Pulse Pile-Up and Pile-Up Rejectors

pile-up \Rightarrow false amplitude measurement

Two cases:

1.



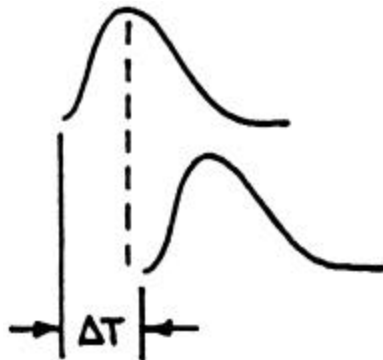
$\Delta T <$ time to peak

Both peak amplitudes are affected by superposition.

\Rightarrow Reject both pulses

Dead Time: $\Delta T +$ inspect time
(\sim pulse width)

2.



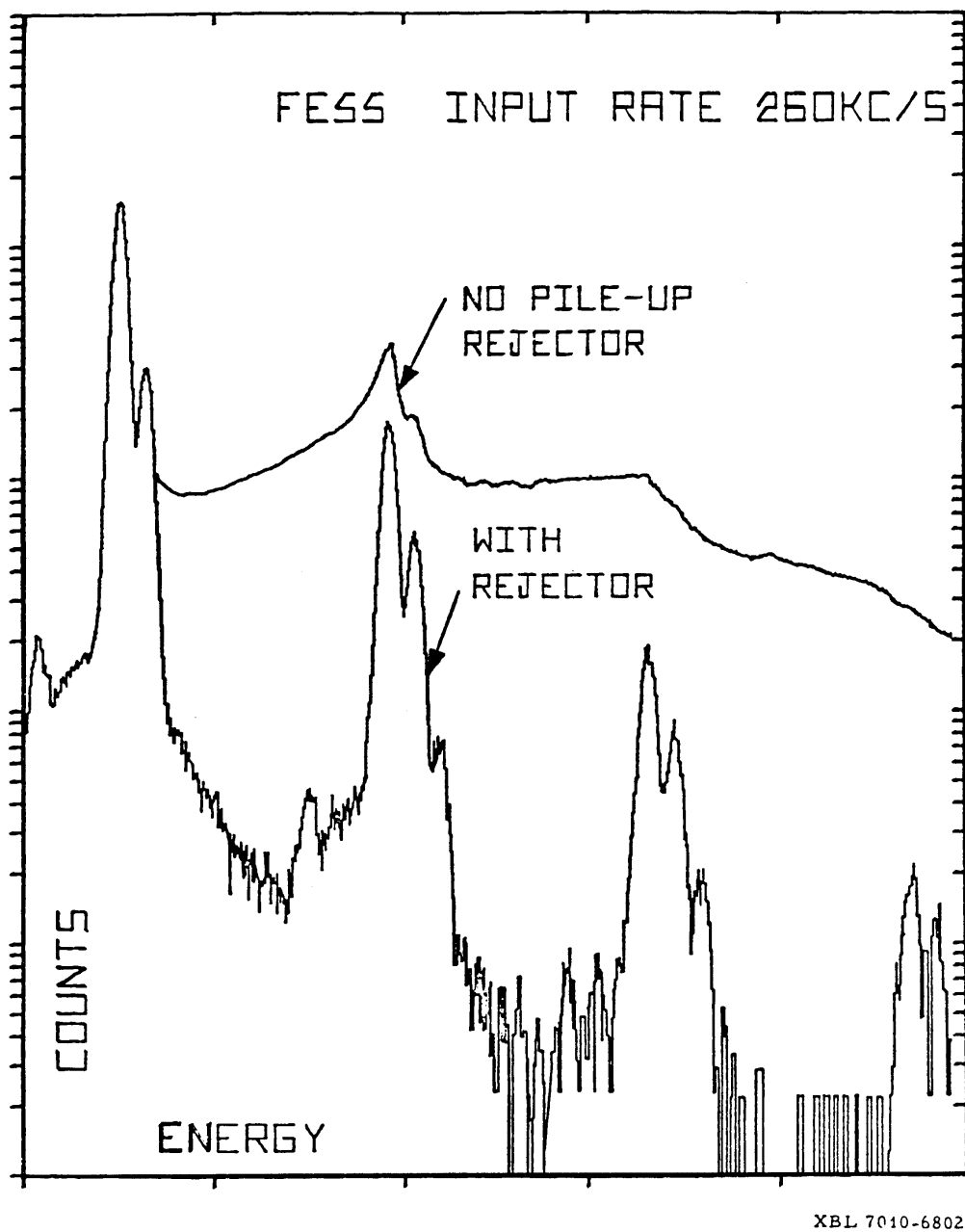
$\Delta T >$ time to peak and
 $\Delta T <$ inspect time, i.e.
time where amplitude of
first pulse \ll resolution

Peak amplitude of first pulse unaffected.

\Rightarrow Reject 2nd pulse only

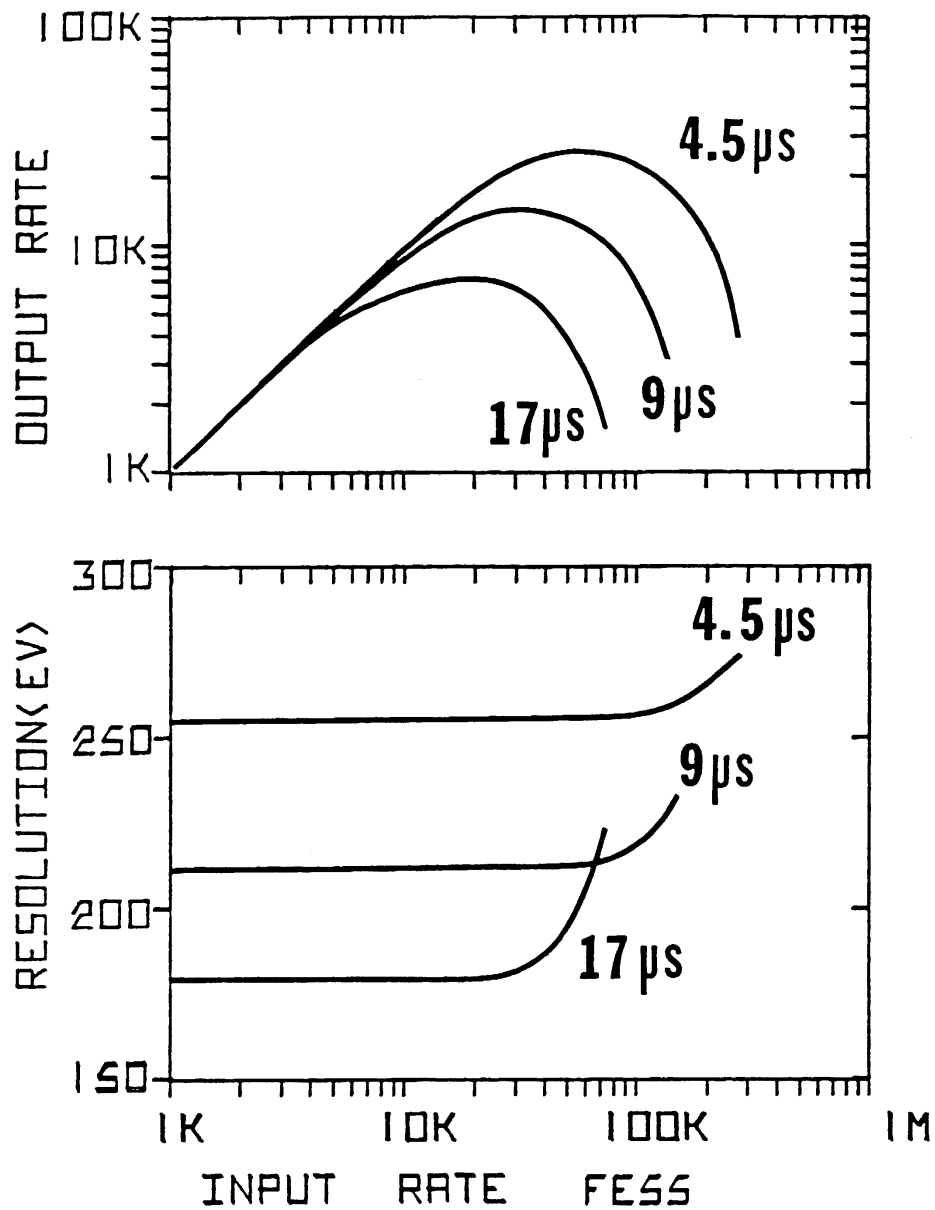
No additional dead time if first pulse accepted for digitization and dead time of ADC $>$
(DT + inspect time)

Typical Performance of a Pile-Up Rejector



(Don Landis)

Dead Time and Resolution vs. Counting Rate



(Joe Jaklevic)

Throughput peaks and then drops as the input rate increases, as most events suffer pile-up and are rejected.

Resolution also degrades beyond turnover point.

- Turnover rate depends on pulse shape and PUR circuitry.
- Critical to measure throughput vs. rate!

Limitations of Pile-Up Rejectors

Minimum dead time where circuitry can't recognize second pulse

⇒ spurious sum peaks

Detectable dead time depends on relative pulse amplitudes

e.g. small pulse following large pulse



⇒ amplitude-dependent rejection factor

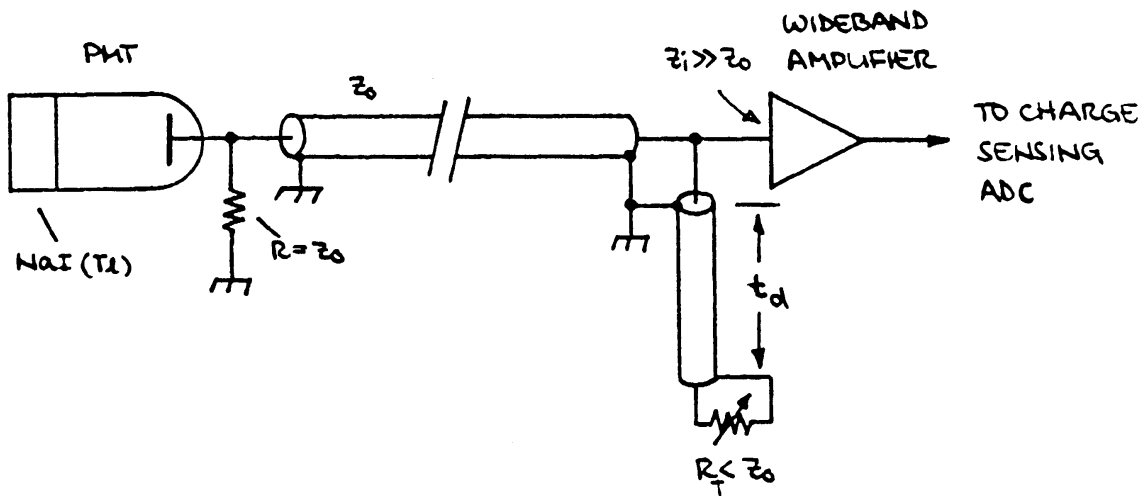
problem when measuring yields!

These effects can be evaluated and taken into account, but in experiments it is often appropriate to avoid these problems by using a shorter shaping time (trade off resolution for simpler analysis).

3.5 Delay-Line Clipping

In many instances, e.g. scintillation detectors, shaping is not used to improve resolution, but to increase rate capability.

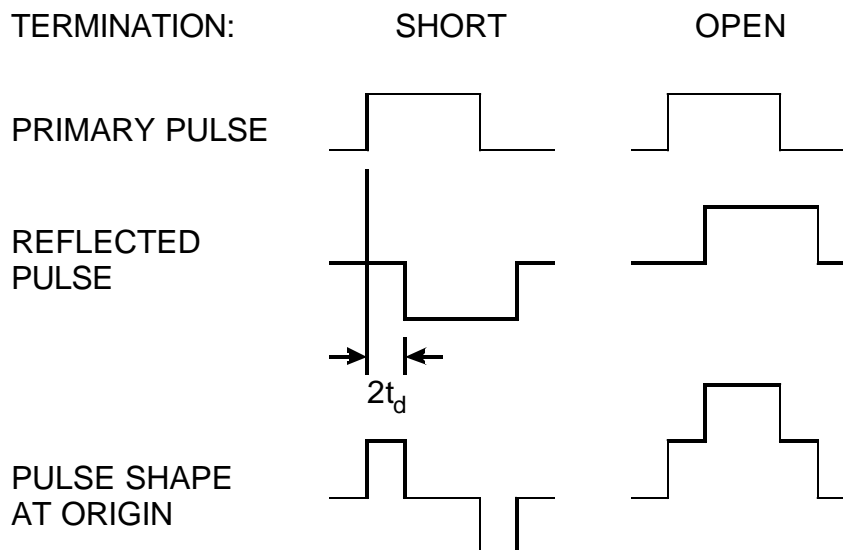
Example: delay line clipping with NaI(Tl) detector



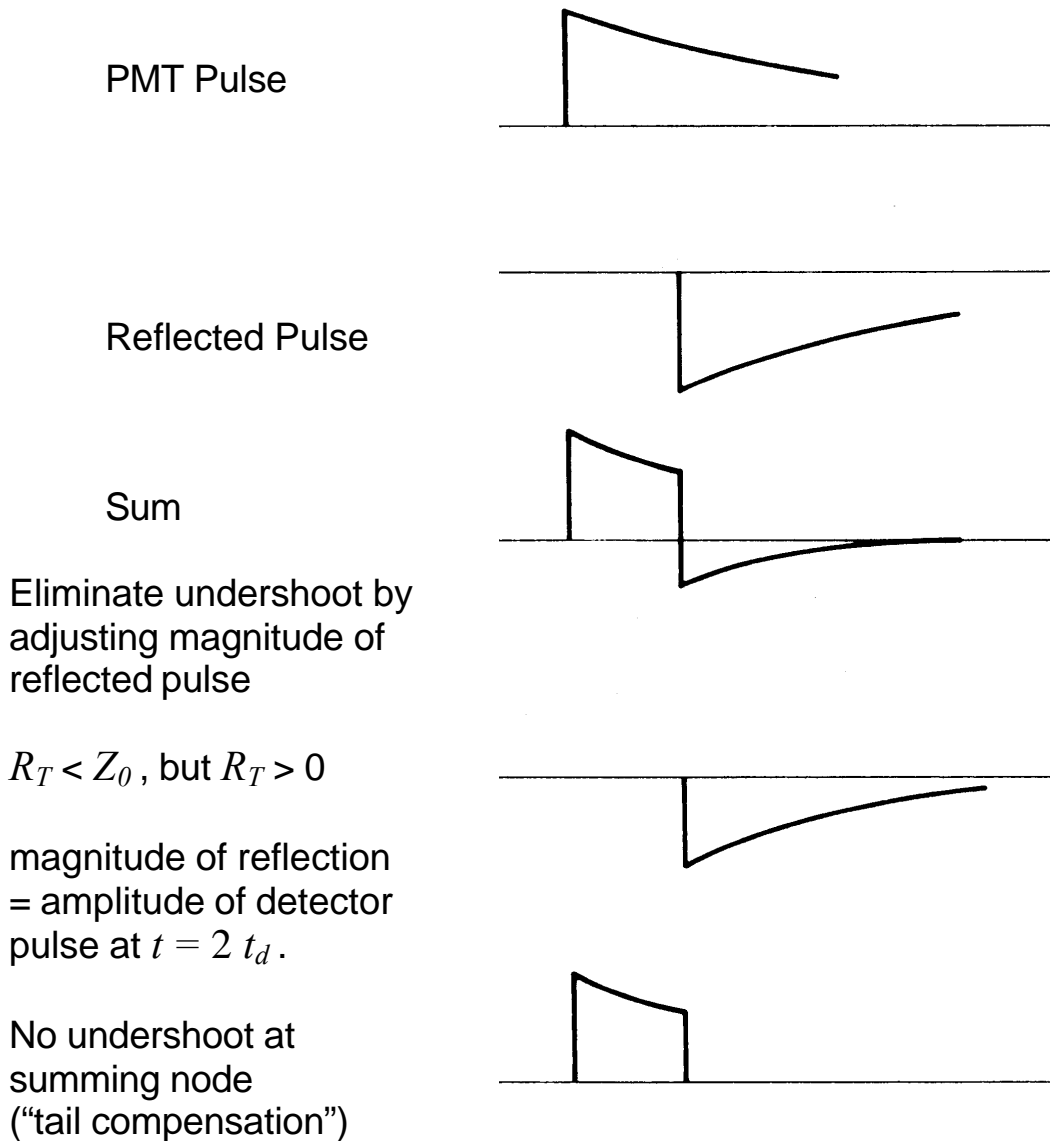
Reminder: Reflections on Transmission Lines

Termination $<$ Line Impedance: Reflection with opposite sign

Termination $>$ Line Impedance: Reflection with same sign



The scintillation pulse has an exponential decay.



Only works perfectly for single decay time constant, but can still provide useful results when other components are much faster (or weaker).

4. Timing Measurements

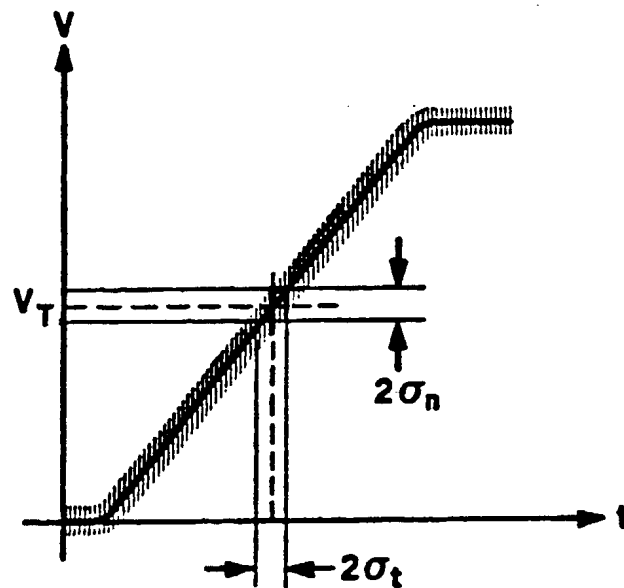
Pulse height measurements discussed up to now emphasize accurate measurement of signal charge.

- Timing measurements optimize determination of time of occurrence.
- For timing, the figure of merit is not signal-to-noise, but slope-to-noise ratio.

Consider the leading edge of a pulse fed into a threshold discriminator (comparator).

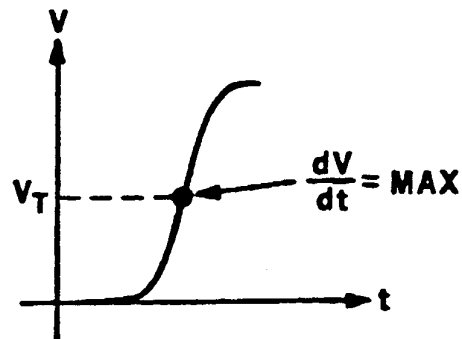
The instantaneous signal level is modulated by noise.

⇒ time of threshold crossing fluctuates



$$\sigma_t = \frac{\sigma_n}{\left. \frac{dV}{dt} \right|_{V_T}}$$

Typically, the leading edge is not linear, so the optimum trigger level is the point of maximum slope.



Pulse Shaping

Consider a system whose bandwidth is determined by a single RC integrator.

The time constant of the RC low-pass filter determines the

- rise time (and hence dV/dt)
- amplifier bandwidth (and hence the noise)

Time dependence: $V_o(t) = V_0(1 - e^{-t/\tau})$

The rise time is commonly expressed as the interval between the points of 10% and 90% amplitude

$$t_r = 2.2 \tau$$

In terms of bandwidth

$$t_r = 2.2 \tau = \frac{2.2}{2\pi f_u} = \frac{0.35}{f_u}$$

Example: An oscilloscope with 100 MHz bandwidth has 3.5 ns rise time.

For a cascade of amplifiers: $t_r \approx \sqrt{t_{r1}^2 + t_{r2}^2 + \dots + t_{rn}^2}$

Choice of Rise Time in a Timing System

Assume a detector pulse with peak amplitude V_0 and a rise time t_c passing through an amplifier chain with a rise time t_{ra} .

If the amplifier rise time is longer than the signal rise time,

$$\text{Noise} \propto \sqrt{f_u} \propto \sqrt{\frac{1}{t_{ra}}}$$

$$\frac{dV}{dt} \propto \frac{1}{t_{ra}} \propto f_u$$

increase in bandwidth \Rightarrow gain in dV/dt outweighs increase in noise.

In detail ...

The cumulative rise time at the amplifier output (discriminator output) is

$$t_r = \sqrt{t_c^2 + t_{ra}^2}$$

The electronic noise at the amplifier output is

$$V_{no}^2 = \int e_{ni}^2 df = e_{ni}^2 \Delta f_n$$

For a single RC time constant the noise bandwidth

$$\Delta f_n = \frac{\pi}{2} f_u = \frac{1}{4\tau} = \frac{0.55}{t_{ra}}$$

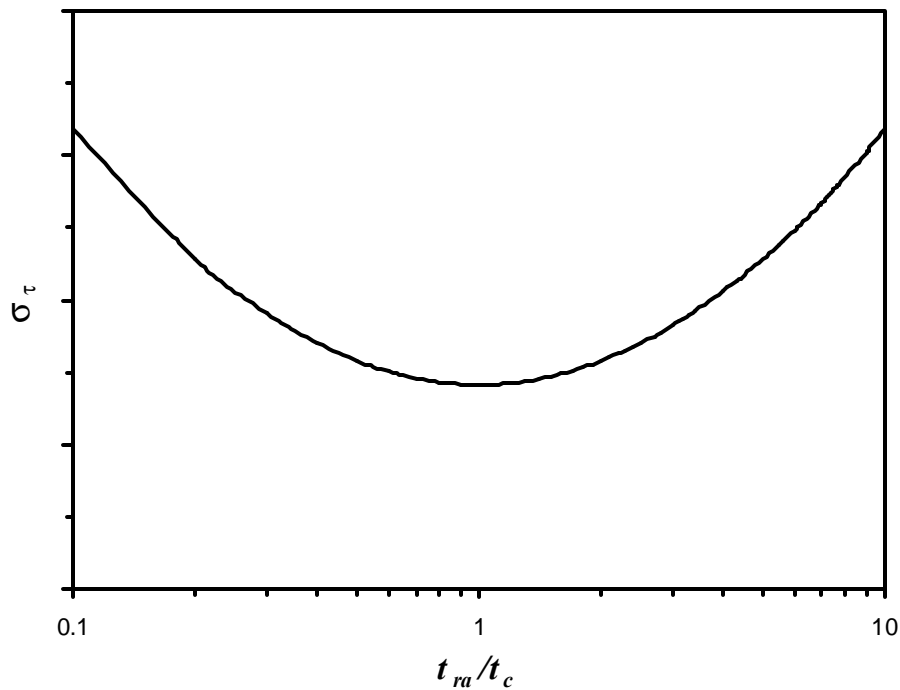
As the number of cascaded stages increases, the noise bandwidth approaches the signal bandwidth. In any case

$$\Delta f_n \propto \frac{1}{t_{ra}}$$

The timing jitter

$$\sigma_t = \frac{V_{no}}{dV/dt} \approx \frac{V_{no}}{V_0/t_r} = \frac{1}{V_0} V_{no} t_r \propto \frac{1}{V_0} \frac{1}{\sqrt{t_{ra}}} \sqrt{t_c^2 + t_{ra}^2} = \frac{\sqrt{t_c}}{V_0} \sqrt{\frac{t_c}{t_{ra}} + \frac{t_{ra}}{t_c}}$$

The second factor assumes a minimum when the rise time of the amplifier equals the collection time of the detector $t_{ra} = t_c$.



At amplifier rise times greater than the collection time, the time resolution suffers because of rise time degradation. For smaller amplifier rise times the electronic noise dominates.

The timing resolution improves with decreasing collection time $\sqrt{t_c}$ and increasing signal amplitude V_0 .

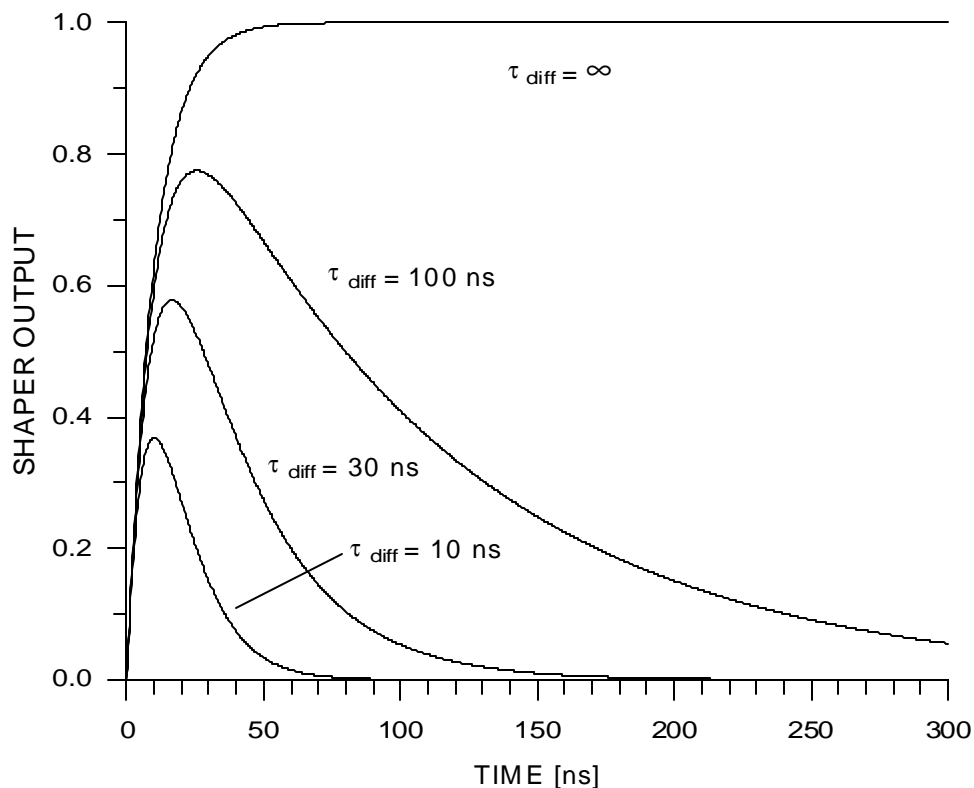
The integration time should be chosen to match the rise time.

How should the differentiation time be chosen?

As shown in the figure below, the loss in signal can be appreciable even for rather large ratios τ_{diff}/τ_{int} , e.g. >20% for $\tau_{diff}/\tau_{int} = 10$.

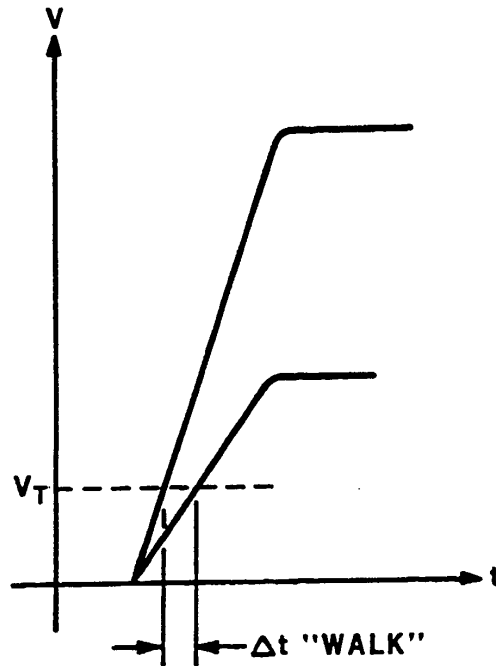
Since the time resolution improves directly with increasing peak signal amplitude, the differentiation time should be set to be as large as allowed by the required event rate.

CR-RC SHAPER
 FIXED INTEGRATOR TIME CONSTANT = 10 ns
 DIFFERENTIATOR TIME CONSTANT = ∞ , 100, 30 and 10 ns



Time Walk

For a fixed trigger level the time of threshold crossing depends on pulse amplitude.



⇒ Accuracy of timing measurement limited by

- jitter (due to noise)
- time walk (due to amplitude variations)

If the rise time is known, “time walk” can be compensated in software event-by-event by measuring the pulse height and correcting the time measurement.

This technique fails if both amplitude and rise time vary, as is common.

In hardware, time walk can be reduced by setting the threshold to the lowest practical level, or by using amplitude compensation circuitry, e.g. constant fraction triggering.

Lowest Practical Threshold

Single RC integrator has maximum slope at $t=0$.

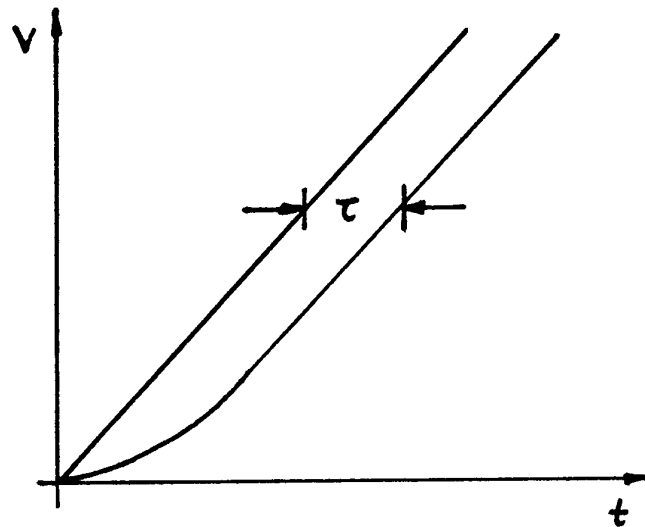
$$\frac{d}{dt}(1 - e^{-t/\tau}) = \frac{1}{\tau} e^{-t/\tau}$$

However, the rise time of practically all fast timing systems is determined by multiple time constants.

For small t the slope at the output of a single RC integrator is linear, so initially the pulse can be approximated by a ramp $\propto t$.

Response of the following integrator

$$V_i = \alpha t \quad \rightarrow \quad V_o = \alpha(t - \tau) - \alpha\tau e^{-t/\tau}$$



⇒ The output is delayed by τ and curvature is introduced at small t .

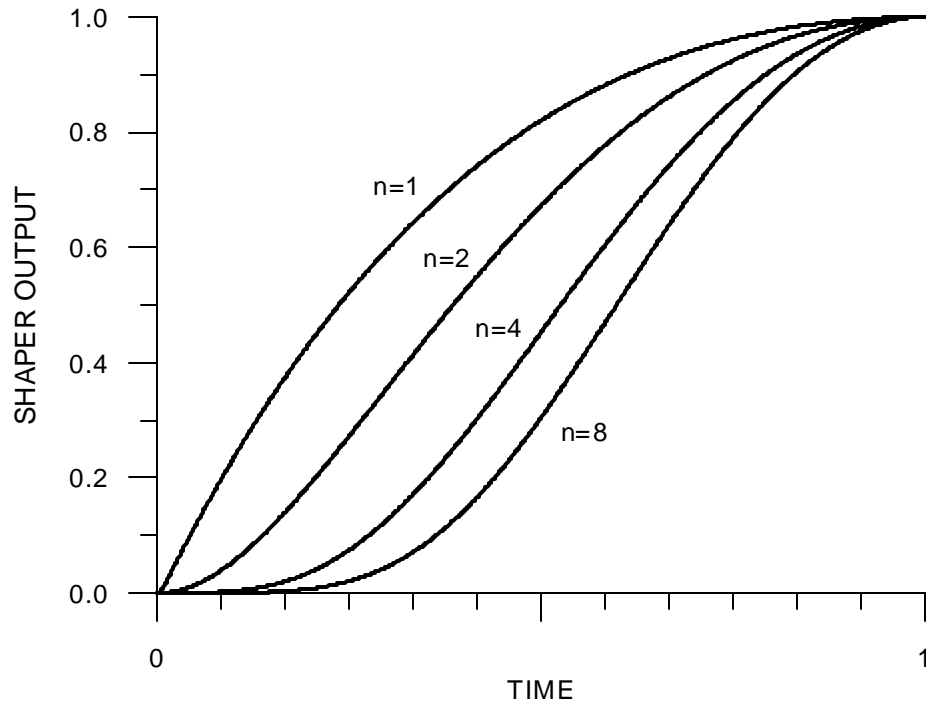
Output attains 90% of input slope after $t = 2.3\tau$.

Delay for n integrators = $n\tau$

Additional RC integrators introduce more curvature at the beginning of the pulse.

Output pulse shape for multiple RC integrators

(normalized to preserve the peaking time $\tau_n = \tau_{n=1}/n$)



Increased curvature at beginning of pulse limits the minimum threshold for good timing.

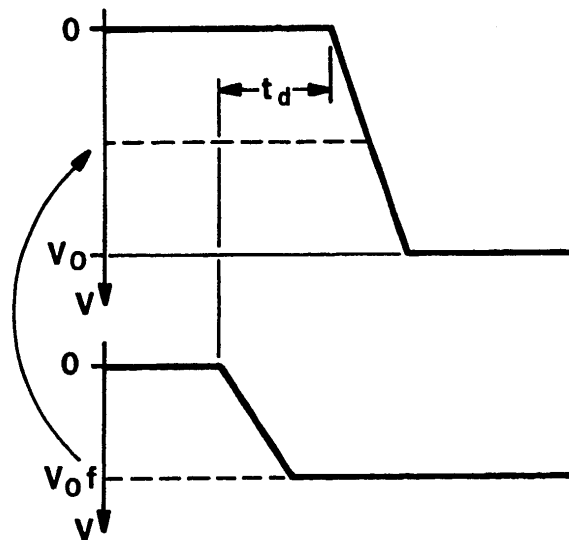
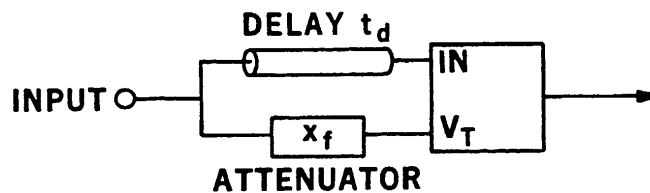
⇒ One dominant time constant best for timing measurements

Unlike amplitude measurements, where multiple integrators are desirable to improve pulse symmetry and count rate performance.

Constant Fraction Timing

Basic Principle:

make the threshold track the signal



The threshold is derived from the signal by passing it through an attenuator $V_T = f V_s$.

The signal applied to the comparator input is delayed so that the transition occurs after the threshold signal has reached its maximum value $V_T = f V_0$.

For simplicity assume a linear leading edge

$$V(t) = \frac{t}{t_r} V_0 \quad \text{for } t \leq t_r \quad \text{and} \quad V(t) = V_0 \quad \text{for } t > t_r$$

so the signal applied to the input is

$$V(t) = \frac{t - t_d}{t_r} V_0$$

When the input signal crosses the threshold level

$$f V_0 = \frac{t - t_d}{t_r} V_0$$

and the comparator fires at the time

$$t = f t_r + t_d \quad (t_d > t_r)$$

at a constant fraction of the rise time independent of peak amplitude.

If the delay t_d is reduced so that the pulse transitions at the signal and threshold inputs overlap, the threshold level

$$V_T = f \frac{t}{t_r} V_0$$

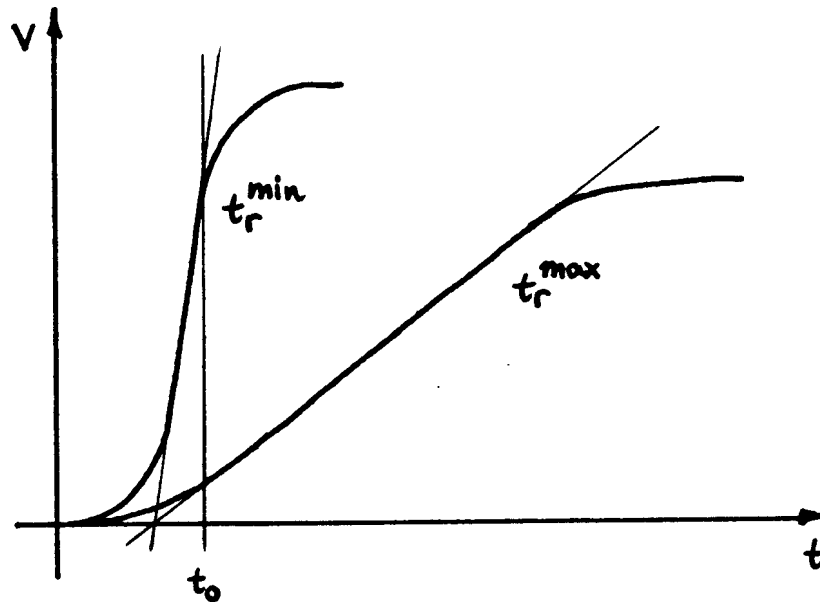
and the comparator fires at

$$f \frac{t}{t_r} V_0 = \frac{t - t_d}{t_r} V_0$$

$$t = \frac{t_d}{1 - f} \quad (t_d < (1 - f) t_r)$$

independent of both amplitude and rise time (amplitude and rise-time compensation).

The circuit compensates for amplitude and rise time if pulses have a sufficiently large linear range that extrapolates to the same origin.



The condition for the delay must be met for the minimum rise time:

$$t_d \leq (1 - f) t_{r,\min}$$

In this mode the fractional threshold V_T/V_0 varies with rise time.

For all amplitudes and rise times within the compensation range the comparator fires at the time

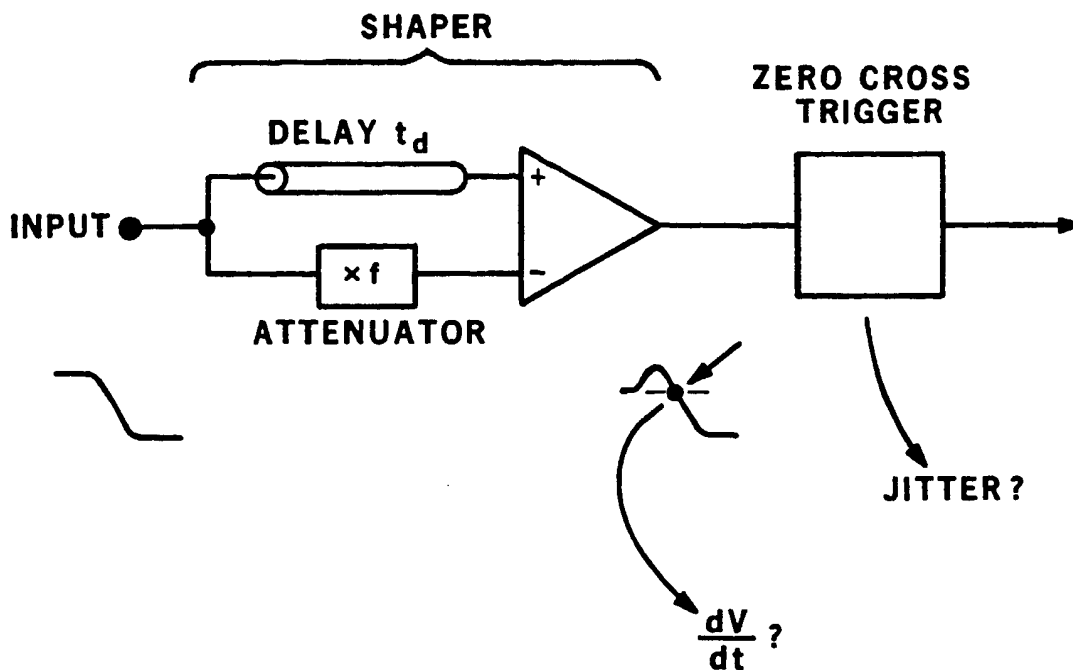
$$t_0 = \frac{t_d}{1 - f}$$

Another View of Constant Fraction Discriminators

The constant fraction discriminator can be analyzed as a pulse shaper, comprising the

- delay
- attenuator
- subtraction

driving a trigger that responds to the zero crossing.

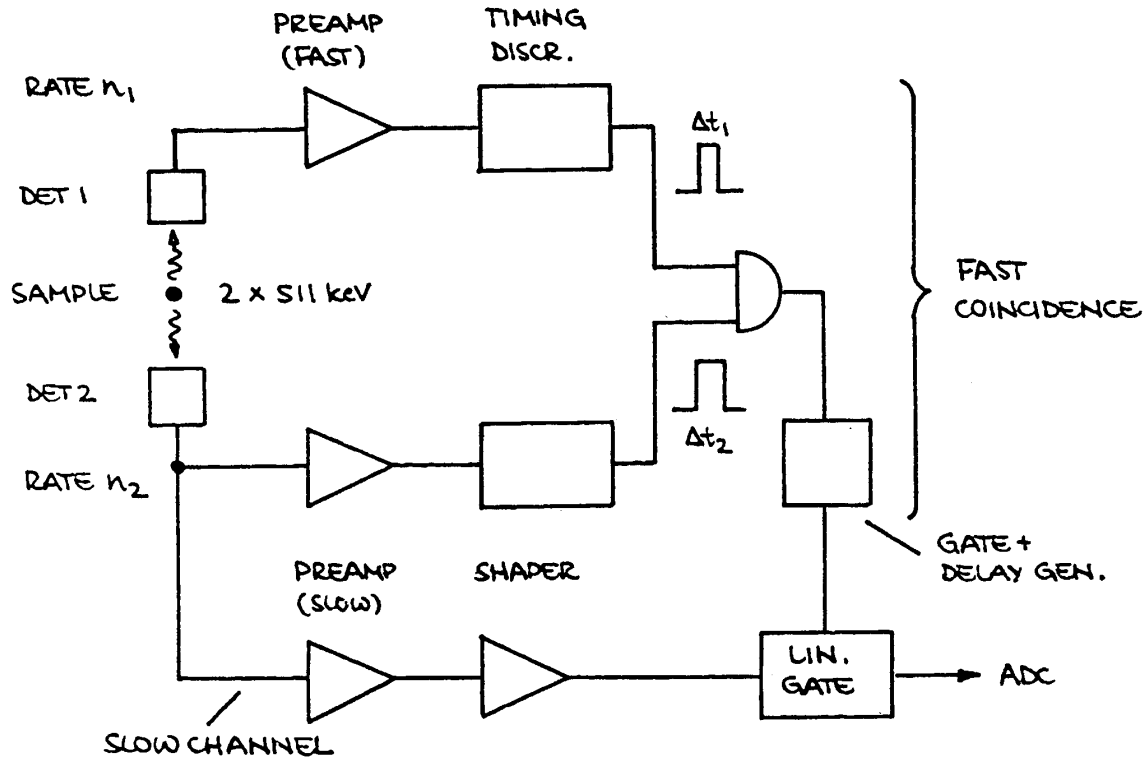


The timing jitter depends on

- the slope at the zero-crossing
(depends on choice of f and t_d)
- the noise at the output of the shaper
(this circuit increases the noise bandwidth)

Examples

1. γ - γ coincidence (as used in positron emission tomography)



Positron annihilation emits two collinear 511 keV photons.

Each detector alone will register substantial background.

Non-coincident background can be suppressed by requiring simultaneous signals from both detectors.

- Each detector feeds a fast timing channel.
- The timing pulses are combined in an AND gate (coincidence unit). The AND gate only provides an output if the two timing pulses overlap.
- The coincidence output is used to open a linear gate, that allows the energy signal to pass to the ADC.

This arrangement accommodates the contradictory requirements of timing and energy measurements. The timing channels can be fast, whereas the energy channel can use slow shaping to optimize energy resolution (“fast-slow coincidence”).

Chance coincidence rate

Two random pulse sequences have some probability of coincident events.

If the event rates in the two channels are n_1 and n_2 , and the timing pulse widths are Δt_1 and Δt_2 , the probability of a pulse from the first source occurring in the total coincidence window is

$$P_1 = n_1 \cdot (\Delta t_1 + \Delta t_2)$$

The coincidence is “sampled” at a rate n_2 , so the chance coincidence rate is

$$n_c = P_1 \cdot n_2$$

$$n_c = n_1 \cdot n_2 \cdot (\Delta t_1 + \Delta t_2)$$

i.e. in the arrangement shown above, the chance coincidence rate increases with the square of the source strength.

Example: $n_1 = n_2 = 10^6 \text{ s}^{-1}$

$$\Delta t_1 = \Delta t_2 = 5 \text{ ns}$$

$$\Rightarrow n_c = 10^4 \text{ s}^{-1}$$

2. Nuclear Mass Spectroscopy by Time-of-Flight

Two silicon detectors

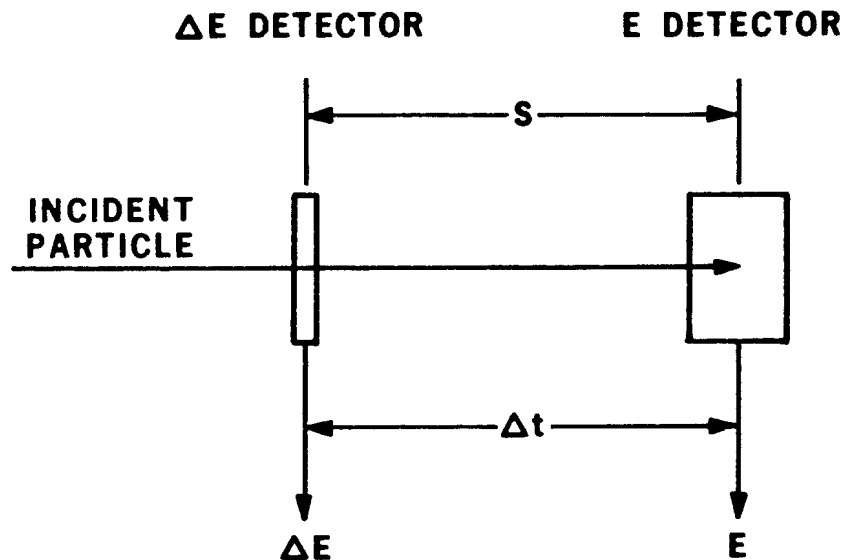
First detector thin, so that particle passes through it
(transmission detector)

⇒ differential energy loss ΔE

Second detector thick enough to stop particle

⇒ Residual energy E

Measure time-of-flight Δt between the two detectors



$$\Delta E + E \rightarrow E_{TOT}$$

$$\Delta E, E \rightarrow Z$$

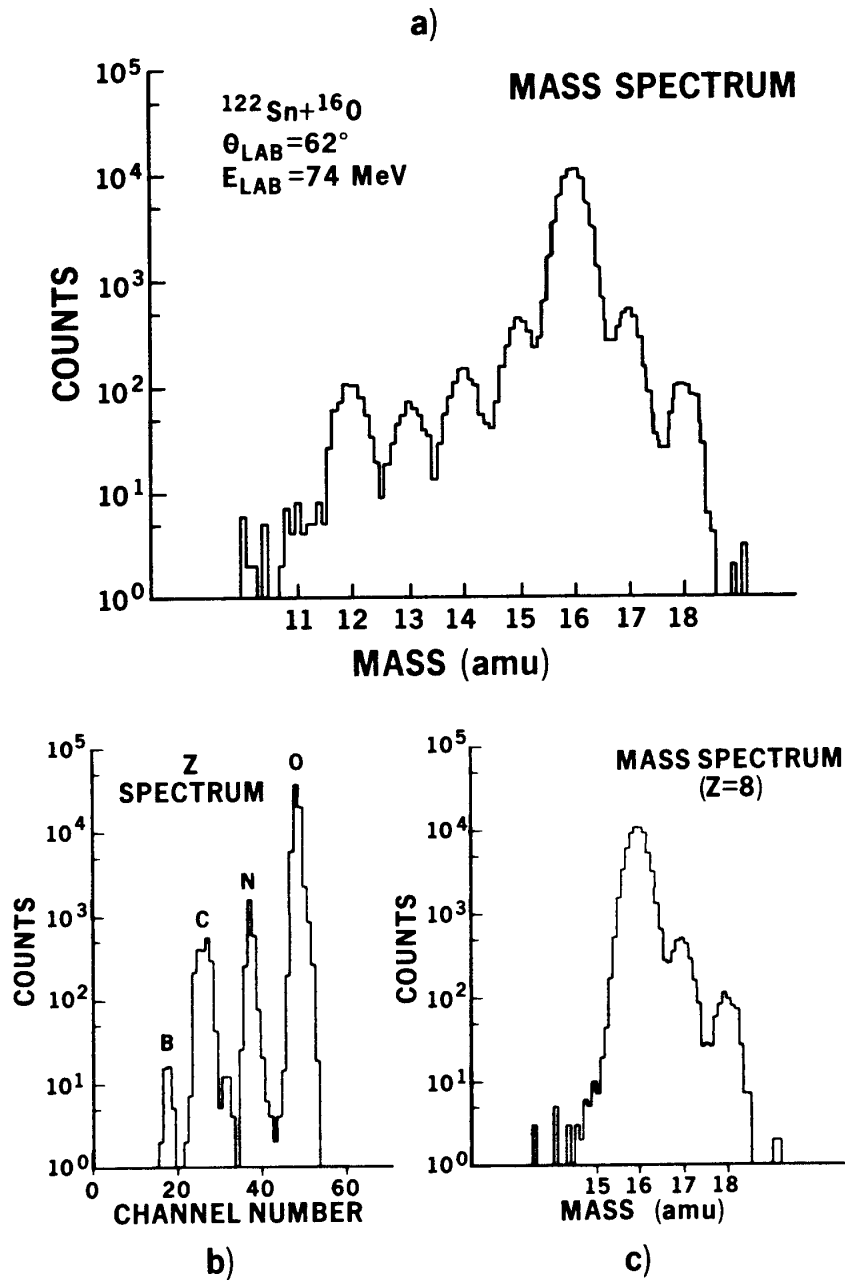
$$\Delta t, E \rightarrow A$$

$$E_{tot} = \Delta E + E \qquad Z \propto \sqrt{\Delta E \cdot E_{tot}} \qquad A \propto E \cdot (\Delta t / s)^2$$

“Typical” Results

Example 1

Flight path 20 cm, $\Delta t \approx 50$ ps FWHM
 $\sigma_t = 21$ ps



(H. Spieler et al., Z. Phys. **A278** (1976) 241)

Example 2

1. ΔE -detector: 27 μm thick, $A = 100 \text{ mm}^2$, $\langle E \rangle = 1.1 \cdot 10^4 \text{ V/cm}$

2. E -detector: 142 μm thick, $A = 100 \text{ mm}^2$, $\langle E \rangle = 2 \cdot 10^4 \text{ V/cm}$

For 230 MeV ^{28}Si : $\Delta E = 50 \text{ MeV} \Rightarrow V_s = 5.6 \text{ mV}$

$E = 180 \text{ MeV} \Rightarrow V_s = 106 \text{ mV}$

$\Rightarrow \Delta t = 32 \text{ ps FWHM}$

$\sigma_t = 14 \text{ ps}$

Example 3

Two transmission detectors,

each 160 μm thick, $A = 320 \text{ mm}^2$

For 650 MeV/u ^{20}Ne : $\Delta E = 4.6 \text{ MeV} \Rightarrow V_s = 800 \mu\text{V}$

$\Rightarrow \Delta t = 180 \text{ ps FWHM}$

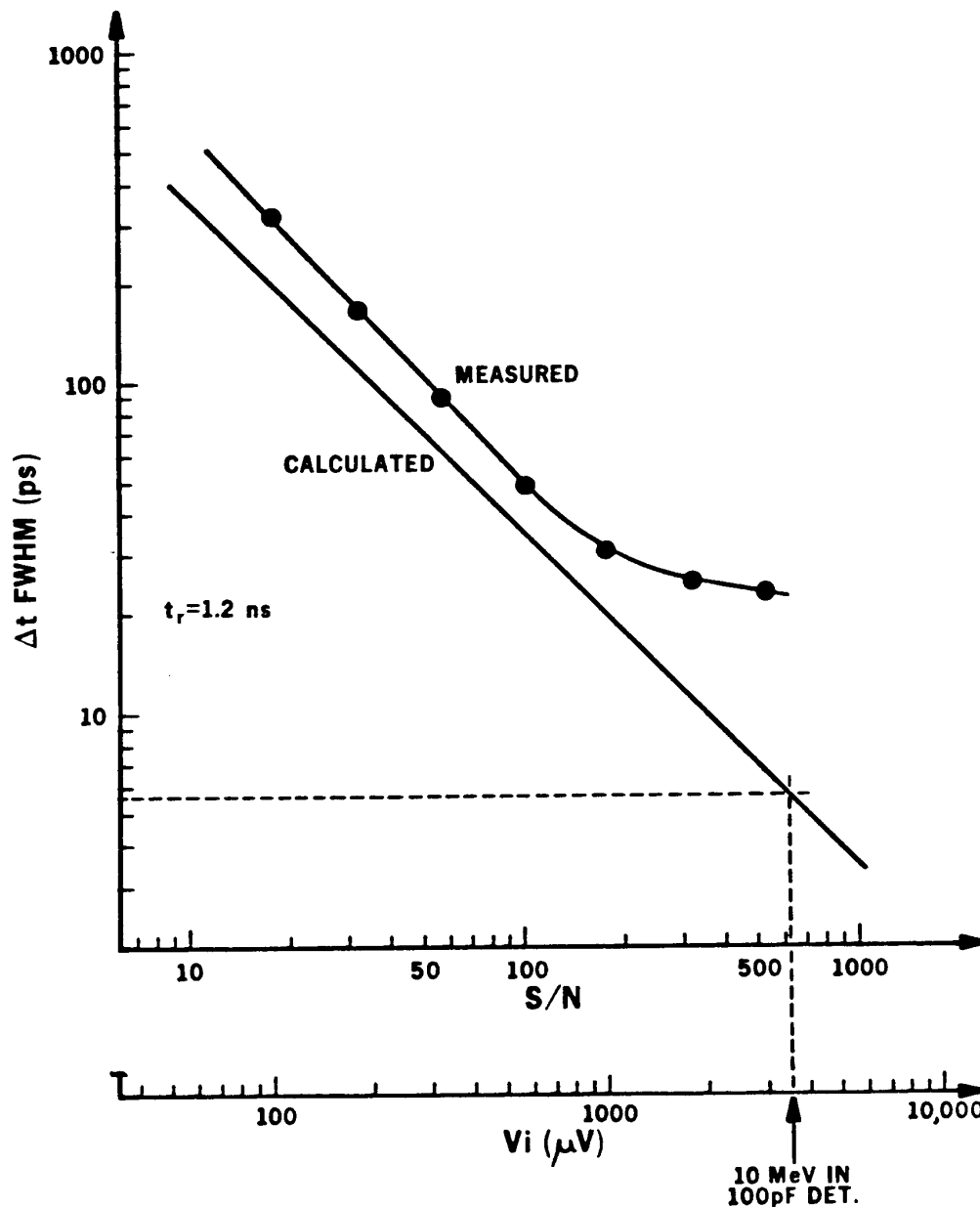
$\sigma_t = 77 \text{ ps}$

For 250 MeV/u ^{20}Ne : $\Delta E = 6.9 \text{ MeV} \Rightarrow V_s = 1.2 \text{ mV}$

$\Rightarrow \Delta t = 120 \text{ ps FWHM}$

$\sigma_t = 52 \text{ ps}$

Fast Timing: Comparison between theory and experiment



At $S/N < 100$ the measured curve lies above the calculation because the timing discriminator limited the rise time.
 At high S/N the residual jitter of the time digitizer limits the resolution.

For more details on fast timing with semiconductor detectors, see H. Spieler, IEEE Trans. Nucl. Sci. **NS-29/3** (1982) 1142.

5. Digitization of Pulse Height and Time – Analog to Digital Conversion

For data storage and subsequent analysis the analog signal at the shaper output must be digitized.

Important parameters for ADCs used in detector systems:

1. Resolution
The “granularity” of the digitized output
2. Differential Non-Linearity
How uniform are the digitization increments?
3. Integral Non-Linearity
Is the digital output proportional to the analog input?
4. Conversion Time
How much time is required to convert an analog signal to a digital output?
5. Count-Rate Performance
How quickly can a new conversion commence after completion of a prior one without introducing deleterious artifacts?
6. Stability
Do the conversion parameters change with time?

Instrumentation ADCs used in industrial data acquisition and control systems share most of these requirements. However, detector systems place greater emphasis on differential non-linearity and count-rate performance. The latter is important, as detector signals often occur randomly, in contrast to measurement systems where signals are sampled at regular intervals.

1. Resolution

Digitization incurs approximation, as a continuous signal distribution is transformed into a discrete set of values. To reduce the additional errors (noise) introduced by digitization, the discrete digital steps must correspond to a sufficiently small analog increment.

Simplistic assumption:

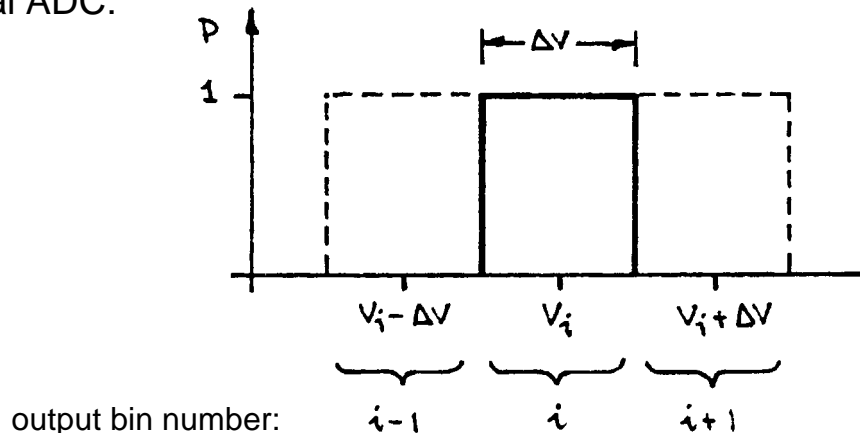
Resolution is defined by the number of output bits, e.g.

$$13 \text{ bits} \rightarrow \frac{\Delta V}{V} = \frac{1}{8192} = 1.2 \cdot 10^{-4}$$

True Measure: Channel Profile

Plot probability vs. pulse amplitude that a pulse height corresponding to a specific output bin is actually converted to that address.

Ideal ADC:



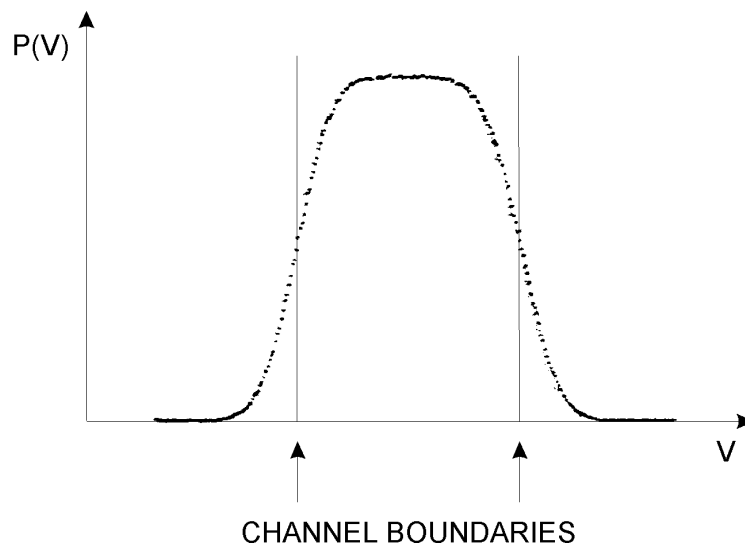
Measurement accuracy:

- If all counts of a peak fall in one bin, the resolution is ΔV .
- If the counts are distributed over several (>4 or 5) bins, peak fitting can yield a resolution of $10^{-1} - 10^{-2} \Delta V$, *if the distribution is known and reproducible* (not necessarily a valid assumption for an ADC).

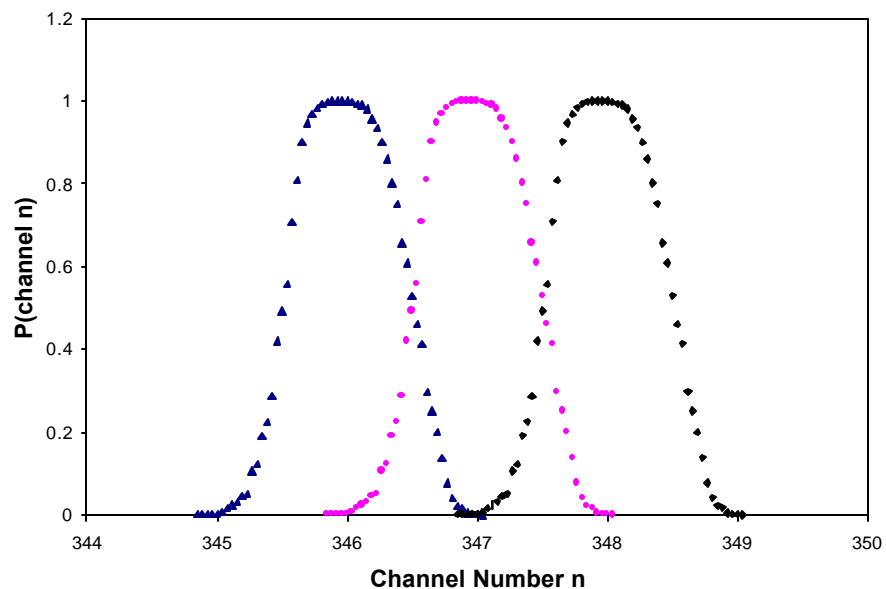
In reality, the channel profile is not rectangular as sketched above.

Electronic noise in the threshold discrimination process that determines the channel boundaries “smears” the transition from one bin to the next.

Measured channel profile (13 bit ADC)



The profiles of adjacent channels overlap

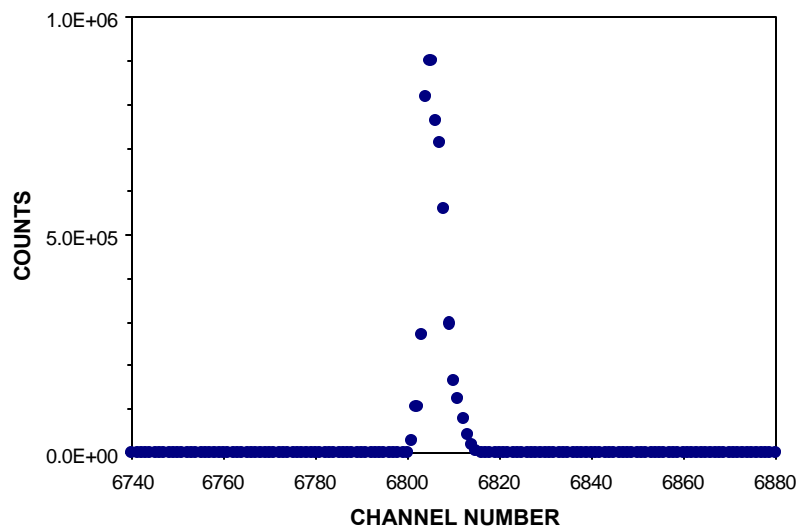


Channel profile can be checked quickly by applying the output of a precision pulser to the ADC.

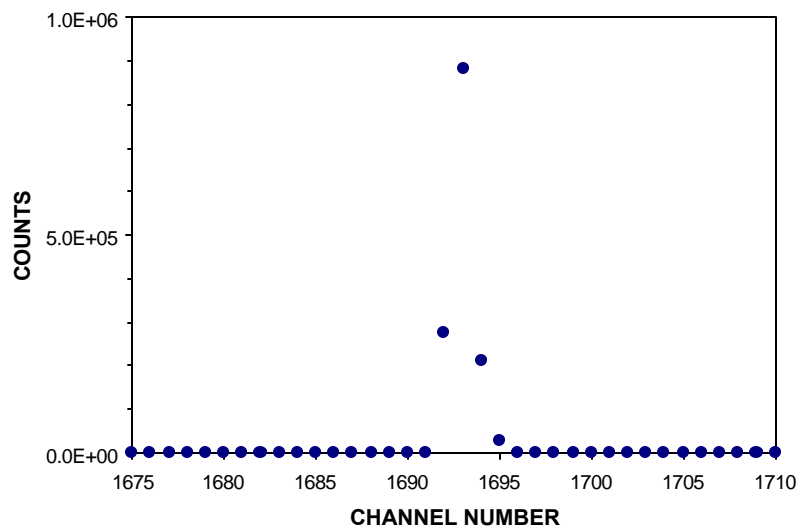
If the pulser output has very low noise, i.e. the amplitude jitter is much smaller than the voltage increment corresponding to one ADC channel or bin, all pulses will be converted to a single channel, with only a small fraction appearing in the neighbor channels.

Example of an ADC whose digital resolution is greater than its analog resolution:

8192 ch conversion range (13 bits)



2048 ch conversion range (11 bits)

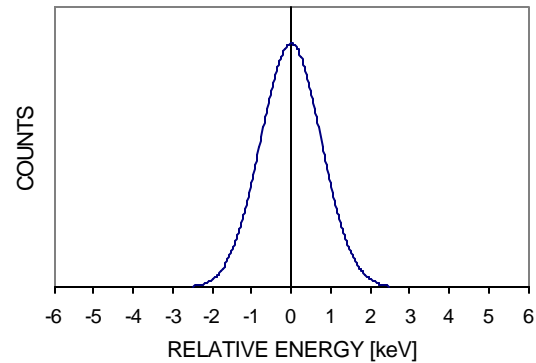


2K range provides maximum resolution – higher ranges superfluous.

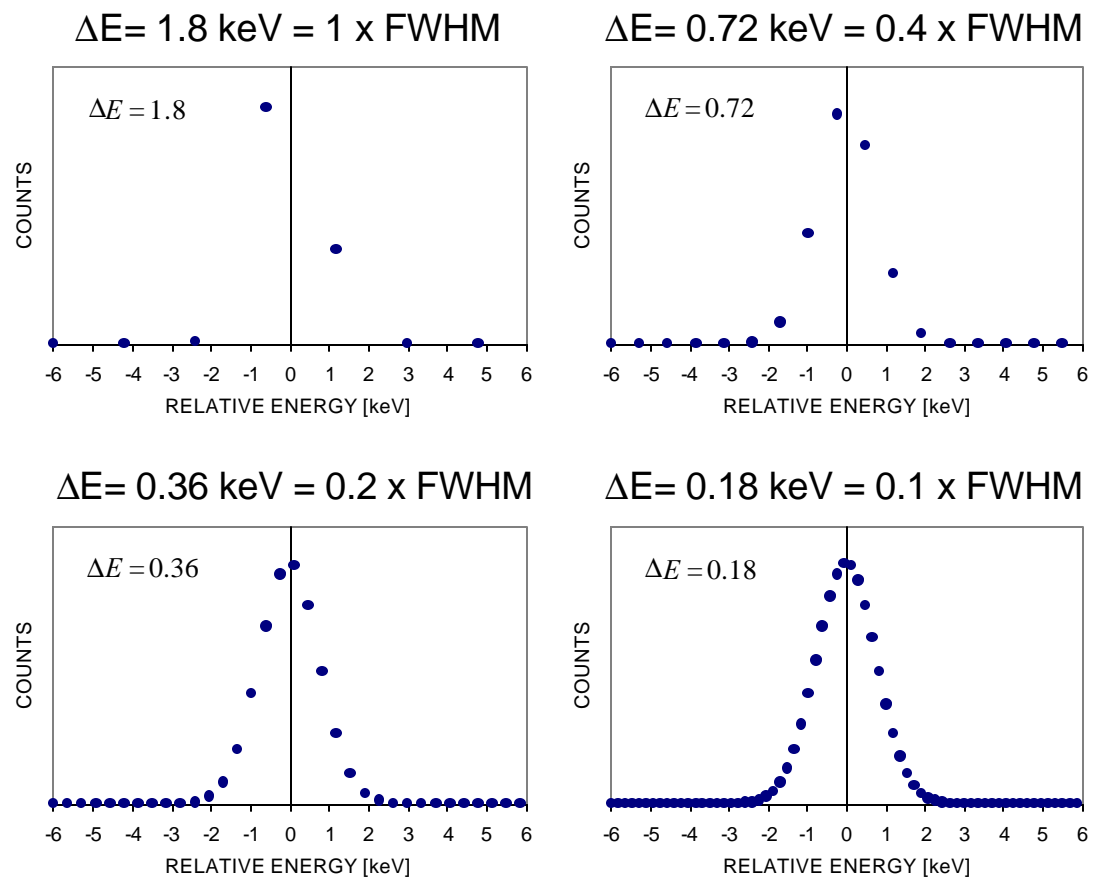
How much ADC Resolution is Required?

Example:

Detector resolution
1.8 keV FWHM



Digitized spectra for various ADC resolutions (bin widths) ΔE :



Fitting can determine centroid position to fraction of bin width even with coarse digitization, **if the line shape is known.**

Five digitizing channels within a linewidth (FWHM) allow robust peak fitting and centroid finding, even for imperfectly known line shapes and overlapping peaks.

2. Differential Non-Linearity

Differential non-linearity is a measure of the inequality of channel profiles over the range of the ADC.

Depending on the nature of the distribution, either a peak or an rms specification may be appropriate.

$$DNL = \max \left\{ \frac{\Delta V(i)}{\langle \Delta V \rangle} - 1 \right\}$$

or

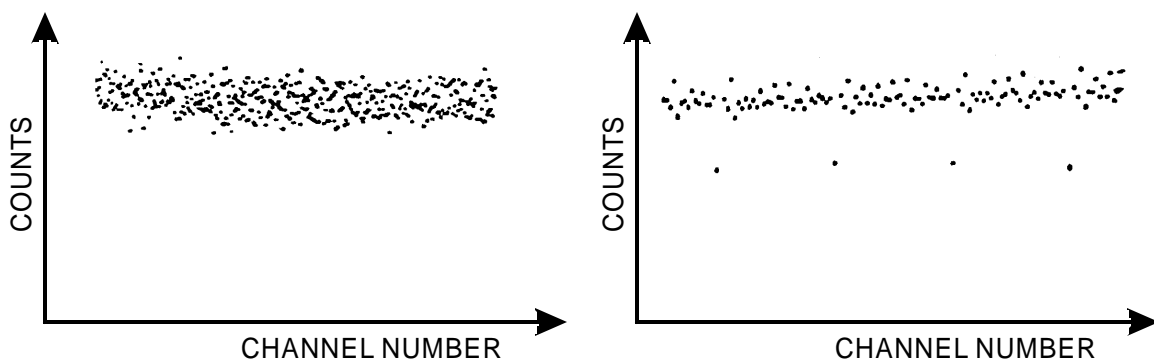
$$DNL = \text{r.m.s.} \left\{ \frac{\Delta V(i)}{\langle \Delta V \rangle} - 1 \right\}$$

where $\langle \Delta V \rangle$ is the average channel width and $\Delta V(i)$ is the width of an individual channel.

Differential non-linearity of $< \pm 1\%$ max. is typical, but state-of-the-art ADCs can achieve 10^{-3} rms, i.e. the variation is comparable to the statistical fluctuation for 10^6 random counts.

Note: Instrumentation ADCs are often specified with an accuracy of ± 0.5 LSB (least significant bit), so the differential non-linearity may be 50% or more.

Typical differential non-linearity patterns (“white” input spectrum).

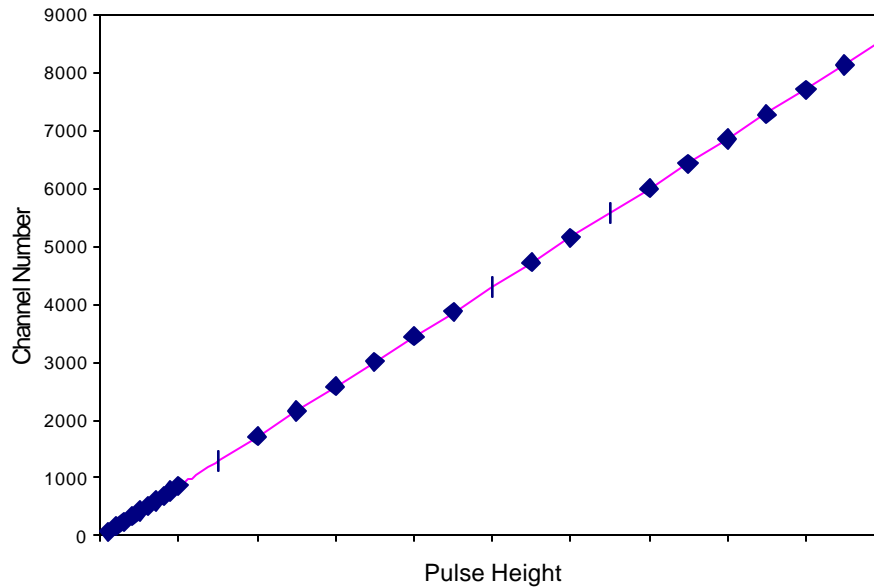


An ideal ADC would show an equal number of counts in each bin.

The spectrum to the left shows a random pattern, but note the multiple periodicities visible in the right hand spectrum.

3. Integral Non-Linearity

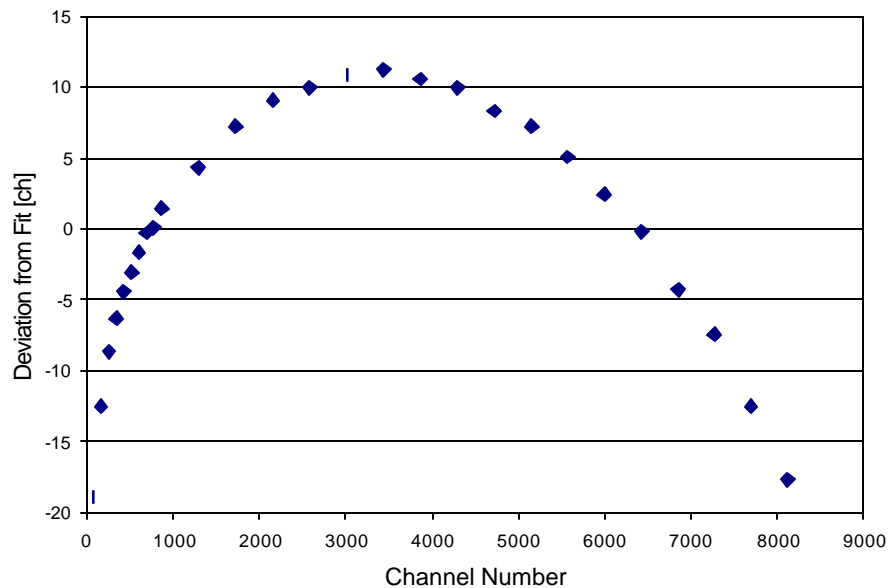
Integral non-linearity measures the deviation from proportionality of the measured amplitude to the input signal level.



The dots are measured values and the line is a fit to the data.

This plot is not very useful if the deviations from linearity are small.

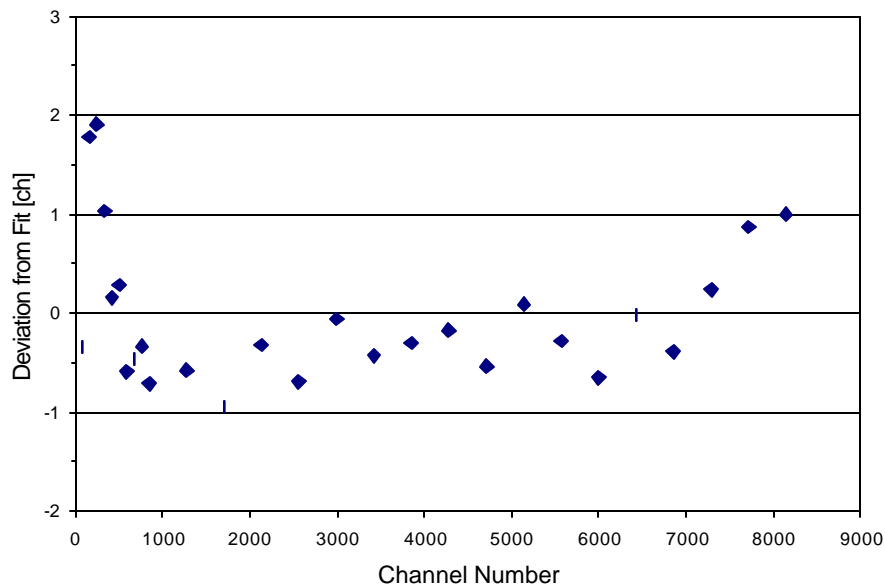
Plotting the deviations of the measured points from the fit yields:



The linearity of an ADC can depend on the input pulse shape and duration, due to bandwidth limitations in the circuitry.

The differential non-linearity shown above was measured with a 400 ns wide input pulse.

Increasing the pulse width to 3 μ s improved the result significantly:



4. Conversion Time

During the acquisition of a signal the system cannot accept a subsequent signal (“dead time”)

Dead Time =

- signal acquisition time → time-to-peak + const.
- + conversion time → can depend on pulse height
- + readout time to memory → depends on speed of data transmission and buffer memory access - can be large in computer-based systems

Dead time affects measurements of yields or reaction cross-sections. Unless the event rate $\ll 1/(\text{dead time})$, it is necessary to measure the dead time, e.g. with a reference pulser fed simultaneously into the spectrum.

The total number of reference pulses issued during the measurement is determined by a scaler and compared with the number of pulses recorded in the spectrum.

Does a pulse-height dependent dead time mean that the correction is a function of pulse height?

Usually not. If events in different part of the spectrum are not correlated in time, i.e. random, they are all subject to the same average dead time (although this average will depend on the spectral distribution).

- Caution with correlated events!

Example: Decay chains, where lifetime is $<$ dead time.
 The daughter decay will be lost systematically.

5. Count Rate Effects

Problems are usually due to internal baseline shifts with event rate or undershoots following a pulse.

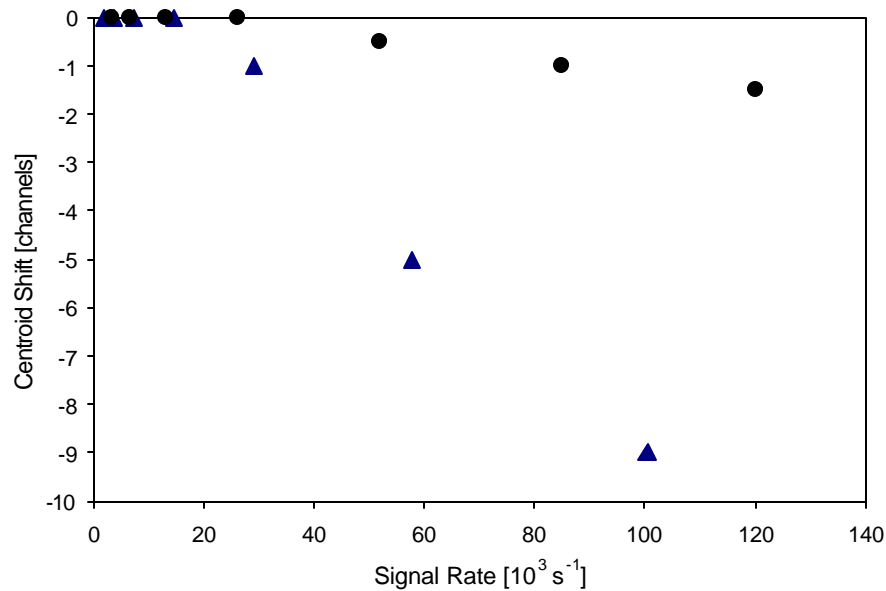
If signals occur at constant intervals, the effect of an undershoot will always be the same.

However, in a random sequence of pulses, the effect will vary from pulse to pulse.

⇒ spectral broadening

Baseline shifts tend to manifest themselves as a systematic shift in centroid position with event rate.

Centroid shifts for two 13 bit ADCs vs. random rate:



6. Stability

Stability vs. temperature is usually adequate with modern electronics in a laboratory environment.

- Note that temperature changes within a module are typically much smaller than ambient.

However: Highly precise or long-term measurements require spectrum stabilization to compensate for changes in gain and baseline of the overall system.

Technique: Using precision pulsers place a reference peak at both the low and high end of the spectrum.

(Pk. Pos. 2) – (Pk. Pos. 1) → Gain, ... then

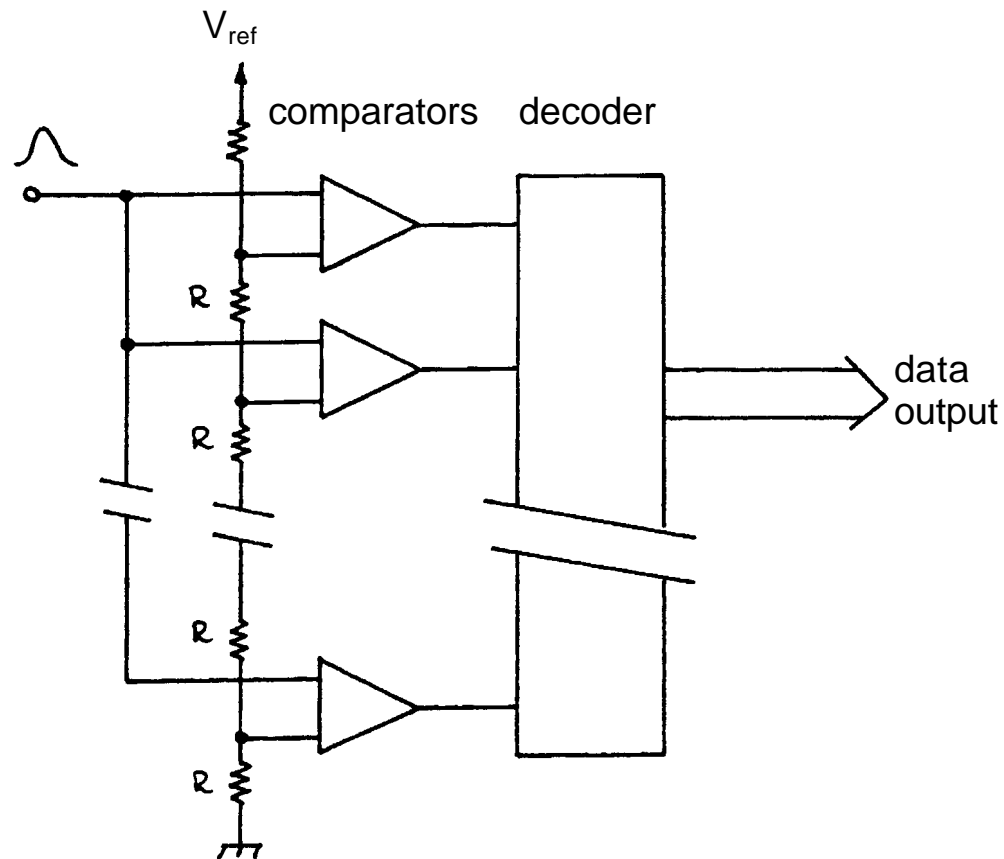
(Pk. Pos. 1) or (Pk. Pos. 2) → Offset

Traditional Implementation: Hardware,
spectrum stabilizer module

Today, it is more convenient to determine the corrections in software. These can be applied to calibration corrections or used to derive an electrical signal that is applied to the hardware (simplest and best in the ADC).

Analog to Digital Conversion Techniques

1. Flash ADC



The input signal is applied to n comparators in parallel. The switching thresholds are set by a resistor chain, such that the voltage difference between individual taps is equal to the desired measurement resolution.

2^n comparators for n bits (8 bit resolution requires 256 comparators)

Feasible in monolithic ICs since the absolute value of the resistors in the reference divider chain is not critical, only the relative matching.

Advantage: short conversion time (<10 ns available)

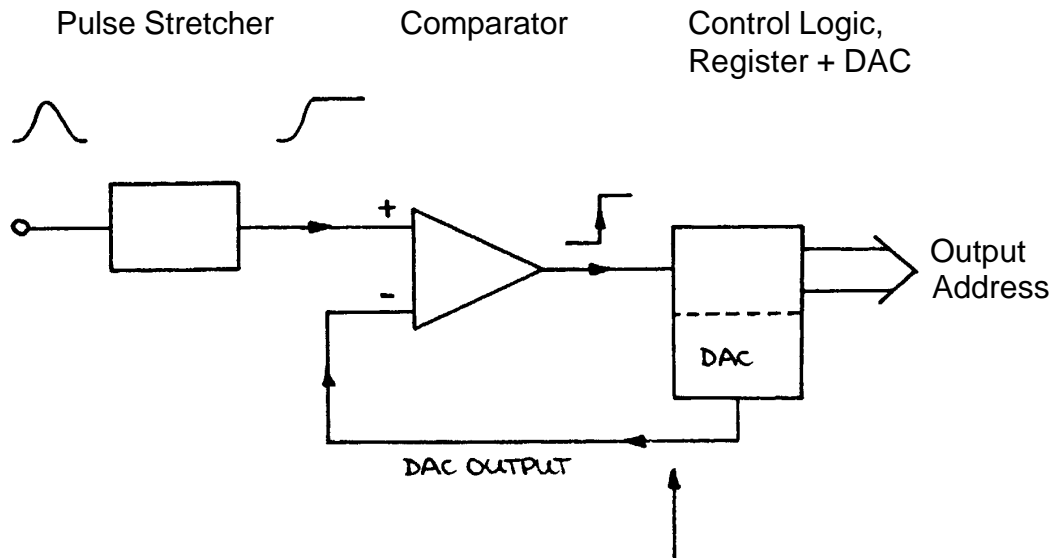
Drawbacks: limited accuracy (many comparators)

power consumption

Differential non-linearity $\sim 1\%$

High input capacitance (speed is often limited by the analog driver feeding the input)

2. Successive Approximation ADC



Sequentially add levels proportional to $2^n, 2^{n-1}, \dots, 2^0$ and set corresponding bit if the comparator output is high (DAC output < pulse height)

n conversion steps yield 2^n channels,
i.e. 8K channels require 13 steps

Advantages: speed ($\sim \mu\text{s}$)
high resolution
ICs (monolithic + hybrid) available

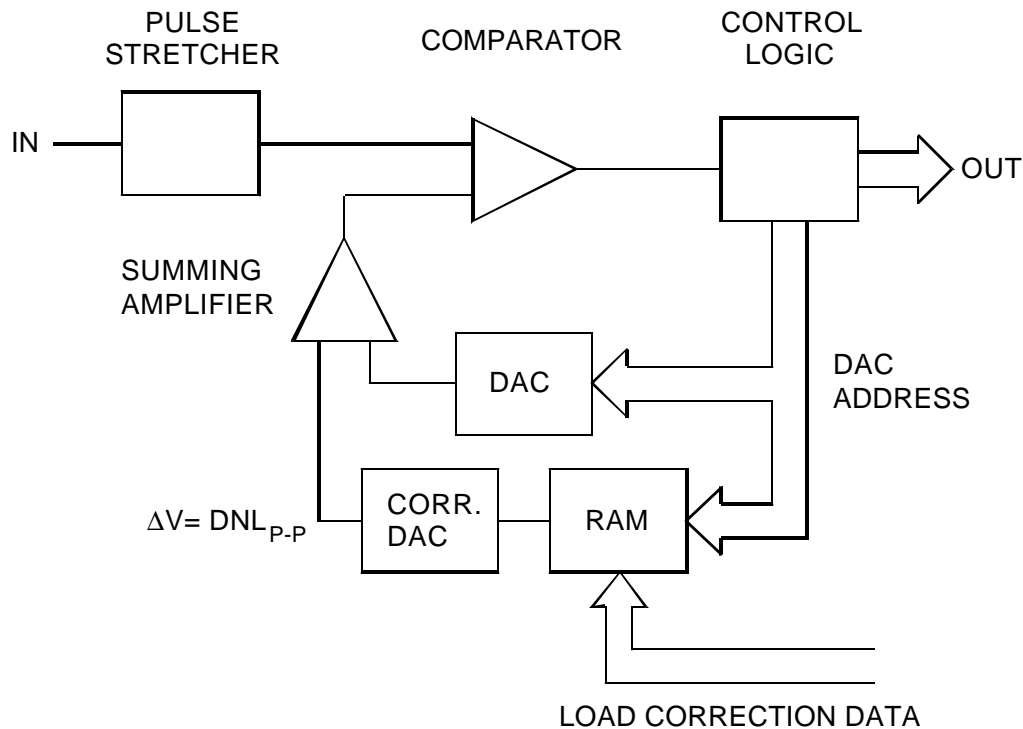
Drawback: Differential non-linearity (typ. 10 – 20%)

Reason: Resistors that set DAC output must be extremely accurate.

For DNL < 1% the resistor determining the 2^{12} level in an 8K ADC must be accurate to $< 2.4 \cdot 10^{-6}$.

DNL can be corrected by various techniques:

- averaging over many channel profiles for a given pulse amplitude (“sliding scale” or “Gatti principle”)
- correction DAC (“brute force” application of IC technology)



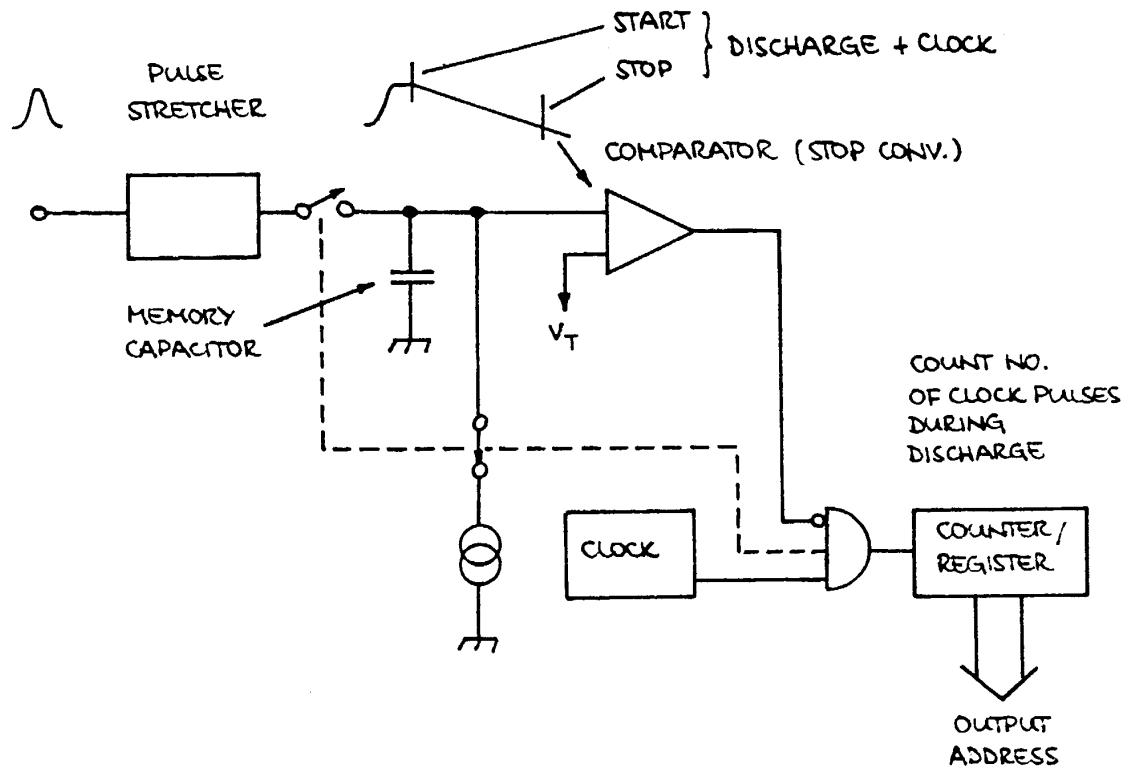
The primary DAC output is adjusted by the output of a correction DAC to reduce differential non-linearity.

Correction data are derived from a measurement of DNL. Corrections for each bit are loaded into the RAM, which acts as a look-up table to provide the appropriate value to the correction DAC for each bit of the main DAC.

The range of the correction DAC must exceed the peak-to-peak differential non-linearity.

If the correction DAC has N bits, the maximum DNL is reduced by $2^{-(N-1)}$ (if deviations are symmetrical).

3. Wilkinson ADC



The peak signal amplitude is acquired by a pulse stretcher and transferred to a memory capacitor. Then, simultaneously,

1. the capacitor is disconnected from the stretcher,
2. a current source is switched to linearly discharge the capacitor,
3. a counter is enabled to determine the number of clock pulses until the voltage on the capacitor reaches the baseline.

Advantage: excellent differential linearity
(continuous conversion process)

Drawbacks: slow – conversion time = $n \cdot T_{clock}$
(n = channel number \propto pulse height)

$$T_{clock} = 10 \text{ ns} \rightarrow T_{conv} = 82 \mu\text{s} \text{ for 13 bits}$$

Clock frequencies of 100 MHz typical, but
>400 MHz possible with excellent performance

“Standard” technique for high-resolution spectroscopy.

Hybrid Analog-to-Digital Converters

Conversion techniques can be combined to obtain high resolution and short conversion time.

1. Flash + Successive Approximation or Flash + Wilkinson (Ramp Run-Down)

Utilize fast flash ADC for coarse conversion
(e.g. 8 out of 13 bits)

Successive approximation or Wilkinson converter to provide fine resolution. Limited range, so short conversion time:

256 ch with 100 MHz clock \Rightarrow 2.6 μ s

Results: 13 bit conversion in $< 4 \mu$ s
with excellent integral and differential linearity

2. Flash ADCs with Sub-Ranging

Not all applications require constant absolute resolution over the full range. Sometimes only *relative* resolution must be maintained, especially in systems with a very large dynamic range.

Precision binary divider at input to determine coarse range + fast flash ADC for fine digitization.

Example: Fast digitizer that fits in phototube base.
Designed at FNAL.

17 to 18 bit dynamic range
Digital floating point output
(4 bit exponent, 8+1 bit mantissa)
16 ns conversion time

Time Digitizers

1. Counter

Simplest arrangement.

Count clock pulses between start and stop.

Limitation: Speed of counter

Current technology limits speed of counter system to about 1 GHz

$$\Rightarrow \Delta t = 1 \text{ ns}$$

Multi-hit capability

2. Analog Ramp

Commonly used in high-resolution digitizers ($\Delta t = 10 \text{ ps}$)

Principle: charge capacitor through switchable current source

Start pulse: turn on current source

Stop pulse: turn off current source

$$\Rightarrow \text{Voltage on storage capacitor}$$

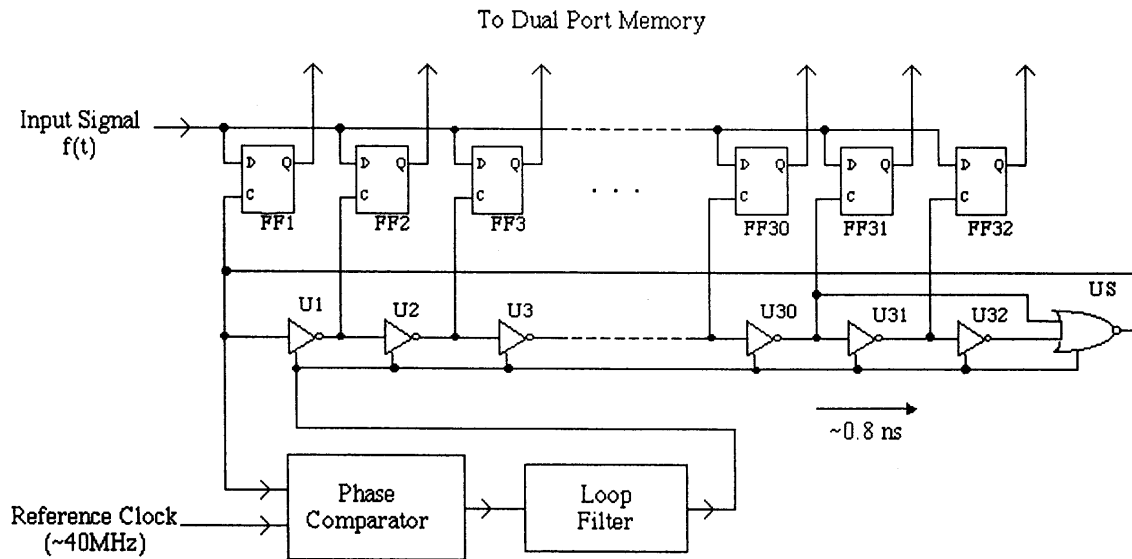
Use Wilkinson ADC with smaller discharge current to digitize voltage.

Drawbacks: No multi-hit capability
Deadtime

3. Digitizers with Clock Interpolation

Most experiments in HEP require multi-hit capability, no deadtime

Commonly used technique for time digitization (Y. Arai, KEK)



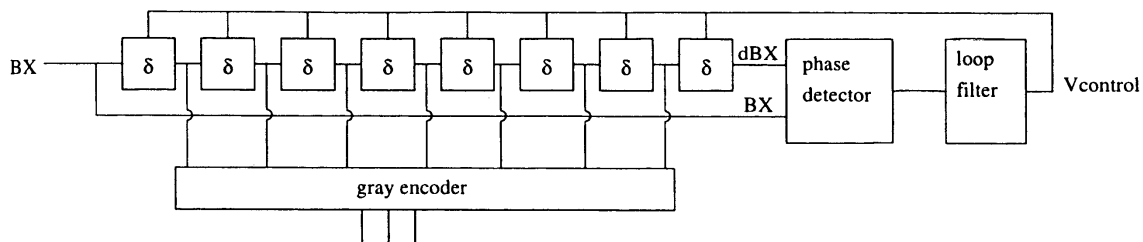
- Digitizing an external signal at a period of internal gate delay of ~ 0.8 ns.
- High Stability with a Phase Locked Loop.
- Long time range (> 3 μ s) & No deadtime by a Dual Port Memory.
- High precision, High Density & Low Cost LSI.

Patent Pending
 • S63-067314 (JP)
 • H3-133169 (JP)
 • H6-69507 (JP)
 • 95300652.5 (EU)

Clock period interpolated by inverter delays (U1, U2, ...).

Delay can be fine-tuned by adjusting operating point of inverters.

Delays stabilized by delay-locked loop

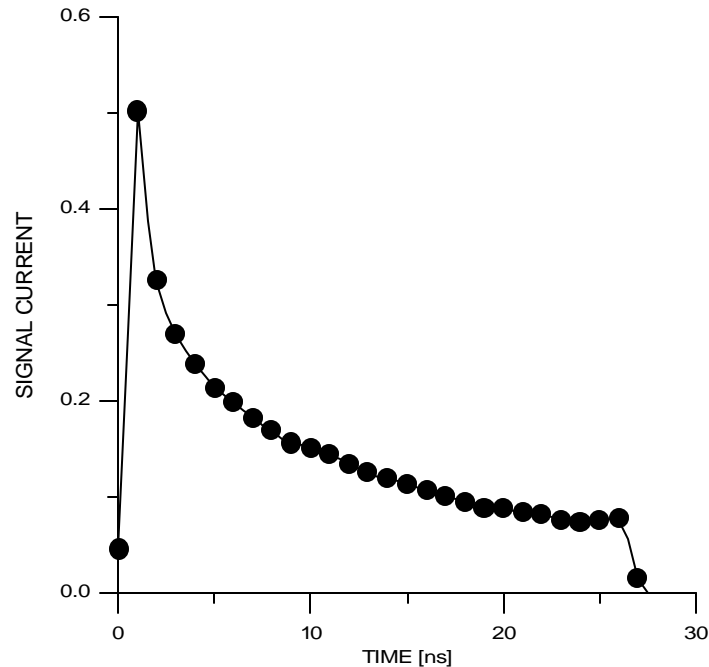


Devices with 250 ps resolution fabricated and tested.

see Y. Arai et al., IEEE Trans. Nucl. Sci. **NS-45/3** (1998) 735-739
 and references therein.

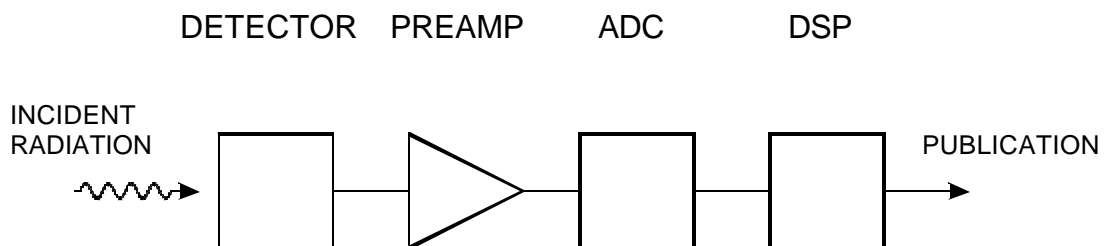
6. Digital Signal Processing

Sample detector signal with fast digitizer to reconstruct pulse:



Then use digital signal processor to perform mathematical operations for desired pulse shaping.

Block Diagram

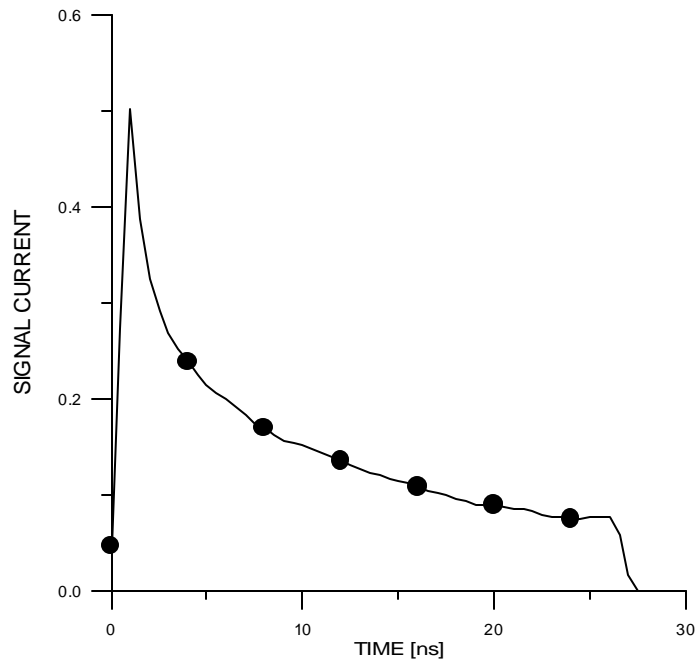


DSP allows great flexibility in implementing filtering functions

However: increased circuit complexity
 increased demands on ADC,
 compared to traditional shaping.

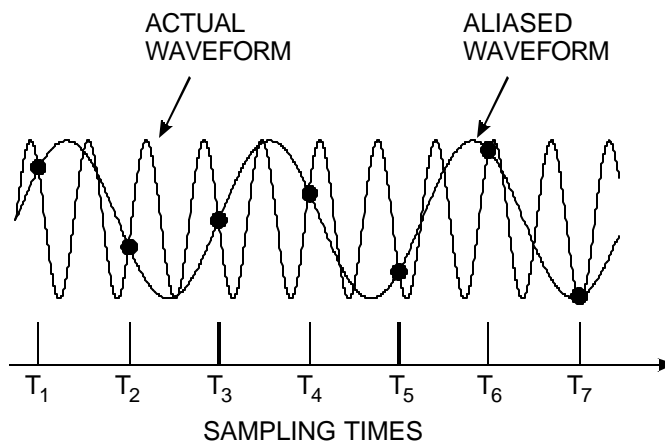
Important to choose sample interval sufficiently small to capture pulse structure.

Sampling interval of 4 ns misses initial peak.

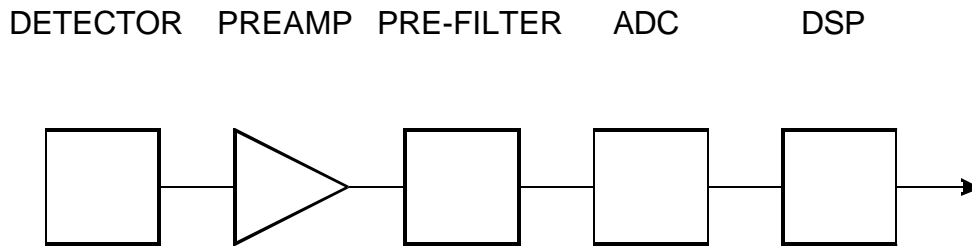


ADC must be capable of digitizing at twice the rate of the highest frequency component in the signal (Nyquist criterion).

With too low a sampling rate high frequency components will be “aliased” to lower frequencies:



⇒ Fast ADC required + Pre-Filter to limit signal bandwidth



- Dynamic range requirements for ADC may be more severe than in analog filtered system (depending on pulse shape and pre-filter).
- ADC can introduce additional noise (differential non-linearity introduces quasi-random noise)
- Electronics preceding ADC and front-end of ADC must exhibit same precision as analog system, i.e.

baseline and other pulse-to-pulse amplitude fluctuations less than order $Q_n/10$, i.e. typically 10^{-4} in high-resolution systems.

For 10 V FS at the ADC input in a high-resolution gamma-ray detector system, this corresponds to < 1 mV.

⇒ ADC must provide high performance at short conversion times

Today this is technically feasible for some applications, e.g. detectors with moderate to long collection times (γ and x-ray detectors).

Systems commercially available.

Benefits of digital signal processing:

- Flexibility in implementing filter functions
- Filters possible that are impractical in hardware
- Simple to change filter parameters
- Tail cancellation and pile-up rejection easily incorporated
- Adaptive filtering can be used to compensate for pulse shape variations.

Where is digital signal processing appropriate?

- Systems highly optimized for
Resolution
High counting rates
- Variable detector pulse shapes

Where is analog signal processing best (most efficient)?

- Fast shaping
- Systems not sensitive to pulse shape (fixed shaper constants)
- High density systems that require
small circuit area
low power

Both types of systems require careful analog design.

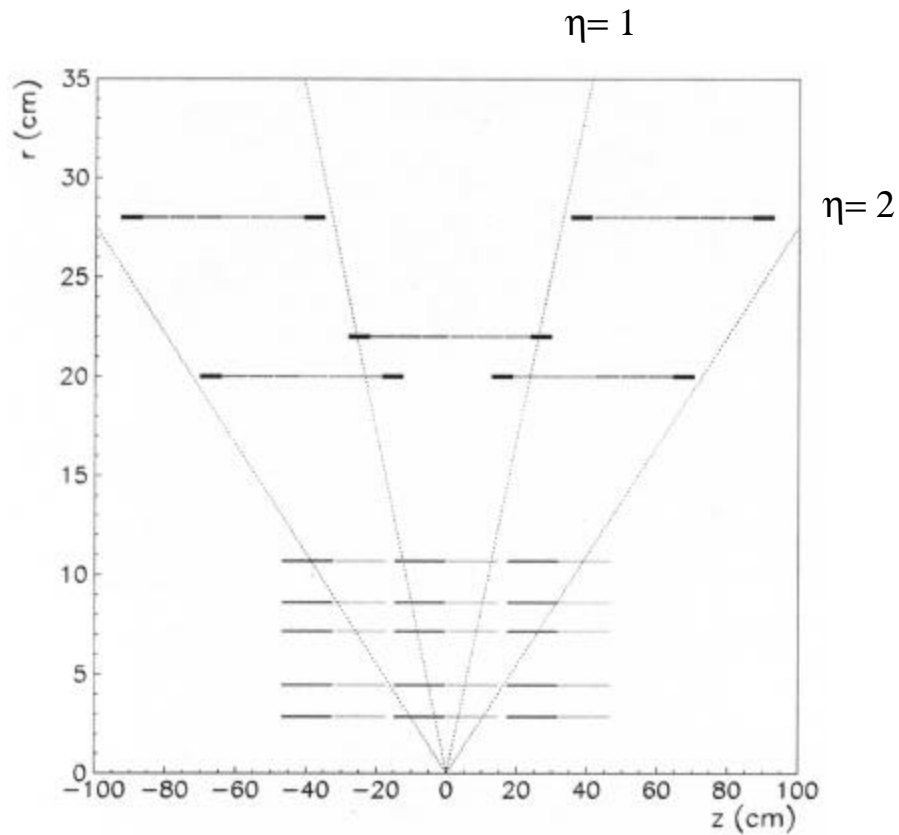
Progress in fast ADCs (precision, reduced power) will expand range of DSP applications

7. Detector Systems – Some Examples

7.1 CDF Vertex Detector Upgrade: SVX2

Expand coverage of existing vertex detector

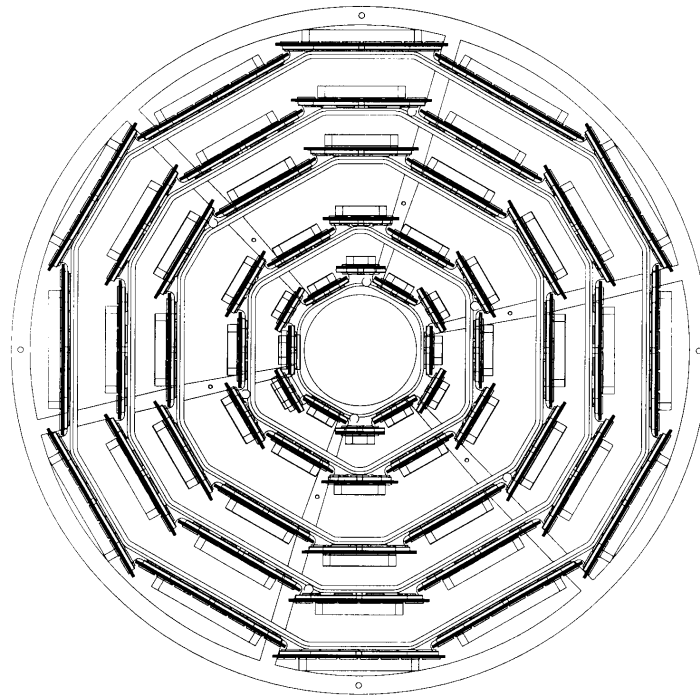
a) side view ($z = \text{beam axis}$)



Inner 5 layers: SVX2

Outer 2 layers: ISL

b) Axial view of vertex detector



Property	Layer 0	Layer 1	Layer 2	Layer 3	Layer 4
Radial distance (cm)	2.45	4.67	7.02	8.72	10.6
Stereo angle (degrees)	90	90	+1.2	90	-1.2
$r\phi/z$ readout channels	256/512	384/576	640/640	768/512	896/896
$r\phi/z$ readout chips	2/2	3/3	5/5	6/4	7/7
$r\phi/z$ strip pitch (μm)	60/141	62/125.5	60/60	60/141	65/65
Total width (mm)	17.14	25.59	40.30	47.86	60.17
Total length (mm)	74.3	74.3	74.3	74.3	74.3

Layers 0, 1 and 3 use 90° stereo angle, whereas layers 4 and 5 use 1.2° stereo angle to reduce ghosting.

Electronic Readout

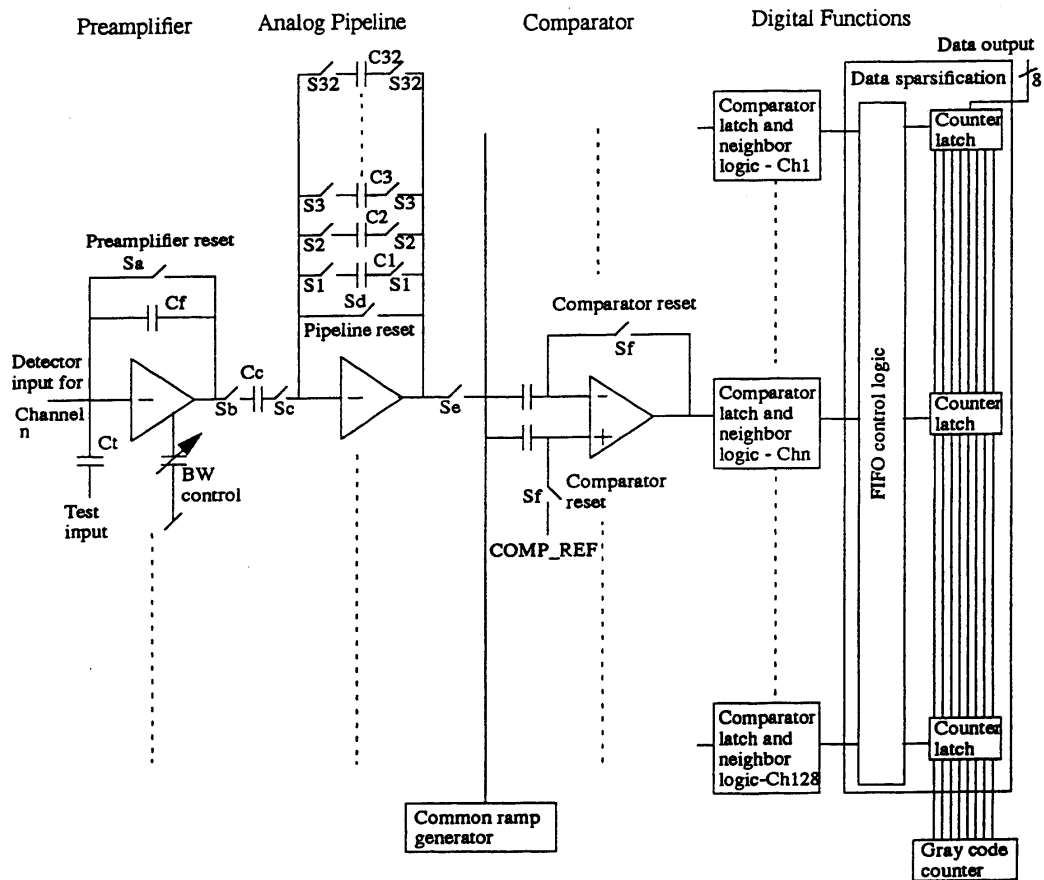
SVX2 uses the SVX3 chip, which is a further development of the SVX2 chip used by DØ.

Include on-chip digitization of analog signal

Threshold, calibration via on-chip DACs

All communication to and from chip via digital bus

Block diagram of SVX2



Wilkinson ADC integrated with pipeline + comparator, which is also used for sparsification. Adds $100\ \mu\text{m}$ to length and $300\ \mu\text{W}/\text{ch}$ power.

ADC clock runs at 106 MHz in experiment, tested to 400 MHz

Total power: 3 mW/ch

SVX2 die layout

Dimensions: 6.3 x 8.7 mm
0.8 μm , triple-metal rad-hard CMOS

Input Pads

Preamplifiers

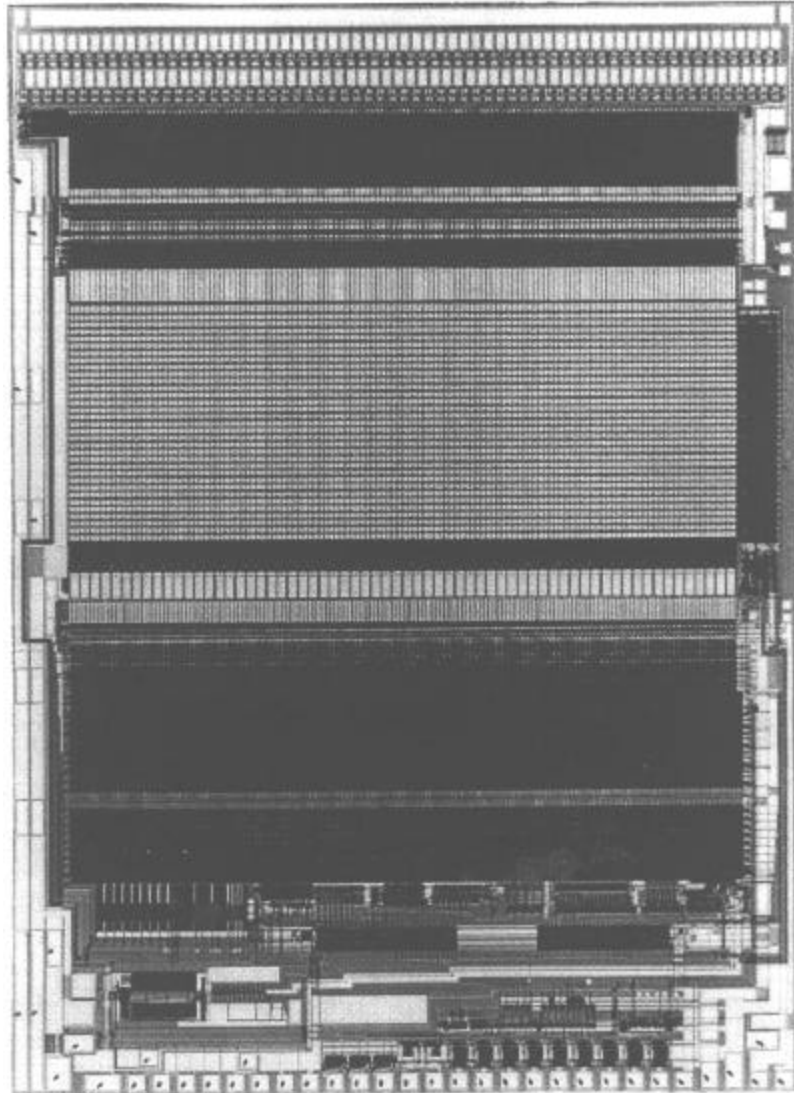
Analog Pipeline

ADC Comparator

Neighbor Logic

Sparsification +
Readout

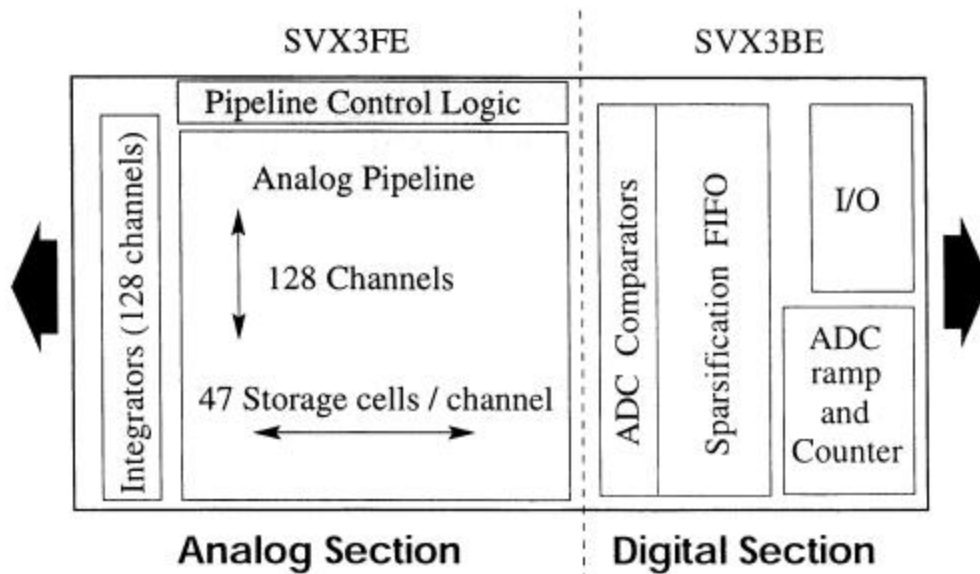
ADC Ramp +
Counter, I/O



SVX2 (used by DØ) is designed for sequential signal acquisition and readout.

SVX3 (used by CDF) allows concurrent read-write, i.e. signal acquisition and readout can proceed concurrently.

SVX3 Floor Plan

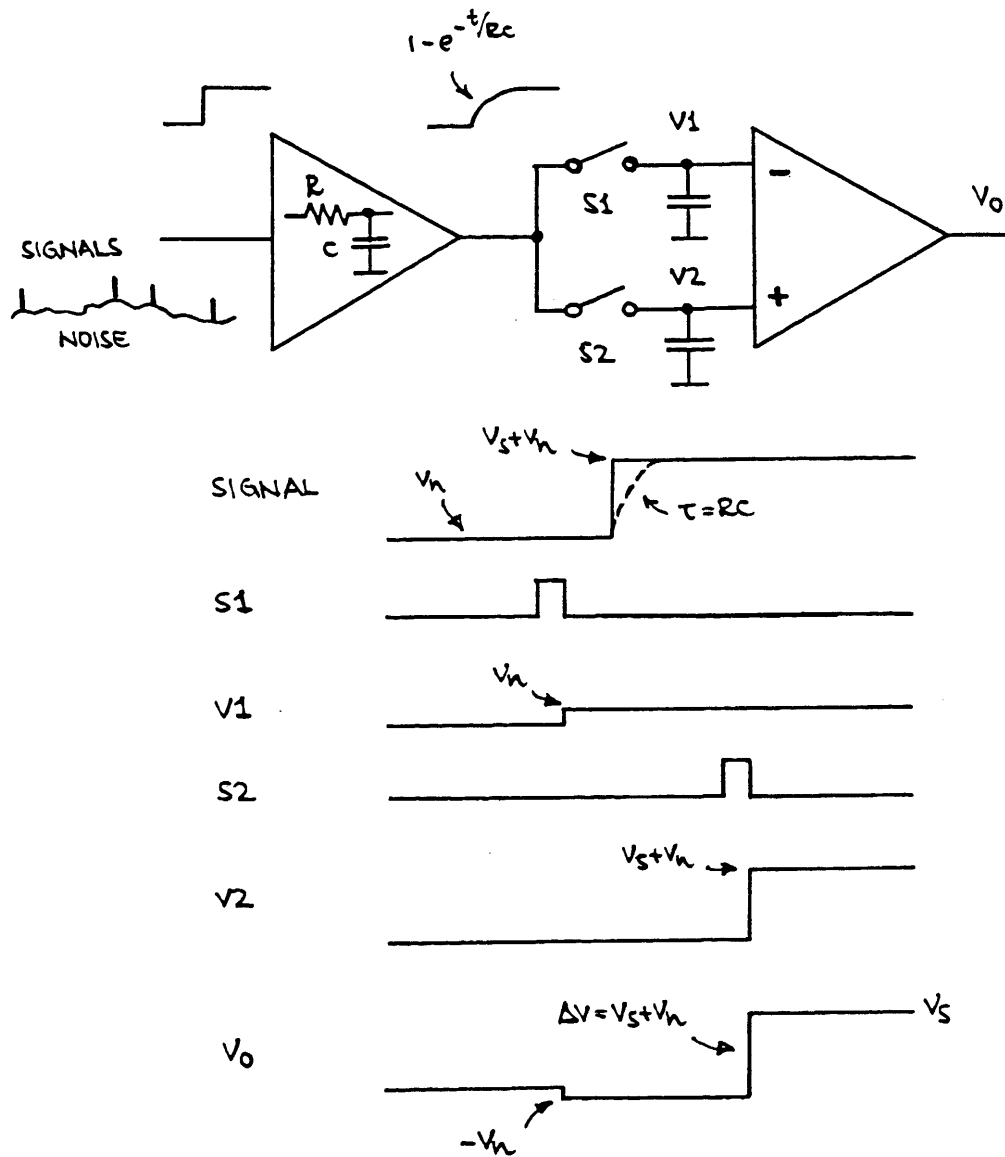


Analog section:	$6.26 \times 8.06 \text{ mm}^2$
Digital section:	$6.26 \times 4.97 \text{ mm}^2$
Combined in 1 chip:	$6.26 \times 12 \text{ mm}^2$

Measured Noise: $Q_n = 500 \text{ el} + 60 \text{ el/pF rms}$

Both chips fabricated in rad-hard CMOS.

SVX2 and SVX3 utilize correlated double sampling for pulse shaping



Correlated double sampling requires prior knowledge of signal arrival.

OK for colliders if $\Delta T_{beam} > T_{shaper}$, but not for random signals.

High luminosity colliders (B Factories, LHC) have much shorter beam crossing intervals

⇒ continuous shaping required

7.2. BaBar Silicon Vertex Tracker

B mesons from $Y(4S)$ production have low momentum.

Asymmetry in beam energies (9 GeV e^- on 3.1 GeV e^+) used to provide boost ($\beta\gamma = 0.56$) that allows conventional vertex detectors to cope with short B meson lifetime.

Vertex detector must provide resolution in boost direction, i.e. parallel to beam axis, rather than in $r\phi$.

Resolution requirement not stringent:

Less than 10% loss in precision in the asymmetry measurement if the separation of the B vertices is measured with a resolution of $\frac{1}{4}$ the mean separation (250 μm at PEP-II)

\Rightarrow 80 μm vertex resolution required for both CP eigenstates and tagging final states.

Resolution is multiple-scattering limited

beam pipe: 0.6% X_0

Use crossed strips

z -strips for vertex resolution

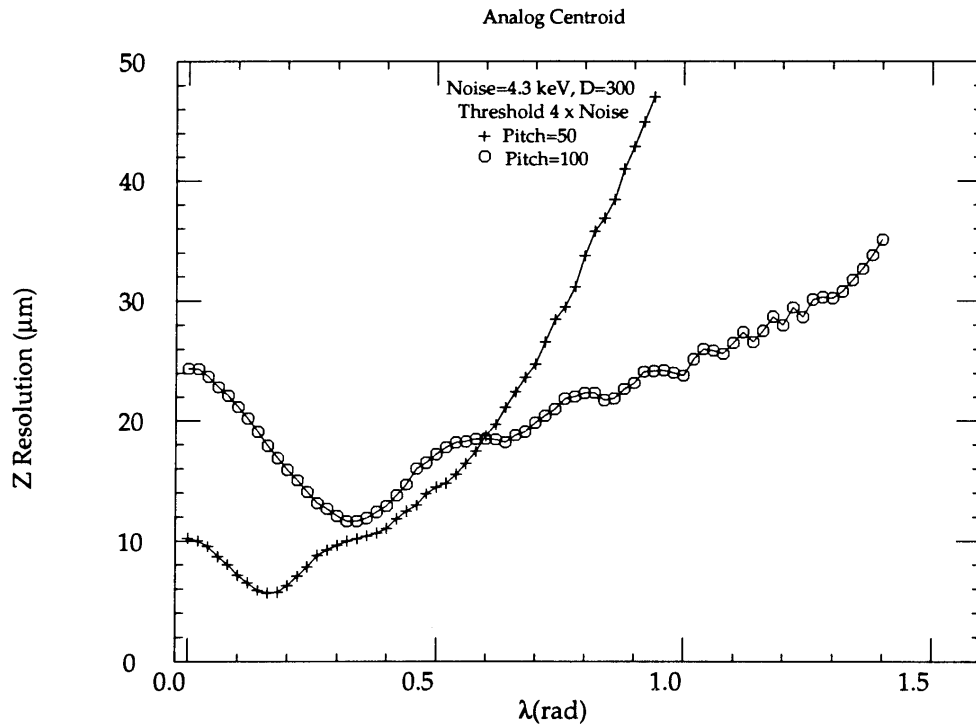
$r\phi$ strips for pattern recognition

Measurement does not require utmost position resolution

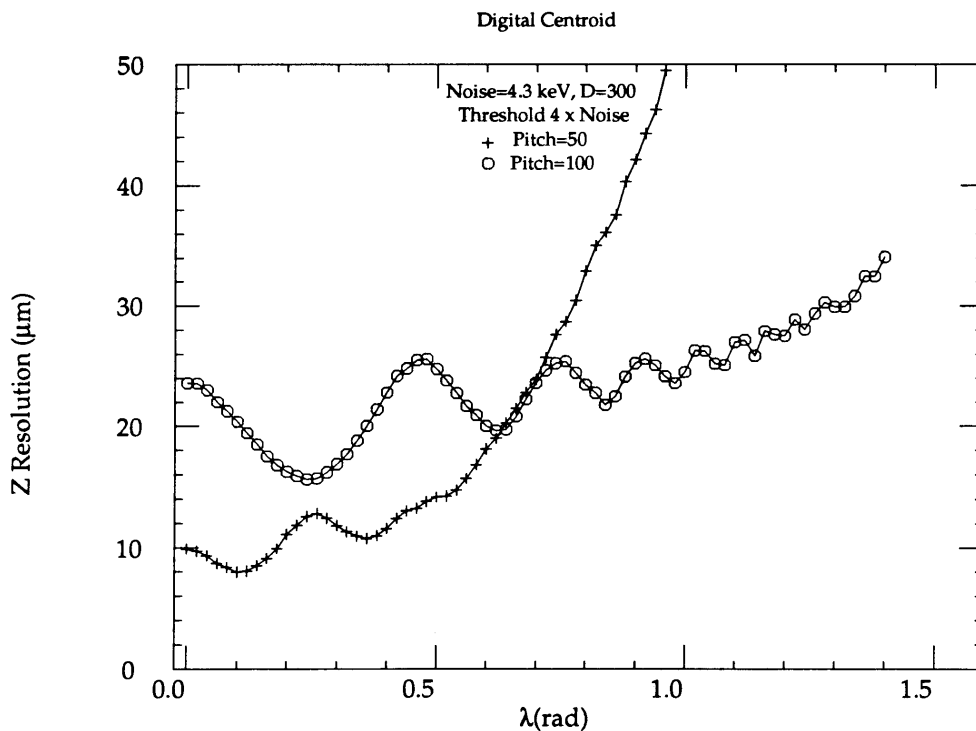
\Rightarrow use binary readout

Position resolution for analog and binary readout vs dip angle λ .

Analog readout (50 and 100 μm pitch)

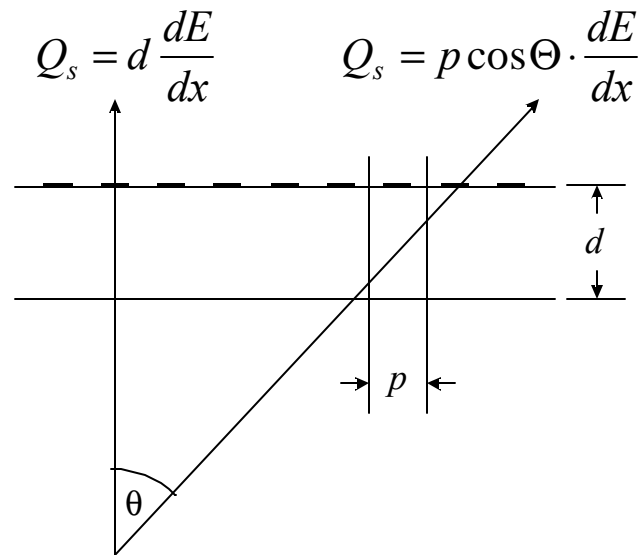


Binary readout (50 and 100 μm pitch)



Why does 100 μm pitch yield better resolution at large dip angles?

Signal in z -strips degrades at large dip angles



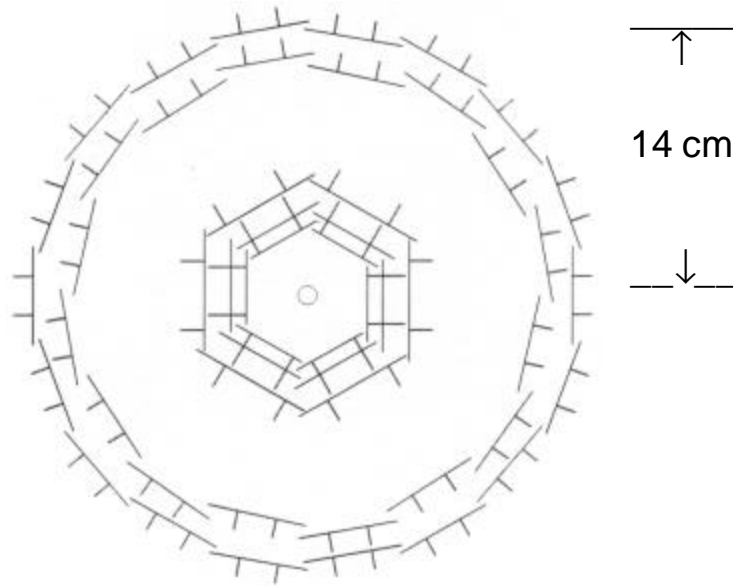
Change strip pitch at $\lambda > 0.7$ radians

Furthermore

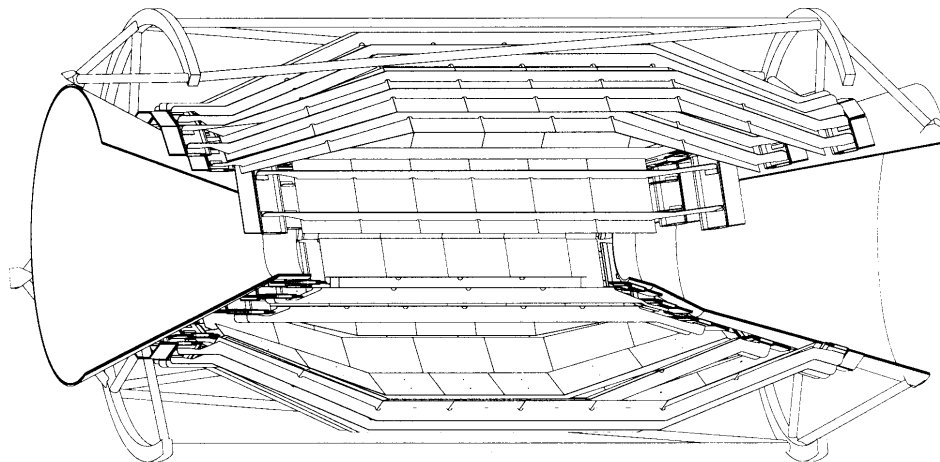
add coarse analog information (3 – 4 bits adequate)

Mechanical arrangement of detector

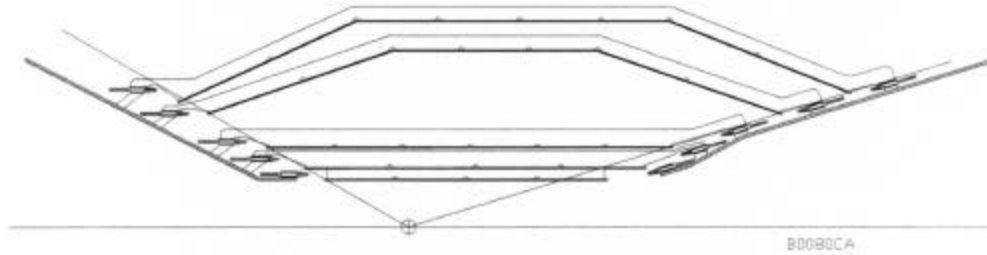
Axial view



Side view



Outer layers use “lampshade” geometry instead of disks



Electronics mounted outside of active region
(connected to detectors by kapton cables)

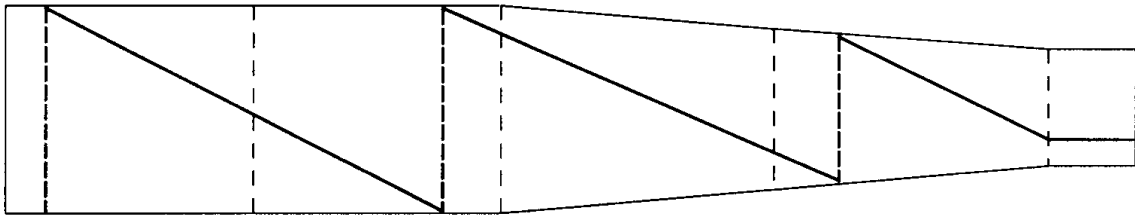
⇒ long strips (high capacitance) in outer layers

Layer	Fanout Type	Length (cm)	Number of Readout		Typical Pitch at		Number of Circuits
			Strips	Channels	Input (μm)	Output (μm)	
1	$z, F+B$	12.5	950	768	100	50	12
	$\phi, F+B$	3.0	768	768	50	50	12
2	$z, F+B$	14.5	1150	1024	100	50	12
	$\phi, F+B$	3.0	960	1024	50	50	12
3	$z, F+B$	15.6	1360	1280	100	50	12
	$\phi, F+B$	2.0	1280	1280	50	50	12
4a	z, F	19.7	885	512	200	50	8
	z, B	24.3	1115	512	200	50	8
	$\phi, F+B$	2.0	512	512	65	50	16
4b	z, F	20.6	930	512	200	50	8
	z, B	24.2	1160	512	200	50	8
	$\phi, F+B$	2.0	512	512	65	50	16
5a	z, F	25.2	1160	512	200	50	9
	z, B	25.1	1205	512	200	50	9
	$\phi, F+B$	2.0	512	512	65	50	18
5b	$z, F+B$	26.1	1205	512	200	50	18
	$\phi, F+B$	2.0	512	512	65	50	18

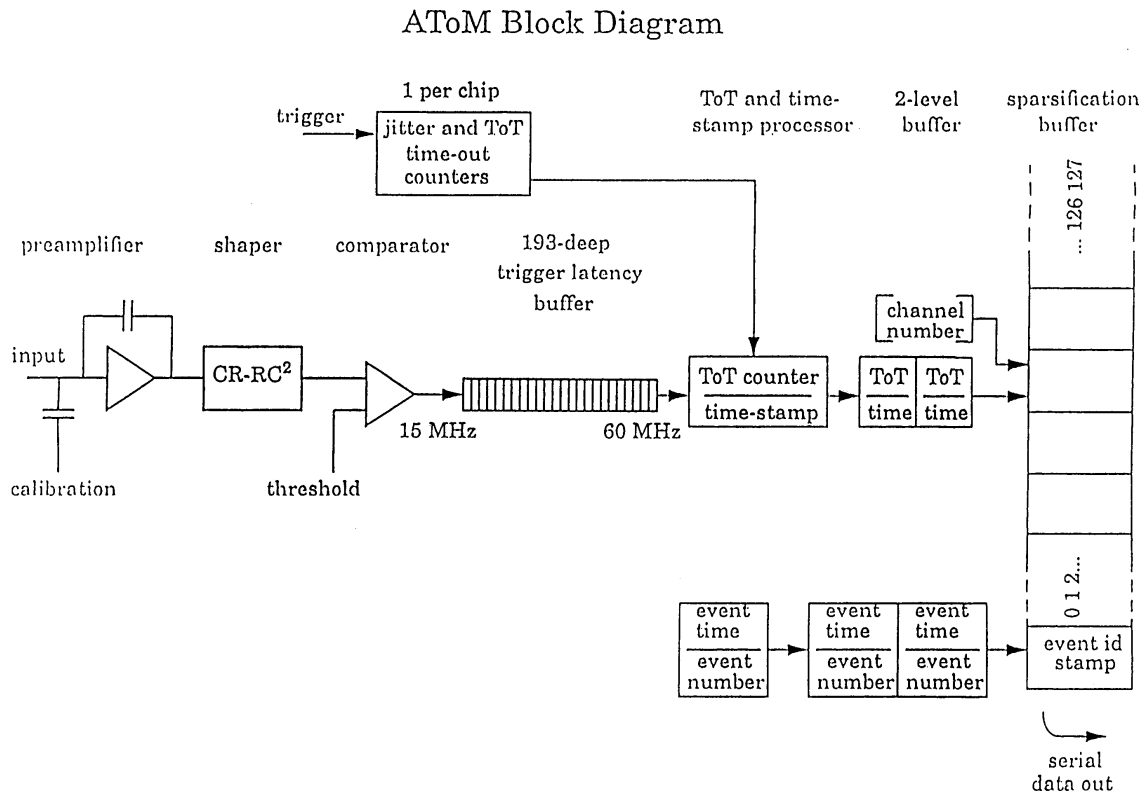
z -strips are connected at ends, to avoid cables in middle of detector.

Kapton connecting cables that connect multiple detector segments
(use $r\phi$ resolution to disentangle ambiguities)

Connections made along diagonals:



AToM – Readout IC for BaBar Vertex Detector (LBNL, Pavia, UCSC)



Preamplifier with continuous reset

CR-RC² shaper with selectable shaping times (100, 200 and 400 ns)

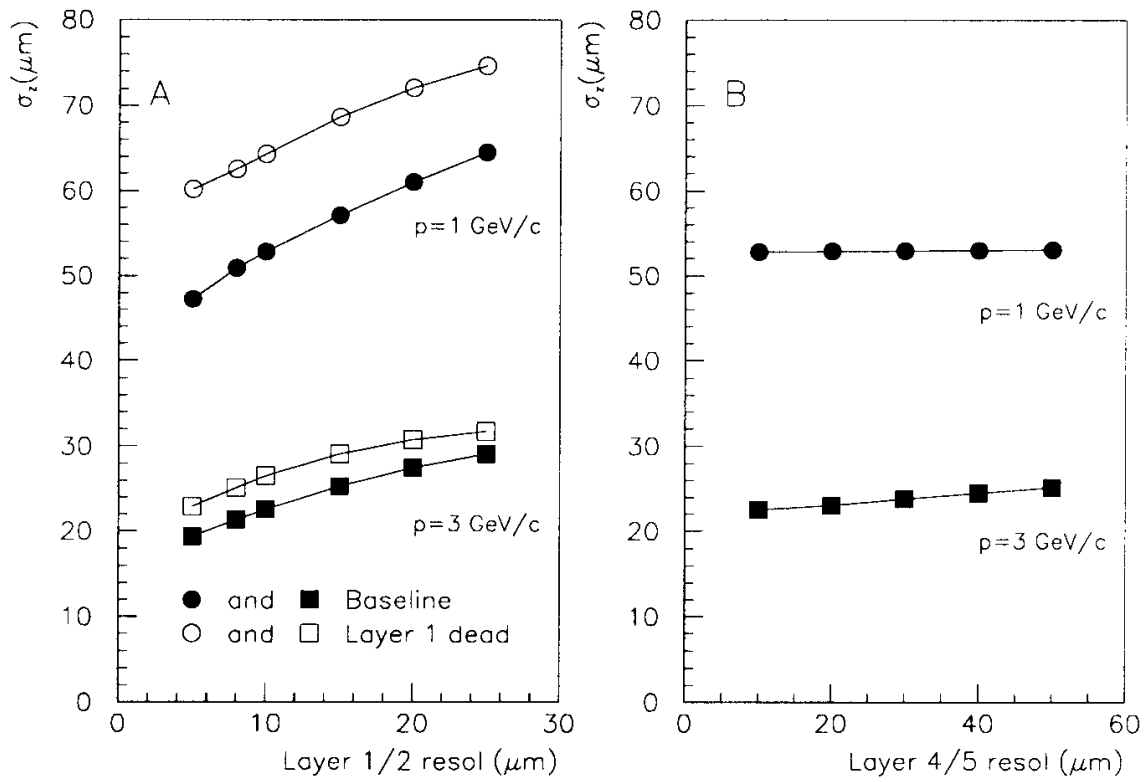
Outer layers of tracker have longer strips (higher capacitance) than inner layers. Lower occupancy allows use of longer shaping time to maintain electronic noise.

Coarse digitization via Time-Over-Threshold
(analog information for position interpolation only requires 3 – 4 bit resolution)

Measured noise (pre-production run) for 3 shaping times

100 ns:	$Q_n = 350 \text{ el} + 42 \text{ el/pF}$
200 ns:	$Q_n = 333 \text{ el} + 35 \text{ el/pF}$
400 ns:	$Q_n = 306 \text{ el} + 28 \text{ el/pF}$

Simulated vertex resolution



8. Why Things Don't Work

or

Why S/N Theory Often Seems to be Irrelevant

Throughout the previous lectures it was assumed that the only sources of noise were

- random
- known
- in the detector, preamplifier, or associated components

In practice, the detector system will pick up spurious signals that are

- not random,
- but not correlated with the signal,

so with reference to the signal they are quasi-random.

⇒ Baseline fluctuations superimposed on the desired signal

⇒ Increased detection threshold,
Degradation of resolution

Important to distinguish between

- pickup of spurious signals, either from local or remote sources (clocks, digital circuitry, readout lines),
and
- self-oscillation
(circuit provides feedback path that causes sustained oscillation due to a portion of the output reaching the input)

A useful reference:

H.W. Ott, *Noise Reduction Techniques in Electronic Systems*
Wiley, 1976, ISBN 0-471-65726-3, TK7867.5.087

Common Types of Interference

1. Light Pick-Up

Critical systems:

- Photomultiplier tubes
- Semiconductor detectors
(all semiconductor detectors are photodiodes)

Sources

- Room lighting (Light Leaks)
- Vacuum gauges

Interference is correlated with the power line frequency
(60 Hz here, 50 Hz in Europe, Japan)

Pickup from incandescent lamps has twice the line frequency
(light intensity \propto voltage squared)

Diagnostics:

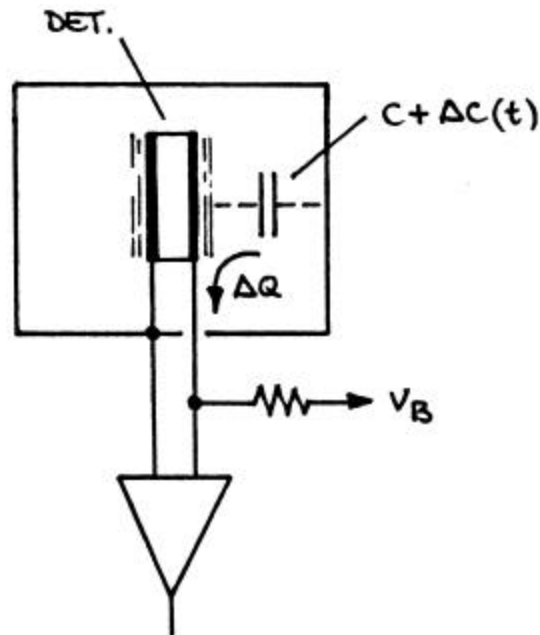
- a) inspect signal output with oscilloscope set to trigger mode "line". Look for stationary structure on baseline

Analog oscilloscope better than digital.

- b) switch off light

- c) cover system with black cloth (preferably felt, or very densely woven – check if you can see through it)

2. Microphonics



If the electrode at potential V_B vibrates with respect to the enclosure, the stray capacitance C is modulated by $\Delta C(t)$, inducing a charge

$$\Delta Q(t) = V_B \Delta C(t)$$

in the detector signal circuit.

Typically, vibrations are excited by motors (vacuum pumps, blowers), so the interference tends to be correlated with the line frequency.

Check with

- a) oscilloscope on line trigger
- b) hand to feel vibrations

This type of pickup only occurs between conductors at different potentials, so it can be reduced by shielding the relevant electrode.

- a) additional shield at electrode potential
- b) in coaxial detectors, keep outer electrode at 0 V.

3. RF Pickup

All detector electronics are sensitive to RF signals.

The critical frequency range depends on the shaping time. The gain of the system peaks at

$$f \approx \frac{1}{2\pi\tau}$$

and high-gain systems will be sensitive over a wide range of frequencies around the peaking frequency.

Typical sources

- Radio and TV stations
 - AM broadcast stations: 0.5 – 1.7 MHz
 - FM broadcast stations: ~ 100 MHz
 - TV stations: 50 – 800 MHz
- Induction furnaces (13.6, 27, 40 MHz)
- Accelerators

⇒ sine waves

- Computers (10's to 100's MHz)
- Video Displays (10 – 100 kHz)
- Radar (GHz)
- Internal clock pulses (e.g. digital control, data readout)

⇒ Pulses (or recurring damped oscillations)

Pulsed UHF or microwave emissions can affect low-frequency circuitry by driving it beyond linearity (the bandwidth of the preamplifier can be much greater than of the subsequent shaper).

Diagnostic Techniques

a) Inspect analog output on an oscilloscope.

Check with different trigger levels and deflection times and look for periodic structure on the baseline.

Pickup levels as low as 10% of the noise level can be serious, so careful adjustment of the trigger and judicious squinting of the eye is necessary to see periodic structure superimposed on the random noise.

Again, an “old fashioned” analog oscilloscope is best.

b) Inspect output with a spectrum analyzer

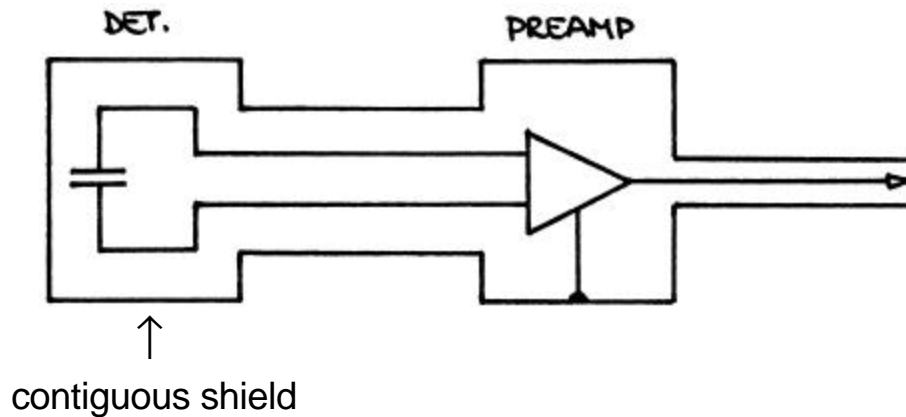
This is a very sensitive technique.

Indeed, for some it may be too sensitive, as it tends to show signals that are so small that they are irrelevant.

Ascertain quantitatively what levels of interfering signals vs. frequency are important.

Remedial Techniques

a) Shielding



Conducting shield attenuates an incident electromagnetic wave because of

a) reflection of the incident wave

$$E_{0r} = E_0 \left(1 - \frac{Z_{shield}}{Z_0} \right)$$

where

$$Z_0 = \sqrt{\frac{\mu}{\epsilon}} = 377 \Omega$$

is the impedance of free space.

The impedance of the conductor is very low, so most of the incident wave is reflected.

b) attenuation of the absorbed wave

The absorbed wave gives rise to a local current, whose field counteracts the primary excitation.

The net current decreases exponentially as the wave penetrates deeper into the medium

$$i(x) = i_0 e^{-x/\delta}$$

where i_0 is the current at the surface of the conductor and

$$\delta = \frac{1}{2 \cdot 10^{-4}} \left[\sqrt{\text{cm} \cdot \text{s}^{-1}} \right] \sqrt{\frac{\rho}{\mu_r f}}$$

is the penetration depth or “skin depth”. μ_r and ρ are the permeability and resistivity of the conductor and f is the frequency of the incident wave.

In aluminum, $\rho = 2.8 \mu\Omega \cdot \text{cm}$ and $\mu_r = 1$, so

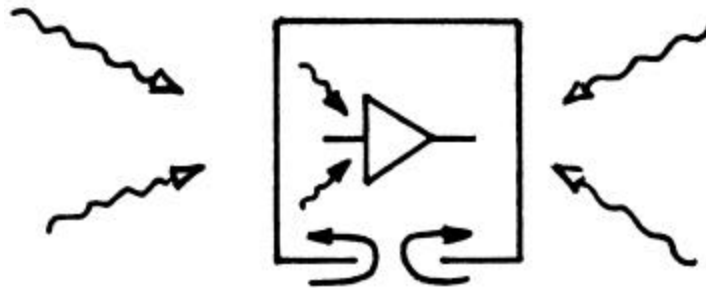
at $f = 1 \text{ MHz}$ the skin depth $\delta = 84 \mu\text{m} \approx 100 \mu\text{m}$.

The skin depth decreases with the square root of

- increasing frequency
- decreasing resistivity (increasing conductivity)

If the shield is sufficiently thick, the skin effect isolates the inner surface of a shielding enclosure from the outer surface.

However, this isolation only obtains if no openings in the shield allow the current to flow from the outside to the inside.



External fields can penetrate significantly if openings $> \lambda/1000$ (diameter of holes, length of slots).

To maintain the integrity of the shield,

- covers must fit tightly with good conductivity at the seams (beware of anodized aluminum!),
- all input and output lines (signal and DC supplies) must have good shield connections,
- shield coverage of coax or other cables $>90\%$ and
- connectors must maintain the integrity of the shield connection.

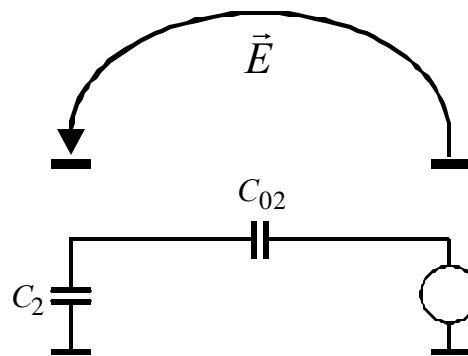
b) “Field Line Pinning”

Full shielding is not always practical, nor is it always necessary.

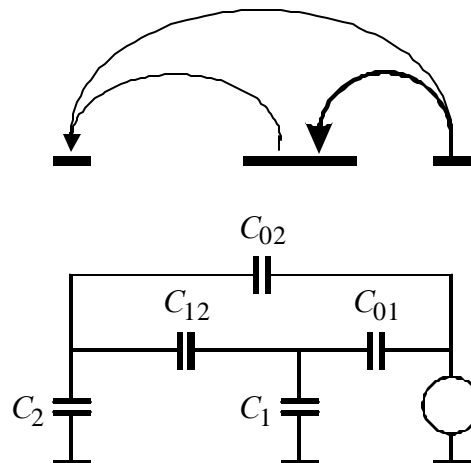
Rather than preventing interference currents from entering the detector system, it is often more practical to reduce the coupling of the interference to the critical nodes.

Consider a conductor carrying an undesired signal current, with a corresponding signal voltage.

Capacitive coupling will transfer interference to another circuit node.



If an intermediate conductor is introduced with a large capacitance to the interference source and to ground compared to the critical node, it will “capture” the field lines and effectively “shield” the critical node.



“Field line pinning” is the operative mechanism of “Faraday shields”.

“Self-Shielding” Structures

The magnitude of capacitive coupling depends on the dielectric constant of the intermediate medium.

Ensemble of electrodes: $\epsilon_r = 1$ in volume between set 2 to set 1 and $\epsilon_r > 1$ between sets 2 and 3.



The capacitance between electrode sets 2 and 3 is ϵ_r times larger than between sets 1 and 2.

Example: Si, $\epsilon_r = 11.9$

- ⇒ 92.2% of the field lines originating from electrode set 2 terminate on set 3,
i.e. are confined to the Si bulk
- 7.8% terminate on set 1.

For comparison, with $\epsilon_r = 1$, 50% of the field lines originating from electrode set 2 terminate on set 1.

- ⇒ high dielectric constant reduces coupling of electrode sets 2 and 3 to external sources.

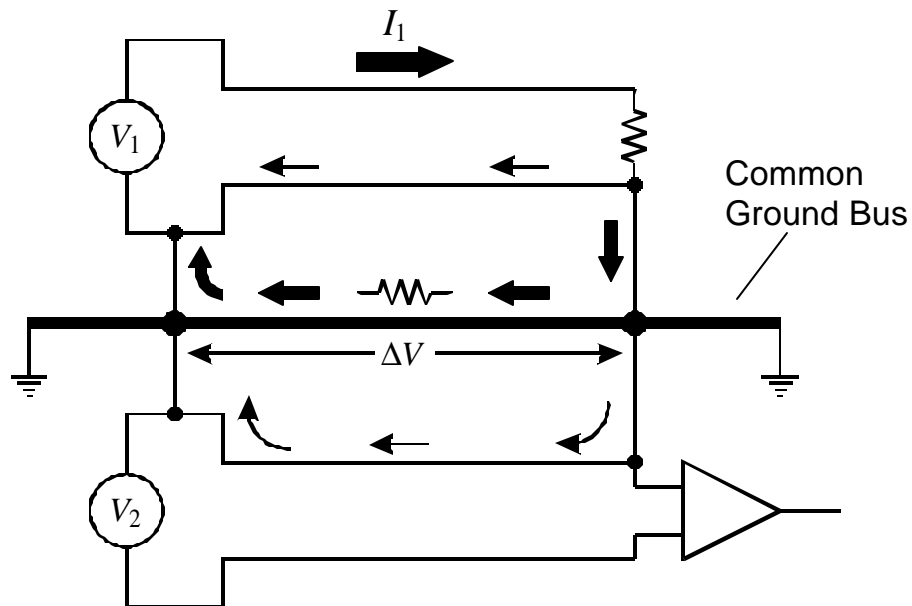
If the interference source is represented by electrode set 1 and sets 2 and 3 represent a detector

- ⇒ Si detector is 6.5 times less sensitive to capacitive pickup than a detector with $\epsilon_r = 1$
(e.g. a gas chamber with the same geometry)

4. Shared Current Paths (“ground loops”)

Although capacitive or inductive coupling cannot be ignored, the most prevalent mechanism of undesired signal transfer is the existence of shared signal paths.

Mechanism:



A large alternating current I_1 is coupled into the common ground bus.

Although the circuit associated with generator V_1 has a dedicated current return, the current seeks the path of least resistance, which is the massive ground bus.

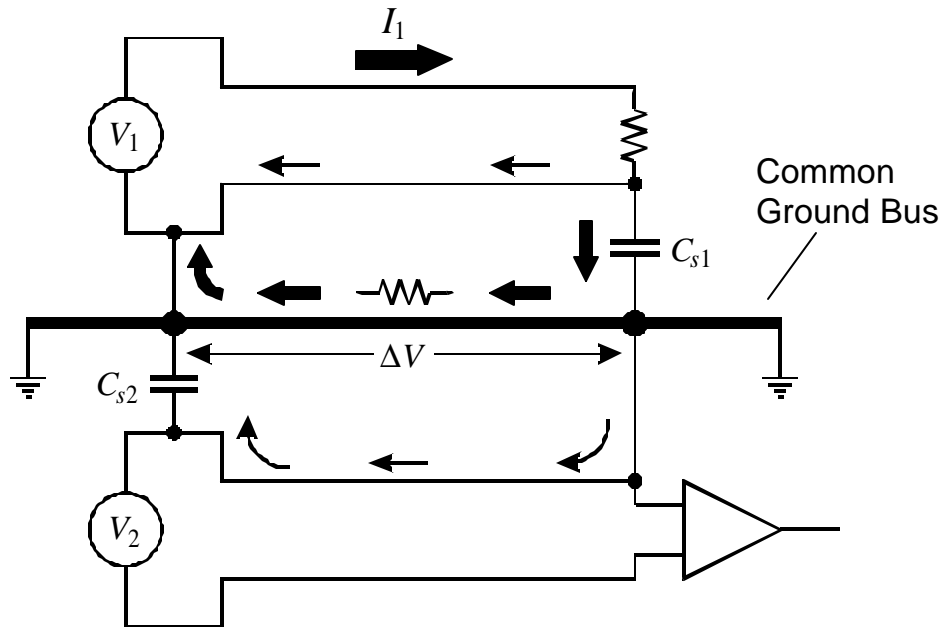
The lower circuit is a sensitive signal transmission path. Following the common wire, it is connected to ground at both the source and receiver.

The large current flowing through the ground bus causes a voltage drop ΔV , which is superimposed on the low-level signal loop associated with V_2 and appears as an additional signal component.

Cross-coupling has *nothing to do with grounding per se*, but is due to the common return path.

However, the common ground caused the problem by establishing the shared path.

In systems that respond to transients (i.e. time-varying signals) rather than DC signals, secondary loops can be closed by capacitance. A DC path is not necessary.



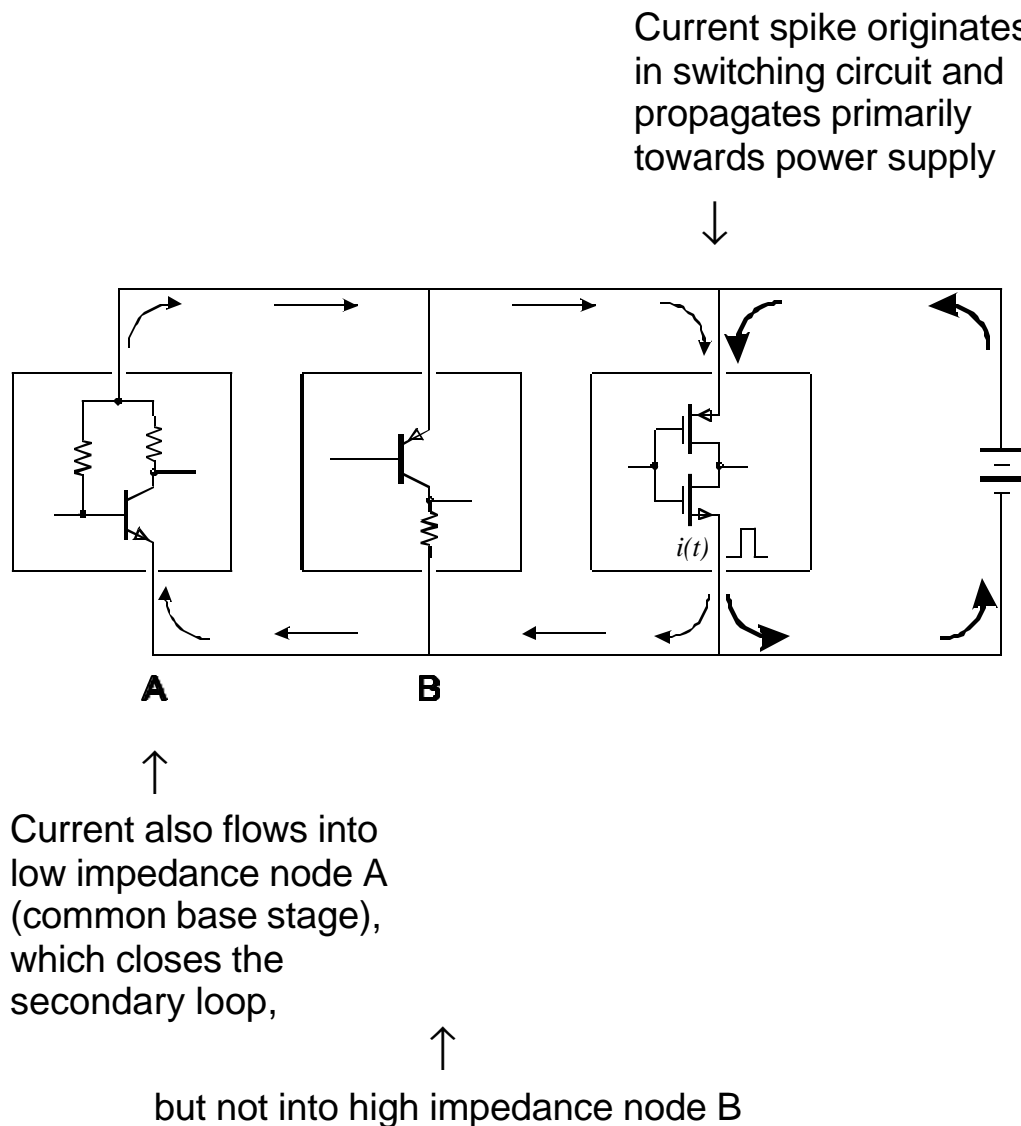
The loops in this figure are the same as shown before, but the loops are closed by the capacitances C_{s1} and C_{s2} . Frequently, these capacitances are not formed explicitly by capacitors, but are the stray capacitance formed by a power supply to ground, a detector to its support structure (as represented by C_{s2}), etc. For AC signals the inductance of the common current path can increase the impedance substantially beyond the DC resistance, especially at high frequencies.

This mode of interference occurs whenever spurious voltages are introduced into the signal path and superimpose on the desired signal.

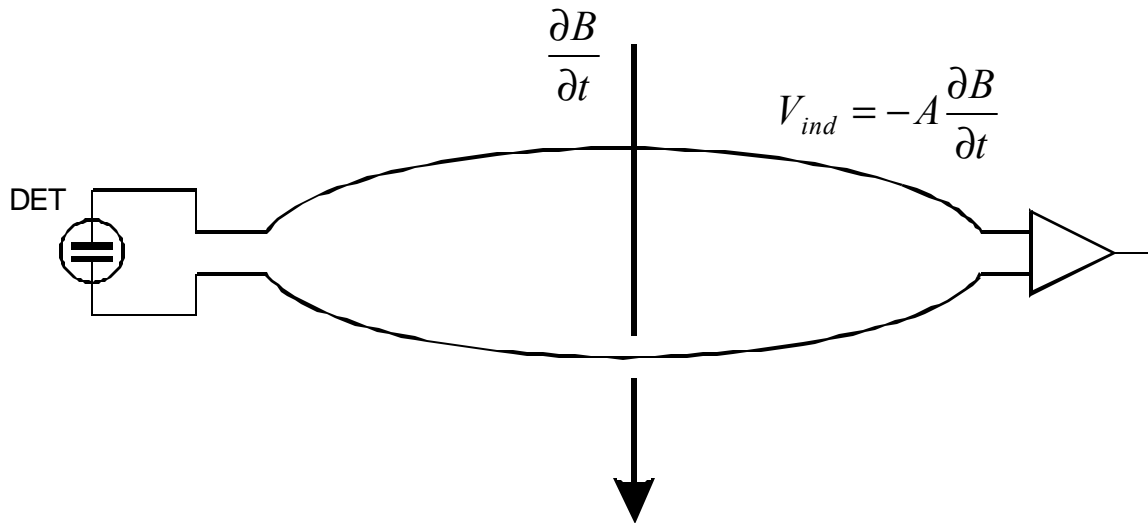
Interference does not cross-couple by voltage alone, but also via current injection.

Current spikes originating in logic circuitry, for example, propagate through the bussing system as in a transmission line.

Individual connection points will absorb some fraction of the current signal, depending on the relative impedance of the node.



Another mechanism, beside common conduction paths, is induction:



Clearly, the area A enclosed by any loops should be minimized.

Accomplished by routing signal line and return as a closely spaced pair.

Better yet is a twisted pair, where the voltages induced in successive twists cancel.

Problems occur when alternating detector electrodes are read out at opposite ends – often done because of mechanical constraints.

Remedial Techniques

1. Reduce impedance of the common path

⇒ Copper Braid Syndrome

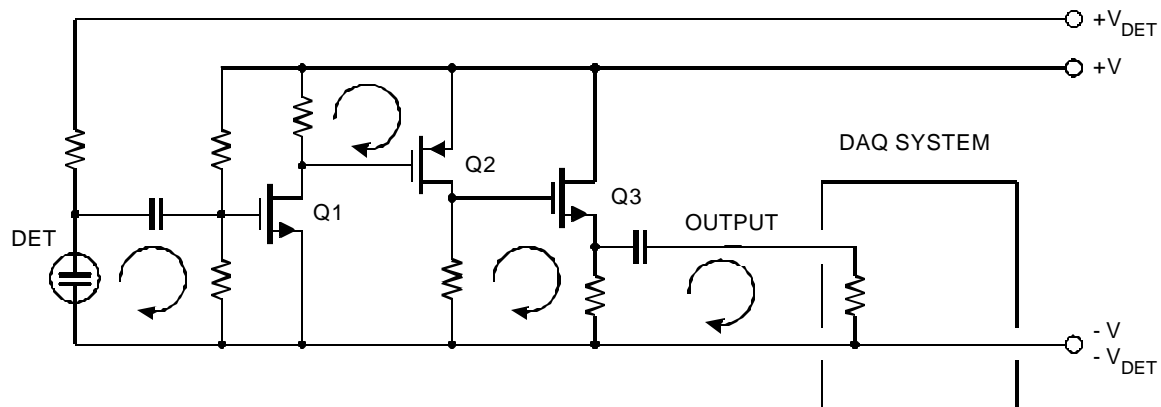
Colloquially called “improving ground”.

(sometimes fortuitously introduces an out-of-phase component of the original interference, leading to cancellation)

Rather haphazard, poorly controlled ⇒ continual surprises

2. Avoid Grounds

Circuits rely on current return paths, not a ground connection!



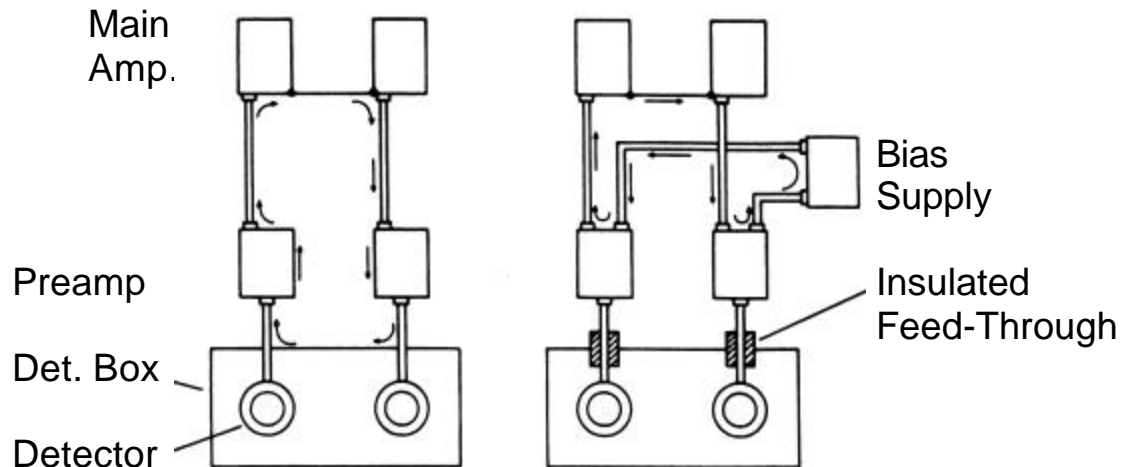
In transferring from stage to stage the signal current flows through local return loops.

1. At the input the detector signal is applied between the gate and source of Q1
2. At the output of Q1 the signal is developed across the load resistor in the drain of Q1 and applied between the gate and source of Q2.
3. The output of Q2 is developed across the load resistor in its drain and applied across the gate and source resistor and load.

Note that – disregarding the input voltage divider that biases Q1 – varying either $+V$ or $-V$ does not affect the local signals.

Breaking parasitic signal paths

Example:



The configuration at the left has a loop that includes the most sensitive part of the system – the detector and preamplifier input.

By introducing insulated feed-throughs, the input loop is broken.

Note that a new loop is shown, introduced by the common detector bias supply. This loop is restricted to the output circuit of the preamplifier, where the signal has been amplified, so it is less sensitive to interference.

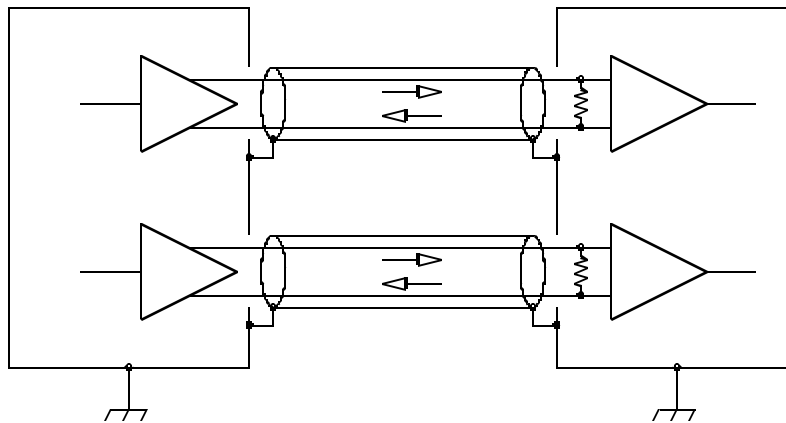
- Note that the problem is not caused by loops *per se*, i.e. enclosed areas, but by the multiple connections that provide entry paths for interference.
- Although not shown in the schematic illustrations above, both the “detector box” (e.g. a scattering chamber) and the main amplifiers (e.g. in a NIM bin or VME crate) are connected to potential interference sources, so currents can flow through parts of the input signal path.

Breaking shared signal paths, cont'd

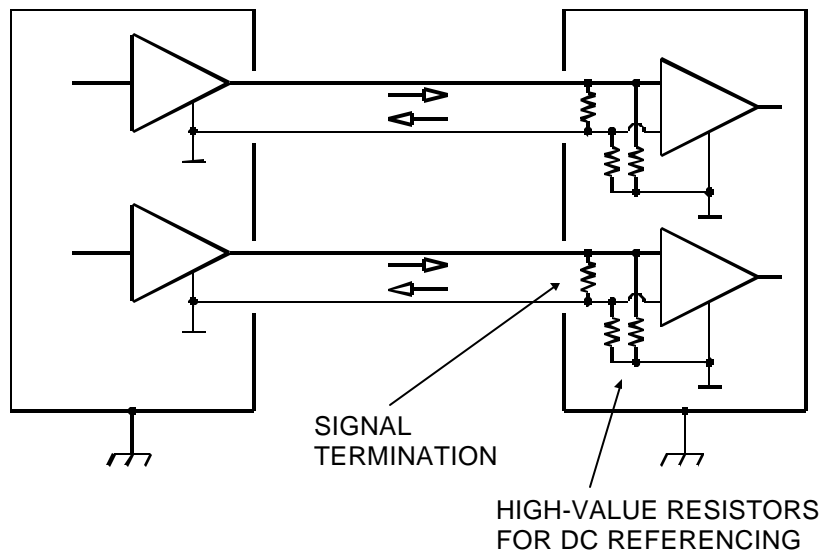
1. Differential Receivers

Besides providing common mode noise rejection, differential receivers also allow “ground free” connections.

Ideal configuration using differential drivers and receivers

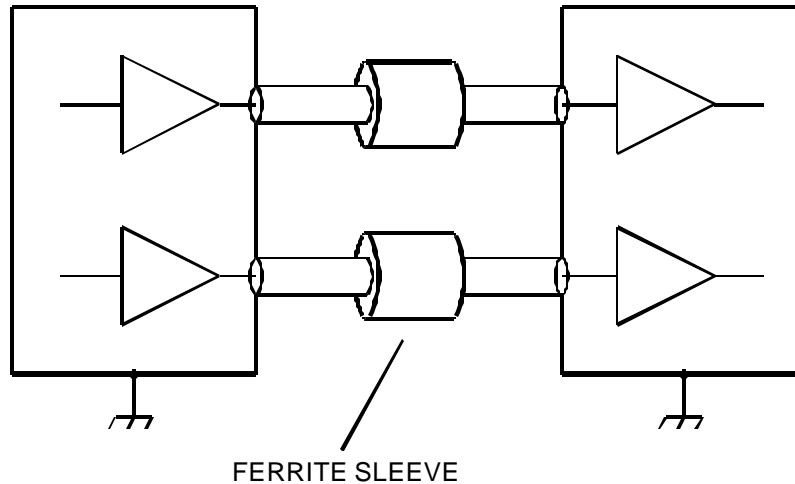


Technique also usable with single-ended drivers



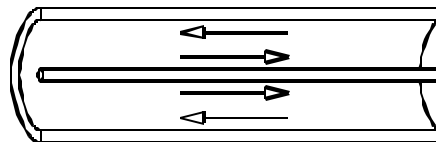
2. Insert high impedances

Ferrite sleeves block common mode currents.



Signal current in coax line flows on

- outer surface of inner conductor
- inner surface of shield.



Net field at *outer surface* of shield is zero.

⇒ Ferrite sleeve does not affect signal transmission.

Common mode currents in the coax line

(current flow in same direction on inner and outer conductor) or current components flowing only on the outside surface of the shield (“ground loops”)

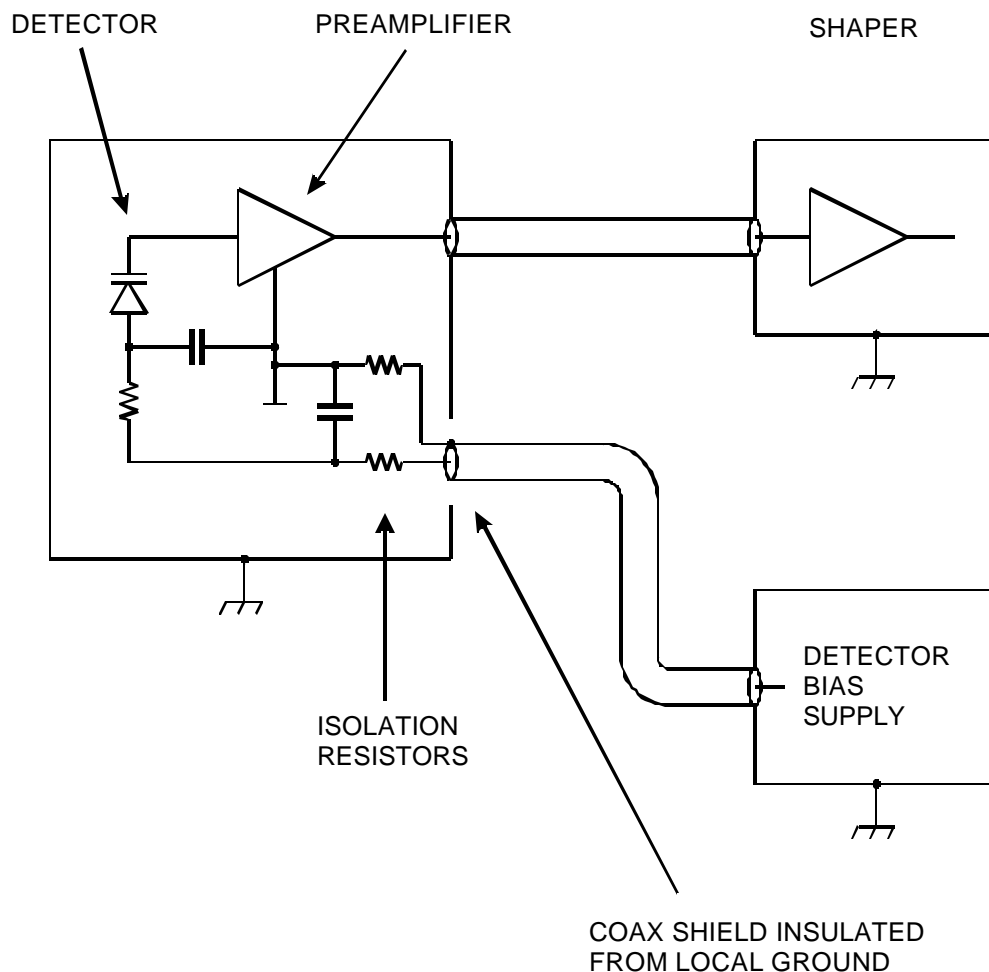
will couple to the ferrite and be suppressed.

Ferrite material must be selected to present high impedance at relevant frequencies.

Technique can also be applied to twisted-pair ribbon cables.

Series resistors isolate parasitic ground connections.

Example: detector bias voltage connection



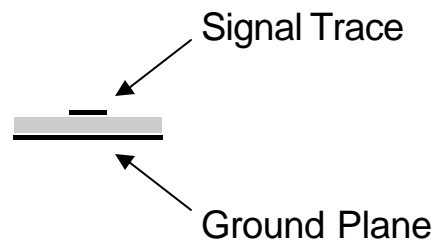
Isolation resistors can also be mounted in an external box that is looped into the bias cable. Either use an insulated box or be sure to isolate the shells of the input and output connectors from another.

A simple check for noise introduced through the detector bias connection is to use a battery.

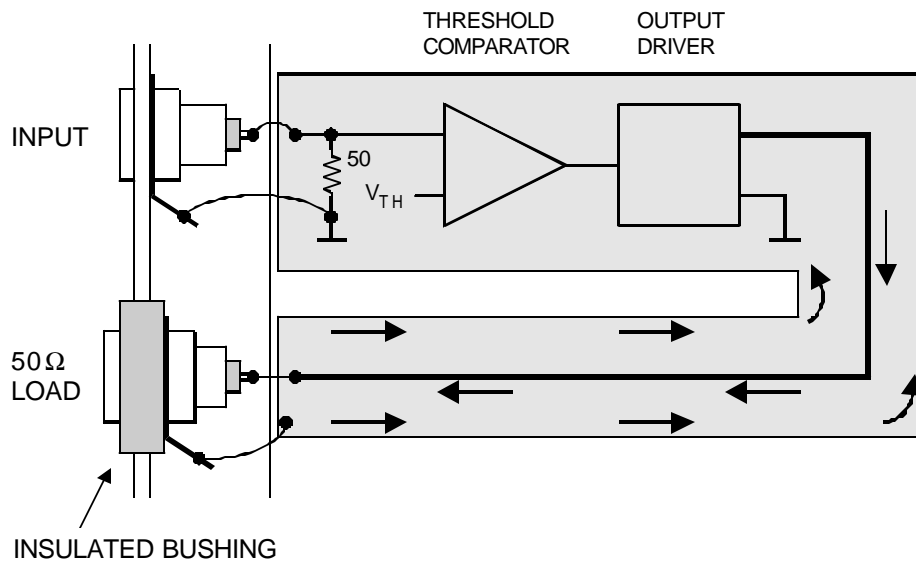
“Ground loops” are often formed by the third wire in the AC power connection. Avoid voltage differences in the “ground” connection by connecting all power cords associated with low-level circuitry into the same outlet strip.

Often it is convenient to replace the coax cable at the output by a strip line integrated on the PC board.

Strip Line:

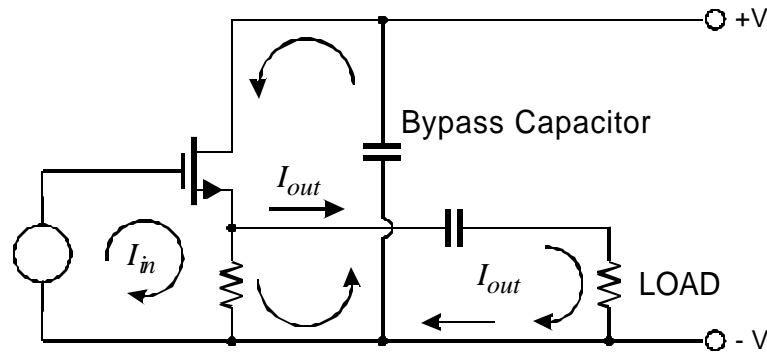


Current paths can be controlled by patterning the ground plane.



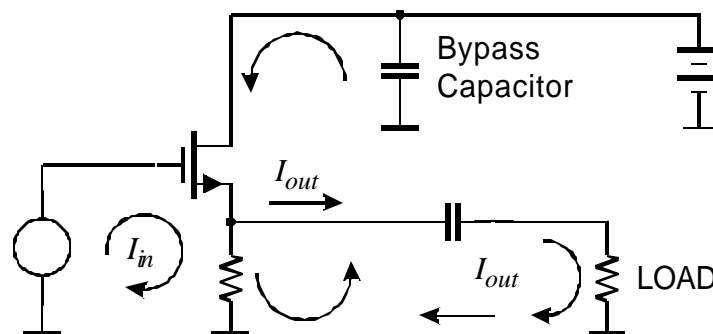
Ground returns are also critical at the circuit level.

Although the desired signal currents circulate as shown on p. 16, there are additional currents flowing in the circuit.



In addition to the signal currents I_{in} and I_{out} , the drain current is also changing with the signal and must return to the source. Since the return through the power supply can be remote and circuitous, a well-defined AC return path is provided by the bypass capacitor.

Since the input and output signal voltages are usually referenced to the negative supply rail, circuits commonly configure it as a common large area bus, the “ground”, and all nodes are referenced to it.



Since the “ground” is a large area conducting surface – often a chassis or a ground plane – with a “low” impedance, it is considered to be an equipotential surface.

The assumption that “ground” is an equipotential surface is not always justified.

At high frequencies current flows only in a thin surface layer (“skin effect”).

The skin depth in aluminum is $\sim 100 \mu\text{m}$ at 1 MHz. A pulse with a 3 ns rise-time will have substantial Fourier components beyond 100 MHz, where the skin depth is $10 \mu\text{m}$.

⇒ Even large area conductors can have substantial resistance!

Example: a strip of aluminum, 1 cm wide and 5 cm long has a resistance of $\sim 20 \text{ m}\Omega$ at 100 MHz (single surface, typical Al alloy)

$100 \text{ mA} \Rightarrow 2 \text{ mV}$ voltage drop,

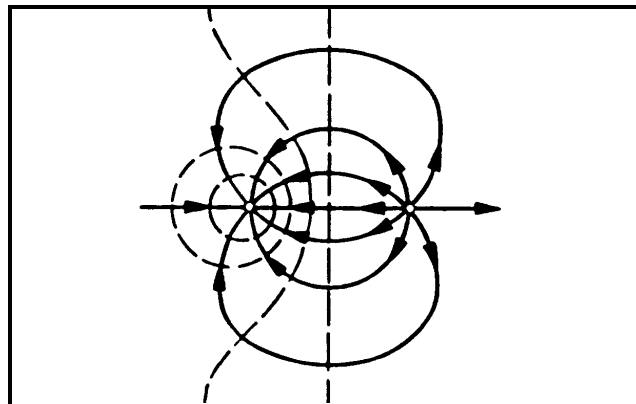
which can be much larger than the signal.

The resistance is determined by the ratio of length to width, i.e. a strip 1 mm wide and 5 mm long will show the same behavior.

Inductance can increase impedances much beyond this value!

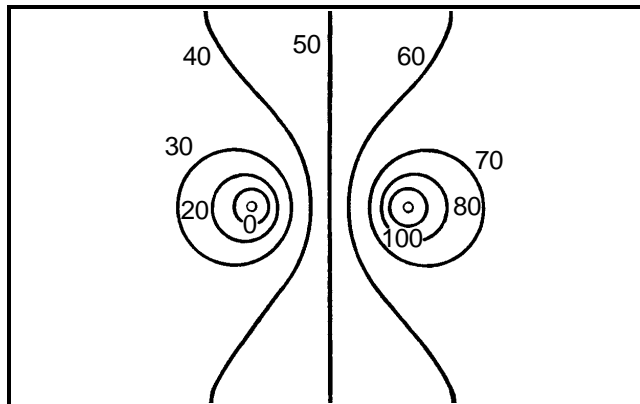
Consider a current loop closed by two connections to a ground plane.

Current distribution around the two connection points:

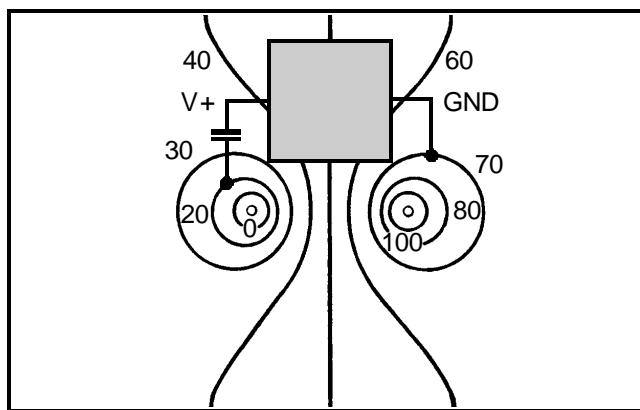


The dashed lines indicate equipotential contours.

Assume a total drop of 100 mV. The resulting potential distribution is

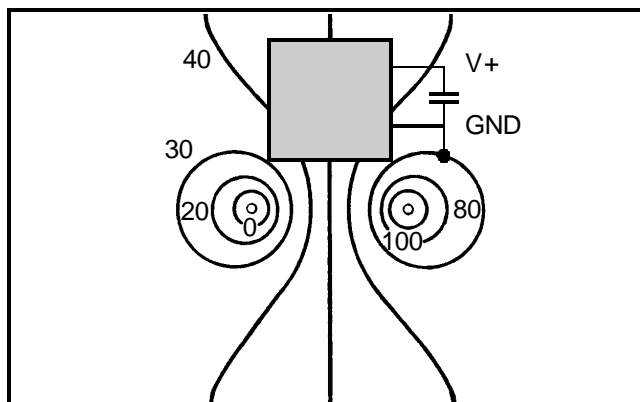


Mounting a circuit block (an IC, for example) with ground and bypass connections as shown below



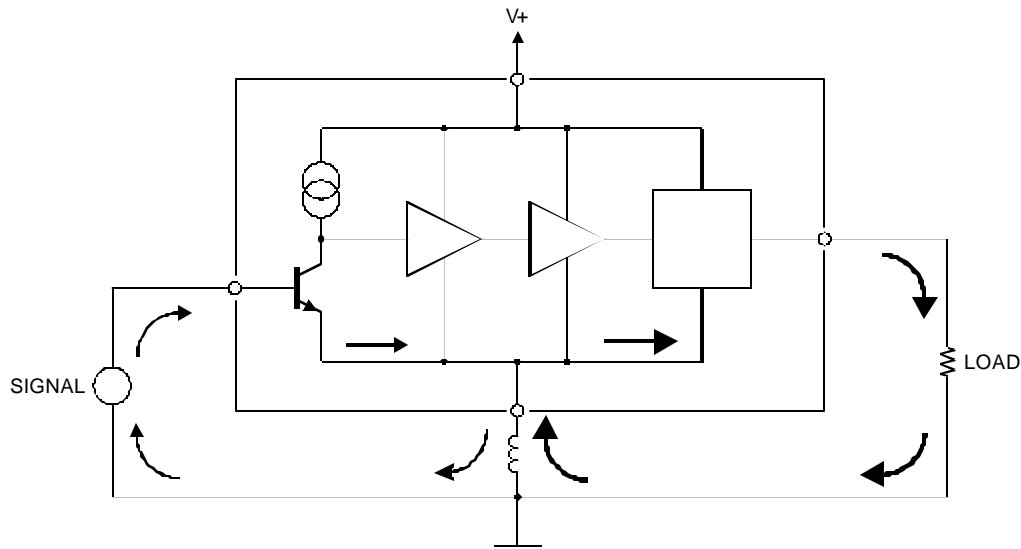
introduces a 50 mV voltage drop in the “ground” path.

Direct connection of the bypass capacitor between the V+ and GND pads avoids pickup of the voltage drop on the ground plane.



“Ground” Connections in Multi-Stage Circuits

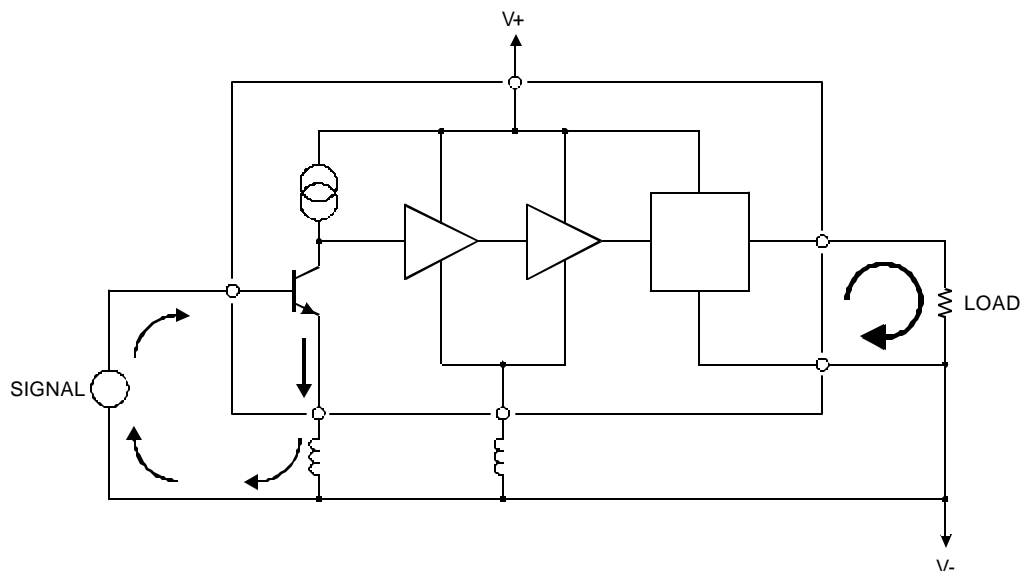
IC comprising a preamplifier, gain stages and an output driver:



The output current is typically orders of magnitude greater than the input current (due to amplifier gain, load impedance).

Combining all ground returns in one bond pad creates a shared impedance (inductance of bond wire). This also illustrates the use of a popular technique – the “star” ground – and its pitfalls.

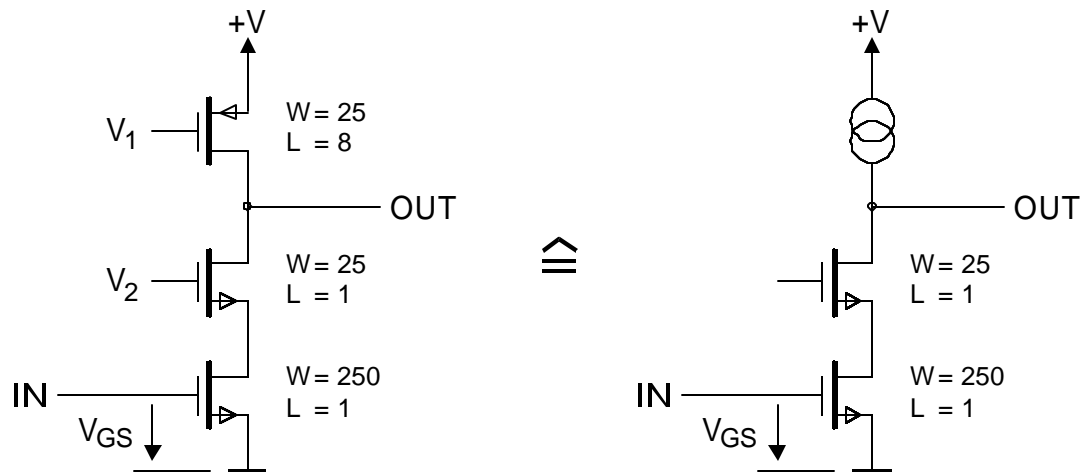
Separating the “ground” connections by current return paths routes currents away from the common impedance and constrains the extent of the output loop, which tends to carry the highest current.



The Folded Cascode

The folded cascode is frequently used in preamplifiers optimized for low power.

Standard cascode with representative transistor sizes:



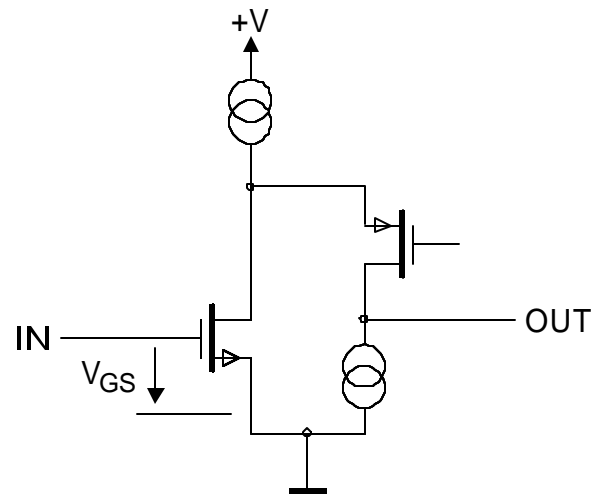
The cascode combines two transistors to obtain

- the high transconductance and low noise of a wide transistor
- the high output resistance (increased by local feedback) and small output capacitance of a narrow transistor
- reduced capacitance between output and input

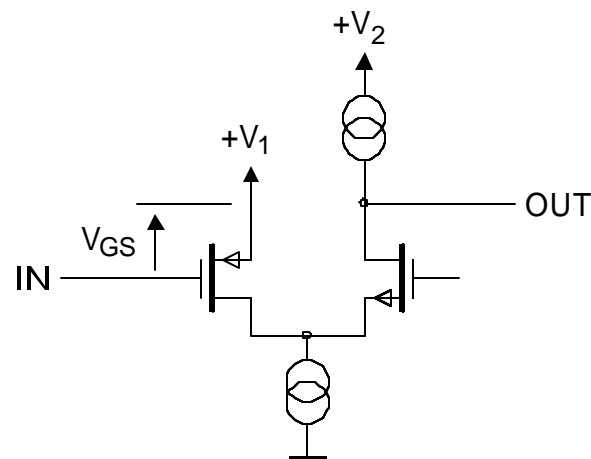
Since the input transistor determines the noise level, its current requirement tends to dominate.

In a conventional cascode the current required for the input transistor must flow through the whole chain.

The folded cascode allows the (second) cascode transistor to operate at a lower current and, as a result, higher output resistance.

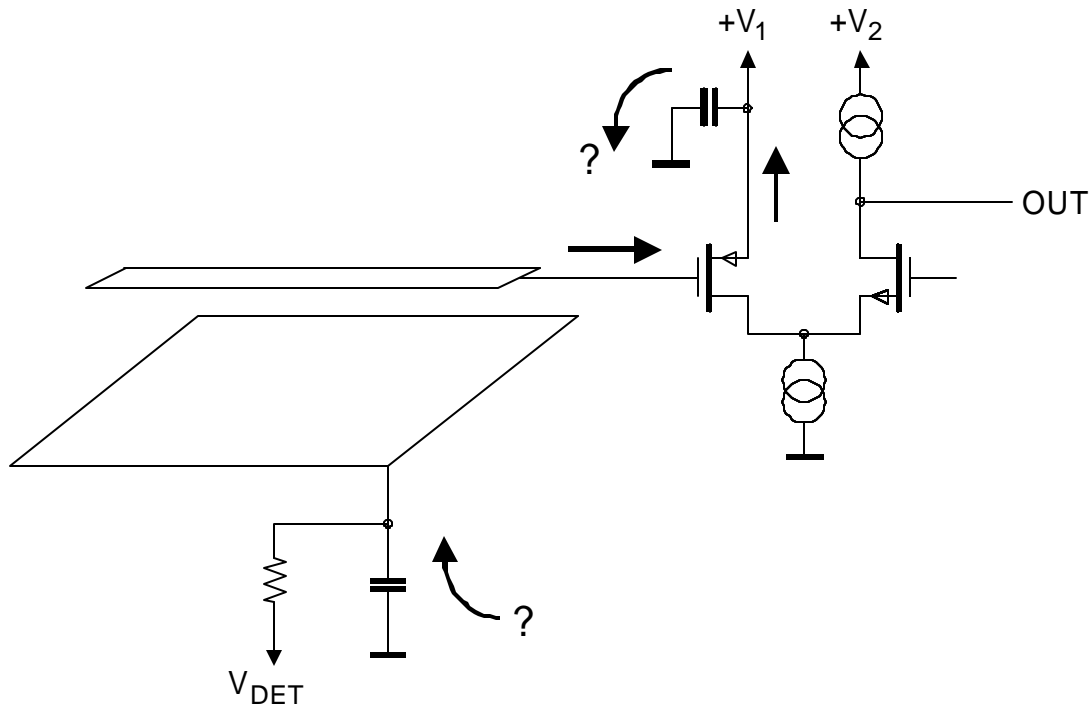


Since PMOS transistors tend to have lower “ $1/f$ ” noise than NMOS devices, the following adaptation is often used:



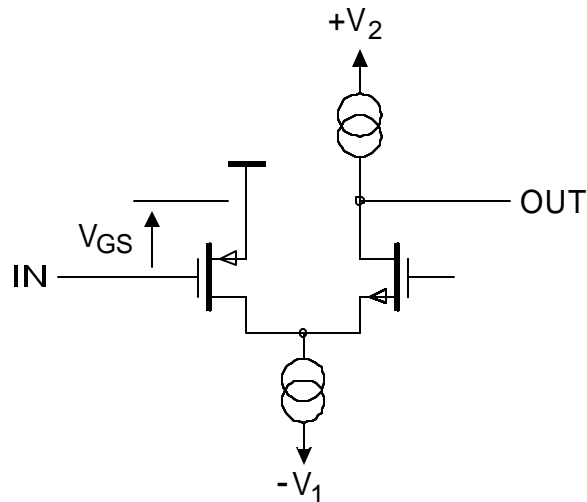
The problem with this configuration is that the supply V_1 becomes part of the input signal path. Unless the V_1 supply bus is very carefully configured and kept free of other signals, interference will be coupled into the input.

Consider the circuit connected to a strip detector:



Unless the connection points of the bypass capacitors from the FET source and the detector backplane are chosen carefully, interference will be introduced into the input signal loop.

It is much better to “ground” the FET source to a local signal reference and use a negative second supply.



System Considerations

1. Choice of Shaper

Although a bipolar shaper has slightly inferior noise performance than a unipolar shaper, it may provide better results in the presence of significant low-frequency noise.

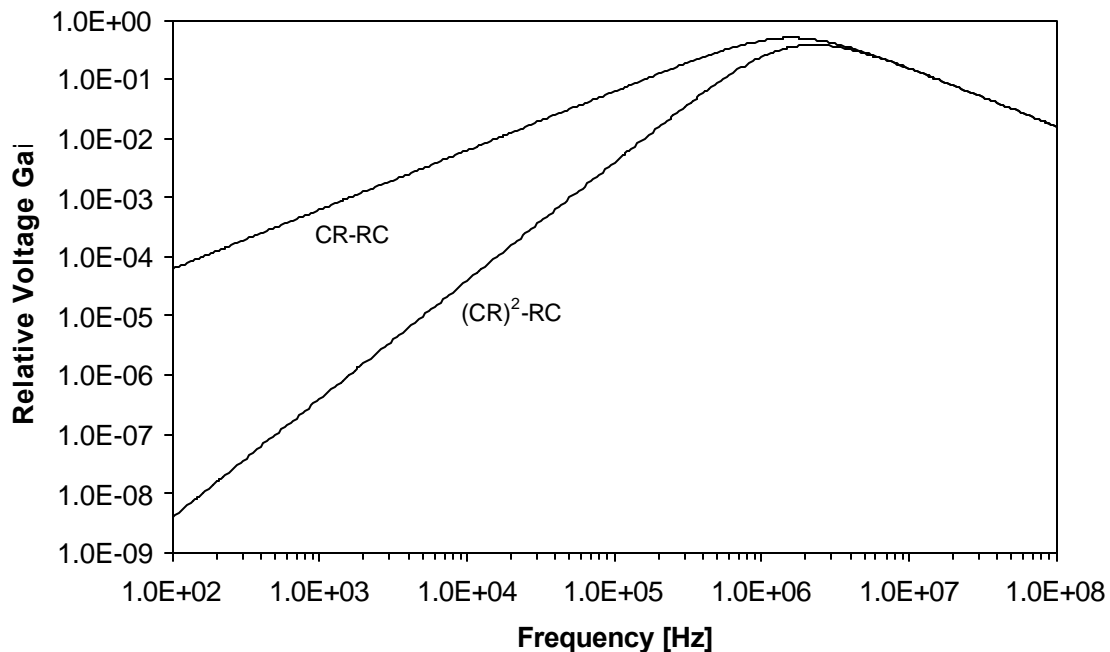
Minimum Noise

$$\text{CR-RC} \quad Q_{n,opt} = 1.355 \sqrt{i_n v_n C}$$

$$(\text{CR})^2\text{-RC} \quad Q_{n,opt} = 1.406 \sqrt{i_n v_n C}$$

In the frequency domain the additional CR-stage (low-pass filter) provides substantial attenuation of low-frequency interference.

Frequency Response of CR-RC and (CR)²-RC Shapers



2. Connections in Multi-Channel Systems

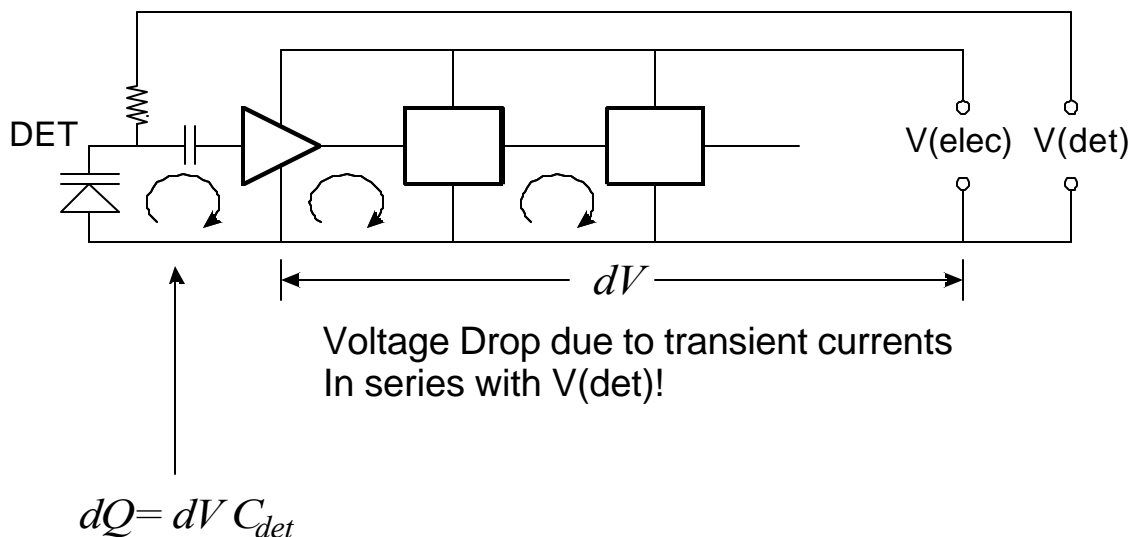
Example: Strip Detector Readout

A single channel of a readout system for strip detectors includes

- low noise preamplification
- additional gain stages
- a comparator for hit recognition
- a clocked pipeline or storage array
- additional multiplexing circuitry to feed the hit flag and possibly analog output signal to the output.

Especially comparators and switching stages inject current spikes into the voltage busses, but even low-level analog stages rely on current changes.

Voltage bussing circuitry on integrated circuitry often has significant resistance, since the lines are narrow and thin, so the current transients cause local voltage changes that can couple into the input.

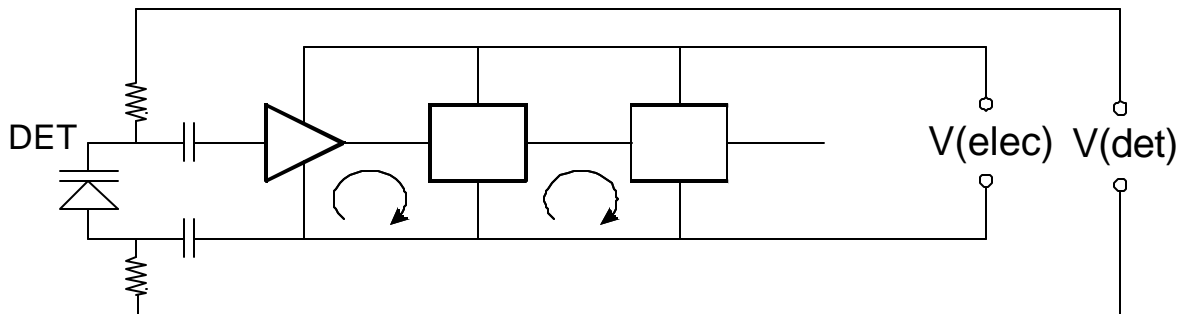


The transient voltage drop dV is superimposed on the detector bias and injects a charge $dQ = dV C_{det}$ into the input.

Propagation of current and voltage transients can be controlled by filter networks comprising resistors or inductors and capacitors.

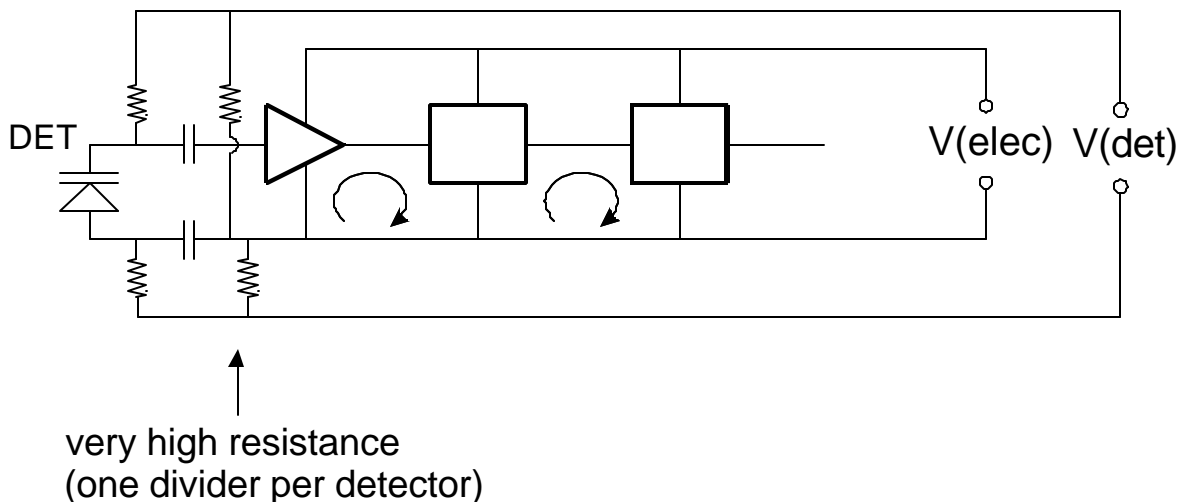
In tracking systems the use of such networks is somewhat restricted, as capacitors can add substantial material and small inductors use ferrite cores that saturate in magnetic fields.

The cross-coupling of detector and electronics voltages can be removed by separating the shared paths:

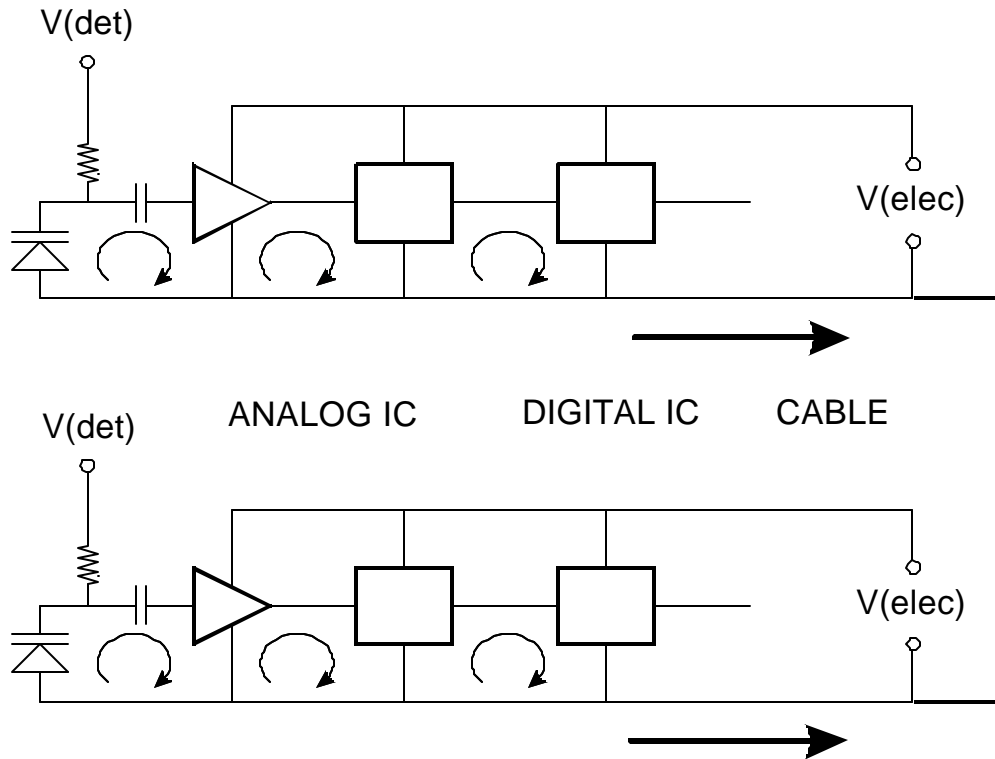


The resistors in both legs of the bias connection isolate the sensitive input node by presenting a high impedance to external signals. Only one of the two capacitors at the input may be necessary, depending on system requirements.

If the detector uses integrated coupling capacitors (often with little voltage margin), the bias and electronics supply voltages must be referenced to one another, for example by a local resistive divider.



Ideally, multiple channels are configured so that only local signal loops exist.



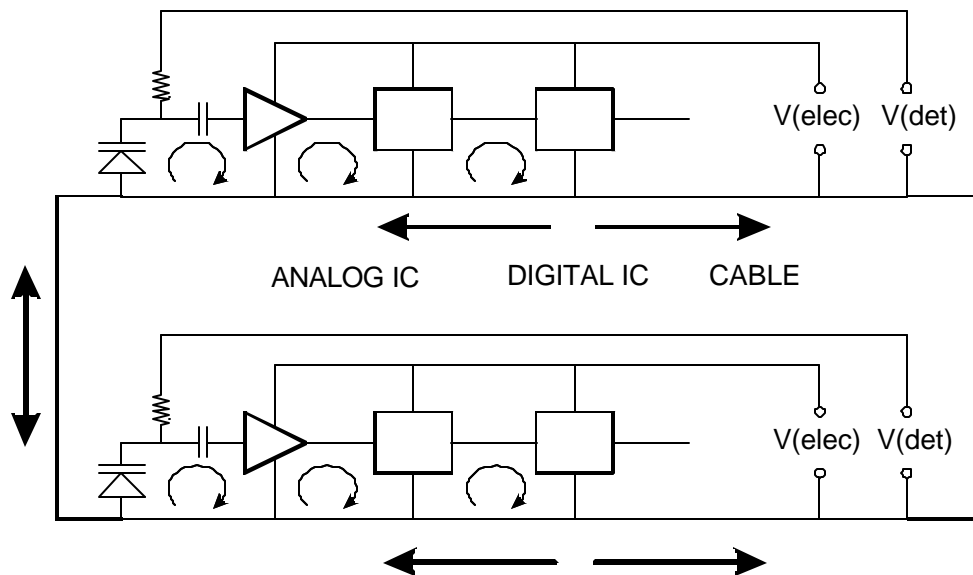
Since the path of least resistance is provided by the cabling and connections to the power supplies and data acquisition system, current transients originating in the front-end circuitry do not flow towards the input.

In reality, the inputs of adjacent channels and chips are coupled by the strip-to-strip capacitance and the common detector substrate.

The loop formed by common connections at both the input and the output allows current transients to propagate to the input.

This also applies to channels on the same side of the detector.

Consider current spikes originating in the digital circuitry:



Since the cross-connection at the input is formed by the connection of multiple chips to the detector, it is unavoidable.

Breaking the cross-connection at the output is impractical (common data line for multiple chips on a hybrid).

What can be done to break the secondary current path?

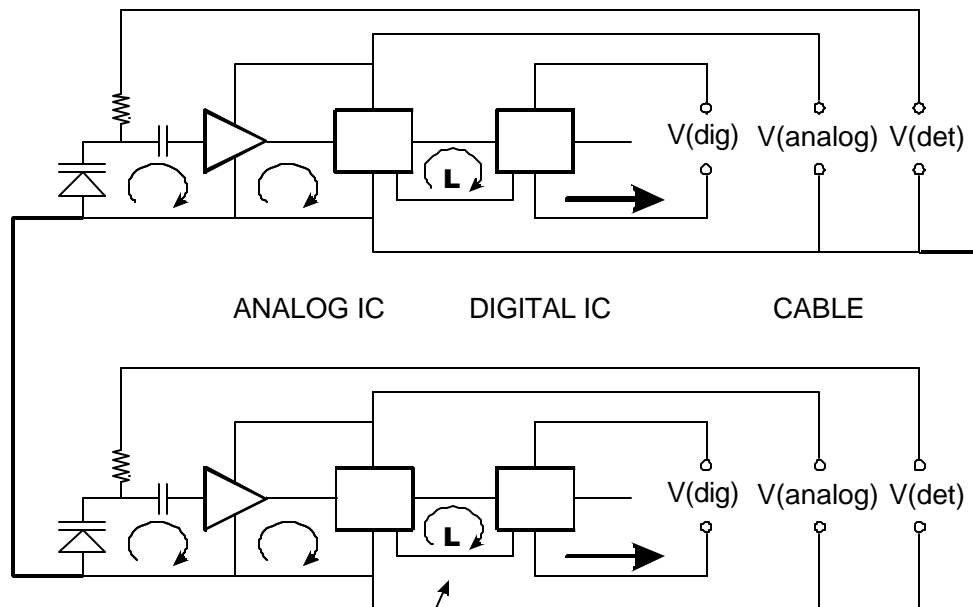
Since the most serious current spikes originate in the digital circuitry, it should be isolated from the analog section.

Commonly, the analog and digital supply voltages are fed separately, but this doesn't address the main problem, which is the common return connection (typically the "ground").

The only necessary connection between the analog and digital circuitry is the data path.

By implementing this in a manner that

- provides a signal path from the analog to the digital circuitry, but
- presents a high impedance from the digital to the analog section, i.e. in the opposite direction, the input loop can be broken.

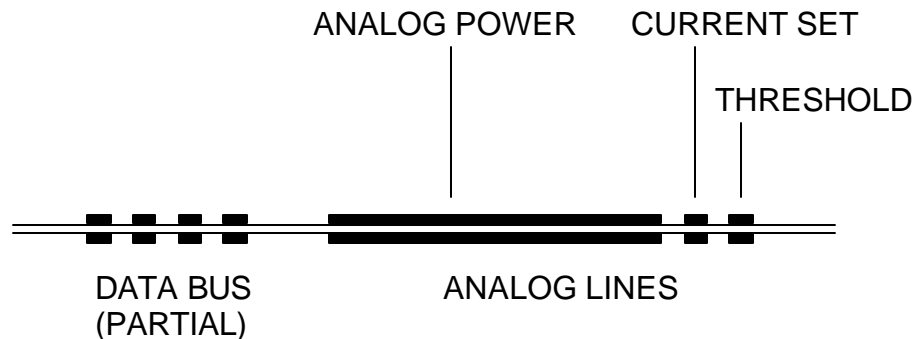


L: Local signal loop
One connection per channel,
but one return per chip (to
limit number of wire bonds).

“Self-Shielding” Cables

In mixed analog-digital systems, radiation from cables, especially digital signal cables, is a concern.

By utilizing broadside-coupled differential lines with a thin intermediate dielectric, the field is confined to the region between the conductors. The extent of the fringing field beyond the conductor edge is about equal to the thickness of the dielectric.



Example:

Conductors:	50 μm thick, 150 μm wide
Dielectric:	50 μm thick
Gap between pairs:	150 μm

Cross-coupling between adjacent pairs:
 $< 2\%$ at 60 MHz for 1 m length

Power connections are made substantially wider (1 – 5 mm), forming a low impedance transmission line with high distributed capacitance.

The geometry shown above is for short runs in the inner region of a tracker, where reduction of material is crucial. Dimensions can be scaled proportionally to achieve lower resistance and signal dispersion in longer cable runs at larger radii.

Why things don't work – some closing remarks

No magic recipes!

All systems involve compromises

Only rarely can they be implemented in a manner that avoids all problems.

Typically, many small details conspire to introduce spurious signals.

However, only one mistake can be enough.

Sometimes doing the wrong thing can improve the situation, but this is a band-aid, not a cure.

When a system has incorporated poor connection schemes, one is often forced to follow that track.

Once shared current paths have been introduced, adding more spurious paths can improve the cross-talk by reducing the common impedances. Cut and try!

Just remember that physics still prevails, even though this topic is dominated by fairy tales.

9. Summary of Considerations in Detector Electronics

1. Maximize the signal

Maximizing the signal also implies reducing the capacitance at the electronic input node. Although we want to measure charge, the primary electric signal is either voltage or current, both of which increase with decreasing capacitance.

2. Choose the input transistor to match the application.

At long shaping times FETs (JFETs or MOSFETs) are best. At short shaping times, bipolar transistors tend to prevail.

3. Select the appropriate shaper and shaping time

In general, short shaping times will require higher power dissipation for a given noise level than long times.

The shaper can be optimized with respect to either current or voltage noise (important in systems subject to radiation damage)

The choice of shaping function and time can significantly affect the sensitivity to external pickup.

4. Position-sensitive detectors can be implemented using either interpolation techniques or direct readout. Interpolating systems reduce the number of electronic channels but require more complex and sophisticated electronics. Direct readout allows the greatest simplicity per channel, but requires many channels, often at high density (good match for monolithically integrated circuits).

5. Segmentation improves both rate capability and noise (low capacitance). It also increases radiation resistance.

6. Timing systems depend on slope-to-noise ratio, so they need to optimize both rise-time and capacitance.

Relatively long rise-times can still provide good timing resolution (\ll rise-time), if the signal-to-noise ratio is high.

Variations in signal transit times and pulse shape can degrade time resolution significantly.

7. Electronic noise in practical systems can be predicted and understood *quantitatively*.
8. From the outset, systems must consider sensitivity to spurious signals and robustness against self-oscillation.

Poor system configurations can render the best low-noise front-end useless, but proper design can yield “laboratory” performance in large-scale systems.

9. Although making detectors “work” in an experiment has relied extensively on tinkering and “cut-and-try”, understanding the critical elements that determine detector performance makes it much easier to navigate the maze of a large system.

It is more efficient to avoid problems than to fix them.

A little understanding can go a long way.